Durham E-Theses

Proteomic analysis of the heat shock and acclimation responses of Cyanobacteria

Hall, John James

Proteomic Analysis of the Heat Shock and Acclimation Responses of Cyanobacteria

John James Hall

A thesis submitted to the University of Durham for the degree of
Doctor of Philosophy

Department of Biological and Biomedical Sciences

2005

Supervisor: Professor A. R. Slabas

1 3 JUN 2005

Thesis
2005/
HAL

John James Hall

Proteomic Analysis of the Heat Shock and Acclimation Responses in Cyanobacteria

Abstract

The cyanobacterium *Synechocystis* sp. PCC 6803 is a model experimental organism for proteomic research because its entire genomic sequence is available and cyanobacteria have high adaptive potential towards a variety of environmental stresses. Heat shock characteristically induces expression of the heat shock proteins (Hsps) and photosynthetic organisms have demonstrated the ability to acclimatise their photosynthetic apparatus to milder elevated temperatures. In this study the proteomic methodology of two dimension gel electrophoresis and peptide mass fingerprinting mass spectrometry (PMF MS) was developed for the analysis of *Synechocystis* proteins. High resolution was attained with the application of narrow acidic pH range 'zoom' gels and of 192 individual soluble protein spots analysed via MALDI ToF, 105 were identified. A 2-D difference gel electrophoresis (2D DIGE) based proteomic approach has been applied to characterise the heat shock response in the soluble protein fraction and determine protein factors involved in the thermal acclimation of the thylakoid membrane and its associated photosynthetic machinery in *Synechocystis*. These analyses together with PMF MS for protein identification characterised 176 and 108 heat shock and heat acclimation responsive protein spots, respectively. In both analyses, molecular chaperones displayed the highest heat elevated level, demonstrating a dual role in stabilisation and refolding of both soluble and membrane-bound proteins. Other proteins identified in the heat shock response included those involved in photosynthesis, carbon fixation, translation, amino acid biosynthesis and several hypothetical proteins. Proteins involved in heat acclimation of the thylakoid membrane included constituents of photosynthesis, respiration, hopene biosynthesis and several hypothetical proteins. Furthermore, a candidate heat sensor involved in the regulation of heat shock gene expression has been characterised through analysis of the heat shock response in a histidine kinase knock out mutant strain of *Synechocystis*, namely *Δhik34*, which displays increased thermal tolerance. The gene product of *hik34* has a possible dual role in both the suppression of *hsp* gene expression under normal growth temperature and enhancement under heat shock.

Contents

Contents continued

Contents continued

Contents continued

Contents continued

Contents continued

Contents continued

Contents continued

List of Figures

List of Figures continued

List of Tables

List of Abbreviations

2-DE	two-dimension gel electrophoresis
A	absorbance
AP	allophycocyanin
APS	ammonium persulphate
amu	atomic mass units
BLAST	basic local alignment search tool
BSA	bovine serum albumin
BVA	biological variation analysis
Ccm	carbon concentrating mechanism
CHAPS	3-[(3-cholamidopropyl)dimethylammonio]-1-propane sulphonate
ChlA	chlorophyll A
CID	collision induced dissociation
CIRCE	controlling inverted repeat of chaperone expression
COG	clusters of orthologous groups of proteins
Cy-Dye	cyanine Dye
Cyt	cytochrome
DIA	differential in-gel analysis
DIGE	difference gel electrophoresis
DMF	dimethylformamide
DMSO	dimethyl ulfoxide
DOC	deoxycholic acid
dpi	dots per inch
DTT	dithiothreitol
EDTA	ethylenediaminetetraacetic acid
ER	endoplasmic reticulum
ESI MS-MS	electrospray ionisation tandem mass spectrometry
EST	expressed sequence tag
FAD	flavin adenine dinucleotide
HEPES	N-2-Hydroxyethylpiperazine-N'-2-Ethane Sulphonic Acid
Hik	histidine kinase
HLP	hemolysin-like protein
HSF	heat shock factor

List of Abbreviations

Hsp	heat shock protein
ICAT	isotope coded affinity tags
ICM	intracytoplasmic membranes
IEF	isoelectric focusing
IGR	in-gel rehydration
IPG	immobilised pH gradient
IT	ion trap
MALDT-ToF	matrix assisted laser desorption/ionisation - Time of flight
MOWSE	molecular weight search
MS	mass spectrometry
MSP	manganese stabilising polypeptide
MW	molecular weight
m/z	mass to charge ratio
NDH-1	NADH dehydrogenase type I complex
NDH-2	NADH dehydrogenase type 2 complex
NEPHGE	non-equilibrium pH gradient electrophoresis
ORF	open reading frame
PAR	photosynthetic active radiation
PB	phycobilisome
PC	phycocyanin
PE	phycoerythrin
pI	isoelectric point
PMF	peptide mass fingerprint
PMT	photon multiplier tube
PPIase	peptidyl prolyl cis-trans isomerse
ppm	parts per million
PSI	photosystem I
PSII	photosystem II
PTM	post translational modifications
Q-TOF	qudrupole time-of-flight
rpm	revolutions per minute
Rre	response regulator

List of Abbreviations
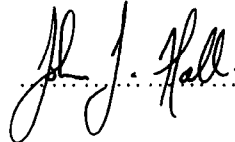
Rubisco	ribulose bisphosphate carboxylase/oxygenase
Spb	substrate-binding proteins
SCA	synthetic carrier ampholytes
SDS	sodium dodecyl suphate
SDS-PAGE	sodium dodecyl suphate polyacrylamide gel electrophoresis
sHsp	small heat shock protein
sp	species
Sp-r	spectinomycin resistance
TAP	tandem affinity purification
TBP	tributyl phosphine
TCA	trichloroacetic acid
TEMED	N,N,N',N' - tetramethylethylene diamine
TFA	trifluroacetic acid
TIF	tagged image file
TQ	triple qudrupole

Declaration

I declare that the work within this thesis, submitted for the degree of Doctor of Philosophy, is my own original work and has not been submitted for a degree at this or any other University.

Signed:

Date: 01 / 05 / 2005

Statement of Copyright

The copyright of this thesis rests with the author. No quotation from it should be published without his prior written consent and information derived from it should be duly acknowledged.

Acknowledgements

I wish to express my gratitude to Professor Toni Slabas for his committed support and guidance throughout this work and to Dr. Bill Simon for his generous technical expertise and to whom I am indebted to for the mass spectrometry data. I also acknowledge the help given by other members of the Integrative Cell Biology Laboratory. In particular, Dr Steve Chivasa, Dr. Dan Maltman and Dr. Bongani Ndimba on specific aspects of two dimensional gel electrophoresis and Dr. Adrian Brown and Dr. Johan Kroon for advice on molecular biology. Thanks are due to John Gilroy for construction of the cyanobacterial growth apparatus and Paul Sidney for colour photography.

Elsewhere I would like to thank Professor Norio Murata and Dr. Iwane Suzuki who kindly supervised fundamental training in the growth of cyanobacteria at the National Institute for Basic Biology and together with Dr. Yoshitaka Nishiyama for an opportunity to collaborate with them.

I also wish to thank my university friends and colleagues for making my time in Durham an enjoyable and rewarding one with a special mention to Dan, Matt and Steve and to friends at Grey College. Last, but certainly not least, I would like to say a huge thank you to my family and loved ones, who have provided me with unconditional support and encouragement and have been there for me every step of the way. Thank you!

CHAPTER 1

General Introduction

1.1   Cyanobacteria

1.1.1   Cyanobacteria – what are they?

Cyanobacteria are aquatic, photo-autotrophic gram-negative prokaryotes, found in both fresh and salt water environments. They are perhaps the largest and most diverse group among the entire prokaryote kingdom (Whitton & Carr, 1982) as shown by their variation of DNA base composition (Herdman *et al*, 1979), a diverse morphology and the different environments they inhabit (Rippka *et al.*, 1979). They are believed to be the first phototrophic organisms, releasing oxygen into the earth's atmosphere. In fact the origins of cyanobacteria date back over 3 billion years to almost the beginning of life on earth (Schopf, 1993). Today, cyanobacteria are abundant throughout the world; found living on a variety of substrates and their phyla ranges from unicellular organisms, such as *Synechocystis* and *Synechococcus* sp., through to complex multicellular filamentous strains, many with specialised differentiated cells, such as heterocysts in nitrogen fixing *Anabaena* and *Nostoc* sp. (Figure 1.1). To date, over 150 genera and over 2000 species have been recorded, with many new species still being discovered (Nagarkar, 2002). Fundamental to this have been the efforts of M. B. Allen who isolated the first unicellular strain *Anacystis nidulans* (Allen, 1952), C. Van Baalen in the purification of strains from marine sources (Van Baalen, 1962), R. W. Castenholz in isolation of thermophilic strains (Peary and Castenholz. 1964), and R. Y. Stanier in isolating a variety of pure cyanobacterial strains (Stanier *et al.*, 1971, Rippka *et al.*, 1979).
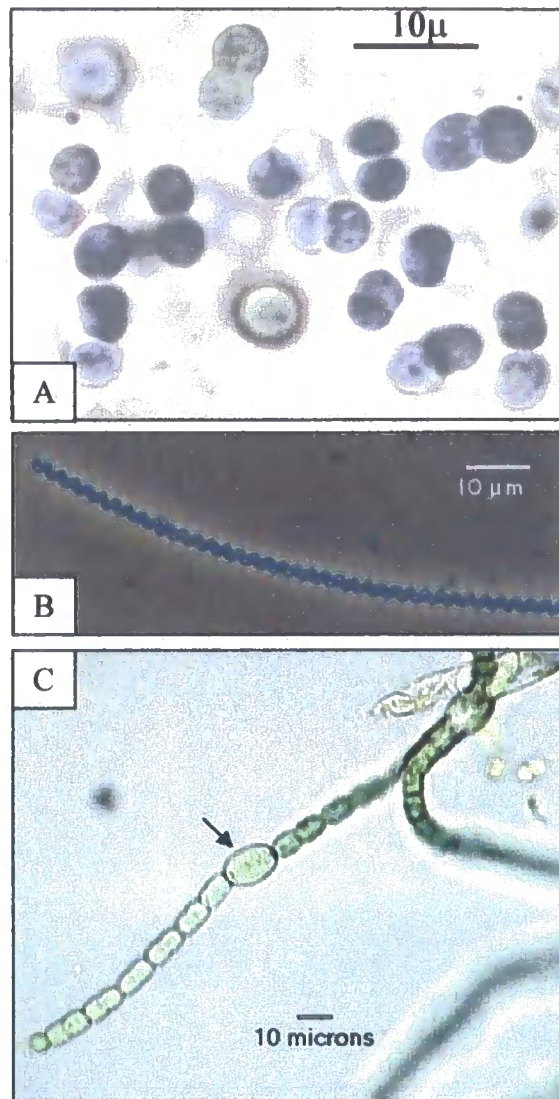
Figure 1.1. Species of cyanobacteria

A, *Synechocystis* sp., B, *Spirulina* sp. and C, *Nostoc* sp. arrow indicates the differentiated heterocyst able to perform nitrogen fixation. Images were obtained from Cyanosite (http://www-cyanosite.bio.purdue.edu) and clearly show the degree of morphological diversity across the numerous cyanobacteria genera.

1.1.2   Cyanobacteria – Biological classification and evolution.

For oxygen-evolving photosynthesis, cyanobacteria possess photosynthetic electron transport systems, which are functionally and structurally similar to those of chloroplasts in photosynthetic eukaryotes, using water as an electron donor and containing the two photopigments chlorophyll a and β-carotene (Stanier and Cohen-Bazire, 1977). Because of this, cyanobacteria were initially incorrectly classified with eukaryotic algae and were designated "blue green algae"; a name so well established that it is still in use today. Recognition of their correct classification with bacteria in the biological hierarchy was achieved with the onset of electron microscopy, which demonstrated the lack a defined nucleus in cyanobacteria, and together with data on cell wall composition and ribosomal structure, helped classify cyanobacteria within the prokaryotic world (Stanier and Van Niel, 1962; Echlin and Morris, 1965).

Explanation for the unmistakable similarity between eukaryotic photosynthetic organisms and cyanobacteria lies with the theory that ancient cyanobacteria are the evolutionary link between bacteria and green plants. This evolutionary theory, originally hypothesised by Mereschkowsky (1905), states that plastids arose in plants as a result of an endosymbiotic event, wherein a eukaryotic ancestral cell engulfed a photosynthetic prokaryote, thus giving rise to the double outer membrane characteristic of each member of the plastid family (Fredrick, 1981).

1.1.3   Photosynthesis in cyanobacteria

Cyanobacteria, like chloroplasts, possess four major membrane-associated protein complexes which act together to form oxygenic photosynthesis. These are the photosystem I and II reaction centre complexes (with their associated chlorophyll-proteins), the cytochrome b_6f complex and the ATP synthase complex (Sidler, 1994) (Figure 1.2). Photosystems I and II and the cytochrome b_6f complex functionally interact with each other and with the use of light form O_2, NADPH and a proton gradient which drives the formation of ATP at the ATP synthase complex. A system typically described through the Z scheme (Blankenship and Prince, 1985). Unlike eukaryotic plants, some species of cyanobacteria have been shown to have the dual capacity for oxygenic photosynthesis and bacterial-type anoxygenic photosynthesis, utilising hydrogen sulphide instead of water as an electron donor. This capability allows cyanobacteria to occupy an intermediate position unsuitable for solely aerobic or anaerobic organisms (Padan and Cohen, 1982).

Despite the similarities between the cyanobacterial and eukaryotic oxygenic photosynthetic machinery, there are two features of the cyanobacterial apparatus which distinguish it from the chloroplast of eukaryotic plants. Firstly, the cyanobacterial photosynthetic apparatus is located on intracytoplasmic membranes (ICM), very similar to the chloroplast thylakoid membranes of higher plants, except they permeate throughout the cytoplasm and are not packaged within a distinct membrane compartment (Golecki and Drews, 1982; Gantt, 1994) (Figure 1.3). Certainly the structure of cyanobacterial thylakoid membranes supports the endosymbiotic evolutionary theory of Mereschkowsky (1905). Secondly,
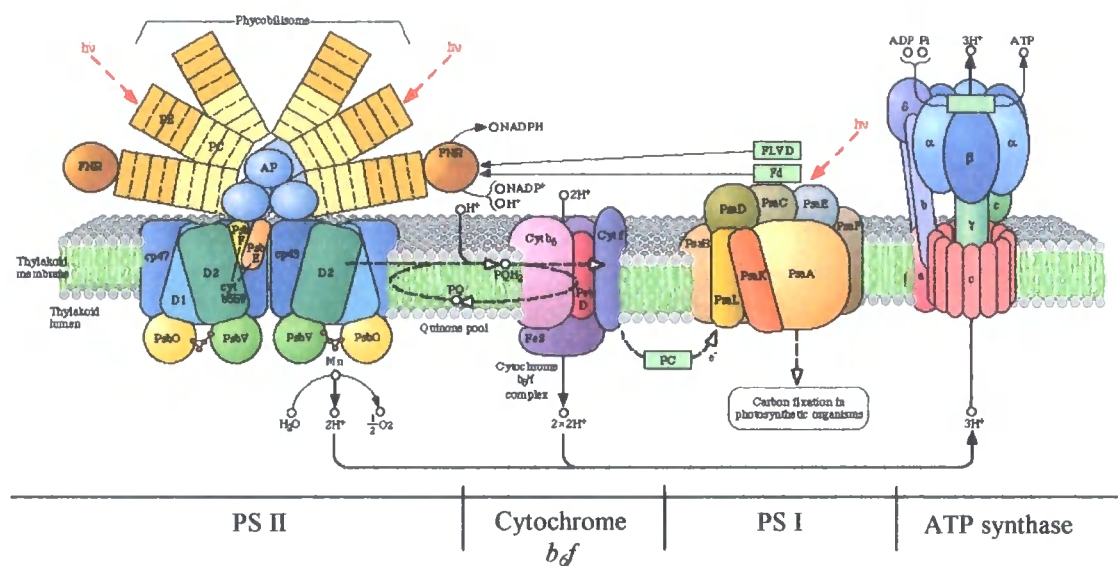
Figure 1.2. Schematic diagram of the cyanobacterial photosynthetic apparatus.

Cyanobacterial photosynthetic membranes, like plants, possess four major protein complexes associated with oxygenic photosynthesis. These are photosystem II (PSII), cytochrome b_6f complex, photosystem I (PSI) and the ATP sythase complex. The PSII complex is the most individual to cyanobacteria where light is harvested through a multi protein complex, namely the phycobilisome, instead of the chlorophyll-*b* containing light harvesting protein complex II (CPII). Phycobilisomes consist of light harvesting rod antennae containing phycoerythrin (PE) and phycocyanin (PC) phycobiliproteins arranged around a central core of allophycocyanin (AP). Figure obtained from KEGG (Kyoto Encyclopaedia of Genes and Genomes) pathways (http://www.genome.jp/).
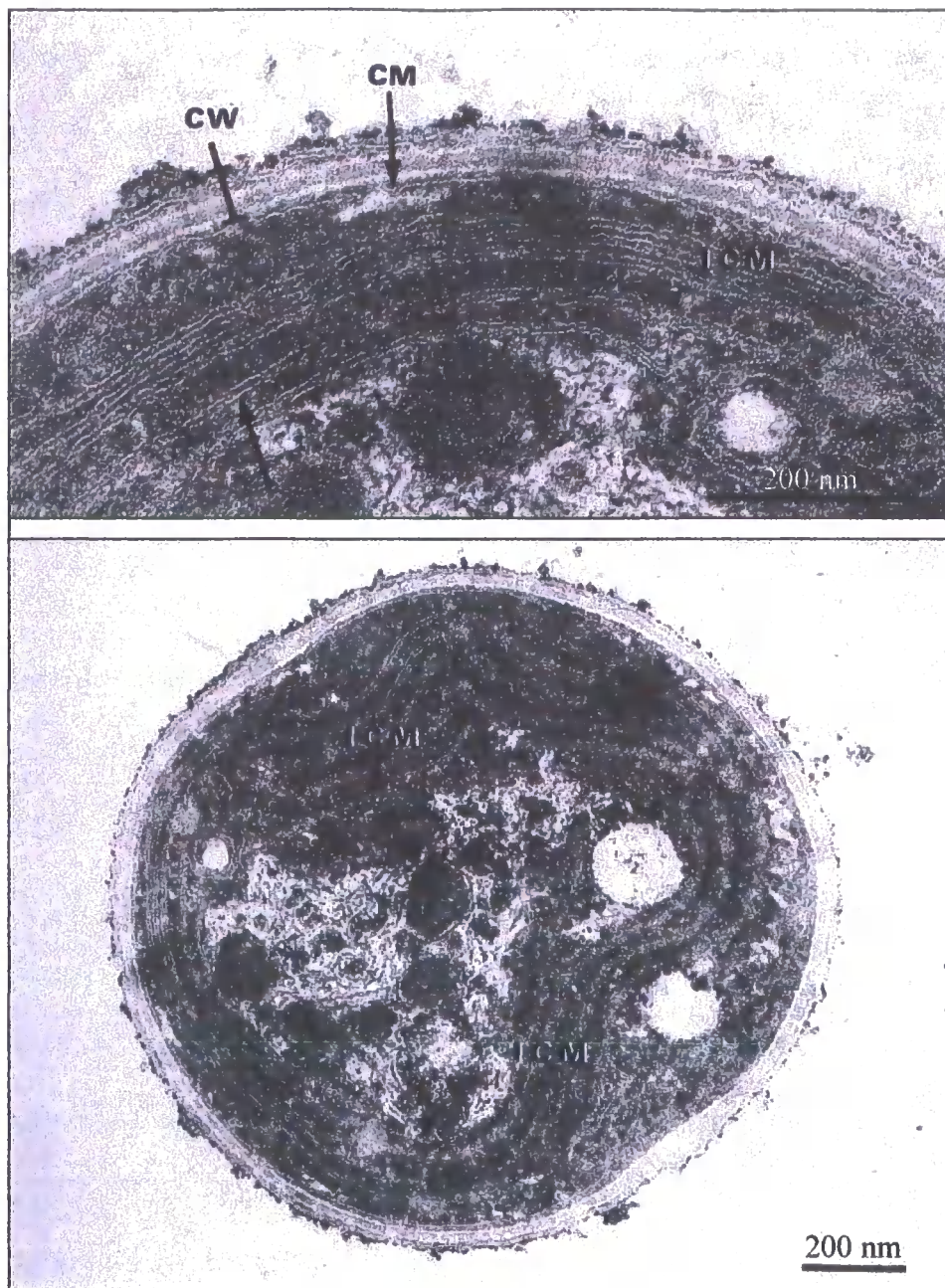
Figure 1.3. Localisation of cyanobacterial intracytoplasmic (thylakoid) membranes within the cell in relation to other membranous structures.

Cell wall (CW), cytoplasmic membrane (CM) and intracytoplasmic membranes/ thylakoids (ICM). Images are adapted from Golecki and Drews (1982). Thylakoid membranes are arranged in parallel and located around the periphery of the cell.

cyanobacteria contain very large (several million daltons) light-harvesting multi protein complexes known as phycobilisomes (PBs) located on the cytoplasmic surface of the thylakoid membranes and are directly attached to PSII (Figure 1.2) (Sidler, 1994; McColl; 1998). In photosynthetic eukaryotes, these structures are substituted for the chlorophyll-*b* containing light harvesting protein complex (CP II), which is located within the photosynthetic membrane, not attached to its surface.

PBs are composed of several different phycobiliproteins subunits and absorb light maximally in 470-660 (yellow-green light) region unlike eukaryotic chlorophyll containing light harvesting complexes (Figure 1.4). This is because little blue or red light reaches the cyanobacteria living in water at a depth of one meter or more as such light is absorbed by water and green plants living above them. The board spectral range over which PB absorb light is owed to the different spectral properties of the various phycobiliproteins subunits which owe their intense absorption properties to the presence of covalently attached open-chain tetrapyrrole chromospheres, commonly known as phycobilins or simply bilins (Cohen-Bazire and Bryant, 1982; MacColl, 1998). The most commonly occurring phycobilins are phycocyanobilin and phycoerythrobilin which maximally absorb at 662.5 nm (Glazer and Fang, 1973) and 555 nm (Glazer and Hixson, 1975), respectively. Phycobiliproteins containing phycocyanobilin and phycoerythrobilin prosthetic groups are known as phycocyanin (PC) and phycoerythrin (PE). These proteins are composed of dissimilar α and β monomers where the number of bilin prosthetic groups per monomer differs from 1 in phycocyanin α subunits to as many as 3 or 4 in phycoerythrin β sunbunits (MacColl, 1998).
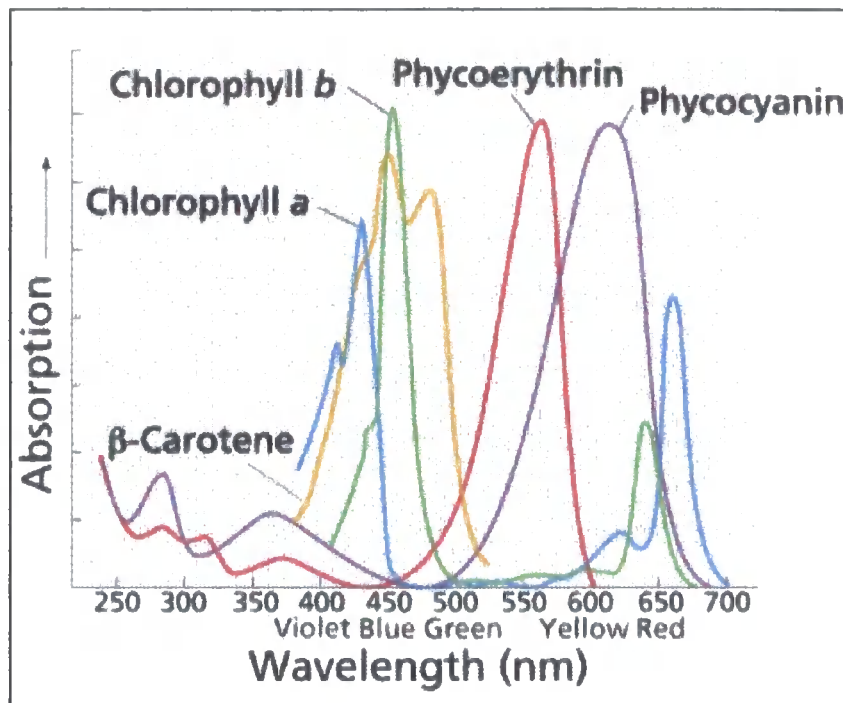
Figure 1.4. Different absorption spectra of cyanobacterial and eukaryotic chloroplast light harvesting tetrapyrole chromophores.

Cyanobacterial light harvesting phycobiliproteins phycoerythrin and phycocyanin contain tetrapyrole chromophores which absorb maximally at 555 nm 662.5 nm, respectively. Eukaryotic chloroplast light harvesting complexes contain chlorophyll *a* and *b* chromophores which absorb maximally at 418 nm and 435 nm, respectively. Image obtained from (http://dwb.unl.edu/Teacher/NSF/C11/C11Links/gened.emc. maricopa.edu/bio/bio181/BIOBK/BioBookPS.html#Stages)

PB structural organisation differs between cyanobacterial species; however, there are basic structural similarities. Phycobilisomes form a hemidiscoidal structure where hexamers of phycoerythrin and phycocyanin proteins are coaxially stacked to form six individual peripheral rods (Bryant and Cohen-Bazire, 1981). The length of rods and ratio of phycoerythrin and phycocyanin in them varies between species and growth conditions (Stanier and Cohen-Bazire, 1977). This ability to alter rod composition enables cyanobacteria to adapt to changes in the environment, including temperature, CO_2 concentration, light intensity and wavelength (Grossman *et al.*, 1993, 2001). The rods protrude from a central triangular core consisting of twelve trimeric allophycocyanin proteins containing phycocyanobilin which link the peripheral rods to the photosynthetic lamellae (MacColl, 1998). One of these twelve trimeric proteins is allophycocyanin-B, which is involved in energy transfer from allophycocyanin to the chlorophyll containing molecules of the PS complex. All these protein subunits are assembled through specific interactions with polypeptides called linkers (de Marsac and Cohen-bazire, 1977). Light energy is absorbed by the phycoerythrin and phycocyanin rods and is subsequently transferred to allophyocyanin, which absorb at longer wavelengths, and then to the chlorophyll containing photosystem II D1/D2 reaction centre (Figure 1.2), an energy transfer which occurs in less than 100 ρs and is greater than 95% efficient (MacColl, 1998). In conclusion the phycobilisomes are sophisticatedly designed harvesting antennae which enable cyanobacteria to occupy habitats which would not support organisms relying solely on chlorophyll for sequestering light energy and allow cyanobacteria to adapt to and survive in ever changing environments.

1.1.4   Carbon metabolism in cyanobacteria

Most cyanobacteria are obligate photoautotrophs and are therefore dependent on light as the only energy source for growth. They use light as the driving force for the formation of NADPH and ATP, which are required for the assimilation of CO_2 and other biosynthetic processes. CO_2 is fixed through the reactions of the Calvin reductive pentose phosphate pathway, the source for all carbon skeletal synthesis in photoautotrophic organisms. However, some cyanobacteria can not only grow in a light dependent fashion but are also capable of growth on exogenous organic compounds. This type of growth is known as heterotrophoic growth, of which there are two different types, photoheterotrophic growth, which is growth in light on an organic substrate in the absence of CO_2 assimilation, and chemoheterotrophic growth, which is growth on an organic substrate in the absence of light (Smith, 1982). In chemoheterotrophic growth, the organic compound supports both the carbon and energy needs of cell, where as in photoheterotrophic growth the organic substrate is only a source of carbon, light provides the energy demands of the cell. Another form of growth which some cyanobacteria are capable of bacteria is mixotrophic growth; here cells simultaneously assimilate both carbon and CO_2, the relative amounts of which vary depending on the culture conditions.

The significance of these various different types of growth in nature has been questioned. Are they irrelevant only characterised as a result of laboratory conditions, or are they further examples of acquired physiological processes enabling cyanobacteria to cope with variations in habitat? Although the majority of cyanobacteria demonstrate photoautotrophic growth, natural populations of

cyanobacteria have been found living in environments where there is little or no light. Furthermore, organic compounds which would support heterotrophic and mixotrophic growth, such as D-glucose, are abundant in many environments (White, 1974). In such specialised environments the majority of, if not all, growth would be heterotrophic. Such observations provide evidence of the need for cyanobacterial heterotrophic growth in nature (Smith, 1982).

1.1.5   Unicellular cyanobacteria – model research organisms

Unicellular cyanobacteria, such as *Synechocystis* sp. and *Synechococcus* sp., are model organisms which have been used in a variety of biochemical and molecular biological studies and there are several factors which contribute to their appeal as research organisms. Firstly, they have simple nutrient requirements for growth; therefore cultures can be easily maintained within the laboratory (Allen, 1968). Secondly, being unicellular organisms all cells within a culture are homogeneous. Consequently, experiments are likely to be more reproducible in comparison to those conducted on organisms with cells of different tissue types, each of which would differ in their response. Thirdly, being photosynthetic, containing a full set of genes for oxygenic photosynthesis, in combination with their simple nature, cyanobacteria provide a simple cellular model for the study of photosynthesis not only from a physiological, structural and biochemical point of view, but also from an evolutionary prospective. Finally, *Synechocystis* sp. and *Synechococcus* sp. are readily transformable and can been grown heterotrophically or mixotrophically on a medium supplemented with glucose (Grigorieva and Shestakov, 1982; Dzelzkalns & Bogorad, 1986). As a result, mutations can be readily introduced and maintained by growth of

cells under non-photosynthetic conditions. A large number of mutant strains have been generated, making functional studies on photosynthesis and a variety of other cellular systems possible.

Cyanobacteria are among the most versatile organisms on earth, possessing a remarkable capacity to adapt and survive in hostile environments. They occur in virtually all known extreme habitats on earth differing in levels of desiccation, salinity, temperature, pH, oxygen and carbon dioxide concentration, light intensity, humidity, radiation and other conditions (Dvornyk and Nevo, 2003). This makes them attractive organisms for investigating adaptive strategies and stress responses of photosynthetic organisms. Such investigations to date include research on salt and osmotic stress (Bagwhat and Apte, 1989; Hagemann *et al.*, 1991, 1993; Iyer *et al.*, 1994; Allakhverdiev *et al.*, 1999, 2000a, 2000b, 2001 and 2002; Huckauf *et al.*, 2000; Ferjani *et al.*, 2003), oxidative stress (Nishiyama *et al.*, 2001; Hihara *at al.*, 2003; Kobayashi *et al.*, 2004), chilling stress (Wada *et al.*, 1990; Deshnium *et al.*, 1997; Los and Murata, 1999; Suzuki *et al.*, 2000b; Dilley *et al.*, 2001), heat shock (Borbély *et al.*, 1985; Bagwhat and Apte, 1989; Lehel *et al.*, 1992; Horvath *et al.*, 1998; Tanaka and Nakamoto, 1999; Huckauf *et al.*, 2000; Nakamoto *et al.*, 2000; Kovács *et al.*, 2001; Rajaram *et al.*, 2003), photo-inhibition (Gombos *et al.*, 1992; Zsiros *et al.*, 2000; Allakhverdiev *et al.*, 2002, 2003a, 2003b, 2004;), nitrogen and sulphur starvation (Duke *et al.*, 1989; Huckauf *et al.*, 2000; Luque *et al.*, 2001; MuroPastor *et al.*, 2001; Richaud *et al.*, 2001; Baier *et al.*, 2004) and studies in acclimatisation to high light (Hihara *et al.*, 1998; Sonoike, *et al.*, 2001; Muramatsu *et al.*, 2003) and high temperature (Nishiyama *et al.*, 1993, 1997, 1999; Kimura *et al.*, 2002). Furthermore, due to their readily transformable nature of *Synechocystis* sp. PCC 6803., several two

component signal transduction mechanisms (Figure 1.5) consisting of histidine kinases (Hiks) and response regulators (Rres) (Saito, 2001) have been characterised for a variety of stimuli/stresses in this organism including cold stress (Suzuki *et al.*, 2000a and 2001; Inaba *et al.*, 2003), salt stress (Marin *et al.*, 2003), high light (Hsiao *et al.*, 2004) adaptation to light-dark transitions (Garcia-Dominguez *et al.*, 2000, Park *et al.*, 2000) phosphate ion sensing (Hirani *et al.*, 2001, Suzuki *et al.*, 2004) manganese ion sensing (Yamaguchi *et al.*, 2002, Ogawa *et al.*, 2002) and photoinhibition (Mikami *et al.*, 2003).

Research using the unicellular cyanobacterium *Synechocystis* sp. PCC 6803 has recently been extended further to functional genomic studies including transcriptomics and proteomics. This is because its entire genome has been completely sequenced (Kaneko *et al*, 1995, 1996) and data on all 3168 predicted genes is freely available (www.kazusa.or.jp/cyano/cyano.html) (Nakamura *et al.*, 1998). Secondly, with only 3168 genes *Synechocystis* has a small complement of genes/proteins. Consequently, DNA microarrays containing 95 % of these genes are readily accessible for gene expression studies and proteomic investigations are less complex in comparison to those conducted in eukaryotic photosynthetic organisms. Current DNA micorrary investigations include acclimation to high light (Hihara *et al.*, 2001), the response to salt and osmotic stress (Kanesaki *et al.*, 2002), the response to cold stress (Suzuki *et al.*, 2001) and phosphate sensing (Susuki *et al.*, 2004). Using proteomic based approaches proteome maps have been generated for several sub-cellular compartments including the soluble (Sazuka *et al.*, 1997, 1999), thylakoid (Wang *et al.*, 2000, Herranen *et al.*, 2004), plasma membrane (Huang *et al.*, 2002) and periplasmisc space (Fulda *et al.*, 2000) and investigations analysing the changes in
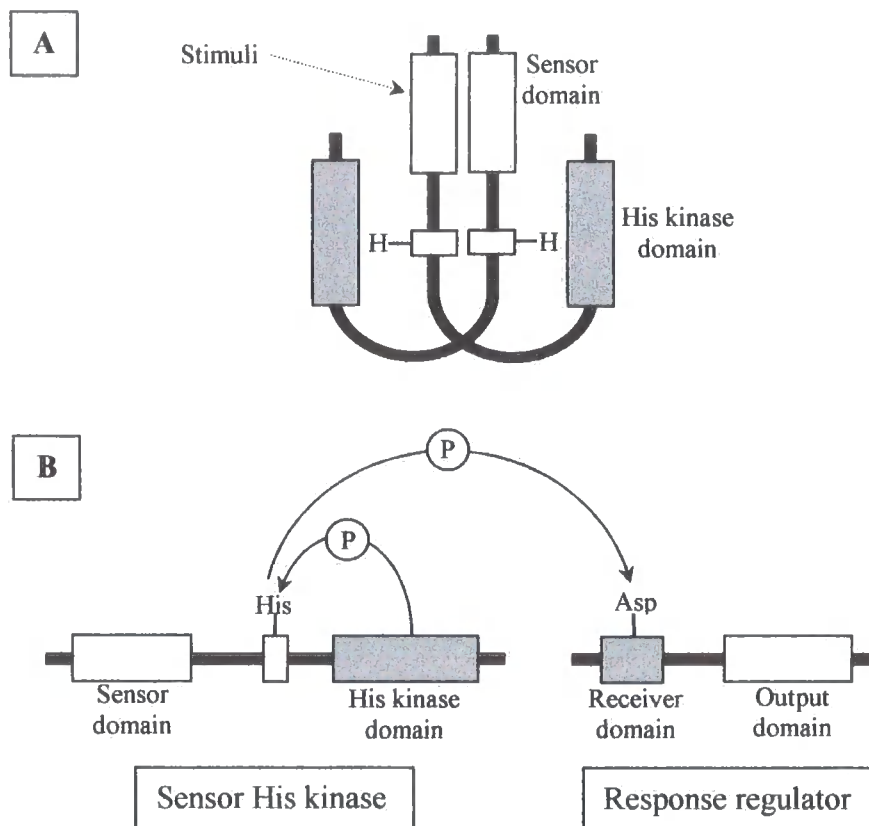
Figure 1.5. Schematic model of a generic two-component signal transduction mechanism.

Most histidine kinases (Hiks) function as homodimers (**A**). Upon receiving an appropriate stimulus the His kinase sensor undergoes a conformational change which brings the histidine phosphorylation sites in close proximity to the kinase domain of one of the two subunits. The His kinase domain autophosphorylates the substrate histidine in an ATP dependant manner. The phosphoryl group on the histidine is subsequently transferred to an aspartate residue in the receiver domain of the response regulator (Rre), resulting in a conformational change and exposure of the output domain activity (**B**). Most output domains are DNA binding transcriptional regulators, others control the activity of other enzymes directly. Figure adapted from Satio (2001).

protein steady state levels in response to high light (Choi *et al.*, 2000) and salt stress (Fulda *et al.*, 2000) have been performed.

In this thesis I have chosen to investigate the heat shock response and its regulation in cyanobacteria and the strategies employed in acclimation of the photosynthetic machinery to high temperature. The current knowledge in these fields will now be discussed.

1.2   The heat shock response

1.2.1   Introduction

Cells have evolved a number of mechanisms to help them survive in harmful environments. Often a disruption in homeostasis activates the expression of several genes which function to protect the cell from the effects of the stress. One such mechanism shared by all cells is the heat-shock response, which is evoked by the sudden exposure of cells to unusually high temperatures and causes proteins to denature and irreversibly aggregate. The cell responds chiefly by reducing the synthesis of normal cellular proteins and at the same time transiently enhancing the expression of a group of proteins called heat-shock proteins (Hsps). These induced Hsps, predominantly molecular chaperones and ATP-dependant proteases, function to control and stabilise the level of denatured protein and restore homeostasis by refolding or degrading the non-native proteins respectively (Bukau and Horwich, 1998). This response to elevated temperature is universal among all living organisms

and the induced Hsps are some of the most conserved proteins in nature (Neidhardt *et al.* 1984), suggesting that they play important roles in fundamental cellular processes.

1.2.2   Heat shock proteins

Hsps were first discovered in 1962 in *Drosophila melanogaster* larvae that were exposed to temperatures above that optimal for normal growth and development, and were described as a set of proteins whose expression is selectively induced by heat shock (Ritossa, 1962; Tissieres *et al.*, 1974). Since then, Hsps have been identified in every species in which they have been sought and in a variety of subcellular compartments, including the cytosol, mitochondria, endoplasmic reticulum, chloroplast and nucleus. The genes encoding Hsps (*hsps*) are highly conserved and many have been categorised into families based on their sequence homology, molecular weight and function (Georgopoulos and Welch, 1993; Hendrick and Hartl, 1993) The principal Hsps, range in molecular mass from ~10 to 110 kDa and have been classified into several families, these being Hsp10, small Hsps (sHsps) (15-42 kDa), Hsp60, Hsp70, Hsp90 and Hsp100 (the number corresponding to their respective approximate molecular weight i.e. Hsp10 ~ 10 kDa).

Over the last 4 decades Hsps have been extensively studied, especially with regard to their function and regulation (Welch, 1992; Hartl, 1996; Yura and Nakahigashi, 1999; Pirkkala *et al.*, 2001). Early indication of Hsp function came about from the observations that, like cells exposed to heat-shock, cells manipulated to accumulate levels of non-native proteins also demonstrated increased expression of the Hsps (Georgopoulos & Welch 1993). Consequently, this led to the proposed hypothesis that

any stress, resulting in the accumulation of abnormally folded proteins with in the cell, leads to an increased expression of Hsps which function to deal with the non-native proteins.

Stress-inducible *hsps* genes respond to a variety of stresses, if sufficiently intense, including extremes of temperature, cellular energy depletion, extremes of ion concentration, other osmolytes, gases and various toxic substances. Such stresses all result in proteins having non-native conformations (Somero, 1995). Despite their inducible gene expression, most Hsps are expressed at significant levels in cells grown under normal conditions and are essential for growth at all physiologically relevant temperatures (Georgopoulos & Welch 1993). These observations, supported by the discovery that not all Hsp homologues are stress-inducible, suggested that Hsps have an important role in normal cell growth and development. In various experiments, under normal growth conditions Hsps were demonstrated to function as molecular chaperones, interacting with and governing the correct folding and assembly of newly synthesised proteins. Such a function is paramount because, growing polypeptide chains emerging from the ribosomes and even newly synthesised proteins not yet correctly folded and translocated to their organellar localisation expose hydrophobic surfaces, susceptible to premature interactions with other polypeptides. Such interactions lead to protein misfolding and aggregation of non-native species (Jaenicke, 1991). Molecular chaperones bind and sequester non-native proteins and their reactive hydrophobic surfaces of polypeptides. By doing so, they minimise inappropriate associations with other reactive surfaces, thus preventing aggregation and favouring correct folding. Because under stress conditions, such as heat shock, proteins denature and aggregate through hydrophobic interactions, it is

understandable that there is an extra requirement for molecular chaperone activity. Indicating why the expression of such proteins is elevated in cells exposed to high temperatures (Ellis and van der Vies, 1991; Jaenicke 1991).

Molecular chaperones not only function to sequester non-native proteins and minimise their aggregation, they also target non-native or aggregated proteins for degradation and removal through proteolytic pathways, maintain non-native proteins in a folding-competent state, help re-fold and assemble abnormally folded proteins and they are involved in protein organellar localisation, import and export (secretion). Chaperone binding and release of non-native proteins is usually dependent upon the association with or the hydrolysis of nucleotide triphosphates, where some chaperones as oligomers of multiple chaperones and in association with co-chaperones, without covalently modifying their polypeptide substrates and without being part of their final structure (Ellis and van der Vies, 1991).

The function of the major Hsps groups will now be discussed, with the main focus being in prokaryotes.

1.2.2.1   Hsp60 Family

The Hsp60 family of proteins, approximately 60 kDa in size, exist in the prokaryotic cytosol and a variety of eukaryotic cellular locations, including the cytosol (Gupta, 1990), chloroplast and mitochondria (Hemmingsen *et al.*, 1988). Due to their chaperone-like function they are also known as chaperone 60s (Cpn60s) and both stress-inducible and non-inducible (constitutively expressed) members have been

found. The Hsp60 homologues in the prokaryotic cytosol, and the eukaryotic chloroplast and mitochondria have high sequence homology (Hemmingsen *et al.*, 1988; Reading *et al.*, 1989), which is substantial similarity since these genes are nuclear encoded in their respective organisms. However, very little homology is observed between prokaryotic and eukaryotic cytosolic Hsp60 proteins. The prokaryotic Hsp60 homologue, GroEL, is one of the most extensively studied chaperonins. It was first discovered in *Escherichia coli* as a host protein required for the assembly and morphogenesis of many bacteriophages, including λ (Georgopoulos *et al.*, 1973), T4 and T5 (Zeilstra-Ryalls *et al.*, 1991). GroEL also functionally operates with a 10 kDa protein, GroES and were both shown to be essential for *E. coli* growth at all temperatures, both physiological and under heat shock (Fayet *et al.*, 1989). In prokaryotes, the *groEL* and *groES* genes are located within a single bicistronic operon, *groE*, so called because mutation blocks bacteriophage λ growth (gro) and the first λ compensatory mutation was in the *λE* gene. The *groE* L and S suffixes denote small and large gene products (Friedman *et al.*, 1984). The mitochondrial Hsp60 was first identified in *Tetrahymena* (McMullin & Hallberg, 1987) and was subsequently shown to be involved in protein import (Hartl and Neupert, 1990) and oligomeric assembly (Cheng *et al.*, 1989). The chloroplast Hsp60 chaperone is required for the assembly of ribulose-bisphosphate carboxylase/oxygenase (rubisco), justly named the rubisco binding-protein (Gatenby *et al.*, 1985; Cannon *et al.*, 1986; Ellis and van der Vies, 1991). The discovery of which helped develop the concept of molecular chaperones. Both mitochondrial and chloroplast Hsps also functionally operate with a 10 kDa co-chaparonin like GroES.

Proteins encoded by the *groEL* and *groES* genes are found in the cell as oligomers. GroEL assembles into a 14-subunit oligomer to form two stacked rings of 7 subunits with a central cavity (Hendrix 1979; Langer *et al.* 1992b), the native form of GroES is a single ring of 7 subunits (Hemmingsen *et al.*, 1988). These two multi oligomeric complexes come together to form a functionally active chaperone machine, where one GroES heptamer binds to one end of the GroEL cylinder, forming a characteristic bullet shape (Langer *et al.* 1992b). This chaperone complex has been demonstrated to assist the complete folding of partially folded polypeptides after their release from the ribosome (Ostermann *et al.*, 1989) and has a low substrate specificity (Ellis, 2000), binding to many unfolded proteins. GroEL has been shown to be able to make stable complexes with over 50 % of all *E. coli* proteins (Viitanen *et al*, 1992) and where 10 – 15 % of all newly synthesised *E. coli* proteins are present in a complex with the GroEL/GroES machine under physiological growth and 30 % under heat shock conditions (Ewalt *et al.*, 1997).

The GroEL cavity acts as a cage in which to sequester non-native proteins, preventing inadvertent inter-polypeptide aggregation and providing an ideal environment in which a single protein can fold (Ellis, 1996). After binding of the unfolded polypeptide to GroEL the binding of GroES and ATP releases the polypeptide inside the cage and GroES remains bound to prevent the protein from re-emerging (Ostermann *et al.*, 1989; Ellis, 2001). Subsequent ATP hydrolysis allows the re-folded protein to be released, however if hydrophobic domains are still exposed the protein will be re-internalised by GroEL (Frydman, 2001).

1.2.2.2   Hsp70 family

The Hsp70 family of proteins have been found to exist in many organisms, in prokaryotic and eukaryotic cells (Craig and Gross *et al.*, 1991) where both heat inducible and constitutively expressed homologues have been identified. They have also been shown to take part in the transport of proteins in to the ER (Sanders *et al.*, 1992), mitochondria (Hartl and Neupert, 1990; Kang *et al.*, 1990) and chloroplast (Yalovsky *et al.*, 1992). The prokaryotic cytosolic Hsp70 homologue, DnaK, thus named as is required for DNA replication (Friedman *et al.*, 1984) is present at high levels under normal growth and is inducible upon heat treatment. Research has shown that DnaK and its corresponding homologues are able to interact with a variety of unfolded polypeptides and that they have no strict specificity (Hartl *et al.*, 1992). They associate with polypeptide chains as they emerge from the ribosome (Nelson *et al.*, 1992) and thus facilitate the exit from the ribosome and prevent premature aggregation. The polypeptide release mechanism from DnaK is ATP dependant and functions through the interaction with two co-chaperones, DnaJ and GrpE. Where, DnaJ and GrpE increase the ATPase activity of DnaK (Liberek, 1991a, 1991b) and also GrpE has been shown to act as a DnaK substrate and compete for binding (Langer *et al*, 1992a).

1.2.2.3   Hsp90 Family

Hsp90 proteins exist primarily in the cytosol, but homologues have also been discovered in the ER (Buchner, 1999). The bacterial Hsp90, namely HtpG, unlike GroEL is dispensable for growth under both normal and heat shock conditions

(Bardwell and Craig et al., 1988; Versteeg et al., 1999). This is in contrast to the yeast Hsp90 homologue which is essential regardless of the growth temperature (Borkovich et al., 1989). Hsp90 is able to recognise non-native proteins and prevent irreversible aggregation either during refolding (Wiech et al., 1992) or thermal unfolding (Jakob et al., 1995), although, a refolding capacity as seen with GroEL is not observed (Yonehara et al., 1996). Instead Hsp90 maintains non-native proteins in a folding competent state in preparation for refolding by other chaperones such as by the GroEL/GroES and the DnaK/DnaJ/GrpE chaperone machines.

1.2.2.4   Hsp100 family

The Hsp100 proteins, known as Clp proteins, constitute a relatively new family of molecular chaperones and like Hsp60 and Hsp70 chaperones, both constitutively expressed and heat inducible homologues have been identified. Various types of Clp protein exists and have been divided into several types based on their structure and sequence (Schirmer et al., 1996). A member of the Clp/Hsp100 protein family is ClpB and has two ATP-binding domains. Two distinct ClpB proteins are present in both eukaryotes and prokaryotes. Separate genes encode a cytosolic and a mitochondrial (Leonhardt et al., 1993) protein in eukaryotic organisms, whereas in prokaryotes they originate from a single gene with two translation initiation sites in the transcript (Eriksson and Clarke, 1996). The mitochondrial ClpB protein functions to prevent protein denaturisation at high temperatures (Schmitt et al., 1996) where as the cytosolic proteins function as common molecular chaperones with the ability to dismantle multi protein aggregates that accumulate at high temperature (Parsell et al.,

1994). Cytosolic ClpB can also interact with DnaK to assist re-solubilisation of aggregated proteins and promote their refolding (Mogk *et al.*, 1999).

1.2.2.5 Small Hsp Family

Small Hsps (sHsps) are a group of proteins having a molecular mass ranging from 15-42 kDa (Roy *et al.*, 1999, van den Ussel) and have been detected in virtually all organisms. The sequence of these proteins is much less conserved between species than Hsps of higher molecular mass (i.e. GroEL, DnaK). However, they do all have a C-terminal region which is similar to that of the eye lens α-crystallins. sHsps in their native state form oligomers of 9-32 subunits or display a variety of variable and dynamic quaternary structures (Kim *et al.*, 1998; Haley *et al.*, 2000). Like Hsp90, sHsps can bind non-native proteins and prevent their aggregation, holding them in a folding competent state for re-folding by the ATPase GroEL and DnaK chaperone systems (Veinger *et al.*, 1998; Lee and Vierling; 2000).

1.2.3 Regulation of the heat shock response

Although the induction of the *hsp* genes is a universal response to elevated temperature, the regulatory mechanisms controlling Hsp synthesis vary greatly among organisms. Regulation of the heat shock genes in eukaryotes generally occurs via heat shock transcription factors (HSF) which bind to the heat shock promoters to regulate transcription (Morimoto, 1998). In bacteria, regulation occurs by two different mechanisms. Firstly, alternative sigma factors positively control the expression of the heat shock genes by the targeting of RNA polymerase to specific heat shock

promoters. In *E.coli* three different classes of heat shock proteins have been shown to be regulated by different sigma factors, namely σ^{32} (also known as RpoH) (Yura and Nakahigashi, 1999), σ^E (Model *et al.*, 1997) and σ^{54} (Missiakas and Raina, 1998) and in *B. subtilis* an alternative sigma factor σ^B controls *hsp* gene expression (Hecker and Voelker, 1998). The currently understood mechanism for the control of *hsp* gene expression via σ^{32} is as follows. Under normal growth the DnaK chaperone sequesters the σ^{32} factor and maintains it in a destabilised state, increasing its affinity for degradation via the FtsH protease (Herman *et al.*, 1995; Tomoyasu *et al.*, 1995). An increase in temperature leads to a rapid escalation in the level of active σ^{32} due to an elevation in the synthesis of this protein and also stability via the release from DnaK, as this chaperone now focuses on binding misfolded proteins (Tatsuta *et al.*, 1998; Tomoyasu *et al.*, 1998). Active σ^{32} is now available for the activation of *hsp* gene transcription.

The alternative mechanism for the regulation of *hsp* expression in prokaryotes is through transcriptional repressors, which function to limit transcription of the heat shock genes under physiological conditions (Narberhaus, 1999). There are a multiplicity of repressor mechanisms and repressor-controlled regulons; however the most common type of negative regulation involves the HrcA repressor protein. This mechanism has been shown to exist in both *B. subtilis* (Mogk *et al.*, 1997) and *Steptomyces* sp. (Servant and Mazodier, 2001) where the active form of the HrcA repressor proteins binds to a well conserved 9-bp inverted repeat operator named CIRCE (controlling inverted repeat of chaperone expression) to prevent transcription of the *hsp* genes via RNA polymerase. In *B. subtilis* this mechanism controls the expression of *dnaK* and *groE* operons and the GroEL/GroES chaperone (GroE)

regulates the activity of HrcA in a feedback mechanism (Mogk *et al.*, 1997). Under normal growth GroE maintains HrcA in its active form allowing it to bind to the CIRCE element and repress *hsp* gene expression. Under heat shock conditions, GroE interacts with denatured proteins removing its association with HrcA. This inactivates HrcA and prevents it from binding to the CIRCE element leading to the derepression of the two heat shock operons (Zuber and Schumann, 1994; Mogk *et al.*, 1997). Other negative regulators of heat shock gene expression include CtsR in *B. subtilis* which controls the expression of the *clpC* and *clpP* genes (Derre *et al.*, 1999), HspR in *Streptomyces* sp. which controls the expression of the *dnaK* operon and the *clpB* gene (Servant and Mazodier, 2001), and RheA also in *Streptomyces* sp. which regulates the expression of the *hsp18* gene (Servant and Mazodier, 2001).

1.2.4   Heat shock proteins and their regulation in cyanobacteria

The current understating of the heat shock response in cyanobacteria is not as advanced as in other organisms. Studies in cyanobacteria have demonstrated a heat shock response similar to that seen in other bacteria (Borbély *et al.*, 1985; Bhagwat and Apte, 1989, Lehel *et al.*, 1992). GroEL/GroES (Webb *et al.*, 1990), DnaK (Chitnis and Nelson, 1991), HtpG (Tanaka and Nakamoto, 1999), ClpB (Eriksson and Clarke, 1996) and small heat shock proteins (Torok *et al.*, 2001; Nakamoto *et al.*, 2000) have all been shown to be heat inducible in cyanobacteria. In *Synechocystis* sp. PCC 6803, two *groEL*-like genes have been identified, denoted *groEL* and *cpn60* (Chitnis and Nelson, 1991; Lehel *et al.*, 1993b), which differ in their relative heat induciblity (Kovács *et al.*, 2001). Disruption of the *clpB*, *htpG* and sHsp *hsp16.6* gene in cyanobacteria have generated temperature sensitive mutants with much more

sticking thermo-sensitive phenotypes than those observed in *E.coli* (Eriksson and Clarke, 1996; Lee *et al.*, 1998b; Tanaka and Nakamoto, 1999). This suggests the particular importance of these chaperones for thermotolerabce in photosynthetic prokaryotes.

The regulation of cyanobacterial heat shock gene expression remains poorly understood (Nakamoto *et al.*, 2001). An *E. coli*-like σ^{32} heat shock promoter has been identified upstream of the transcriptional start site of both the *groESL* operon in *Synechococcus* sp. PCC 7942 (Webb *et al.*, 1990) and the *cpn60* (*groEL-2*) gene in *Synechocystis* sp. PCC 6803 (Lehel *et al.*, 1993b). However, there is no evidence for the presence of σ^{32} in cyanobacteria, although analysis of sigma factor gene expression under stress conditions has shown that the σ^H gene is noticeably induced in heat shocked *Synechocystis* cells (Huckauf *et al* 2000). Perhaps, other σ factors are involved in the regulation of *hsp* gene transcription in cyanobacteria. The nine-nucleotide inverted repeat CIRCE element has also been identified upstream of *groESL* and *dnaK* genes in cyanobacteria (Lehel *et al.*, 1993b; Tanaka *et al.*, 1997) and a HrcA homolog has been identified in the genome of *Synechocystis* sp. PCC 6803 (Kaneko *et al.*, 1996). This suggests that the expression of these two genes is under the regulation of HrcA and is supported by the observation that deletion of the *hrcA* gene in *Synechocystis* revealed substantial increase in the expression of *groEL* (Nakamoto *et al.*, 2002).

1.2.5   Photosynthetic acclimation to high temperature

Exposure of plants to temperatures above the normal physiological range can cause irreversible inactivation of the photosynthetic apparatus and such inactivation occurs at relatively low elevated temperatures unlike those characteristic of heat shock. However, some photosynthetic organisms have demonstrated the ability to modify their photosynthetic machinery in response to elevated ambient temperatures. By doing so, organisms enhance the thermal-stability of their photosynthetic apparatus (Berry and Björkman 1980) and thus adapt and become acclimatised to high temperatures. This acclimation phenomenon has already been seen in several higher plants (Armond *et al.*, 1978; Pearcy, 1978; Raison *et al.*, 1982; Tanaka *et al.*, 1997) and cyanobacteria (Fork *et al.*, 1987, Lehel; *et al.*, 1993a; Nishiyama *et al.*, 1993) and is referred to as acquired thermotolerance, where the exposure of cells to a mild elevated temperature increases the tolerance at subsequent higher temperatures. Consequently, it is probable that the thermal stability of photosynthetic activity determines cellular thermotolerance in plants.

Of the several photosynthetic components, the Photosystem II (PSII) complex is the most susceptible to high temperature stress (Berry and Bjorkman, 1980; Thompson *et al.*, 1989; Mamedov *et al.*, 1993) and of the several reactions of PSII, the oxygen evolving process is particularly sensitive to heat (Yamashita and Butler, 1968; Santarius, 1975; Thompson *et al.*, 1989; Mamedov *et al.*, 1993). Oxygen evolution, via the oxidation of H_2O, is catalysed by a cluster of four manganese ions attached to the luminal side of the PSII complex. Heat causes dissociation of two of these four manganese atoms from the PSII complex and results in complete inactivation of

oxygen evolution (Nash *et al.*, 1985). Such observations spawned the realisation that adaptation of the photosynthetic apparatus to high temperature is related to the protection of the PSII oxygen-evolving complex.

Several polypeptides have been discovered to be associated with the oxygen-evolving machinery, which vary among organisms that perform oxygenic photosynthesis. In higher plants, proteins of 23 kDa, 17 kDa and a 33 kDa manganese stabilising polypeptide (MSP) associate with the oxygen-evolving complex (Seidler, 1996) whereas in cyanobacteria a 12 kDa protein named PsbU (Nishiyama *et al.*, 1997; Shen *et al.*, 1997), a 15 kDa low redox potential *c-type* monoheme cytochrome, named cytochrome c_{550} (Cyt c_{550}) (Nishiyama *et al.*, 1994; Shen *et al.*, 1995a, 1995b) and the MSP (Shen *et al.*, 1995a; Morgan *et al.*, 1998; Al-Khaldi *et al.*, 2000) are associated. Additionally, red algae contain a fourth protein of 20 kDa together with the PsbU, Cyt c_{550} and MSP proteins (Enami *et al.*, 1998).

Targeted mutagenesis of the genes which encode the MSP, Cyt c_{550} and PsbU proteins in *Synechocystis*, namely *psbO*, *psbV*, *psbU*, respectively, revealed that they were not essential for growth and oxygen evolution under normal conditions (Kimura *et al.*, 2002). However, they do function to optimise the oxygen evolving activity under physiological temperature. It has been reported that the MSP and Cyt c_{550} proteins maintain the affinity of the manganese cluster for calcium and chloride ions, required for maximum oxygen evolving activity (Morgan *et al.*, 1998; Shen *et al.*, 1998), while PsbU functions to maintain the normal S-state transitions of the oxygen evolving machinery (Shen *et al.*, 1998). Therefore, these intrinsic proteins function to maintain the activity and stability of the oxygen-evolving complex.

Although the MSP, Cyt c_{550} and PsbU proteins are not essential for growth under physiological conditions they are required for the maintenance of thermal stability of the oxygen evolving machinery. In the cyanobacterium, *Synechococcus* sp. PCC 7002, biochemical studies revealed that Cyt c_{550} and PsbU stabilised the oxygen evolving machinery against thermal inactivation (Nishiyama *et al.*, 1994, 1997). Subsequent targeted mutagenesis of the *psbU* gene in this organism revealed PsbU is required for the enhancement of oxygen evolving thermal stability and for the development of acquired thermoltolerance (Nishiyama *et al.*, 1999). Similar investigations in *Synechocystis* revealed the same to be true for the MSP, Cyt c_{550} and PsbU proteins in this organism (Kimura *et al.*, 2002).

In cyanobacteria, the MSP and Cyt c_{550} proteins are thought to be closely associated with the manganese cluster and function to prevent the dissociation of manganese ions caused by high temperatures (Shen *et al.*, 1998). This was demonstrated by deletion of the genes encoding these two proteins which resulted in rapid heat inactivation of oxygen evolving activity, complete loss of the ability to enhance thermal stability and thus develop thermotolerance (Kimura *et al.*, 2002). Furthermore, analysis of the nucleotide sequence of both these genes revealed the presence of a transit peptide, indicating both proteins to be located on the luminal side of the thylakoid membrane. Such an observation was consistent with the prediction that these proteins would protect the oxygen evolving machinery, also located on the lumen side of the thylakoid membrane. Deletion of the *psbU* gene, on the other hand, only resulted in partial loss of ability to enhance thermal stability and *ΔpsbU* mutant cells displayed a reduced level of thermotolerance, not a complete loss (Nishiyama *et al.*, 1999). Consequently, it was predicted that this protein is not directly associated with the

manganese cluster and performs a more subtle function in thermal stabilisation. This was supported by the observation that PsbU requires both the presence of MSP and Cyt c_{550} to bind to PSII (Shen *et al.*, 1995a). These results demonstrate that the enhancement of thermal stability of the oxygen-evolving machinery provided by the MSP, Cyt c_{550} and PsbU proteins is essential for the development of acquired thermotolerance. A schematic diagram demonstrating the association of these proteins to the manganese cluster of PSII is shown in Figure 1.6).

In this thesis proteomics has been implemented as the primary research technique, therefore its origins and methodology will now be discussed in detail.

1.3   Post-genomic research

1.3.1   Introduction

The first genome sequencing project was completed for a free-living organism in 1995 (Fleischmann *et al.*, 1995) and since then the number of complete genome sequences has been increasing at an ever accelerating pace. As of September 2004 there have been 215 published complete genomes, with a further 524 prokaryotic and 441 eukaryotic projects currently in progress (http://www.genomesonline.org/) (Kyrpides, 1999). Such organisms include *Bacillus subtilis* (Kunst *et al.*, 1997) *Arabidopsis thaliana* (The Arabidopsis Initiative, 2000), *rattus norvegicus* (Laboratory Rat) (Gibbs *et al.*, 2004) and *homo sapien* (Lander *et al*, 2001) which was finished earlier this year. Although sequenced genomes provide the sequence of every
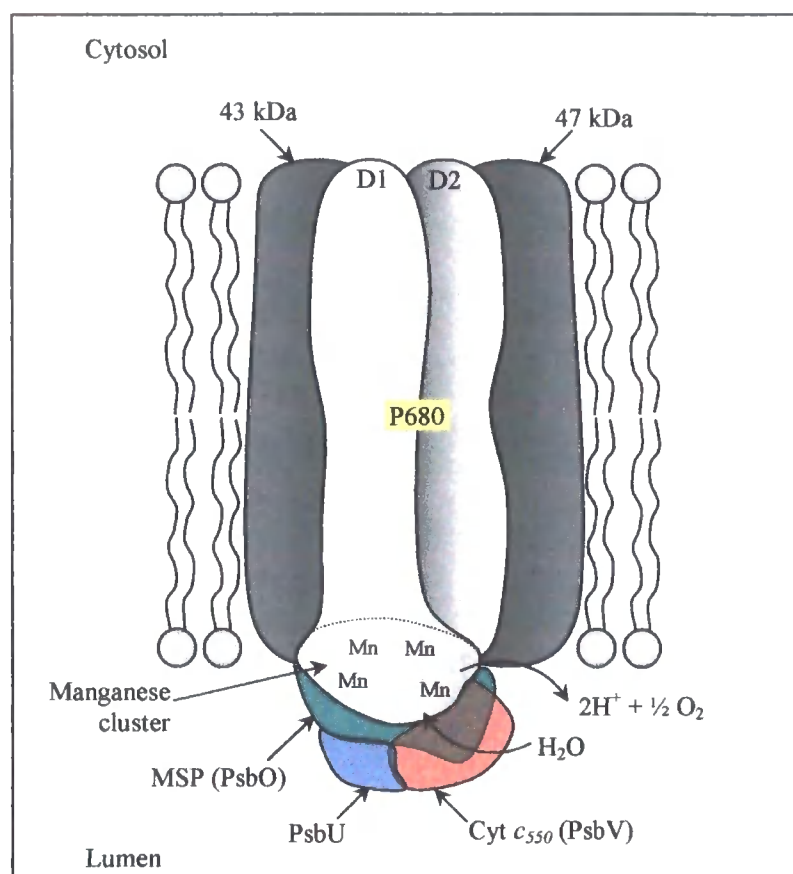
Figure 1.6. Schematic model of the photosystem II core and oxygen evolving unit in cyanobacteria.

The 43 and 47 kDa transmembrane proteins contain antenna chlorophylls that transfer energy to P680. The D1 and D2 transmembrane proteins form the dimeric reaction centre. P680 is the reaction centre and consists of a pair of chlorophyll molecules. The manganese cluster contains for manganese ions and is the site of oxidation of H_2O to O_2. The MSP, PsbU and Cyt c_{550} proteins are associated with the manganese cluster.

gene and potentially every protein encoded by a particular species, on their own they reveal little about the biology of an organism (Dove, 1999; Pennington & Dunn, 2001); however they have and will continue to be used as a platform for post-genomic research.

The aim of post-genomic research is to elucidate gene expression and function, and by doing so describe the state of the biological system. This research encompasses a wide variety of complementary experimental approaches which exploit the availability of sequence information. Such investigations quantitatively measure the system components downstream of the genomic information, i.e mRNA and proteins. Analysis of mRNA expression, termed transcriptomics, has evolved from the use of Northern blotting and conventional PCR techniques. With the development of techniques such as differential display-PCR (DD-PCR) (Liang and Pardee 1992), cDNA microarray and DNA chip technology (Lashkari et al., 1997; Shalon et al., 1996) and serial analysis of gene expression (SAGE) (Velculescu et al., 1995 and 1997) it is possible to conduct quantitative analysis of mRNA expression on a genome wide scale. The application of cDNA microarrays and DNA chip technology to trascriptomics for high throughput analysis of mRNA expression has increased the ease and scale of analysis at a high level of sensitivity and allowed the majority of the experimentation to be automated. This technology is well established in post-genomic research and has been instrumental in investigating gene function (Hughes et al., 2000; Young, 2000). However, there are disadvantages to analysing mRNA as an indication of cellular function which promote the need for investigation at the protein level. Firstly, proteins are the biological molecules which carry out cellular function and mRNA abundance does not always correlate well with protein abundance

(Haynes *et al.*, 1998, Gygi *et al.*, 1999b; Pennington & Dunn 2001). The reasons being, transcription and translation are two independently regulated systems and the longevity of both mRNA and protein species can also be independently regulated to alter their abundance. Secondly, the biological activity of mature proteins is regulated beyond their mRNA or protein expression, such as the extent of post-translational modification (PTM), of which there are over 400 different types, or the association with other molecules, such as DNA, RNA, proteins and organic and inorganic co-factors (Haynes *et al.*, 1998; Pennington & Dunn 2001). These modifications are dynamic and reversible and affect both the activity and subcellular localisation of the proteins and thus the activity of the cell. Furthermore, a single gene can generate several different protein products with different PTM's. Analysis of gene sequence and mRNA abundance does not reveal the types and locations of such modifications and how they affect the subcellular distribution of the protein. Therefore, examination of the proteins will provide the most accurate description of the activity and function of the organism or cell/tissue type. Such investigations have given birth to the emerging scientific filed of proteomics which intend to bridge the gap between genome sequence and cellular function.

1.3.2 Proteomics

The term proteomics, coined approximately 8 years ago by Wilkins *et al* (1996), was originally defined as the characterisation of the protein complement expressed by the genome at a given time, the proteome. The emergence of proteomics is attributed to whole genome sequencing projects; however its success has been dependant on the development of large-scale analytical tools such as two-dimensional gel

electrophoresis and Isotope coded affinity tags (ICAT) for quantification of protein expression, mass spectrometry for protein characterisation and also the integration of informatics for data analysis. Several large scale proteome mapping projects have already been performed for a variety of organisms and cell types, from simple bacteria such as *Escherichia coli* (VanBogelen, 1997) to single celled eukaryotes like *Saccharomyces cerevisiae* (Hodges, 1998) to tissues as complex as the human brain (Pennington *et al.*, 2004). Now regarded as one of the fastest, most sensitive techniques for studying complex mixtures of proteins, proteomics has evolved with the realisation that such investigations are more complex than originally defined and possess greater challenges than sequencing genomes (Dove, 1999, Tyers & Mann, 2003). Not only aimed at identifying all expressed proteins, proteomics aims to characterise all possible protein isoforms and post-translational modifications, the interactions of proteins, protein structure and protein organisation within complexes (Tyers & Mann, 2003). Furthermore, unlike the genome, the proteome is representative of the state of the biological system, such as during cell growth, in response to stress and disease, and during stages in cell cycle or differentiation. Thus having an almost limitless diversity with tissue, developmental, temporal and disease/stress specificity. Although proteomic investigations are by nature extremely complex and a comprehensive project does seem a daunting exercise, proteomics presents a high throughput approach for studying the function of expressed proteins on a global scale, making it easier to discover the many complex interactions between mature gene products (Haynes *et al.*, 1998). It is the hope that the combination of proteomics with other post-genomic approaches and the application of informatics for deconvolutiong complex and interrelated data will contribute to obtaining a full understanding of cellular function (Tyers & Mann, 2003).

1.3.3   Two-dimensional polyacrylamide gel electrophoresis

Fundamental to proteomic methodology is the separation of complex protein mixtures containing up to several thousand individual polypeptides. Although numerous techniques for protein separation exist in proteomic methodology, two-dimensional polyacrylamide gel electrophoresis (2-DE) is the most commonly used. The reasons being, 2-DE has unrivalled simultaneous separation of several thousand individual proteins and a high level of sensitivity, where the resolution of over 10,000 individual protein spots in one 2D gel has been reported (Klose, 1999). Also, 2-D gel separations can be analysed by computer algorithms for the quantification of protein abundance and detection of differentially expressed proteins. Finally, there are well established, high sensitive technologies for the identification of 2-DE separated protein spots such as Edman sequencing and mass spectrometry based techniques (see section 1.3.8). Although, 2-DE does provide the most powerful platform for the separation, quantification and analysis of protein expression it is not without its drawbacks. Firstly, the system excludes very small, very large, low abundant and very hydrophobic proteins; although recent developments have improved the sensitivity of 2-D gels (see section 1.3.6) and the resolution of hydrophobic proteins (Molloy *et al.*, 1998; Santoni *et al.*, 1999, 2000). Secondly, it is difficult to resolve the entire proteome of a cell/tissue type as two or more proteins may resolve at the same location. Thirdly, it may not be possible to characterise all detectable protein spots on a 2-D gel due to their low abundance or lack of MS detectable peptides (see section 1.3.8.2).

2-DE, originally developed by O'Farrell (O'Farrell, 1975), combines the techniques of isoelectric focusing (IEF) and sodium dodecyl sulphate polyacrylamide gel electrophoresis (SDS-PAGE). This methodology separates proteins by two independent physical properties, charge (isoelectric point, pI) and size (relative molecular mass, M_r) in two discrete steps and has been the basis for the majority of developments in 2-DE over the past 30 years. The resolved proteins are subsequently visualised at high sensitivity where a plethora of different techniques are applicable (see section 1.3.6).

1.3.4 First Dimension Isoelectric focusing (IEF)

Proteins are amphoteric macromolecules i.e. they possess positive, negative and neutral net charges. This physical property is reflected by the side chains of the amino acid residues (Table 1.1). Certain amino acids like Arginine, Lysine and Histidine residues are positively charged in free solution where as Glutamic acid and Aspartic acid residues possess a negative charge. The net charge of a particular protein is the sum of all positive and negative charges and depending on the pH of their environment; proteins are either positively or negatively charged. The isoelectric point (pI) of a protein is determined by the pH at which the net charge on their amino acid side chains is zero and proteins are positively charged at pH below their pI and negatively charged at pH above their pI. When a mixture of proteins with different pI's are applied to a pH gradient they acquire a positive, negative or neutral charge.

Under electric current proteins will migrate to the pH where their net charge is zero. A protein with a positive net charge will migrate towards the cathode and a negatively

Amino acid	Code	Side chain	Hydrophilic /phobic (+/-)	Ionisable (pK)	Residue mass	Immonium ion mass
Alanine	Ala (A)	Aliphatic	+		71	44
Asparagine	Asn (N)	Amide	+		114	87
Aspartic acid	Asp (D)	Acidic	+	+ (4.4)	115	88
Arginine	Arg (R)	Basic	+	+ (12.0)	156	129
Cysteine	Cys (C)	Sulphur containing	-	+ (8.5)	103	76
Glutamine	Gln (Q)	Amide	+		128	101
Glutamic acid	Glu (E)	Acidic	+	+ (4.4)	129	102
Glycine	Gly (G)	Aliphatic	+		57	30
Histidine	His (H)	Basic	+	+ (6.5)	137	110
Isoleucine	Ile (I)	Aliphatic	-		131	86
Leucine	Leu (L)	Aliphatic	-		131	86
Lysine	Lys (K)	Basic	+	+ (10.0)	128	101
Methionine	Met (M)	Sulphur containing	-		131	104
Phenylalanine	Phe (F)	Aromatic	-		147	120
Proline	Pro (P)	Aliphatic*	+		97	70
Serine	Ser (S)	Aliphatic Hydroxyl	+		87	60
Threonine	Thr (T)	Aliphatic Hydroxyl	+		101	74
Tryptophan	Trp (W)	Aromatic	-		186	159
Tyrosine	Tyr (Y)	Aromatic		+ (10.0)	163	136
Valine	Val (V)	Aliphatic	-		99	70
Oxidised Methionine	Mo				147	120
Acrylocysteine	C^a				174	147
Carbamido-methylcysteine	C*				186	159

Table 1.1 Amino acids – their biochemical properties.

Residue and immonium ion masses were obtained from Jardine (1990)

charged protein will migrate towards the anode. This allows a mixture of proteins with very small charge differences to be separated via IEF (Figure 1.7).

O'Farrell's original method for IEF protein separation was performed through polyacrylamide cylinders containing synthetic carrier ampholyte (SCA) generated pH gradients (O'Farrell, 1975). However, there was considerable variability between carrier ampholyte batches, limiting the reproducibility of first dimension separation. Moreover, SCA were not fixed within the IEF gels and consequently, due to the electroendosmotic flow of water which occurs during IEF, SCA migrated towards the cathode. This phenomenon, known as cathodic drift, disrupts the pH gradient resulting in the loss of the basic end of the gradient. This problem was later remedied by O'Farrell, who developed non-equilibrium pH gradient electrophoresis (NEPHGE) specifically for basic proteins (O'Farrell *et al* 1977). However, gel-to-gel reproducibility was again difficult to maintain.

The greatest advancement in 2-DE technology came with the establishment of immobilised pH gradient (IPG) IEF (Bjellqvist *et al.*, 1982). Görg and co-workers later developed the use of IPG IEF specifically for the first dimension separation of 2-DE (Görg *et al.*, 1988, 2000). IPGs are prepared using Immobilines (Amersham Biosciences), weak acid or base acrylamide derivatives possessing either a carboxyl or a tertiary amino group respectively. These IPG gels are fixed to acetate film to facilitate the ease of handling and cut to 0.5 mm wide. Immobilised pH gradients have several advantages over SCA generated pH gradient; i) they are highly reproducible, ii) not subjected to the effects of cathodic drift and iii) allow the separation of proteins over liner and nonlinear (Bjellqvist *et al.*, 1993) and also wide and narrow pH
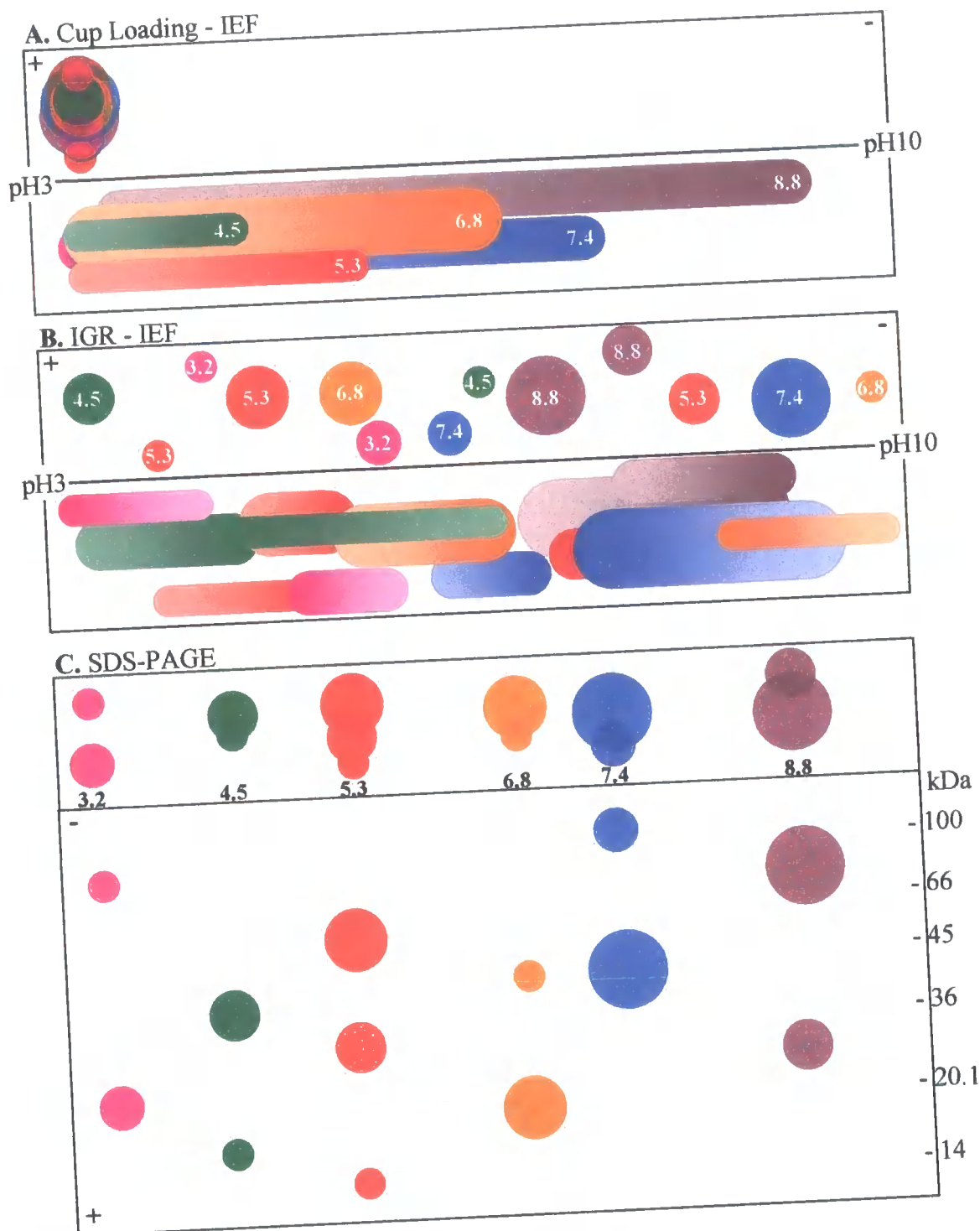
Figure 1.7. Principle of IEF and SDS-PAGE of two-dimensional gel electrophoresis.

Mixtures of proteins can be loaded into pH gradient strips, referred to as IEF or IPG gels, using two different methods, cup loading (A) and IGR (B). When subjected to an electrical current positively charged proteins migrate towards the basic end and of the gradient and vice versa, until they have reached their isoelectric point (p*l*). Focused IEF gels are then equilibrated in a solution containing SDS, following which they are layered onto a polyacrylamide resolving gel for separation of by MW.

gradients (Görg *et al.*, 1999, 2000). The latter is a very important feature of IPGs for several reasons. Firstly, although pH 3-10 is often used for initial analysis of a particular sample, the majority of proteins in many samples focus between pH 4-7, resulting in poor separation of these proteins (Dunn and Görg, 2001). This can be remedied with the use of nonlinear pH 3-10 gradients, where the pH 4-7 region is much broader, allowing increased separation of the acidic proteins while still resolving the more basic species (Bjellqvist *et al.*, 1993). Or also through the use of pH 4-7 IPG gel strips, providing even greater separation (Görg *et al.*, 2000). A variety of narrow pH range IPG strips are available form commercial sources providing strips covering just 1 pH unit. Such strips have been used over the entire pH range to obtain powerful resolution of complex protein mixtures (Wildgruber *et al.*, 2000).

Protein is loaded into IPG gels using one of three available methods, including paper bridge (Sabounchi-Schütt, *et al.*, 2000), in-gel rehydration (IGR) (Rabilloud *et al.*, 1994) and cup loading (Görg *et al.*, 1988, 2000). The latter two methods are the most universally used, where with cup loading protein sample is applied to the IPG gel via a plastic cup at either the anode or cathode (depending on the particular sample) during IEF, but with IGR the sample is rehydrated into the IPG strip prior to IEF (Figure 1.7). Cup loading is more frequently used for low loaded gels where IGR is preferred for resolution of high sample loadings. This is because when cup loading high protein loads, proteins tend to precipitated at the point of application and cause streaking (Rabilloud *et al.*, 1994; Sanchez *et al.*, 1997).

1.3.5   Second dimension SDS-PAGE

Before second dimension separation, IPG gel strips are equilibrated in SDS to ensure proteins will migrate correctly during electrophoresis. This equilibration solution also contains glycerol and urea to prevent electroendosmotic effects which result in reduced protein transfer into the second dimension (Görg *et al.*, 1988). Two separate equilibration solutions are sequentially used, the first contains dithiothreitol (DTT) to ensure proteins remain fully reduced, the second contains iodoacetamide to alkylate any remaining DTT which can otherwise migrate through the second dimension and cause an artefact known as point streaking (Dunn and Görg, 2001). Alternatively, non charged reducing agents such as tributyl phosphine (TBP) can be used instead of DTT which do not migrate during SDS-PAGE (Herbert *et al.*, 1998). For second dimension SDS-PAGE, equilibrated IPF gels are directly loaded onto a polyacrylamide resolving gel. There is no need for a stacking gel, as with one dimension SDS-PAGE, because within the IPG gel proteins are already concentrated (Dunn and Görg, 2001). Protein samples are most universally electrophoresed using the discontinuous buffer system of Laemmli (1970) where under an electric current SDS coated proteins migrate with a uniform charge to mass ratio. Single acrylamide concentrations are most commonly used, or linear/nonlinear polyacrylamide concentration gradients may be employed to increase the distance over which proteins of different size can be effectively resolved.

1.3.6   Protein 'in-gel' detection

After two-dimensional gel electrophoresis, resolved protein spots can be visualised 'in-gel' using a variety of different staining techniques including, Coomassie Brilliant

Blue, Silver, Negative Zinc-Imidazole and Fluorescent staining. Proteins can also be fluorescently labelled or radiolabelled prior to electrophoresis for detection. These different techniques will now be discussed individually, although it should be noted that there are other protein stains used for protein detection not discussed here (for a review see Patton, 2001).

1.3.6.1 Coomassie Brilliant Blue Staining

Coomassie staining is a simple quantitative method for protein detection and is one of the most commonly used methods since its initial application with polyacrylamide gels (Meyer & Lamberts, 1965). It stains almost all polypeptides and is compatible with mass spectrometry techniques. However, its limitation is sensitivity, with a capacity to detect down to only 100 ng/protein spot and a dynamic range of approximately a 20-fold concentration range (Neuhoff *et al.*, 1988). A colloidal version of the Coomassie stain has been developed which boasts background free staining and increased sensitivity of down to 10 ng (Neuhoff *et al.*, 1988). Although this method does introduce complications when attempting to identify proteins via MS techniques as this it can cause methylation of carboxyl side chain groups on glutamic acid residues (Haebel *et al.*, 1998).

1.3.6.2 Silver staining

Silver staining was first introduced for detection of proteins resolved through polyacrylamide gels in 1979 (Switzer *et al.*, 1979). It is an extremely sensitive method for protein staining with an ability to detect below 1 ng, over 100 times more sensitive

than Coomassie, and possesses a dynamic range over a 40-fold concentration range (Switzer *et al.*, 1979). However, the methodology is tedious involving the preparation of solutions which demand quality and numerous separate steps which increase the possibility for contamination. Also, silver staining, unlike Coomassie, is not quantitative and therefore can not be used for determination of protein abundance. Other drawbacks of silver staining include reduced detection of glycoproteins (Jay *at al.*, 1990) and the use of glutaraldehyde and formaldehyde which alkylate α- and ε-amino groups, preventing protein identification by Edman-sequencing or mass spectrometry techniques (Patton, 2001). However, at the cost of reduced sensitivity and increased background, the silver staining method can be altered by removal of gluteraldehyde for MS compatibility (Shevchenko *et al.*, 1996b). Although, proteins stained in the way have shown reduced sequence coverage in MALDI-TOF peptide mass finger printing (PMF) experiments, thought to be a result of formaldehyde modification (Scheler *et al.*, 1998).

1.3.6.3   Negative Zinc–Imidazole

Zinc-imidazole staining is different from other protein visualisation stains in that it stains the polyacrylamide gel and therefore highlighting the resolved proteins as clear areas contrasted against an opaque background. The detection limit of this stain is approximately 15 ng of protein (Fernandez-Patron *et al.*, 1998) and is compatible with MALDI-TOF PMF; however like silver it is not a good quantitative technique.

1.3.6.4 Fluorescent staining

The most commonly used fluorescent stains include SYPRO™ Orange and SYPRO™ Ruby dyes (Steinberg *et al.*, 1996a, 1996b). These dyes become fluorescent upon association with SDS-protein complexes and because the stoichiometry of SDS protein binding is relatively constant, SYPRO dyes can be used in quantitative proteomic analyses. SYPRO dyes can detect protein down to 2 ng and have a linear dynamic range of 10^4; making it the only quantitative commercially available protein stain able to match the dynamic range of gene expression levels (Patton, 2001). However, resent analysis of SYPRO staining has revealed a specking artefact which can compromise protein abundance quantification.

1.3.6.5 Fluorescent Cyanine Dye (CyDye) labelling

Propyl-Cy3 and methyl-Cy5 cyanine NHS-ester dyes (Figure 1.8) are available for fluorescently labelling two different protein samples, via lysine residues, and allowing their co-resolution on the same 2D gel (Unlu *et al.*, 1997). See section 1.3.7.1 for the application of this technology in differential analysis of two proteins samples, a method known as 2D difference gel electrophoresis (DIGE) (Unlu *et al.*, 1997; Tonge *et al.*, 2001). A present Cy labelling protein samples involves labelling 1-2 % of all lysine resides. This method allows the detection of 0.25-1 ng of protein, sensitivity similar to that of silver, and a dynamic range of four orders of magnitude (Tonge *et al.*, 2001). Although proteins of lower abundance are not detectable using this method, a DIGE technique is being developed were all cysteine resides are labelled and thus increasing the sensitivity, a method known as saturation labelling (Shaw *et*
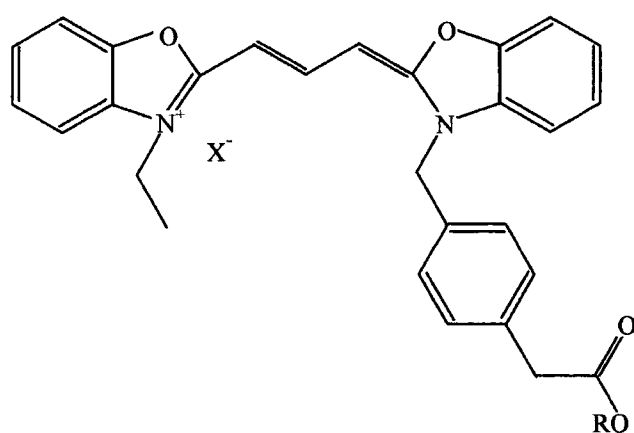
Cy2
MW = 550.5837
MW + to protein = 436.5062
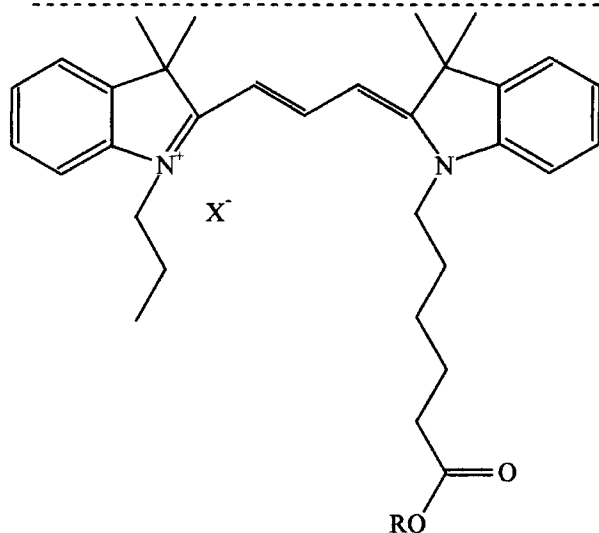
Cy3
MW = 582.7573
MW + to protein = 468.6789
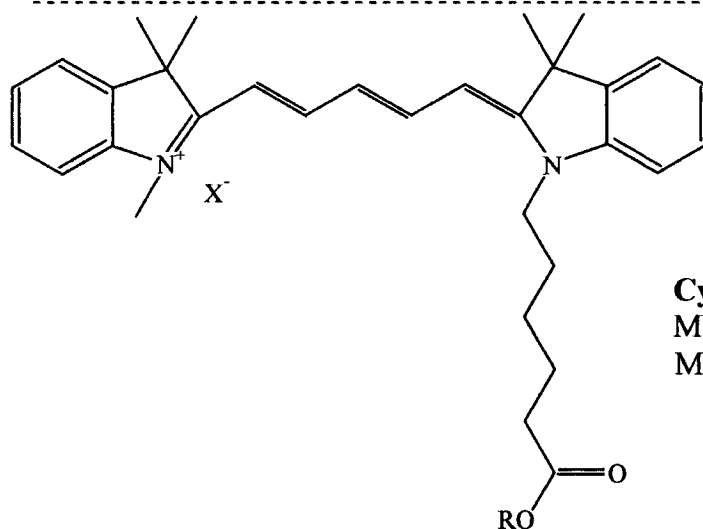
Cy5
MW = 580.7415
MW + to protein = 466.664
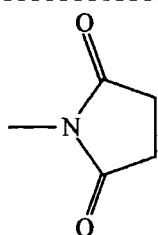
R-group
N-hydroxy succinimidyl (NHS) ester

Figure 1.8. Structures of Cyanine dyes

al., 2003). These dyes were demonstrated to have superior sensitivity to that of minimal Cy-labelling, silver stain and Sypro Ruby. However, 2-D spot patterns were significantly altered from that of unlabelled or minimal-labelled protein (Shaw *et al.*, 2003).

1.3.7 Quantification of changes in protein abundance

The global quantitative measurement of all expressed proteins in a particular cell or tissue is one of the chief aims of proteomics (Blackstock and Weir, 1999). Previously, to detect differences in protein abundance between two samples using 2-DE methodology, samples had to be processed individually on separate 2-D gels and the resultant images spot-matched and compared. Unfortunately, due to variations in electric fields, thermal fluctuations and the un-homogenous nature of polyacrylamide gels (system variation), no two 2-D gels are identical, even when the gels are prepared and processed simultaneously. Consequently, spot matching and image comparison is difficult, a problem elevated by the need to be confident that the differences seen are a reflection of the biological system studied, something achieved by generating repeat 2-D gels of each sample type. Although a variety of software algorithms have been designed which warp 2-D gel images allowing them to be superimposed and also synthesise hypothetical average gels which can be subsequently compared (Pleissner *et al.*, 200), image comparison is still complex, especially with samples of distinctly different spot patterns or where discrete changes in protein abundance are sought after. In order to solve this problem two techniques have been developed, one being a 2-DE based technique, namely 2D Difference gel electrophoresis (DIGE) (Unlu *et al.*,

1997), the other involving isotope tagging of proteins, namely Isotope coded affinity tags (Gygi *et al.*, 1999a).

1.3.7.1   2D Difference gel electrophoresis (DIGE)

2D DIGE involves the pre-2-DE labelling of two different protein samples with separate fluorescent Cy-Dyes, Cy3 and Cy5 (Figure 1.8), distinct by their different fluorescent spectra. Consequently two different protein samples can be co-resolved in the same 2-D gel, thus subjecting them to the same environment throughout the 2-DE run. Following electrophoresis protein 2-D profiles are visualised by fluorescence imaging at a level of sensitivity equal to that of silver staining (Unlu *et al.*, 1997). The current 2D DIGE method also involves labelling a third sample with a different Cy-Dye, namely Cy2 (Figure 1.8) (Alban *et al.*, 2003; Tonge *et al.*, 2001). This sample is a pooled mixture of all repeat samples in the experiment and is co-resolved with each set of replicate samples. It allows accurate normalisation and thus quantification of spot abundance and also better spot matching between replicate gels (Alban *et al.*, 2003; Tonge *et al.*, 2001). Although each sample is imaged separately, gel images can be easily overlaid and spots matched because they originate from the same gel. Consequently differences in protein abundance between two samples either due to changes in gene expression, protein translation or post translational modification can be easily identified. For a diagrammatical description of the 2D DIGE process see Figure 1.9).

Figure 1.9. Flow diagram of the 2D DIGE experimental process.

Protein samples are first labelled with the appropriate Cy-Dye, sample A (control) with Cy3, sample B (treated) with Cy5, and the pooled sample with Cy2. Equal quantities of each sample (i.e. Cy2, Cy3 and Cy5) are mixed together and subjected to 2-DE. After electrophoresis, samples are visualised using the appropriate excitation and emission wavelengths for each Cy fluor. The three images are overlaid and analysed for differences in protein abundance between the Cy3 and Cy5 labelled samples. For accurate quantification Cy3 and Cy5 samples are normalisation against the Cy2 sample.

Extract A Cy3 | Extract B Cy5 | Pooled standard Cy2

1. Cy Labelling

NHS ester reactive group

2. Mix Labelled Extracts

3. 2-DE

Cy3   Cy5   Cy2

3. Overlay image

4. Differential analysis

Cy3   Cy5
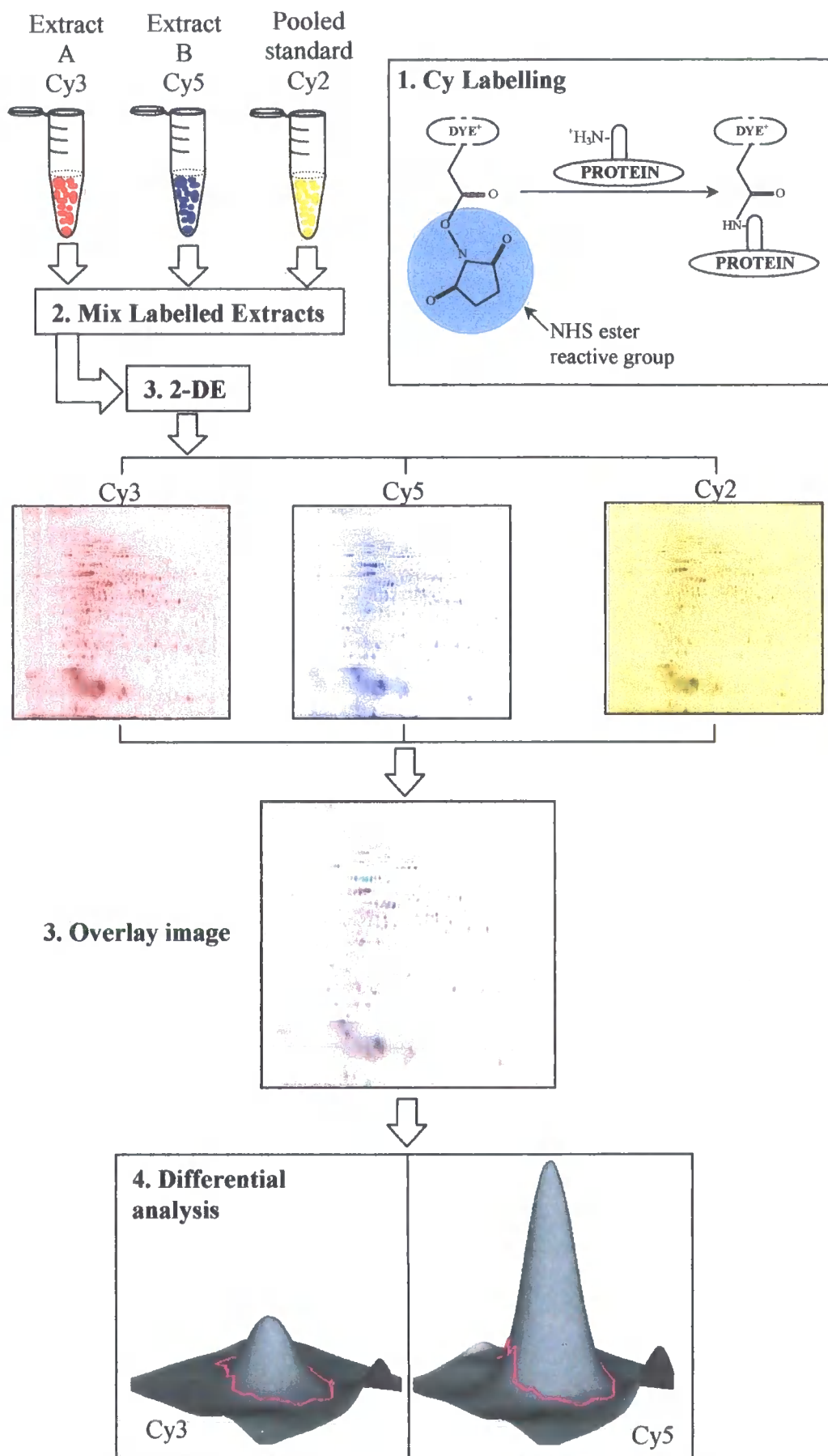
CyDyes carry an NHS ester reactive group which forms a covalent amide bond with the epsilon amino group of lysine residues in proteins (Figure 1.9). The dyes have different fluorescence properties allowing them to be discriminated, yet they also have similar MW and charge properties (Figure 1.8), therefore ensuring the same proteins, differentially labelled, migrate to the same position on a 2-D gel. Moreover, Cy-Dye labelled proteins are not significantly perturbed in their electrophoretic mobility during both IEF and SDS-PAGE. Because lysine residues carry a single positive charge at acidic or neutral pH, the CyeDyes also carry a single positive charge, which when bound to lysine residues, ensures that the proteins pI is not significantly distorted (Unlu *et al.*, 1997; Tonge *et al.*, 2001). Also, using the minimal labelling method, on average each protein is only modified on one lysine residue, consequently this only adds approximately 500 daltons (Figure 1.8) to the proteins MW, a mass shift which does not greatly affect the 2-D pattern (Unlu *et al.*, 1997; Tonge *et al.*, 2001). This is important when matching Cy labelled analytical gels to separate higher loaded unlabelled preparative gels for identification of select proteins via peptide mass fingerprinting (PMF).

2D DIGE technology has been used in a variety of investigations including, analysis of human colon cancer where 52 unique proteins were identified and shown to demonstrate a cancer specific change in abundance (Friedman *et al.*, 2004) and analysis of *E. coli* after benzoic acid treatment where 179 differentially expressed protein spots were identified (Yan *et al*, 2002). Although there are still limitations with sensitivity and identification by subsequent MS techniques, Cy-Dyes present a state-of-the-art protein detection technology for 2-DE and through their

implementation in 2D DIGE an improved 2-DE method for measuring changes in protein abundance.

1.3.7.2 Isotope coded affinity tags (ICAT)

ICAT technology makes use of the stable isotope labelling technique (De Leenheer and Thienpont 1992) a method which involves the addition of a tag, to the sample proteins, composed of three functional groups, (i) a specific chemical reactivity, (ii) an isotopically coded linker containing stable heavy isotopes (such as ^{2}H, ^{13}C and ^{15}N), and (iii) an affinity tag. Differential profiling of protein abundance between two samples from different cell states or conditions is achieved where one sample is labelled with the tag containing the heavy isotopes and the other sample is labelled with an identical tag containing normal elemental isotopes. The ICAT reagent itself is composed of a thiol specific reactive group, an eightfold deuterated linker, and a biotin affinity tag (Gygi *et al.*, 1999b). Proteins are labelled on the side chains of cysteinyl residues in a reduced state. The proteins from one cell state/condition are labelled with the isotopically light form of the ICAT reagent and the proteins from the other cell state/condition are labelled with the isotopically heavy form. The two samples are subsequently mixed and digested generating peptide fragments, those of which contain cysteine are tagged. The tagged peptides are purified by avidin affinity chromatography and the peptides are separated and analysed by microcapillary liquid chromatography tandem mass spectrometry (μLC-MS/MS). In this last step, both the relative quantity and the sequence of the tagged peptides are obtained. This system has been currently used to characterise human liver proteins (Yan *et al.*, 2004).

As previously mentioned the commonly used 2-DE MS technique is a platform technology for global proteome analysis due to the ability to simultaneously separate several thousand proteins in a single gel and quantify there abundance (Shevchenko *et al.*, 1996a). However, the global capacity of this system is in question due to its inability to resolve and detect certain classes of proteins, including very small, very large, low abundant and very hydrophobic proteins. This is a particularly important consideration to address as certain classes of proteins such as transcription factors and proteins kinases are low abundant within the cell. ICAT presents an alternative method to 2-DE where protein abundance is not an issue, allowing the quantification and identification of low abundant proteins, as long as sufficient material can be prepared for analysis via MS (Gygi *et al.*, 1999b). Also, unlike 2-DE, ICAT is not selective towards the mass of the protein, where both low and high MW proteins can be detected and analysed. However, the analysis of hydrophobic proteins, like 2-DE, is still dependant upon solubilisation and extraction strategies and because only cysteine residues are tagged, proteins not possessing cysteine in their primary structure will be omitted from the investigation. Despite this, ICAT does present a broadly applicable alternative approach to 2-DE for the quantification of protein expression although neither provide a comprehensive coverage on a proteome-wide scale (Patton *et al.*, 2002).

1.3.8   Protein identification approaches

The methods described in this section depend upon the purity of the sample for successful identification and therefore require that protein separation techniques are employed. As mentioned high resolution 2-DE is most commonly used and forms the

basis for many proteomic investigations. For a review of non mass spectrometry based proteome analyses see Wilkins *et al.*, (1996) and for mass spectrometry based methods see Aebersold and Goodlett (2001).

1.3.8.1 Edman sequencing

In early proteomic investigations, Edman sequencing was the principal method for protein identification as the methodology was well established and automated sequencers were readily available (Hewick *et al* 1981). Also during this time, the amount of gene sequence information readily available was limited and therefore protein sequence information was required in order to identify the corresponding genes. The establishment of electroblotting gel-separated proteins onto polyvinylidine difluoride (PVDF) membrane allowed the integration of this technique with 2-DE (Aebersold *et al.*, 1986). Blotted proteins are sequenced by sequential chemical degradation from the N-terminus and subsequent identification of the liberated amino acids by correlation of their retention time against a series of standards, separated by reverse phase HPLC. Although Edman sequencing of 2-DE resolved proteins is a well established technique, N-terminally blocked proteins are not directly sequencable. This problem was later solved through the development of chemical and enzymatic digestion methods for low quantities of gel separated proteins, an approach which allowed N-terminally blocked proteins to be sequenced from internal peptides (Aebersold *et al.*, 1987; Rosenfeld *et al.*, 1992). Internal sequencing also generated much more sequence data than N-terminal sequencing. In recent years Edman sequencing has been superseded by more sensitive mass spectrometry based methods. However, because mass spectrometry based methods are dependant on protein

sequence data, usually generated from genome sequencing projects, Edman sequencing continues to be an important tool in the identification of proteins from organisms with little or no genome sequence data.

1.3.8.2 Mass Spectrometry in proteomics

The rapidly growing quantity and availability of large scale genomic and expressed sequence tag (EST) sequence databases changed the way in which proteins could be identified by their amino acid sequence. However, the development of two methods for the ionisation of large, non-volatile analytes, such as polypeptides perhaps had the greatest impact in the application of MS to proteomics. These two methods, namely matrix-assisted laser desorption/ionisation (MALDI) (Karras and Hillenkamp, 1988) and electrospray ionisation (ESI) (Fenn *et al.*, 1989) allowed the ionisation of such molecules with minimal fragmentation and were subsequently referred to as 'soft' ionisation methods. The creation of commuter algorithms for the rapid identification of proteins by correlation of primary structural data (obtained from the mass spectrometer) with predicted sequences (translated from nucleotide sequences) was also important, as was the establishment of methods for the digestion of gel-separated proteins generating peptide fragments (Rosenfeld *et al.*, 1992; Shevchenko *et al.*, 1996b).

The mass of a protein/peptide is an attractive method for identification because it is very specific to the particular protein being analysed and it can be determined with high accuracy, speed and sensitivity using mass spectrometry. Mass spectrometers calculate the mass of an ionisable molecule by measuring its mass-to-charge ratio

(*m/z*). All MS instruments consist of three distinct components, these being (i) an ionisation source, (ii) a mass analyser and (iii) a detector and although there are several different types of mass spectrometer available with different combinations of ionisation sources and mass analysers, there are two which are most commonly used in proteomics. These are matrix-assisted laser desorption/ionisation time-of-flight mass spectrometry (MALDI ToF MS) and electrospray ionisation tandem mass spectrometry (ESI MS-MS), each of which will be discussed in detail.

1.3.8.3   MALDI ToF MS

In proteomics investigations, MALDI is used primarily in peptide mass fingerprinting (PMF). Here the accurate mass measurement of a group of peptides derived from a protein by sequence-specific proteolysis (a peptide mass fingerprint, PMF) compared to predicted peptide masses from protein sequence data is a highly efficient means of identification, with a level of detection between 5-50 pmol (Patterson, 1995a). Several methods have been developed for the automation of this process (review by Patterson and Aebersold, 1995b) but they generally include the following steps. Firstly, sample proteins are digested by a sequence specific protease, e.g. trypsin which cleaves at lysine (K) and arginine residues (R). Secondly, peptide masses are accurately measured in a mass spectrometer (Figure 1.10). Here, peptides are mixed with a low molecular weight matrix, usually α-cyano-4-hydroxy cinnamic acid or 2,5-dihydroxybenzoic acid, which have absorption maximums at the wavelength of a UV laser (Beavis and Chait, 1989). This mixture is applied and dried onto a metal MALDI target grid which causes the peptide to crystallise with the matrix. Peptides are ionised with a pulsed UV laser which has a wavelength of 337 nm and are subsequently
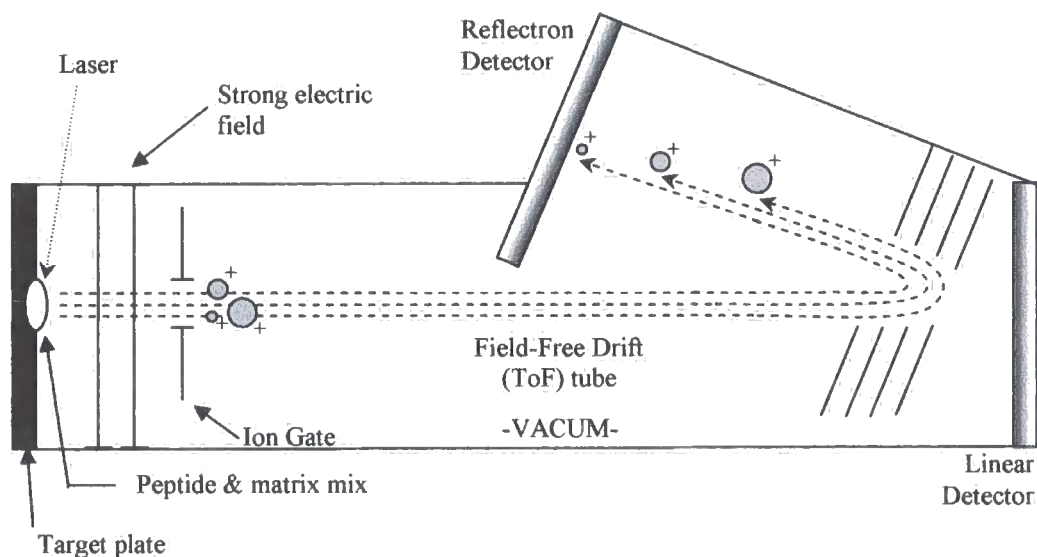
Figure 1.10. Schematic diagram showing the basic principle of MALDI-ToF.

Peptides are mixed with a UV absorbing matrix and loaded onto the target plate. A UV laser is used to ionise the peptides which are subsequently accelerated down the field-free drift tube. The detector measures the time-of-flight for each peptide and calculates their mass/charge ratio (m/z). Figure adapted from Patterson *et al.*, 2001).

accelerated in an electric field at high voltage towards the field-free drift tube. Time-of-flight (ToF) through the field-free drift tube is measured for each peptide ion by the detector usually in reflectron mode. The velocity of the ions is inversely proportional to their mass/charge ratio (m/z) where smaller ions fly faster than larger ones. By measuring the time-of flight for each ion their m/z ratio can be calculated and thus their peptide mass, which is measured down to a 50 ppm mass accuracy (Patterson *et al.*, 2001). Finally, the generated set of measured peptide masses is used to interrogate a theoretical tryptic digest database and matches are assigned a molecular weight search (MOWSE) score relating to the degree of confidence for the identification given (Pappin *et al*, 1993). The parameters involved in calculating this score include the proteins molecular weight range, the cleavage enzyme used and the number of matching peptide masses present in the fingerprint. The more peptide masses match the greater the MOWSE score and thus confidence in the attained identification. Multiple identifications for searched peptide mixtures are often obtained and the MOWSE score algorithm ranks the list of positive hits according to their score. The highest scoring identification is usually the positive hit.

Although MALDI PMF is a highly effective means by which proteins can be accurately identified, it is not without its problems. Because it is ultimately dependent upon the correlation of several peptide masses with corresponding theoretical data in a database, complex protein mixtures can not be analysed nor can EST databases used for identification. EST sequence data can not be used because only a small proportion of the gene sequence is represented which is probably insufficient to cover the entire peptides mass fingerprint. Complex protein mixtures present a problem because it is difficult to determine which peptides originate from the same protein. Consequently,

this technique is best suited to organisms with completely sequenced genomes and in combination with protein separation via 2-DE. Other problems associated with this technique include the inability to detect all predicted peptides in a particular protein and the detection of peptide masses which are not assigned to the theoretical list of masses. The former is due to a number of reasons including, the detection of small peptides and selective ionisation. However, because only a low number of peptides are required for protein identification this is only an issue when sample quantity is low. The latter is a more significant problem and miss identifications can often arise as a result. Several reasons can be responsible for the presence of unassigned masses including (i) post translation modifications (e.g. phosphorylation) which add additional mass to the peptide, (ii) miss peptide cleavages generating longer than predicted peptides, (iii) modification of amino acid residues during sample preparation including oxidation of methionine or acrylamide modification of cysteine (Table 1.1) or (vi) the presence of peptides from other protein species (Jensen *et al.*, 1997; Eriksson *et al.*, 2000). However, some of these modifications can be accounted for in the database search and thus improve search results.

1.3.8.4   ESI Tandem mass spectrometry (MS-MS)

Peptide amino acid sequence is more constraining for protein identification via database interrogation than peptide mass (Zubarev *et al.*, 1996). Tandem mass spectrometers have the ability to further fragment peptides ions at the amide bonds and record the resultant fragment ion spectra. This is most frequently performed using either a triple qudrupole (TQ) (Lee *et al.*, 1998) ion trap (IT) (Davis and Lee, 1997) or qudrupole time-of-flight (QTOF) (Borchers *et al.*, 2000) mass spectrometer. These

mass spectrometers do this via low energy collision-induced dissociation (CID) and are usually used in conjunction with electrospray ionisation (ESI). Although a MALDI ionisation source may be used instead. For the ESI TQ MS method (Figure 1.11), peptide digests are passed through a metal capillary needle for extended periods (60 minutes) at high potential. This causes the sample flow to disperse as a fine spray of charged droplets, which are directed into the inlet orifice of the mass spectrometer held at a lower potential. As the droplets travel from the needle to the inlet orifice they are desolvated by the application of heated nitrogen gas, which releases the ions from the liquid phase and into the gas phase (Patterson *et al.*, 2001). These ions are then directed through the orifice and into the first quadrupole (under vacuum). Quadrupoles consist of four parallel rods and by varying the voltage through opposite pairs of rods, this first quadruple can be used as a mass filter allowing only peptide ions with a specific m/z ratio through. Also, if applied voltages are varied over time and the numbers of ions exiting the filter quadrupole are recorded as a function of the m/z ratio, a mass spectrum can be attained for the selected peptide fragment. The selected ions are subsequently accelerated into the second quadrupole which functions as a collision chamber where peptides are fragmented in a sequence specific manner along the peptide backbone. Fragmentation is caused by low energy CID in which peptides are collided with a heavy inert gas, usually argon or nitrogen. The ionic products of the CID reaction are called fragmentation or product ions, the masses of which are determined in the third quadrupole via their m/z ratio.

ESI usually generates multiply charged ions, and if tryptic peptides are analysed both the N-terminal NH_2 group and the lysine/arginine NH_2 side chain group will be charged. These ions are referred to as $[M + 2H]^+$ ions and are preferentially selected
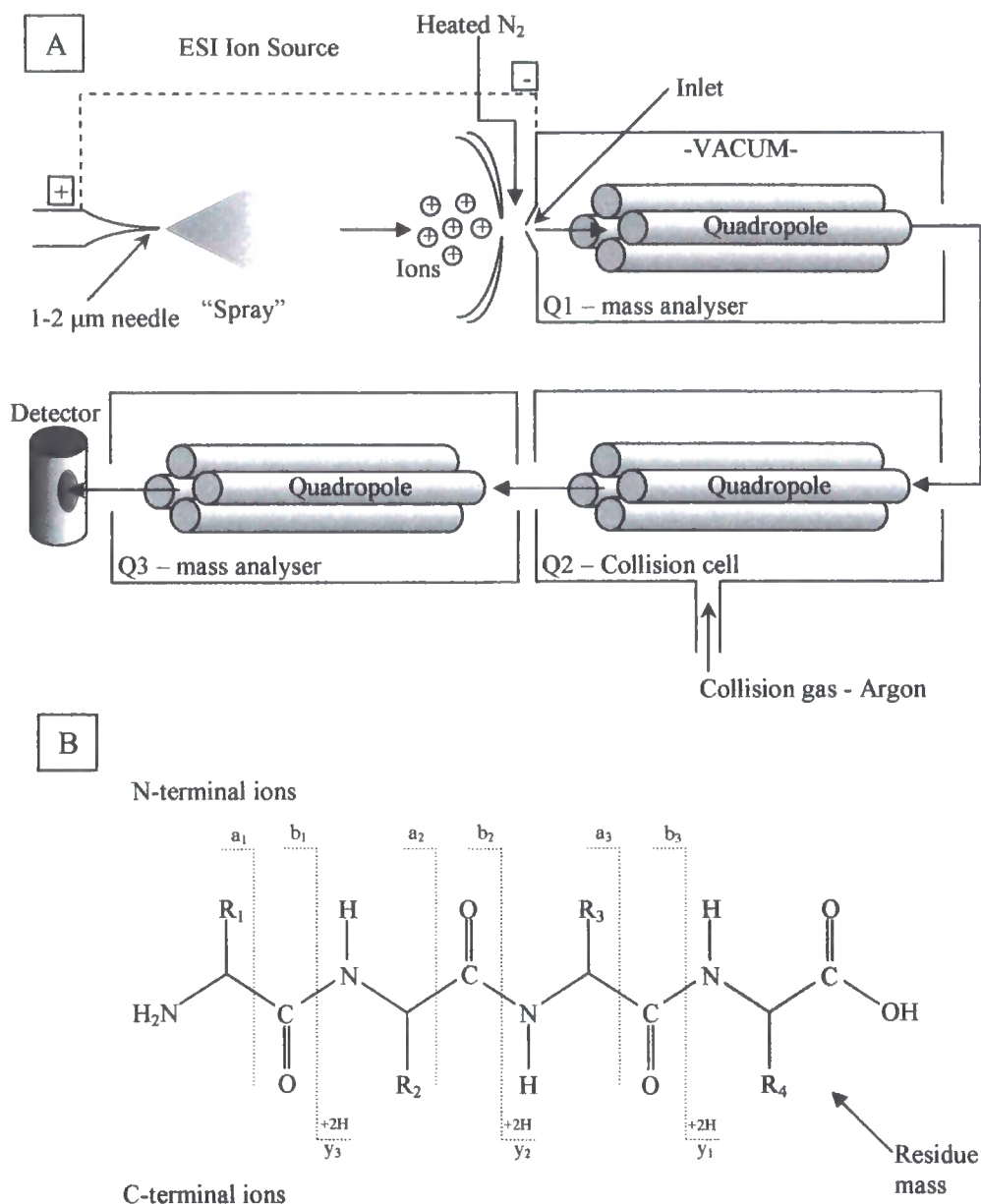
Figure 1.11. Schematic diagram of ESI MS/MS using a TQ mass spectrometer and the principle of fragment ion nomenclature.

A, Peptides are ejected from a metal needle as a fine spray and the high potential causes the droplets to become charged. Charged droplets become desolvated by drying with heated N_2 gas which generates protonated peptide ions. These ions enter the first quadrupole where $[M + 2H]^+$ peptide ions are selected for further fragmentation. In the collision cell (second quadrupole) these peptides are fragmented by colliding with argon in process known as CID. The mass of the generated fragmentation ions are calculated in the third quadrupole. B, three major types of fragment ions: y ions result from N-terminal deletions, b ions result for C-terminal deletions, a ions result from the loss of carbon monoxide from the b ion.

for fragmentation because [M + H]$^+$ fragmentation ions, which are more readily interpreted in comparison to other ion species, can be generated by loss of a residue, and thus charge, from either the carboxyl-terminus or amino-terminus and therefore provide a greater quantity of sequence data. As a result a nomenclature has been generated to differentiate the fragment ions according to the amide bond which fragments and also the end of the peptide which retains the charge (Figure 1.11) (Biemann, 1990; Roepstorff and Fohlman, 1984). If the positive charge of the parent ion remains on the N-terminus of the fragment ion, the ion is referred to as a *b* ion. However, the fragmentation ion is referred to as a *y* ion if the positive charge remains on the carboxyl-terminus. Therefore *b* ions represent fragmentation ions with losses at the C-terminus and an intact N-terminus and vice versa. Also a subscript numbering is used to reflect the number of amino acid residues remaining on the fragment ion, counting from the N- or C-terminus depending on the end of the peptide which retains the charge. A satellite *b* ion series is also generated as a result of the fragmentation process through the loss of carbon monoxide (Figure 1.11). This ion series is referred to as the *a* ion series and each ion is 28 amu less in mass than it corresponding *b* ion. Other ion species can be present in the fragmentation spectra due internal fragmentation, particularly at proline or aspartic acid residues, where particular ions undergo multiple fragmentation events (Loo *et al.*, 1993). This internal fragmentation generates either acyl ions consisting of at least two amino acid residues or immonium ions (Table 1.1). The latter represent individual amino acids and provide partial amino acid composition of the peptide.

The fragment ion mass spectra together with the parent ion mass provide extremely constraining criteria which can be used for identification. Also, because partial amino

acid sequence data is generated the need for complete genomic sequence is not essential and consequently translations of EST database can be used. In order to automatically interpret the MS-MS data complex algorithms have been developed (Mann and Wilm, 1994; Yates *et al.*, 1995). However, the quantity of data does complicate the interpretation of the sequence and often it is not immediately apparent which ion series a particular ion belongs to, consequently it is sometime necessary to manually interpret the data (Pardo *et al.*, 2000). In addition to amino acid sequence MS-MS can also be used to identify post translation modifications, of which the methodologies for the identification of phosphorylation and glycosylation have been most developed (Annan and Carr, 1997; revived by Jensen, 2004). Furthermore, due to the sequencing capability of MS-MS it can be used to identify subunits form multi protein complexes. For this MS-MS is often coupled to multi dimensional liquid chromatography (LC/LC) (Link *et al.*, 1999) or via the employment of the TAP tag purification method (Rigaut *et al.*, 1999).

In conclusion 2-DE and MS represent an integrated technology by which several thousand protein species can be separated, detected and quantified in a single operation, and hundreds of the detected proteins can be identified in a highly automated fashion by sequential analysis of the peptide mixtures generated by digestion of individual gel spots.

1.4   Aims of this study

There were four major aims of this thesis. Firstly, the aim was to establish 2D electrophoresis and PMF technology for the analysis of *Synechocystis* proteins and to use this technology to determine the complexity of the *Synechocystis* proteome and identify proteins on 2D maps. Secondly, with limited information on the heat shock response and its regulation in cyanobacteria the developed proteomic technology would be used to characterise the heat shock induced changes in protein steady state levels. Due to the capacity of 2-DE to simultaneously resolve several thousand spots, this analysis would provide a wider picture of the cellular response to heat shock than currently known and characterise proteins not previously associated with the heat shock response. Thirdly, a mutant of *Synechocystis*, *Δhik34*, has been demonstrated to have an elevated thermotolerant phenotype (unpublished data Iwane Susuki, NIBB, Okasaki, Japan – personal communication). It was the aim to compare the proteomes of wild type and *Δhik34* knockout mutant *Synechocystis* strains to determine the role of Hik34 in the perception and regulation of the heat shock response. It is predicted that this protein is active at physiological temperature and suppresses the expression of *hsp* genes, following heat shock this protein is inactive relieving the repression of the *hsp* genes. Consequently, the *Δhik34 Synechocystis* mutant has high basal levels of Hsps and is preconditioned to the effects of heat shock enabling to survive at higher temperatures than the wild type and other *hik* gene mutants. Fourthly, protein factors have been demonstrated to stabilise the photosynthetic machinery in cyanobacteria and allow development of acquired thermotolerance. It was the aim to compare the thylakoid associated proteins from heat acclimated cells and non-acclimated cells to

identify protein factors involved in the thermo stabilisation of the photosynthetic machinery and establishment of acquired thermotolerance in cyanobacteria.

CHAPTER 2

Materials and Methods

2.1   Materials

2.1.1   Lab chemicals

All materials used during the course of this study were, unless stated, obtained from Sigma Chemical Company Ltd., Fancy Road, Poole, Dorset, BH17 7NH or BDH chemicals Ltd., Merck Ltd., Merck House, Poole, Dorset BH15 1TD.

2.1.2   Cyanobacterial strains

Synechocystis sp. PCC 6803 (here after called *Synechocystis*) wild type strain was obtained from the American Type Culture Collection (ATCC no. 27184). *Synechocystis* Glucose tolerant strain was kindly given by Professor Murata, National Institute of Basic Biology, Okasaki, Japan, originally obtained from Dr. Williams, Dupont Co. Ltd. *Synechocystis* histidine kinase (Hik) knockout mutant strain $\Delta hik34$ was also kindly given by Professor Murata. This strain was created by the insertion of a Spectinomycin resistance (Sp-r) gene (Figure 2.1) (Suzuki *et al.*, 2000a, 2003). Sequence of the Sp-r gene is available from Genbank "M60473" and reported by Prentki *et al* (1991).
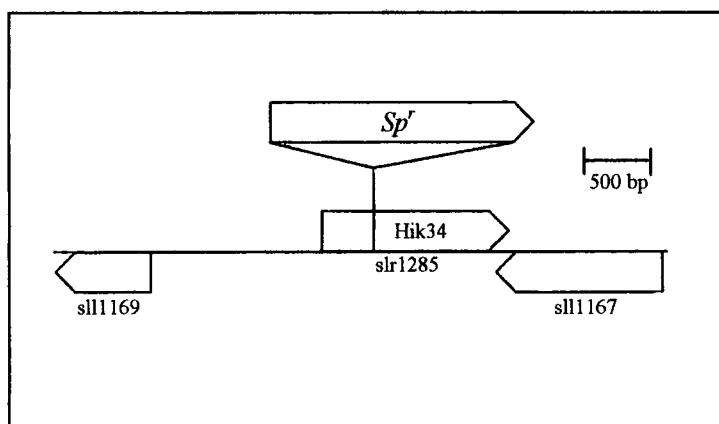
Figure 2.1 Diagram of gene structure and the insertion site of antibiotic-resistance gene cassette in ΔHik34 mutant.

2.2 Methods

2.2.1 Cyanobacterial culture methods

2.2.1.1 Cyanobacterial growth and maintenance

All cell culture experimentation was performed aseptically within a lamina flow cabinet wiped with 80 % (v/v) ethanol. *Synechocystis* strains were cultured in BG-11 media (Allen, 1968) (see section 2.2.1.2) which supports growth both in air or in an atmosphere slightly enriched with CO_2 (Stanier *et al.*, 1971). For routine maintenance, *Synechocystis* strains were grown in air, in liquid media as shaking suspension cultures (see section 2.2.1.3) and on solid media as agar plates or slopes (see section 2.2.1.4). However more rapid growth and higher cell yields are obtained if suspension cultures are continuously aerated with 1 % CO_2 in air (Stanier *et al.*, 1971) (see section 2.2.1.7). The latter method was used for growing cultures on which experiments were conducted, here after are referred to as gassed cultures. *Synechocystis* strains were also reserved as dimethyl sulfoxide (DMSO) stocks stored in liquid nitrogen. Every 6 months a fresh DMSO stock was used to initiate a new suspension culture from which all future cultures were grown (see section 2.2.1.6). DMSO stocks were made when required from freshly initiated suspension cultures (see section 2.2.1.5).

2.2.1.2 BG-11 culture media

BG-11 media is essentially a mineral media; first devised by M. M. Allen (Allen M. 1968), its composition is shown in Table 2.1a and 2.1b. Because the majority of constituents were required in small quantities (i.e. all those excluding $NaNO_3$ and

Table 2.1a. Composition of Medium BG-11

Constituent	Amount (ml) or (g) per litre
$NaNO_3$	1.5 g
K_2HPO_4	0.04 g
$MgSO_4 \cdot 7H_2O$	0.075 g
$CaCl_2 \cdot 2H_2O$	0.036 g
Citric Acid	0.006 g
Ferric Ammonium citrate	0.006 g
EDTA (disodium magnesium salt)	0.001 g
Na_2CO_3	0.02 g
HEPES	4.77 g
Trace Metal Mix A5 (Table 1b)	1.0 ml

Table 2.1b. Composition of trace metal mix

Constituent	Amount (g) per litre
H_3BO_3	2.86
$MnCl_2 \cdot 4H_2O$	1.81
$ZnSO_4 \cdot 7H_2O$	0.222
$Na_2MoO_4 \cdot 2H_2O$	0.36
$CuSO_4 \cdot 5H_2O$	0.079
$Co(NO_3)_2 \cdot 6H_2O$	0.0494

Table 2.1c. BG-11 constituent stock solution

Constituent	(g) per litre	x conc.	Stock vol. (ml)	Stock mass (g)	Vol. for 1 litre BG-11
K_2HPO_4	40	1000	50	2	1 ml
$MgSO_4 \cdot 7H_2O$	75	1000	50	3.75	1 ml
$CaCl_2 \cdot 2H_2O$	36	1000	50	1.8	1 ml
Citric Acid	6	1000	50	0.3	1 ml
Ferric Ammonium citrate	3	500	50	0.15	0.5 ml
EDTA	1	1000	50	0.05	1 ml
Na_2CO_3	20	1000	50	1.0	1 ml

HEPES), stock solutions of high concentration were prepared (Table 2.1c). BG-11 has low phosphate content and is consequently poorly buffered; therefore in order maintain a neutral pH during 1 % CO_2 aeration, BG-11 is buffered with 20 mM HEPES-NaOH pH 7.5. After titration with 10 M NaOH to pH 7.5, the media was decanted into the desired culture vessels and autoclaved for 20 minutes. Required quantities of media were made excluding ferric ammonium citrate due to its tendency to precipitate during autoclave sterilisation; it was therefore separately filter sterilised and added aseptically at the time of inoculation.

2.2.1.3   Cyanobacterial shaking suspension cultures

All *Synechocystis* strains were maintained as 100 ml cultures in 500ml conical flasks shaken at 120 rpm using an orbital shaker at 32°C and illuminated with florescent tubes providing 30 $\mu E \ m^{-2} \ s^{-1}$ of photosynthetic active radiation (PAR). Cultures were shaken to increase the circulation of air into and within the conical flask, thus maintaining the availability of air for gaseous exchange. Shaking suspension cultures were inoculated to a starting optical density measured at A_{730nm} of approximately 0.05 and allowed to grow for 1 month before being re-inoculated into fresh media.

2.2.1.4   Cyanobacterial growth on solid media

For the preparation of solid media, the mineral base is supplemented with 1.5 % (w/v) agar. Equal volumes of double strength solutions of BG-11 media (minus the Ferric ammonium citrate) and agar were made and autoclaved separately. These solutions were allowed to cool to approximately 50°C (placed in a 50°C water bath) before adding the required volume of the 500 x ferric ammonium citrate stock solution. The agar solution was added to the BG-11 media and mixed by swirling. This solution was

poured into Petri dishes, approximately 25-30 ml in each Petri dish, or pre-autoclaved 30 ml glass universal bottles, resting at an angle, for slope cultures. The media was allowed to solidify and the moisture to evaporate before sealing the Petri dishes and universal bottles and storing at 4°C.

Agar plates and slopes were inoculated from both liquid and agar cultures. Typically, 100 μl aliquots of liquid culture were used to inoculate the agar media. Cultures were allowed to grow for 1 month before inoculating a new plate/slope. After inoculation, Petri dishes were positioned upside down and sealed with Parafilm to prevent the media drying-out and universal bottle lids were left slightly ajar to allow gaseous exchange. The cultures were grown at 32°C and illuminated with florescent tubes providing 30 μE m^{-2} s^{-1} of photosynthetic active radiation (PAR). The *Synechocystis* histine kinase mutant strain *Δhik34* was grown on agar media supplemented with the antibiotic spectinomycin at a concentration of 20 μg/ml. This was added immediately prior to pouring the agar media. When growing the *Δhik34* mutant strain on agar media containing antibiotics, light intensity was reduced to 20 μE m^{-2} s^{-1}. This was because in the initial stage of growth cell density is low and will therefore not interfere with the light intensity. At this stage, exposure to excess light may cause photo-inhibition.

2.2.1.5   Preparation of cyanobacterial DMSO stocks

DMSO stocks were made from fresh logarithmic gassed suspension cultures with an A_{730} of approximately 1.0. Prior to harvesting the cells, the cultures were tested for contamination on various media types (Table 2.2) and under a light microscope at x 40 magnification. Cells were pelleted by centrifugation at 3,000 *g* for 5 minutes at

Table 2.2. Contamination test plates

Media Type	Constituent	Quantity (g) per litre dd.H_2O
NB	Nutrient Broth	25
	Agar	10
PG	Glucose	1
	Bacto-peptone	1
	Agar	10
SST	Glucose	10
	Bacto-tryptone	10
	Agar	10
Y	Yeast Extract	5
	Agar	10

room temperature and the supernatant discarded. The cell pellet was re-suspended in a small volume of sterilised BG-11 media, approximately 1 ml or 1/10th of the original culture volume, so that a concentrated cell suspension was attained. A sterilised 70 % (v/v) DMSO solution was added to the concentrated cell suspension so that the final concentration of DMSO is 7 % (v/v). Small aliquots, 0.5 to 1.0 ml, of the suspension were dispensed into 1.5 ml pre-sterilised cryovials and stored in liquid N_2.

2.2.1.6   Initiation of cell suspension cultures from DMSO stocks

Fresh DMSO stocks were removed from storage in liquid nitrogen and thawed in a 37°C water bath. After thawing, aliquots of 0.25 ml were plated out onto fresh BG-11 agar plates, remembering to use those plates containing spectinomycin for the *Δhik34 Synechocystis* cells. Cultures were grown at 32°C under 30 μE m^{-2} s^{-1} illumination and plates were positioned upside down and sealed with parafilm. After 1-2 weeks the majority of bacteria on the plate were scraped off and used to inoculate 100 ml of fresh liquid BG-11 media in a 500 ml conical flask. This suspension culture was grown at 32°C under 30 μE m^{-2} s^{-1} illumination and shaken at 120 rpm. After 1-2 weeks the A_{730} of the culture was sufficient to generated new gassed cultures.

2.2.1.7   Growth of gassed cultures

Gassed cultures were those on which experiments were conducted and they varied in volume from 50 – 1000 ml, depending on the amount biological material required. They were grown using a purpose built apparatus (see section 3.2.1) in glass flasks of varying size and gassed continuously with air containing 1% CO_2 for rapid division. This gas mix was delivered into the culture via a sterilised glass tube which itself was inserted into the culture in sterile conditions and positioned at the very bottom of the

flask to allow the CO_2 enriched air to circulate through the whole culture. The flow of gas was restricted so that only three bubbles were visible on the surface of the culture at any one time. Before being introduced into the culture, the gas was moistened by bubbling through dd.H_2O in order to reduced culture evaporation. Also, a 50 μm filter and a cotton wool bung in the neck of the glass tube ensured the sterility of the gas mix. Lateral illumination was provided via 2 banks of three fluorescent tubes on either side of the flask supplying 70 μE m^{-2} s^{-1} of PAR and temperature was maintained at 34°C through temperature controlled water baths.

Experimental cultures were inoculated from 50 ml gassed pre-cultures. These were grown in the same environment as the experimental culture, but were inoculated from a shaking flask culture and were used to equilibrate the cyanobacteria to the change in environment from a shacking to a gassed flask. *Synechocystis* has a doubling time of approximately 8 hours and therefore pre-cultures were routinely inoculated to a starting A_{730} of either 0.05 or 0.4 and then grown for 2 or 1 days respectively to obtain a culture with an A_{730} of approximately 3.2 in that time. This was then used to inoculate an experimental culture, usually 500 ml in volume, to a starting A_{730} of 0.125 which would achieve an A_{730} of approximately 1.0 after 24 hours. Exponentially growing cultures with an A_{730} of 0.5 – 1.0 were typically used to conduct experiments.

2.2.2 Cellular breakage, cellular fractionation and protein extraction methods

2.2.2.1 Glass bead cell breakage

Synechocystis cells were harvested from gassed suspension cultures by centrifugation at 3,000 g for 10 minutes at 4°C and washed with ice cold extraction buffer (20 mM Tris-HCl pH 8.0, 2 mM DTT (Melford Laboratories Ltd., Bildeston Road, Chelsworth, Ipswich, Suffolk, IP7 7LE, U.K), 1 mM EDTA) to remove any secretory proteins. Cells were re-collected by centrifugation as before and re-suspended in ice cold extraction buffer to $1/10^{th}$ of the original culture volume. This suspension was transferred to a pre-chilled glass test tube containing an equal volume of pre washed glassed beads, 106 μm and smaller in diameter. To break the cells this cell/glass bead suspension was vortexed in 30 second bursts for a total of 6 minuets, where after each vortex burst the suspension was briefly put on ice.

2.2.2.2 French press cell breakage

Synechocystis cells were harvested from gassed suspension cultures with volumes >100 ml by centrifugation at 3,000 g for 10 minutes at 4°C and washed with ice cold extraction buffer (20 mM Tris-HCl pH 8.0, 2 mM DTT (Melford Laboratories Ltd), 1 mM EDTA). Cells were re-collected by centrifugation as before and re-suspended in ice cold extraction buffer to $1/10^{th}$ of the original culture volume or a minimum of 10 ml. To break the cells, this suspension was twice passed through a Basic Z Cell Disrupter (Constant Systems Ltd., Low March, Daventry, Northants, UK. NN11 4SD) at 24.5 KPSI and cooled to 4°C.

2.2.2.3 Cellular fractionation

Broken cell suspensions were immediately centrifuged at 3,000 g for 10 minutes at 4°C to pellet any unbroken cells and the cell debris and the resultant supernatants were transferred to fresh vessels on ice. Chlorophyll concentration of these supernatants was determined spectrophotometrically (see section 2.2.2.4). These suspensions were ultracentrifuged using a Beckman Optima™ L-70 Ultracentrifuge and a Beckman SW28 rotor (Beckman Coulter, Inc., 4300 N. Harbor Boulevard, P.O. Box 3100, Fullerton, CA.) at 100,000 g for 1 hour at 4°C to pellet the membranes. The resultant supernatants were transferred to fresh vessels and the soluble protein acetone precipitated (see section 2.2.2.5). Pelleted membranes were re-suspended in 100-500 µl of ice cold extraction buffer (20 mM Tris-HCl pH 8.0, 2 mM DTT (Melford Laboratories Ltd), 1 mM EDTA,) and transferred to fresh microfuge tubes before being stored at -80°C.

2.2.2.4 Determination of Chlorophyll A concentration

A 20 µl aliquot of broken cell suspension (with unbroken cells and cell debris separated) was transferred to a fresh 2 ml microfuge tube to which 2 ml of ice cold 80% (v/v) acetone was added and subsequently incubated on ice for 5 minutes. The precipitate was pelleted by centrifugation at 3,000 g for 10 minutes at 4°C and the absorbance of the supernatant was measured spectrophotometrically at 418 nm using an Ultra Spec II spectrophotometer (Amersham Biosciences, Amersham Place, Little Chalfont, Buckinghamshire UK. HP7 9NA). Chlorophyll A (ChlA) concentration was determined using the Beer Lambert law with the molar absorption coefficient (ϵ) of ChlA at $\lambda_{418\,nm}$ = 110743 M^{-1} cm^{-1} (Strain *et al.*, 1963).

2.2.2.5   Acetone precipitation of fractionated soluble proteins

Synechocystis soluble protein fractions were mixed with ice cold acetone to a final concentration of 80 % (v/v) acetone and incubated at -20°C for up to 24 hours. The precipitated protein was collected by centrifugation at 3,000 g for 10 minutes at 4°C and the supernatant discarded. Protein pellets were washed twice with ice cold 80 % (v/v) acetone and finally with absolute acetone, where precipitates were harvested by centrifugation (as before) after each wash and the supernatant discarded. Pellets were re-suspended in absolute acetone and stored at -80°C. These three sequential washing steps helped remove any precipitated non-protein compounds, such as salt, which may interfere with isoelectric focusing and electrophoresis.

For electrophoretic analysis, precipitated protein samples stored in absolute acetone at -80°C were harvested by being centrifuged at 3,000 g for 5 minutes at 4°C. The acetone supernatant was discarded and the resultant pellet air dried for 5 minutes, taking care not to over dry which resulted in pellets that were difficult to re-suspend.

2.2.2.6   Membrane subfractionation methodology

This methodology was employed to further fractionate *Synechocystis* membranes, removing contaminating soluble proteins and separating both peripheral and integral membrane associated proteins. Techniques were adapted from previously reported methodologies where NaCl was shown to release phosphatidic acid phosphatase from avocado microsomes (Pearce and Slabas, 1998) and Na_2CO_3 was demonstrated to convert closed vesicles to open membrane sheets and release peripheral proteins (Fujiki *et al.*, 1982).

Fractionated *Synechocystis* membranes were sequentially washed with extraction buffer (20mM Tris pH 8.0, 2mM DTT (Melford Laboratories Ltd), 1mM EDTA), 500 mM NaCl and 100 mM Na_2CO_3 (pH 12.0) at a 1:3 (w/v) ratio of membranes to each wash reagent. All extractions were conducted using ice cold solutions and involved a 5 minute homogenisation step, where membranes were homogenised within a thick wall polycarbonate ultracentrifuge tube using a tight fitting glass rod (Figure 2.2). For fractionation of 100 μg of membranes 0.5 ml polycarbonate tubes (part no. 343776) were used (Beckman Coulter, Inc.) for up to 1 mg 3.0 ml polycarbonate tubes (part no. 349622) were used. This was preceded by a 30 minute incubation period on ice before the membranes were re-harvested by ultracentrifugation at 100,000 *g* for 1 hour at 4°C using a Beckman Optima™ TLX Ultracentrifuge and TLA 120.1 or TLA 100.3 rotors (Beckman Coulter, Inc.) for 0.5 ml and 3.0 ml tubes, respectively. The first buffer wash step removed any soluble protein contaminants. The following NaCl and Na_2CO_3 treatments extracted peripheral proteins situated on the external and luminal faces of the *Synechocystis* microsomes respectively, leaving behind the integral membrane proteins in the pellet.

2.2.2.7 Trichloroacetic acid/acetone precipitation of extracted membrane associated proteins.

The membrane subfractionation methodology utilised various compounds to extract membrane associated proteins. TCA/acetone protein precipitation was used to purify the extracted proteins in preference over acetone precipitation because this method is more effective at removing various non-protein contaminants which can interfere with isoelectric focusing and electrophoresis, such as lipids and salts.

Glass rod

Polycarbonate
ultracentrifuge
tube
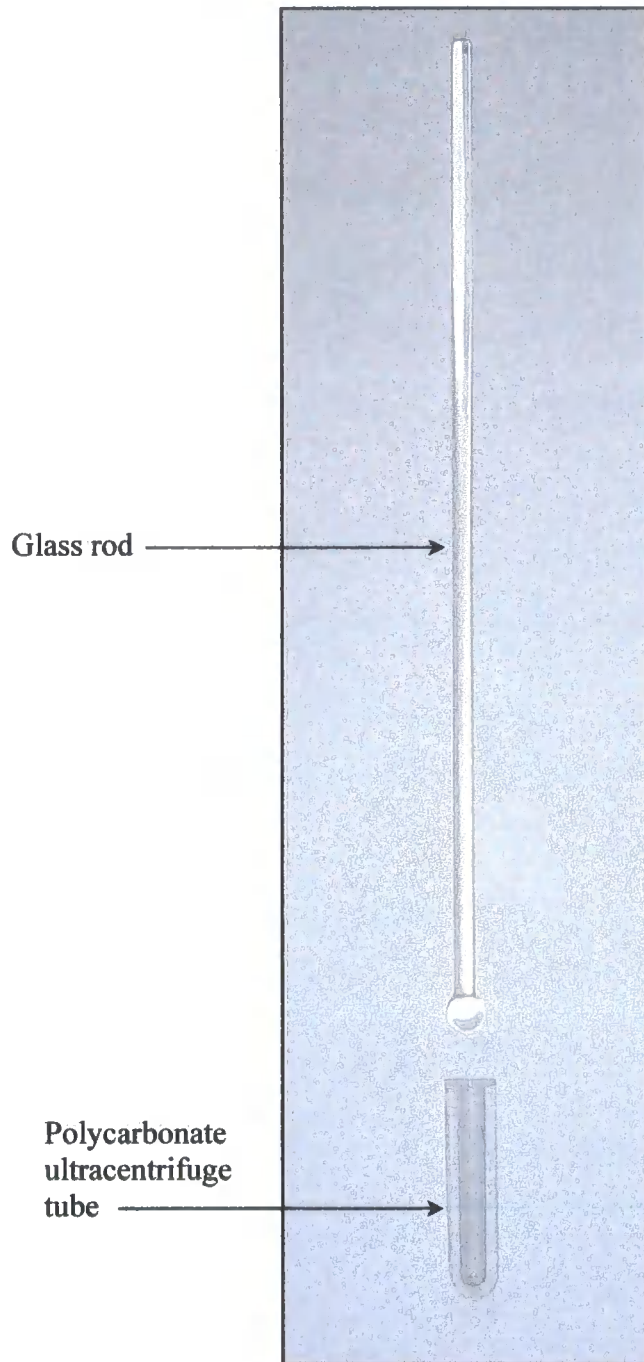
Figure 2.2 Apparatus used for homogenisation of *Synechocystis* membranes in membrane sub-fractionation methodology.

Membrane associated proteins extracted by washing with extraction buffer, 500 mM NaCl and 100 mM Na_2CO_3 were precipitated by addition of ice cold 50 % (w/v) TCA in acetone (stored at room temperature) to give a final concentration of 10 % (w/v) in solution. Samples were incubated at -20°C for 1 hour before the protein precipitates were harvested by centrifugation at 3,000 g for 15 minutes at 4°C. The supernatants were discarded and pellets were twice washed with equal volumes ice-cold 80 % (v/v) acetone and finally with ice cold absolute acetone. After each wash protein precipitates were collected by centrifugation (as before) and the supernatant discarded. Pellets were allowed to air dry for 5 minutes and care was taken to avoid over drying, which resulted in tough pellets that were difficult to re-suspend.

2.2.3   Protein concentration estimation assays

2.2.3.1   Bradford protein concentration estimation assay

First developed by Bradford (Bradford, 1976) this dye-binding assay is based on the principal that upon binding to protein the maximum absorbance for an acidic solution of Coomassie Brilliant Blue G-250 shift from 465 nm to 595 nm. The dye reagent used, Protein Assay Dye Reagent Concentrate, was obtained from Bio-Rad (Bio-Rad Laboratories Ltd., Bio-Rad House, Marylands Avenue, Hemel Hempstead, Hertfordshire HP2 7TD) and the protein concentration estimation assay was performed according to the manufacturer's recommendations for the Micro-assay procedure. Standard curves were constructed using a series of BSA standard solutions in the range 1-25 μg.

2.2.3.2 Modified Bradford protein concentration estimation assay

Used for the estimation of lysis buffer solubilised protein samples this assay is a modified version of the Bradford assay and was first developed by Ramagli and Rodriguez (1985). Its development was instigated by the inability to use either the Lowry or Bradford assays for estimation of protein concentration in lysis buffer solubilised samples, due to the presence of carrier ampholytes and thiol containing compounds. In this modified Bradford method, protein samples are acidified, allowing a stable linear relationship between protein concentration and absorbance to be obtained.

BSA standards and protein samples were prepared as follows and as shown in Table 2.3. A 2 mg/ml BSA stock solution in lysis buffer (9 M urea, 2 M thiourea, 4% (w/v) CHAPS) was prepared, from which a standard BSA series was made ranging from 0-40 μg (usually 0, 1, 2, 5, 10, 20 and 40 μg). Multiple aliquots (usually 3) of each lysis buffer solubilised protein sample were taken, and along with the BSA standards were made up to 20 μl with lysis buffer. To each sample and BSA standard 10 μl of 0.1 M HCl and 70 μl of dd H_2O were added. Finally, 900μl of 25 % (v/v) Protein Assay Dye Reagent Concentrate (Bio-Rad Laboratories Ltd.) was added to each sample and BSA standard and mixed before being allowed to stand at room temperature for 10 minutes. The absorbance of each solution was measured at 595 nm and the protein concentration of each sample calculated from the plotted BSA standard data.

2.2.3.3 TCA Lowry protein concentration estimation method

The protein concentration of membrane bound protein samples was estimated using an adaptation of Lowry's method (Lowry *et al*, 1951) as described by Peterson

Table 2.3. Preparation of protein standards and samples for modified Bradford protein concentration estimation.

BSA standard	BSA (μl) of 2 mg/ml stock	Lysis buffer (μl)	0.1 M HCl (μl)	ddH$_2$O (μl)
0 μg	0.0	20.0	10	70
1 μg	0.5	19.5	10	70
2 μg	1.0	19.0	10	70
5 μg	2.5	17.5	10	70
10 μg	5.0	15.0	10	70
20 μg	10.0	10.0	10	70
40 μg	20.0	0.0	10	70

Protein sample	Volume (μl) *	Lysis buffer (μl)	0.1 M HCl (μl)	ddH$_2$O (μl)
A	2.5	15.5	10	70
B	2.5	15.5	10	70
C	2.5	15.5	10	70

* If protein samples are dilute, larger aliquots can be taken for quantification of concentration.

(Peterson, 1979). This method incorporates a deoxycholate-trichloroacetic acid (DOC-TCA) precipitation step to remove lipid and other potentially interfering compounds and is therefore good for analysing membrane bound proteins. The basis for the assay is the reduction of molybdic-tungstic mixed acid chromagen (Folin and Ciocalteu phenol reagent) by tryptophan and tyrosine aromatic amino acid side chains, and the reaction of copper chelates with polar groups and peptide chains. The reduction of the chromagen results in an increase in absorbance at 750 nm which is maximal at 20-30 minutes after initiation.

Protein standards and sample preparation

A standard BSA series ranging 1-80µg and two-three replicates of the protein sample(s) of interest were made. Volumes of each sample were made up to 1 ml with ddH$_2$O

DOC-TCA precipitation

To each 1 ml protein sample and standard, 100 µl of 0.15% (w/v) deoxycholate acid was added, vortexed and allowed to stand at room temperature for 10 min. 100 µl of 72% (w/v) trichloroacetic acid was added and mixed by further vortexing. Samples were centrifuged for 10 min in a microcentrifuge at 13,000 rpm and the supernatant immediately removed.

The Lowry assay

Pellets were re-suspended in 1 ml of solution C (Table 2.4), vortexed and left at room temperature for 5-10 minutes. 100µl of freshly prepared solution D (Table 2.4) was

added and again vortexed. Samples were incubated for 20-30 minutes at room temperature, before measuring the absorbance at 750 nm.

Table 2.4. TCA Lowry assay reagents

Solutions	Constituents
Solution A	0.5 % (w/v) $CuSO_4.5H_2O$ in 1 % (w/v) sodium tartrate
Solution B	2 % (v/v) Na_2CO_3 in 0.1M NaOH
Solution C	Solution A: Solution B, 1:50 ratio (freshly prepared)
Solution D	ddH_2O: Folin-Ciocateu phenol reagent, 1:1 ratio (freshly prepared)

2.2.4. Mini SDS-Polyacrylamide gel electrophoresis (PAGE)

SDS-PAGE analysis of protein samples was performed according to the method of Laemmli (Laemmli, 1970), using Bio-Rad's Mini Protean II vertical gel apparatus (Bio-Rad Laboratories Ltd.).

2.2.4.1 SDS Polyacrylamide gel casting

Gels routinely used were 0.75 mm thick and were composed of a 12 % acrylamide resolving gel and a 5 % acrylamide stacking gel. These were cast using the Mini-Protean II Cell (Bio-Rad Laboratories Ltd.) and the glass casting plates were wiped clean with 70% (v/v) ethanol prior to use. Resolving gel solutions were prepared containing 12 % (w/v) acrylamide (acrylamide:bis-acrylamide 37.5:1) (Bio-Rad Laboratories Ltd.), 0.375 M Tris-HCl pH 8.8, 0.1 % (w/v) SDS, 0.05 % (w/v) ammonium persulphate (Bio-Rad Laboratories Ltd.), and 0.2 % TEMED (Bio-Rad Laboratories Ltd.) in a total volume of 10 ml. Stacking gels were similarly prepared adjusting acrylamide concentration accordingly and containing 0.125 M Tris-HCl pH6.8 as the buffer. Resolving gel solutions were poured into glass cassettes first, onto which 250 µl of water saturated Butan-1-ol was layered. This created an even

surface onto which the shacking gel could be poured. After polymerisation of the resolving gel, the butan-1-ol was rinsed from the glass cassette with dd.H$_2$O. Residual water was removed from the cassette with blotting paper and the staking gel poured. Teflon combs were immediately inserted to create the desired sample wells. Prior to protein sample loading, wells were rinsed with dd.H$_2$O to remove any remaining un-polymerised acrylamide.

2.2.4.2   Protein sample preparation

Protein sample preparation for SDS-PAGE analysis ranged from direct loading of crude *Synechocystis* soluble fractions, to re-solubilisation of precipitated protein samples using 80 % acetone or TCA/acetone procedures, to direct SDS sample loading buffer solubilisation of membrane associated proteins in crude membrane isolates. The quantity of sample analysed also varied from 2.5-50 µg depending on the visualisation method used. Exact sample preparation procedures are included in the appropriate results sections.

Protein samples were solubilised in 5 x SDS sample loading buffer (10 % (w/v) SDS, 5 % (w/v) DTT (Melford Laboratories Ltd.), 0.05 % (w/v) bromophenol blue, 0.312 M Tris-HCl pH 6.8, 50 % (v/v) glycerol) to give a final 1 x concentration and up to a final volume of 25 µl. Before loading onto SDS PAGE gels, samples were boiled for 2 minutes followed centrifugation in a microfuge at full speed (13,000 rpm) for 5 minutes to pellet any insoluble material.

2.2.4.3 Electrophoresis

Samples were electrophoresed using the discontinuous Tris-glycine buffer system of Laemmli (Laemmli, 1970) (25 mM Tris-HCl pH 8.8, 0.1 % (w/v) SDS, 192 mM glycine) kept as a 10 x stock at room temperature. Electrophoresis was conducted at 60 V until the bromophenol blue dye front left the stacking gel, after which the voltage was increased to 120 V until the dye front had reached the bottom of the gel. After electrophoresis, gels were carefully detached from the apparatus and proteins visualized by either Coomassie Blue R-250, silver-staining or SYPRO™ Ruby staining (see section 2.2.7).

2.2.5 Mini two-dimensional gel electrophoresis (2-DE)

Mini two-dimensional electrophoresis (2-DE) was performed using a MultiPhor™ II Electrophoresis Unit with an accompanying Immobiline™ DryStrip kit (Amersham Biosciences) for first dimension IEF and a Mini Protean II vertical gel apparatus (Bio-Rad Laboratories Ltd.) for second dimension SDS-PAGE. First dimension protein resolution via IEF was conducted using 7 cm Immobiline™ Dry strips (Amersham Biosciences) with linear pH gradients of 3-10, 4-7 and 6-11. These strips are also known as immobilised pH gradient (IPG) strips and the use of specific pH ranges are indicated in the appropriate results section.

2.2.5.1 Protein sample preparation

Precipitated protein samples were air dried and solubilised in lysis buffer (9M urea, 2M thiourea, 4% (w/v) CHAPS) by vortexing for 2-24 hours at room temperature. Insoluble material was removed by centrifugation in a microfuge at full speed (13,000 rpm) for 10 minutes at room temperature. The supernatants were transferred to fresh

microfuge tubes and the protein concentration determined via modified Bradford assay (see section 2.2.3.2).

2.2.5.2   In-gel rehydration protein loading

Dry 7 cm IPG strips (Amersham Biosciences) were rehydrated with 125 µl of rehydration solution (9M urea, 2M thiourea, 4% (w/v) CHAPS, 1% (w/v) DTT (Melford Laboratories Ltd.), 2% (v/v) IPG Buffer (Pharmalyte), 0.002 % (w/v) bromophenol blue) containing the desired quantity of lysis buffer solubilised protein sample. DTT, Pharmalytes and protein sample were all added fresh to the rehydration solution, immediately prior to rehydration. The pH range of the Pharmalytes used corresponded to the pH gradient of the IPG strip being rehydrated. Dry IPG strip rehydration was conducted in an Immobiline™ DryStrip Reswelling Tray (Amersham Biosciences). Prior to use, the reswelling tray was rinsed thoroughly with detergent followed by dd.H₂O removing any residual DryStrip cover fluid and blotted dry. Each sample was pipetted into a separate grove of the reswelling try and the IPG strip placed on top gel-face-down. Care was taken to avoid trapping bubbles underneath the strip which would result in uneven sample uptake. Finally, each strip was covered with 2 ml of DryStrip Cover Fluid (Amersham Biosciences) and left over night.

Various protein quantities were loaded into 7 cm IPG strips depending on the indented stain used for visualisation of resolved proteins. For Coomassie Brilliant Blue staining 200 µg of protein was routinely loaded, where as for silver staining 20 µg of protein was used and finally for SYPRO™ Ruby staining 50 µg of protein was loaded. These differences in protein quantity reflect the sensitivity of the stain.

2.2.5.3   Preparation and running of 1st dimension IEF

The ceramic cooling plate of the MultiPhor™ II Electrophoresis Unit (Amersham Biosciences) was connected to a Grant thermostatic circulating water bath (Grant Instruments Ltd., 29 Station Road, Shepreth, Roysten, Hertfordshire, SG6 6P2, UK). This continually circulated water maintained at 20°C through the cooling plate and prevented gels from over heating during IEF. The position of the ceramic cooling plate was ensured to be level before 3-4 ml of DryStrip cover fluid (Amersham Biosciences) was pipetted onto the surface of the cooling plate. Onto this the Immobiline™ DryStrip tray (Amersham Biosciences) was placed, where the formation of bubbles was avoided. Into the try, 10 ml of DryStrip cover fluid was poured, on top of which the DryStip aligner was placed groove-side-up, taking care to avoid forming any air bubbles between the tray and aligner.

The hydrated IPG strips were removed from the reswelling tray and rinsed with dd.H_2O to wash off any remaining sample which may cause streaking during subsequent IEF. Residual fluid was removed from the strip by blotting on damp 3 mm blotting paper. It was necessary to use damp blotting paper in order to prevent the gel surface from sticking and being damaged. Strips were immediately transferred into the prepared DryStrip aligner and positioned gel-side-up and orientated so the acidic (pointed) end was at the anode and the basic (flat) end was at the cathode. When focusing multiple IPG strips simultaneously, strips were aligned so that all anodic ends were level. Electrode wicks (Amersham Biosciences) were cut to 110 mm in length, soaked with dd.H_2O and blotted to remove excess water as this can cause streaking. These moistened wicks were placed across each end of the aligned IPG strips, where wicks were at least partially in contact with the gel surface of each strip.

The anode and cathode electrodes were placed in contact with the corresponding wick and strips were completely submerged with DryStrip cover fluid (Amersham Biosciences). The length of time which rehydrated strips were not immersed under DryStrip cover fluid was kept to a minimum. This was done to avoid formation of urea crystals in the gel, which could affect subsequent IEF.

Isoelectric focusing was performed using a 3-step program, the intricacies of which varied for each pH gradient i.e. pH 3-10 (Table 2.5a), pH 4-7 and pH 6-11 (Table 2.5b).

2.2.5.4 IPG strip equilibration for SDS PAGE

Focused IPG strips were removed from the DryStip aligner and rinsed with dd.H_2O to wash off residual DryStrip cover fluid. Equilibration of these strips for SDS PAGE involved sequentially soaking in two solutions of equilibration buffer (6 M urea, 30% (v/v) glycerol, 2 % (w/v) SDS, 50 mM Tris-HCl pH 8.8, 0.002 % (w/v) bromophenol blue), the first containing 1% (w/v) DTT (Melford Laboratories Ltd.) and second containing 4.8% (w/v) iodoacetamide. These two incubations were performed in an Immobiline™ DryStrip Reswelling Tray (Amersham Biosciences), where each strip was immersed in 2 ml of each solution and was gently agitated using an orbital shaker at room temperature for 15 minutes each.

2.2.5.5   Preparation and running of 2nd dimension SDS PAGE

Mini SDS-PAGE gels were prepared as described previously in the mini SDS-PAGE protocol (section 2.2.4.1). Equilibrated IPG strips were rinsed with dd.H_2O and aligned on top of Mini-Protean II (Bio-Rad Laboratories Ltd.) 12% acrylamide

Table 2.5a. Mutiphor™ IEF program for 7 cm pH 3-10 IPG strips.

Phase	Volts (V)	Current (μA/strip)	Power (W)	Time[a] (hrs:mins)	Volt hours (Vh)
1	200	50	5	0:01	1
2	3,500	50	5	5:00	2,800
3	3,500	50	5	5:00	3,700
Total				10:01	6,501

Table 2.5b. Multiphor™ IEF program for 7 cm pH 4-7 and pH 6-11 IPG strips.

Phase	Volts (V)	Current (μA/strip)	Power (W)	Time[a] (hrs:mins)	Volt hours (Vh)
1	200	50	5	0:01	1
2	3,500	50	5	5:00	2,800
3	3,500	50	5	8:00	4,400
Total				13:01	7,201

[a] Time is not the limiting factor determining the length of the IEF run; therefore it is always grossly in excess. Volt hours determine the length of the run.

resolving gels. The void volume in the glass cassettes above the resolving gels was filled will dd.H$_2$O to facilitate the layering of IPG strips. The water was drained off, taking care not to dislodge the IPG strip, and residual fluid was removed by blotting with filter paper. The IPG strip was sealed in place by covering with agarose sealing solution (1 % (w/v) low melting point agarose, 0.002 % (w/v) bromophenol blue in Tris-glycine SDS electrophoresis buffer). Gels were electrophoresed using a Mini Protean II vertical gel apparatus (Bio-Rad Laboratories Ltd.) in a Tris-glycine electrophoresis buffer (25 mM Tris-HCl pH 8.8, 0.1 % (w/v) SDS, 192 mM glycine) at 60 V for 30 minuets followed by 120 V until the bromophenol blue dye front reached the bottom of the gel. Upon completion of the second dimension, SDS gels were removed and the resolved spots visualised with either Coomassie Brilliant Blue or silver staining (see section 2.2.7).

2.2.6 Large format two-dimensional gel electrophoresis

In this thesis, large format 2-DE was performed using two different systems for both IEF and SDS-PAGE. For first dimension IEF a MultiPhor™ II Electrophoresis Unit (Amersham Biosciences) and an Ettan™ IPGphor™ Isoelectric Focusing System (Amersham Biosciences) were utilised. For second dimension SDS-PAGE a Hoefer™ DALT Large Format Vertical System (Amersham Biosciences) and an Ettan™ DALT*twelve* Large Format Vertical System (Amersham Biosciences) were employed. Both in gel rehydration (IGR) and cup loading methods were used to load protein samples into IPG strips for large format 2-DE and 18 cm Immobiline™ Dry strips (Amersham Biosciences) with linear pH gradients of 3-10, 4-7 and 4.5-5.5 were used. Also both acrylamide and Duracryl (Patton *et al.*, 1991) were utilised at 12 % and 15 % concentration for second dimension separation. The methodology for these

techniques is described below, but the application of these various methods is stipulated in the appropriate result sections.

2.2.6.1 Protein sample preparation

Protein samples were prepared as previously described in the mini 2-DE protocol (section 2.2.4.2).

2.2.6.2 In-gel rehydration protein loading

Dry 18 cm IPG strips (Amersham Biosciences) were rehydrated in an Immobiline™ DryStrip Reswelling Tray (Amersham Biosciences) with 340 µl of rehydration solution (9M urea, 2M thiourea, 4% (w/v) CHAPS, 1% (w/v) DTT (Melford Laboratories Ltd), 2% (v/v) IPG Buffer (Pharmalyte), 0.002 % (w/v) bromophenol blue) containing the desired quantity of lysis buffer solubilised protein sample.

2.2.6.3 Anodic cup sample loading

Cup sample loading was only performed using an Ettan™ IPGphor™ IEF system (Amersham Biosciences). Dry 18 cm IPG strips were rehydrated in an Immobiline™ DryStrip Reswelling Tray (Amersham Biosciences) with 340 µl of rehydration solution (9M urea, 2M thiourea, 4% (w/v) CHAPS, 1% (w/v) DTT (Melford Laboratories Ltd), 2% (v/v) IPG Buffer (Pharmalyte), 0.002 % (w/v) bromophenol blue). DTT and IPG Buffer were added fresh, immediately prior to rehydration. The pH range of the IPG Buffer corresponded to the pH gradient of the IPG strip being rehydrated. Strips were immersed with 2 ml of DryStrip Cover Fluid (Amersham Biosciences) and left over night.

Rehydrated IPG strips were removed from the Immobiline™ DryStrip Reswelling Tray (Amersham Biosciences) and individually transferred to separate ceramic IPGphor™ Cup Loading Strip Holders (Amersham Biosciences). Strips were positioned gel-side-up and with the basic (flat) end flush with the flat end of the strip holder. Electrode wicks, 5 mm x 15 mm, soaked with dd.H₂O were blotted with filter paper to remove excess water (which may cause horizontal streaking) and placed at the acidic and basic ends of each strip. Electrodes were clipped firmly onto each electrode wick ensuring a good contact. Sample loading cups were positioned at the anodic end of each strip, as close to the electrode wick as possible without actually touching it. Cups were filled with DryStrip Cover Fluid and the level of fluid monitored to identify any leaks between the sample cup and IPG strip. If leaks were detected, the DryStrip Cover Fluid was removed and the cup repositioned. Once good seals were obtained, strips were immersed in at least 4 ml of DryStrip Cover Fluid, ensuring the entire strip was completely submerged. Prepared protein samples solubilsed in Rehydration buffer (9M urea, 2M thiourea, 4% (w/v) CHAPS, 1% (w/v) DTT (Melford Laboratories Ltd), 2% (v/v) IPG Buffer (Pharmalyte), 0.002 % (w/v) bromophenol blue) to a maximum final volume of 100 μl were pipetted into the bottom of each sample cup. The clear plastic strip covers were positioned over each strip holder and at which point were ready to load on the Ettan™ IPGphor™ IEF unit for first dimension IEF.

2.2.6.4   First dimension IEF using a MultiPhor™ II Electrophoresis unit

Rehydrated 18 cm IPG strips containing protein sample were prepared for IEF using a MultiPhor II Electrophoresis Unit (Amersham Biosciences) as previously described

for mini 2D-E (see section 2.2.5.3). Isoelectric focusing was performed using a 3-step program (Table 2.6a).

2.2.6.5   First dimension IEF using an Ettan™ IPGphor™ IEF system

IPGphor Strip Holders containing the rehydrated IPG strips and samples were positioned onto the Ettan IPGphor unit in the correct orientation. Isoelectric focusing of protein samples through 18 cm IPG strips using this apparatus was conducted at 50 μA/strip for 70 kVh at 20°C using a 5–step program (Table 2.6b).

2.2.6.6   IPG strip equilibration for SDS PAGE

Focused IPG strips were removed and rinsed with dd.H_2O to wash off residual DryStrip cover fluid. Equilibration of these strips for SDS-PAGE involved sequentially soaking in two solutions of equilibration buffer (6 M urea, 30 % (v/v) glycerol, 2 % (w/v) SDS, 50 mM Tris-HCl pH 8.8, 0.002 % (w/v) bromophenol blue), the first containing 1% (w/v) DTT (Melford Laboratories Ltd.) and second containing 4.8% (w/v) iodoacetamide. These two incubations were performed in Equilibration tubes (Amersham Biosciences) for 15 minutes each, where each strip was immersed in 5 ml of solution and was gently agitated at 100 rpm using an orbital shaker at room temperature.

2.2.6.7   Second dimension SDS PAGE using a Hoefer™ DALT system

Large format SDS PAGE gels were cast the day before their intended use to ensure complete polymerisation, using a DALT Multiple gel caster (Amersham Biosciences) and DALT glass cassettes 240 x 200 x 1.5 mm (Amersham Biosciences). Before casting, glass cassettes were wiped clean with 1 % (v/v) Decon™, rinsed with

Table 2.6a. Multphor™ II IEF program for 18cm IPG strips.

Phase	Volts (V)	Current (μA/strip)	Power (W)	Time[a] (hrs:mins)	Volt hours (Vh)
1	500	50	5	0:01	1
2[b]	3,500	50	5	5:00	3,000
3[b]	3,500	50	5	30:00	67,000
Total				35:01	70,001

[a] Time is not the limiting factor determining the length of the IEF run; therefore it is always grossly in excess. Volt hours determine the length of the run.
[b] No difference between phases 1 and 2 except time. The purpose of the two phases is to allow the user to monitor the main stage of the IEF run and alter it if they see fit.

Table 2.6b. Ettan™ IPGphor™ IEF program for 18cm IPG strips[c].

Step	Step Type (gradient or step n' hold)	Volts (V)	Time (hrs:mins)
1	GRADIENT	500	00: 10
2	GRADIENT	1,000	01: 20
3	GRADIENT	4,000	01: 40
4	Step n' Hold	6,500	10: 00
5	Step n' Hold	1,000	60: 00

[c] Ettan™ IPGphor™ IEF program was performed over night for at least 70 kVh, which equalled ~15 hours.

dd.H$_2$O, soaked in 1 % HCl (v/v) for 1 hour followed by a final rinsing with dd.H$_2$O and subsequently dried using a lint free tissue. This was done to remove any residual polyacrylamide from previous experimentation and ensure glass cassettes were clean. Resolving gel solutions, both acrylamide and Duracryl, were prepared as indicated in Table 2.7a and Table 2.7b, adjusting the quantity as required and initially omitting APS and TEMED from the mix. This solution was degassed by vacuum suction for a minimum of 1 hour to remove air which inhibits the polymerisation process. During this time the DALT gel casting apparatus was prepared, inserting the required number of cassettes and filling the remaining space with acrylic blocks. The resolving gel solution was poured into the DALT casting apparatus at a constant steady pace reducing the addition of bubbles into the system until the level reached approximately 4 cm from the top of the cassette. Displacing solution (375 mM Tris-HCl pH 8.8, 50 % glycerol, 0.002 % (w/v) bromophenol blue) was then used to force the remaining acrylamide solution out of the bottom reservoir and into the glass cassettes until the level reach 1cm from the top of the cassette. Finally, 1 ml of water saturated Butan-1-ol was layered on top of each gel to create an even surface onto which the IPG strip could be layered. Gels were allowed to polymerise overnight, after which the butan-1-ol was rinsed from the glass cassette with dd.H$_2$O.

Equilibrated IPG strips were rinsed with dd.H$_2$O and aligned on top of the cast gels. The void volume in the glass cassettes above the resolving gels was filled will dd.H$_2$O to facilitate the layering of IPG strips. The water was drained off, taking care not to dislodge the IPG strip, and residual fluid was removed by blotting with filter paper. The IPG strip was sealed in place by covering with agarose sealing solution (1 % (w/v) low melting point agarose, 0.002 % (w/v) bromophenol blue in Tris-glycine

Figure 2.7a. Composition of large format 12 % and 15 % acrylamide SDS-PAGE gels.

Constituent	12 % Acrylamide		15 % Acrylamide	
	Volume (ml)	Final conc.	Volume (ml)	Final conc.
10 % (v/v) SDS	10	1 %	10	1 %
1.5 M Tris-HCL pH 8.8	250	375 mM	250	375 mM
40 % (v/v) acrylamide[a]	300	12 %	375	15 %
dd.H$_2$O	434	-	359	-
10 % (v/v) APS[b]	5	0.01 %	5	0.01 %
TEMED[b]	1	0.001 %	1	0.001 %
Total	1000		1000	

Figure 2.7b. Composition of large format 12 % Duracryl (Genomic Solutions) SDS-PAGE gels.

Constituent	12 % Duracryl	
	Volume (ml)	Final conc.
10 % (v/v) SDS	10	1 %
1.5 M Tris-HCL pH 8.8	250	375 mM
30 % (v/v) Duracryl[c]	400	12 %
dd.H$_2$O	334	-
10 % (v/v) APS[b]	5	0.01 %
TEMED[b]	1	0.001 %
Total	1000	

Materials were obtained from BDH Chemicals Ltd. ([a]), BioRad Laboratories Ltd. ([b]) and Genomic Solutions ([c]).

[a] Acrylamide:bis-acrylamide = 37:1
[b] Added immediately prior to casting.
[c] Acrylamide:bis-acrylamide = 37.5:1

SDS electrophoresis buffer). Gels were electrophoresed using a Hoefer™ DALT Large Format Vertical System (Amersham Biosciences) requiring 20 litres of Tris-glycine electrophoresis buffer (25 mM Tris-HCl pH 8.8, 0.1 % (w/v) SDS, 192 mM glycine) at 20 mA per gel for approximately 15 hours until the bromophenol blue dye front reached the bottom of the gel. Upon completion of the second dimension, SDS gels were removed from the glass cassettes taking care not to tare the gel and the resolved spots visualised with either Coomassie Brilliant Blue, silver or SYPRO™ ruby fluorescence staining (see section 2.2.7).

2.2.6.8   Second dimension SDS-PAGE using a Ettan™ DALT*twelve* system

Large format SDS-PAGE gels were cast in an Ettan™ DALT*twelve* gel caster and using both Ettan™ DALT glass cassettes and low fluorescence glass cassettes (260 x 200 mm) 1.5 mm and 1 mm thick, respectively. The 1 mm thick low fluorescence cassettes were used to generate analytical fluoresce gels either as DIGE gels or backed SYPRO™ Ruby stained gels (see section 2.2.6.9). The 1.5 mm thick cassettes were used to generate preparative gels for spot picking, the extra thickness reduced the tendency of the gel to tare.

Gels were cast and IPG strips inserted as described in the Hoefer™ DALT protocol above. Electrophoresis was conducted using an Ettan™ DALT*twelve* Large Format Vertical System (Amersham Biosciences) requiring 7.5 litres of Tris-glycine electrophoresis buffer (25 mM Tris-HCl pH 8.8, 0.1 % (w/v) SDS, 192 mM glycine) in the bottom reservoir of the tank and 2.5 litres of 2 x Tris-glycine electrophoresis buffer in the top reservoir of the tank. Gels were electrophoresed at 25°C at 5 W per gel for 30 minutes followed by 17 W per gel for 4 hours or until the bromophenol

blue dye front reached the bottom of the gel. Usually, 1.5 mm thick gels took longer to run than 1 mm gels. Upon completion of the second dimension, DIGE gels were imaged directly within the glass cassette (see section 2.2.11.6), backed gels were stained attached to the glass plate with SYPRO™ Ruby and 1.5 mm preparative gels were removed from the glass cassette and stained with either Coomassie blue, silver or SYPRO™ Ruby (see section 2.2.7).

2.2.6.9   Preparation of backed gels

Backed gels were generated by smearing 2-4 ml of Bind-silane solution (80 % (v/v) ethanol, 0.01 % (v/v) PlusOne Bind-Silane (Amersham Biosciences), 0.2 % (v/v) glacial acetic acid) using a CREW® wipers lint free tissue over the entire surface of the low fluorescence glass plate without attached 1 mm spacers. The solution was subsequently allowed to dry for 1.5 hours underneath a CREW® wipers lint free tissue to prevent dust from sticking to the plate. Glass cassettes were prepared and the gels cast in the usual way.

2.2.7   In-gel protein staining methods

2.2.7.1   Coomassie Brilliant Blue R-250 protein staining

SDS PAGE gels were treated sequentially with three different Coomassie solutions designated Coomassie I, II, and III (Table 2.8). This sequential staining method enhances protein staining by gradually destaining the background and thus is more sensitive than conventional Coomassie staining techniques. Solutions were pre-heated in a microwave oven on full power for 2 min, before incubating the gel by gentle agitation for 20-30 min. After the third incubation, gels were subjected to a prolonged

incubation in the destaining solution (Table 2.8) until all background had diapered. The volume of stain used depended of the size of the gel, typically 100 ml and 500 ml were used for mini and large format gels, respectively. Coomassie solutions were re-used but fresh solutions were made when separated protein bands/spots were intended for mass spectrometry analysis.

Table 2.8. Coomassie Blue protein staining solutions.

Ingredient	Coomassie Solutions			
	I	II	III	Destain
Coomassie Stock solution [a]	2%	0.25%	0.25%	-
Propan-2-ol	25%	10%	-	-
Glacial acetic acid	10%	10%	10%	10%
Glycerol	-	-	-	10%

[a] 1.25% (w/v) Coomassie brilliant blue R-250,

2.2.7.2 Disruptive silver staining of SDS PAGE separated proteins

This silver staining method is according to Heukeshoven and Dernik (1988), with some modifications. Following electrophoresis gels were removed from the apparatus and placed in fixing solution (40 % (v/v) ethanol, 10 % (v/v) glacial acetic acid) for a minimum of 30 minutes. Fixed gels were transferred to a sensitising solution (30 % (v/v) ethanol, 0.13 % (w/v) glutaraldehyde, 6.8 % (w/v) sodium acetate·$3H_2O$, 0.2 % (w/v) sodium thiosulphate·$5H_2O$) and incubated for 30 minutes to over night. Gels were washed three times in fresh dd.H_2O, 5 minutes for each wash, before incubating in silver nitrate solution (0.1 % (w/v) silver nitrate, 0.008 % (w/v) formaldehyde) for 40 minutes. After a brief rinse in dd.H_2O, gels were incubated in developing solution (2.5 % (w/v) anhydrous sodium carbonate, 0.004 % (w/v) formaldehyde) for up to 15 minutes. The time required to develop the stained proteins varied, but the reaction was

allowed to continue until protein bands/spots were dark without the background darkening. The developing reaction was stopped by transferring gels into stop solution (1.46 % (w/v) EDTA-Na$_2$·2H$_2$O) for 10 minutes. Gels were washed twice in ddH$_2$O, 10 minutes for each wash, before preserving by soaking the gels in 10 % (v/v) Glycerol. All solutions were made fresh and all incubations and washes were performed with gentle agitation. After staining gels were scanned (see section 2.2.8.2) and then either dried directly (see section 2.2.7.5) or stored in heat sealed polythene bags.

If gels were over stained they could be de-stained with Farmer's reducer solution (0.15 % (w/v) potassium hexacyanoferrate III, 0.3 % (w/v) sodium thiosulphate and 0.05 % (w/v) sodium carbonate) and then re-stained by proceeding with the above method immediately after the sensitising step.

2.2.7.3   MS compatible silver staining of PAGE separated proteins

This protein staining method was performed according to the PlusOne® Silver Staining Kit (Amersham Biosciences) and is similar to the modified silver staining protocol of Shevchenko (Shevchenko *et al.*, 1996b). Unlike conventional silver staining (see section 2.2.7.2) this method is compatible with mass spectrometry techniques due to the omission of glutaraldehyde, a peptide cross linking reagent, from the sensitising solution. However as a side effect, this reduces the sensitivity of the stain.

Following electrophoresis gels were fixed twice in fresh fixing solutions (40 % (v/v) methanol, 10 % (v/v) glacial acetic acid) for 15 minutes each and may be left

overnight. Fixed gels were transferred to a sensitising solution, absent of glutaraldehyde (30 % (v/v) methanol, 6.8 % (w/v) sodium acetate·3H$_2$O, 0.2 % (w/v) sodium thiosulphate·5H$_2$O) and incubated for 30 minutes. Gels were washed 3 times in fresh dd.H$_2$O, 10 min for each wash, before incubating in 0.5 % (w/v) silver nitrate for 40 minutes. After twice rinsing in dd.H$_2$O, 1 minute for each wash, gels were incubated in developing solution (2.5 % (w/v) anhydrous sodium carbonate, 0.008 % (w/v) formaldehyde) for up to 15 minutes. The time required to develop the separated proteins varied, but the reaction was allowed to continue until protein bands/spots were dark without the background darkening. The developing reaction was stopped by transferring gels into stop solution (1.46 % (w/v) EDTA-Na$_2$·2H$_2$O) for 10 minutes. Gels were washed three times in dd.H$_2$O, 10 minutes for each wash, before preserving by soaking the gels in 10 % (v/v) Glycerol. All solutions were made fresh and all incubations and washes were performed with gentle agitation.

2.2.7.4 SYPRO™ Ruby Fluorescent stain for SDS PAGE gels

SYPRO™ Ruby fluorescent stain (Genomic Solutions) has a level of sensitivity greater than Coomassie but less than silver (Steinberg *et al.*, 1996a, 1996b; Patton, 2001). However; it is compatible this MS techniques and has a wide dynamic range for quantification.

After electrophoresis gels were fixed twice in fresh fixing solutions (40 % (v/v) methanol, 10 % (v/v) glacial acetic acid) for 2 hours each. Fixed gels were incubated in SYPRO™ Ruby Protein Stain (Genomic Solutions Ltd., 8 Blackstone Road, Huntingdon, Cambridgeshire, PE29 6EF, UK) over night in a light minimal environment. After removal of SYPRO™ Ruby stain, gels were rinsed twice with

dd.H$_2$O, for 1 minute each, before incubating in destaining solution (10 % (v/v) methanol, 6 % (v/v) acetic acid) for 1-2 hours. All solutions were made fresh and all incubation and washing steps were performed with constant gentile agitation. Staining was performed in polypropylene or polycarbonate trays, as glass interferes with the staining process. Gels were imaged directly at 100 nm resolution using a Typhoon 9200 imager (Amersham Pharmacia Biosciences) or ProXPRESS imager (Genomic Solutions) (see section 2.2.8.3) and subsequently stored in the plastic staining trays or heat-sealed plastic bags in 2 % (v/v) glycerol. SYPRO™ Ruby stain was reused several times, but was filtered beforehand due to the stains tendency to precipitate during use. The precipitate can stick to the surface of the gel and interfere with the image. After considerable reuse, the stain became less concentrated and was therefore supplemented with fresh stain at 5-10 % (v/v) concentration.

2.2.7.5   Drying of PAGE mini gels

Gels were held between water soaked sheets of cellophane using an Easy Breeze™ drying frame (Hoefer Scientific Instruments, 654 Minnesota Street, San Francisco, CA) and dried in a Hoefer Easy Breeze™ Gel Dryer.

2.2.8   Gel Imaging

2.2.8.1   Transferring gels into scanning apparatus

Gels were always handled with gloves as fingerprints can mark the gel and keratin proteins in hair can contaminate protein samples intended for MS identification. When handling fluorescently labelled gels powder-free gloves were worn as the powder used in laboratory gloves can fluoresce and can also cause light scattering,

both which can affect image quality. Loose polyacrylamide gels were transferred onto the various scanning surfaces using a nylon mesh. This was positioned underneath the gel whilst in the staining tub and used to lift the gel out of the tube and place onto the desired scanning surface. This method dramatically reduced the possibility of tearing gels whilst handling them.

2.2.8.2 Coomassie and silver stained gels

Gels stained with Coomassie Brilliant Blue or silver were imaged using either an ImageMaster scanner (Amersham Biosciences) with Power Scan software (Non Linear Dynamics, Newcastle, UK) or a ProXPRESS Imager (Genomic Solutions) with ProFinder software (Genomic Solutions).

Image Master

Gels were scanned at 300 dpi using an Image Master flat bed scanner (Amersham Biosciences) and Phoretix Power Scan V 3.01b software (Non Linear Dynamics) and were saved as 16 bit TIF files.

ProXPRESS Imager

Gels were transferred into the scanning glass cassette, imaged on the hollow adaptor base plate and orange flat field acrylic sheet with bottom illumination using the 530/30 emission filter at 100 μm resolution and typically a 10 second exposure time. The resultant gel scans were 16-bit images, i.e. each pixel had a value between 1 and 65,536. The image exposure time was varied in order to achieve maximal use of this 16-bit dynamic range and yet avoid pixel saturation (i.e. > 65,536). Images were saved as 16-bit TIF files.

The ProXPRESS imager illuminates the gel with UV light and therefore when scanning Coomassie or silver stained gels a UV to white light conversion plate was used. To image gels, the ProXPRESS uses a high resolution camera which photographs the gel in sections. As a result uneven illumination occurs across the frame in the camera's filed of view. To correct for this, the ProFinder software uses a pre-captured image of the empty glass cassette, called a "flat field image", as a base line. These 16-bit TIF flat field images were generated at the start of each scanning session, using the same parameters as used for scanning the intended gel. The exposure time varied to obtain a peak pixel range of 30,000 – 40,000.

2.2.8.3   SYPRO™ Ruby stained gels

SYPRO™ Ruby stained polyacrylamide gels were imaged using either a ProXPRESS Imager (Genomic Solutions, Huntingdon, UK) with ProFinder software (Genomic Solutions) or a Typhoon Variable Mode Imager (Amersham Biosciences).

ProXPRESS Imager

A flat field image was generated prior to scanning the gel (see section 2.2.8.2). Gels were transferred to the scanning glass cassette, imaged on the solid base plate and green flat field acrylic with top illumination using the 480/30 excitation filter and 620/30 emission filter at 100 μm resolution and typically exposed for 10 seconds. However, image exposure time was varied in order to achieve maximal use of the 16-bit dynamic range and yet avoid pixel saturation (i.e. > 65,536). Images were saved as 16-bit TIF files.

Typhoon 9200 Variable Mode Imager – in fluorescence acquisition mode

Both backed gels and loose gels, stained with SYPRO™ Ruby, were imaged using a Typhoon Variable Mode Imager and the specific parameters used to scan these different gel types are detailed bellow. In preparation for scanning the Typhoon Imager was allowed to warm up for 30 minutes and the glass platen scanning surface was wiped using a CREW® wipers lint free tissue with 70 % (v/v) ethanol to remove any particles that may fluoresce. Gels were scanned in fluorescence acquisition mode at normal sensitivity and using the scan parameters listed in Table 2.9. Pre-scans at 1000 μm pixel resolution were initially performed and subsequently analysed using ImageQuant software (Amersham Biosciences) to aid the identification of a suitable photon multiplier tube (PMT) voltage. Higher 100 μm resolution scans with maximum pixel values > 60,000 but < 100,000* were subsequently obtained using the identified PMT value. These images were ideal for analysis and saved as ".gel" modified 16 bit TIF files.

Scanning of loose SYPRO™ Ruby stained polyacrylamide gels

After de-staining, gels were transferred onto a low fluorescence glass plate (dimensions: 290 x 250 mm), previously wiped clean using a CREW® wipers lint free tissue with 70 % (v/v) ethanol. Any bubbles between the gel and the glass plate were removed. This was subsequently transferred onto the glass platen scanning surface of the Typhoon imager. Plastic spacers, 1 mm thick, were positioned at each corner between the glass plate and glass platen to set the height of the gel at 3 mm and allow for a 3 mm focal plane scan. The scanning area was selected using the user select function in the tray selection window and the sample pressing option was turned off.

Table 2.9. **Typhoon imaging parameters for visualisation of fluorescently labelled proteins.**

Dye/Stain	Emission filter (nm)	Laser
Cy2	520 BP 40	Blue 2 (488)
Cy3	580 BP 30	Green (532)
Cy5	670 BP 30	Red (633)
SYPRO Ruby	610 BP 30	Blue 1 (457)

Scanning of backed SYPRO™ Ruby stained polyacrylamide gels

Polyacrylamide gels were backed onto low fluorescence glass plates prior to electrophoresis and stained attached to the glass plate. After de-staining, the glass plate surface was wiped dry with a CREW® wipers lint free tissue. Gels were transferred onto the glass platen of the Typhoon imager glass face down and positioned between the gel alignment guides. Gels were scanned using the 3 mm focal plane and the predefined single DIGE Ettan DALT tray selection area.

2.2.9   Radiochemical methods

2.2.9.1   *In vivo* L-[^{35}S] labelling of *Synechocystis de novo* synthesised proteins

Preparation of cultures

Glass test tubes (125 ml) containing 50 ml of sterilised BG-11 media were inoculated with *Synechocystis* cells to a starting A_{730} of ~ 0.02. These cultures were incubated within the Cyanobacterial culture apparatus under normal growth conditions at 34°C, illuminated with 70 µE m^{-2} s^{-1} PAR and gassed with 1% CO_2 in air. Cultures were grown for approximately 2 days until culture turbidity (A_{730}) was ~ 1.0.

Radiolabelling

Labelling was conducted in the cyanobacterial growth apparatus within a laboratory fume cupboard. The extractor fan of the fume cupboard was used to draw away any radioactive gas that may be produced. Redivue™ PRO-MIX™ L-[^{35}S] *in vitro* Cell Labelling Mix (Amersham Biosciences) was used as the labelling reagent with a specific activity > 37 TBq mmol^{-1} (1000 Ci mmol^{-1}). This reagent contains both L-

[^{35}S] methionine and L-[^{35}S] cysteine in a ratio of approximately 70:30. To each 50 ml gassed *Synechocystis* culture 125 µCi of Redivue PRO-MIX was added. For heat shock experiments, cells were immediately exposed to elevated temperature once radioactivity had been added. Aliquots of cells were removed from the labelled cultures at set points and transferred to pre-chilled falcon tubes containing 50 µl of 100 mM non-radioactive (cold) L-methionine. Cells were collected by centrifugation and 4,500 *g* for 15 minutes and the supernatant discarded according to correct radiochemical disposal procedure. Cells were washed with ice cold extraction buffer, re-collected and frozen in liquid nitrogen. Quantities of radioactivity remaining in culture media and incorporated into cells and proteins was measured using a 1600 TR liquid scintillation analyser (Packard, Brook House, 14 Station Road, Pangbourne, Berkshire, UK) by analysing 10 µl or 20 µl aliquots of sample mixed with 4 ml of scintillate compared against a blank control.

Isolation of radiolabelled proteins

Cells were broken with glass beads as described in section 2.2.2.1 and broken cells were fractionated into soluble and membrane isolates as described in section 2.2.2.3.

2.2.9.2   Autoradiography

SDS-PAGE and 2-D gels of radiolabelled *Synechocystis* proteins were stained with Coomassie Brilliant Blue, dried between cellophane sheets (see section 2.2.7.5) and exposed to X-ray Hyperfilm™ (Amersham Biosciences) for 2 days. Films were developed in a solution of 20 % (v/v) Ilford Phenisol high contrast film developer (Ilford, Moberly, Cheshire, UK) and fixed in a solution of Kodak Unifix (Kodak-

Pathé, 26e rue Villiot, Paris) using a Compact X4 automatic x-ray film processor (X-ograph Imaging Systems, Malmesbury, Wiltshire SN16 9JS).

2.2.10   Image analysis

2.2.10.1   Analysis of 1D gels

Phoretix 1D Advance software V 5.00 (Non Linear Dynamics) was used to analyse 16 bit TIF images of 1D (SDS-PAGE) gels. Lanes and protein bands were automatically detected and background subtracted using the valley to valley algorithm.

2.2.10.2   Analysis of 2D gels

Phoretix Evolution software (Non Linear Dynamics) was used to analyse large format 2D gels. Spots were automatically detected, background subtracted using the 'mode of non-spot' algorithm and volume normalised using the 'total spot volume x 100' parameter. Average gels were generated for differential analysis of repeat experiments.

2.2.11   2-D Difference gel electrophoresis (DIGE)

2-D DIGE technology (Unlu *et al.*, 1997; Tonge *et al.*, 2001) involves the differential labeling of different protein samples allowing their comparison in a singe 2D gel and the subsequent detection of changes in proteomes. Protein samples are labeled with Cyanine dyes and the methodology for protein labeling, 2-DE of labeled samples, fluorescent imaging of DIGE gels and software analysis are described bellow.

2.2.11.1 Sample clean up and preparation for CyDye DIGE minimal dye labelling

Lysis buffer (9 M urea, 2 M thiourea, 4 % (w/v) CHAPS) solubilised protein samples intended for CyDye DIGE Fluor minimal dye labeling were first cleaned using Amersham's 2-D Clean-Up kit (Amersham Biosciences). This precipitates the protein removing any compounds that may affect the CyDye labelling process and was performed according to the manufactures recommendations. Protein pellets were dried in air for 2-5 minutes, taking care not to over dry, and solublised by vortexing for 2 hours in labelling buffer (9 M urea, 2 M thiourea, 4 % (w/v) CHAPS, 25 mM Tris-HCL pH 9.5) to a protein concentration between 5-10 mg/ml. Labelling buffer was prepared by adding 25 μl of a 1 M Tris-HCl pH 9.5 stock solution to 1 ml of lysis buffer. The pH of these protein samples was measured by pipetting a small volume, typically 1 μl, onto pH indicator strips (pH 7-14) and adjusted, if necessary, using 1 M NaOH to between pH 8.0-9.0. This was essential for optimal CyDye labelling. Because the majority of *Synechocystis* soluble proteins have an acidic pI, the pH of these samples containing 100 μg of total protein was routinely adjusted using 1 μl of 1 M NaOH. Furthermore, *Synechocystis* soluble protein samples are blue in colour, due to the presence of the phycobilisome proteins, which affected pH determination using colour pH indicator strips. Therefore, to dilute the colour, 10 fold dilutions of protein samples in lysis buffer (not containing 25 mM Tris-HCl pH 9.5) were analysed. Finally the protein concentration was quantified by modified Bradford assay.

2.2.11.2 Reconstitution of stock CyDye DIGE Fluor minimal dyes in dimethylformamide (DMF)

CyDye DIGE Fluor minimal dyes (Amersham Biosciences) (here after referred to as Cy-Dyes) are supplied as solids and are reconstituted in DMF for use. The storage and reconstitution of Cy-Dyes is important to the success of sample labelling. If low quality DMF is used or the Cy-Dyes are incorrectly stored, protein labelling will not be efficient. High quality DMF ($\leq 0.005\%$ H_2O, $\geq 99.8\%$ pure) was used and care was taken to ensure it was not contaminated with water. Furthermore, DMF once opened will start to degrade generating amine compounds. Amines will react with the Cy-Dyes reducing the concentration of dye available for protein labelling. Therefore a new bottle of DMF was used every 3 months.

Stock solutions

Cy-Dye vials (Cy™2, Cy3 and Cy5) were removed form the freezer and allowed to equilibrate to room temperature for 5-10 minutes. This prevented exposure of the dyes to condensation which may have caused hydrolysis. Vials were centrifuged briefly in a microcentrifuge at full speed (13,000 rmp) to collect the dye powder at the bottom before opening. Vial contents were resuspended in N,N-dimethylformamide (anhydrous 99.8 %) by vortexing for 30 seconds to prepare a primary stock of 1 nmol/µl (1 mM). This dye stock was stable for 2 months at -20°C and for storage vials were sealed with Parafilm and placed in a heat sealed bag containing desiccant. After reconstitution in DMF the Cy-Dyes were deep colours; Cy2-yellow, Cy3-red, Cy5-blue.

Stock dye solutions were removed form the freezer, allowed to equilibrate to room temperature for 5-10 minutes and centrifuged to collect the contents to the bottom. Cy-Dye working solutions of 400 pmol/µl (0.04 mM) were prepared where typically 2 µl of Cy-Dye was diluted with 3 µl of DMF. However, this did vary depending on the number of labelling reactions. These working dye solutions were stable for approximately 2 weeks at -20°C.

2.2.11.3 Protein labelling with the CyDye DIGE Fluor minimal dyes

To comply with the recommended 2-D DIGE experimental design, control samples were labelled with Cy3, treated samples were labelled with Cy5 and a pooled internal standard was created containing equal quantities of all samples and labelled with Cy2. Sufficient internal standard must be prepared to allow enough to be included on every gel in the experiment. In the following text I describe the method used for a 5 gel experiment where 5 control and 5 treated samples were labelled, however for different sample numbers, labelling reaction volumes were adjusted accordingly. For this particular 5 gel experiment labelling reactions were routinely performed in 19 µl for Cy3 and Cy 5 and 95 µl for Cy2 where the ratio of dye to protein was maintained at 400 pmol dye:50 µg protein.

Volumes of each protein sample equivalent to 50 µg were dispensed into fresh microfuge tubes, made up to 18 µl with labelling buffer, mixed by vortexing and placed on ice. To prepare the pooled standard, volumes of each protein sample equivalent to 25 µg were dispensed into the same microfuge tube, made up to 90 µl with Labelling buffer, mixed by vortexing and placed on ice. To each control sample

1 μl (400 pmol) of Cy3, to each treated sample 1 μl of Cy5 and to the polled standard 5 μl of Cy2 working dye solutions were added. Samples were mixed thoroughly by vortexing and incubated on ice for 30 min in the dark. After this time, labelling reactions were stopped by addition of 10 mM L-lysine, the volume of which was identical to the amount of dye added, i.e. 1 μl for Cy3 and Cy5 labelled samples and 5 μl for the Cy2 labelled sample. Therefore, final sample volumes were 20 μl for control (Cy3) and treated (Cy5) samples and 100 μl for the pooled standard (Cy2) where the protein concentration was 2.5 μg/μl in each case. Samples were mixed by vortexing and left of ice and in the dark for a further 10 minutes, after which they were stored at -70 °C in the dark where they were stable for at least 3 months.

Samples were labelled (by adding the appropriate Cy-Dye) and stopped (by adding the appropriate volume of 10 mM L-lysine) sequentially with 1 minute intervals between each sample. This was done to ensure each sample was labelled for the correct amount of time.

2.2.11.4 Labelling efficiency quality control

To check the labelling efficiency, each sample was resolved via SDS-PAGE and visualised using a Typhoon 9200 Variable Mode Imager (Amersham Biosciences). Because the samples were solubilised in urea (Lysis buffer) which interferers with electrophoresis, they were precipitated with 80 % (v/v) acetone and re-dissolved in 1 x SDS-loading buffer before running.

To a 1 μl aliquot of each Cy labelled sample containing 2.5 μg of protein, 50 μl of dd.H$_2$O, 200 μl of ice cold acetone and 5 μl of 1.5 M Tris-HCl pH 8.8 were added.

Samples were mixed by briefly vortexing and left on ice for 10-20 minutes. Precipitated protein was collected by centrifugation in a microcentrifuge at 13,000 rpm for 5 minutes. The supernatants were discarded and the pellets allowed dried in air for 2-5 minutes before being re-solubilised in 1 x SDS sample loading buffer (see section 2.2.4.2) and boiled for 2 minutes. Samples were loaded onto 12 % resolving gels and electrophoresed as described in section 2.2.4.3. Resolved protein bands were visualised using a Typhoon Variable Mode Imager (Amersham Biosciences) directly on the glass platen in fluorescence acquisition mode using the Cy-Dye detection parameters listed in Table 2.9.

2.2.11.5 Large format 2-DE of Cy-Dye labelled protein samples

Equal 12.5 μg quantities of control (Cy3 labelled) and treated (Cy5 labelled) samples from the same experiment were mixed together with the same quantity (12.5 μg) of pooled internal standard (Cy2 labelled). The protein concentration of all labelled samples was 2.5 μg/μl (see section 2.2.11.3); therefore 12.5 μg protein quantities equated to 5 μl sample volumes. Consequently each sample mix contained a total of 37.5 μg of protein in a total of 15 μl. To these samples, 1.4 μl of fresh 50 % (w/v) DTT (Melford Laboratories Ltd) in Lysis buffer and 1.4 μl of IPG Buffer (Ampholytes) were added (final concentrations 1 % (w/v) DTT and 2 % (v/v) Ampholytes) and each sample was made up to a final volume of 70 μl with rehydration buffer (9M urea, 2M thiourea, 4% (w/v) CHAPS, 0.002 % (w/v) bromophenol blue). Samples were mixed by briefly vortexing and centrifuged for 3 minutes in a microcentrifuge at 13,000 rpm to pellet any insoluble material. Samples were loaded on to pre-hydrated IPG strips via an anodic sample cup and focused using an Ettan™ IPGphor IEF system (Amersham Biosciences) (see section 2.2.6.3). IPG

strips were equilibrated and electrophoresed using an Ettan™ DALT*twelve* system (Amersham Biosciences) (see section 2.2.6.8) and the fluorescently labelled resolved protein spots were detected using a Typhoon variable mode imager (Amersham Biosciences) (see section 2.2.11.6).

2.2.11.6 Imaging of large format 2-D DIGE gels using a Typhoon Variable Mode Imager

In preparation for scanning the Typhoon Variable Mode Imager was allowed to warm up for 30 minutes and the glass platen scanning surface was wiped using CREW® wipers lint free tissue with 70 % (v/v) ethanol to remove any particles that may fluoresce. Immediately after electrophoresis the low fluorescence glass cassettes were removed from the Ettan™ DALT electrophoresis unit and rinsed with distilled H₂O. When handling these cassettes powder free gloves were worn as the powder used in laboratory gloves can fluoresce and may also cause light scattering which can affect image quality. The Typhoon imager can only scan two DIGE gels simultaneously and therefore the reaming gels waiting to be scanned were rapped in Clingfilm™ and stored at 4°C in the dark. Before scanning the low fluorescence glass cassettes were wiped dry with lint free tissue and positioned onto the glass platen scanning surface between the gel alignment guides. DIGE gels were scanned in fluorescence acquisition mode using the 3 mm focal plane and the predefined DIGE Ettan™ DALT tray selection area specifying the boundaries of each gel. It was necessary to set the 3 mm focal plane in order to focus the scanning laser onto the gel surface between the glass cassettes. Gel cassettes were also pressed while scanning to prevent them from shifting and distorting the gel image.

The three Cy images (Cy™2, Cy3 and Cy5) for each gel were obtained by scanning at normal sensitivity and using the scan parameters listed in Table 2.9. Pre-scans at 1000 μm pixel resolution were initially performed for each Cy image. These rapid scans were not suitable for quantitative analysis, but when analysed using ImageQuant software (Amersham Biosciences) gave an approximation of the expected signal values. This aided the identification of a suitable photon multiplier tube (PMT) voltage which achieved the target maximum pixel value of 50,000 – 60,000. This usually equated to a maximum pixel value between 60,000 – 90,000 on subsequent higher 100 μm resolution scans. Providing maximum pixel values did not exceed 100,000 these gel images were acceptable for quantitative analysis using DeCyder™ Differential Analysis software (Amersham Biosciences). Once the PMT voltages for each Cy image had been optimised for one gel, these settings were used for all other gels within the same experiment. However, to enable accurate quantification of spot volumes, the maximum pixel values for all Cy images had to be above 60,000 but below 100,000. Therefore, if necessary, different PMT settings were used for different gels in the same experiment.

2.2.11.7 DeCyder™ Differential Analysis

2-D DIGE gels were saved as data set file formats (.ds files) and cropped using ImageQuant Tools software (Amersham Biosciences). Spot detection, matching and volume abundance quantification was conducted across multiple 2-D DIGE gels using DeCyder™ Batch processor software (Amersham Biosciences). This required previous estimation of total spot number obtained from analysis of a single DIGE gel via DeCyder™ DIA software (Amersham Biosciences). Quantification of average changes in protein abundance between control and treated samples across multiple

repeat 2-D DIGE gels was automatically calculated using DeCyder™ BVA software. This software also determined the variance of the average data using a statistical paired T-test. Spots showing a > 1.10 fold (10 %) change in abundance and a > 95 % statistical confidence were selected for identification via MS.

2.2.12 Excision of proteins from SDS-polyacrylamide gels for peptide mass fingerprinting mass spectrometry (PMF-MS)

2.2.12.1 Staining and handling considerations of polyacrylamide gels intended for PMF-MS

SDS-PAGE gels intended for protein excision were stained with fresh solutions in polypropylene tubs previously scrubbed clean with 1 % (v/v) Decon and rinsed with dd.H$_2$O. To reduce the extent of keratin contamination, gels were kept immersed in dd.H$_2$O in sealable staining tubes at all times and handling of gels was kept to a minimum. When gels were handed it was always with laboratory gloves as protein samples can be contaminated with keratin.

2.2.12.2 Manual excision of protein bands from mini SDS PAGE gels

Excision of protein bands from min 1D gels was performed within a laminar flow sterile air cabinet. Acrylamide gels were transferred onto a glass plate previously wiped clean with 70% (v/v) ethanol and rinsed with dd.H$_2$O and protein bands were excised using a separate fresh razor blade for each band. Any excess acrylamide was trimmed off and the gel slices were subsequently transferred into separate un-autoclaved 0.5 ml microfuge tubes, pre-rinsed with dd.H$_2$O immediately prior to use. Gel pieces were submerged with 100 µl of dd.H$_2$O and stored at 4°C.

2.2.12.3 Manual excision of protein spots from large format 2D gels

Large format 2D gels were transferred from the staining tub on to a low fluorescence glass plate (290 x 250 mm) previously wiped clean with 70 % (v/v) ethanol and rinsed with dd.H_2O. Due to the fragile nature of large format polyacrylamide gels, a sheet of nylon mesh was used to transfer the gel from the staining tub onto the glass plate (see section 2.2.8.1). Manual excision of protein spots was performed within a lamina flow sterile air cabinet and spots were excised using One Touch Plus Spot Picking Pipettes (The Gel Company, San Francisco, California, USA) into separate wells of a 96 well microtitre plate (Genomic Solutions) where separate fresh picking tips were used for each spot. Laboratory gloves were worn at all times to avoid keratin contamination and the 2-D gel was periodically spayed will dd.H_2O to prevent dehydration.

2.2.12.4 Robot excision of protein spots from large format 2D gels

Large format 2D gels were transferred from the staining tub using a sheet of nylon mesh on to a low fluorescence glass plate (290 x 250 mm) previously wiped clean with 70 % (v/v) ethanol and rinsed with dd.H_2O. Reference holes in each corner of the gel were made and the gel was subsequently imaged using a ProXPRESS imager (Genomic solutions). This image was imported into Phoretix Evolution software (Non Linear Dynamics, Newcastle, UK) and spots selected for identification were detected on the gel image. Following this, the same gel was imaged using the CCTV camera of the ProPick spot picking robot (Genomic Solutions). This image was imported into the Phoretix Evolution software and using the triangulation algorithm and reference holes spots selected for picking were automatically located on the ProPick image. The generated predicted spot boundaries and centres were manually checked before exporting the picking list coordinates to the ProPick robot. During picking the gel was

periodically spayed with dd.H_2O to prevent it from dehydrating and spots were excised into separate wells of a 96 well microtitre plate (Genomic solutions).

2.2.13 Peptide mass fingerprinting mass spectrometry (PMF-MS)

All mass spectrometry and associated procedures reported in this thesis were performed by Dr J. W. Simon (University of Durham, Biological and Biomedical Sciences, South Road, Durham).

2.2.13.1 Automated in-gel tryptic digestion of protein spots excised from polyacrylamide gels in preparation for (PMF-MS)

Microtitre plates containing gel plugs were transferred to a ProGest Workstation (Genomic Solutions) for automated tryptic digestion and peptide extraction according to the ProGest long trypsin digestion protocol. This involved the following steps. Fist gel plugs were equilibrated in 50 µl of 50 mM ammonium bicarbonate which neutralises the acid from the destain solution. Samples were subsequently reductively alkylated with solutions of 10 mM DTT and 100 mM iodoacetamide, followed by destain and desiccation with acetonitrile. Gel plugs are re-hydrated with 50 mM ammonium bicarbonate containing 6.6 % (w/v) trypsin (Promega, Delta House, Chilworth Science Park, Southampton, SO16 7NS, UK) and digested overnight. Following digestion peptides were extracted from the gel plugs with a solution of 50 % (v/v) acetonitrile, 0.1 % (v/v) TFA into a final volume of 50 µl (2 x 25 µl extractions) and lyophilised in a vacuum concentrator. Samples were re-suspended in 10 µl of 0.1 % formic acid and sonicated in an ultra sonic water bath for 1 minute. In this form samples are used directly for both MALDI and MS-MS analyses.

If gel plugs were from silver stained gels an addition de-staining step was introduced at the beginning of the above method. This involved incubation in 50 µl of 300 mM potassium ferricyanide, 100 mM sodium thiosulfate for 10 minutes followed by twice rinsing with dd.H$_2$O to remove the de-staining reagents.

2.2.13.2 Matrix assisted laser desorption/ionisation time of flight peptide mass fingerprinting (MALDI-ToF PMF)

MALDI-ToF PMF was performed using a Voyager-DE™ STR BioSpectrometry™ Workstation (Applied Biosystems, Warrington, Cheshire, UK). MALDI target plates were prepared for sample application using the thin film MALDI target spotting methodology (Vorm et al., 1994). This involved preparing a solution of 2 parts nitrocellulose solution (1 g nitrocellulose dissolved in 100 ml of 50 % (v/v) acetone, 50 % (v/v) isopropanol) and 3 parts saturated α-cyano-4-hydroxy-cinnamic acid solution in acetone (thin film mix) and applying approximately 0.3 µl of this thin film mix onto each MALDI grid position. Following this, 0.5 µl of each concentrated tryptic digest was spotted directly onto separate MALDI grid positions and left to dry of 60 minutes. Each spot was subsequently washed with 5 µl of ice cold 0.1 % (v/v) TFA which acts to remove any salt from the samples. The TFA was subsequently removed and samples allowed to dry.

Spectra were acquired from 480 laser shots using system parameters optimised for the mass range 800-3500 amu. Automated peak detection, noise reduction and peak de-isotoping was subsequently performed on the obtained spectra using Applied Biosystems Data Explorer software. Following this the de-isotoped spectra were internally calibrated using the trypsin autolysis peaks 842.5100 and 2211.1046 m/z

present in the spectra and the resultant calibrated peak list of peptide masses for each sample were used in a MASCOT (www.matrixscience.com) database search of all entries available in the NCBInr database using a mass accuracy of 50 ppm.

2.2.13.3 Liquid chromatography electrospray ionisation tandem mass spectrometry (LC ESI MS-MS) sequencing

Mass spectroscopic peptide separation and sequencing was carried out on a QSTAR PULSARi™ quadrupole time of flight mass spectrometer (Applied Biosystems coupled to an UltiMate™ nano HPLC workstation (LC Packings, Abberdann 144, 1046AA Amsterdam, Netherlands). Following digestion 7.0 µl of each concentrated tryptic peptide digest was loaded into the auto sample which injected 5 µl of digest dirrectly onto a C18, 5 µm PepMap™ nano-precolum (LC Packings). This column was previously washed of salts with 400 µl of 0.5 % (v/v) acetonitrile, 0.05 % (v/v) TFA. Sample was eluted from the 5 µm PepMap™ nano-precolum with a 6 ml linear gradient of 5 % (v/v) acetonitrile, 0.05 % (v/v) TFA to 65 % (v/v) acetonitrile, 0.05 % (v/v) TFA through a flow splitter and onto a C18, 3 µm PepMap™ nano-column (LC Packings) for direct infusion at 200 nl/min through a nano-spray tip into the mass spectrometer.

TOF mass spectra were collected between the mass range 100-2000 amu throughout the gradient elution. Precursor ion selection and product ion spectra were generated using Applied Biosystems BioAnalyst™ software's fully automated switching and acquisition procedures. Only multiply charge precursor ion species were selected for fragmentation and peptide sequencing. For protein identification all Ms-MS product ion spectra generated from each sample were used in a MASCOT

(www.matrixscience.com) database search of all entries available in the NCBInr database.

2.2.13.4 MASCOT database searches and protein identification

Protein identification was attained from both MALDI-PMF and LC MS-MS peptide mass data using the MASCOT (www.matrixscience.com) mass spectrometry database search software to interrogate all available entries in the NCBInr database (www.ncbi.nlm.nih.gov). For MALDI-PMF data, MASCOT database searches were performed allowing for single miss cleavages, oxidised methionines and carboxylmethyl cysteines as potential modifications and data was required to match at better than 50 ppm mass accuracy. For LC MS-MS data, the same modifications were allowed for and precursor ion masses together with all un-interpreted MS-MS fragmentation spectra for peptides eluted during the gradient were used in the search.

MASCOT reports the results with a probability based score, the MOWSE score (Pappin *et al.*, 1993) derived from all the parameters in the data which match the search criteria. The number of peptides which match, the number of fragment ions which match, the accuracy at which the ions match and a weighting for matching of large peptide fragments all contribute to this score. The higher the score the more significant the identification (hit) and the less likely it is a result of a random event. Several hits were obtained for each set of data searched and the highest scoring hit was usually considered as the positive hit.

CHAPTER 3

Establishment of Large Scale Growth, Controlled Culture Conditions, Cellular Subfractionation and Proteomic Analysis of Soluble and Membrane Associated Proteins in *Synechocystis* sp. PCC6803.

3.1 Introduction

All organisms in nature experience continual changes in their immediate environment and depending on their geographical location, risk exposure to extremes of temperature, chemical and gas concentration, nutrient and water availability, radiation and hydrostatic pressure. Animals exposed to such fluctuations in their environment have the ability to move or adopt other behaviours enabling them to avoid such stress-inducing conditions by exploiting temperate microhabitats in otherwise stressful environments (Feder and Hofmann, 1999). Plants on the other hand do not have such luxury to change location (other than through seeds or pollen) and are limited in their ability to adjust heat exchange with their environment. Therefore, in order to survive in ever changing surroundings, photosynthetic organisms have evolved a variety of molecular mechanisms to sense and respond to environmental changes.

Of the many adaptive strategies to changing environmental factors, high temperature resistance of plants is of great economic importance and it is commonly accepted that photosynthesis is the most heat-sensitive biological activity of green cells (Yordanov *et al.*, 1986). Cyanobacteria have a remarkable capacity to adapt to a wide range of environmental conditions and this together with their ease of growth and genetic manipulation mean that cyanobacteria have been extensively used to study the heat shock and heat acclimatisation strategies of photosynthetic organisms. Moreover, investigations utilising unicellular cyanobacteria such as *Synechocystis* and *Synechococcus* species are particularly common due to their ideal characteristics as model research systems. Despite this, little progression has been made in

understanding the mechanisms of high temperature perception and acclimatisation/survival strategies in these organisms.

A large proportion of the data on heat shock and heat acclimatisation responses of photosynthetic organisms has been obtained from genomic and transcriptomic studies. However, it is the proteins that perform cellular functions and few studies have been conducted into "global" changes at the protein level. It has been shown that there can be little correlation between the messenger RNA (mRNA) abundance and protein levels in cells (Haynes et al., 1998, Gygi et al., 1999b; Pennington and Dunn, 2001). Consequently, studies at the transcriptome level would miss vital cellular changes. Furthermore, postranslational modifications, of which there are over 400 different possible types, including acylation, phosphorylation, glycosylation and peptide cleavage can often alter the function and cellular localisation of the modified protein (Haynes et al., 1998; Pennington and Dunn, 2001). Consequently, examination of the changes in cellular mRNA levels in response to elevated temperature will not necessarily reflect the changes in protein diversity, thus requiring examination at the protein level.

The proteomic methodology of two-dimension gel electrophoresis (2-DE) in combination with peptide mass fingerprinting (PMF) has been employed in this investigation in order to discover and characterise the protein responses to elevated temperature. This methodology was chosen for this investigation for two reasons. Firstly, the alternative method of protein identification, Edman N-terminal sequencing, has many disadvantages compared to peptide mass fingerprinting. It has a lower level of sequence coverage and therefore a reduced level of confidence in

protein identities, a lower level of sensitivity and there are also inherent problems with obtaining sequence data from N-terminally blocked proteins (Brown, 1979; Brown and Roberts, 1976). Secondly, 2-DE and peptide mass fingerprinting technology was established in the laboratory, providing an ideal environment for this study. However, both 2-DE and peptide mass fingerprinting techniques would require optimisation for the specific samples under investigation. Development of 2-DE methodology was achieved in this study by conducting a series of experiments, testing a variety of different techniques to establish gel reproducibility and optimal resolution. PMF technology was tested to ascertain the success rate of positive protein identifications, to determine the level of sensitivity and to ensure it could be used as a high throughput method for obtaining protein identifications in this organism.

Fundamental to any proteomic investigation is the availability of amino acid sequence data for the organism under study, this can be derived from either expressed sequence tags (ESTs), whole genome sequencing experiments or protein sequence data. Organisms with an incompletely sequenced genome have a limited number of proteins that can be positively identified which therefore affects the success of a proteomic study. *Synechocystis* sp. PCC 6803 has a completely sequenced genome (Kaneko *et al.*, 1995, 1996) available through the CyanoBase database (www.kazusa.or.jp/cyano/ cyano.html) (Nakamura *et al.*, 1998) and therefore it should be possible to match each protein to its corresponding gene. Analysis of the *Synechocystis* genome using GeneQuiz (http://jura.ebi.ac.uk:8765/ext-genequiz/) has revealed that function has only been assigned to 64 % of the proteins by homology to proteins from other organisms (Iliopoulos *et al.*, 2000). The remaining 36 % encompasses those proteins with no assigned function, whether they have homology

to proteins with no known function (18 %) or have no homologues (18 %). With a third of the proteins assigned as hypothetical, their encounter is highly likely in a proteomic investigation. This is obviously a complication when attempting to elucidate the cellular response to elevated temperature. However, their expression is interesting as they add previously unknown entities to the response being studied and data concerning the regulation of their expression contributes to elucidating their function.

In order to perform an extensive proteomic investigation on *Synechocystis* it was essential to grow large scale cultures capable of generating sizable and unlimited quantities of biological material relatively quickly. Because it is well documented that faster cyanobacterial growth and high cell yields can be obtained if cultures are continually gassed with 1% CO_2 in air (Stanier *et al.*, 1971), *Synechocystis* cells were grown in suspension in this way. Without these gassed large scale cultures, sufficient biological material would not have been generated quickly and any analysis would have been difficult and restricted. It was also important to establish a highly reproducible cell culture system, where environmental factors effecting growth, such as temperature and light intensity, were stringently controlled, thus maintaining biological uniformity between cultures grown on different occasions. Furthermore, an investigation into the response to elevated temperature required two separate culture locations where temperature was independently controlled but where all other environmental factors were maintained constant. This would reduce the amount of biological variability between samples in their responses to elevated temperature. Such, a culture system has been developed in Japan by Professor Norio Murata (NIBB, Okasaki, Japan) and has been extensively used in a variety of experiments on

unicellular strains of cyanobacteria, such as *Synechocystis* sp. and *Synechococcus* sp. Through collaboration with this group, a cyanobacterial cell culture apparatus, adapted from Prof. Murata's design, was constructed by John Gillroy, School of Biological and Biomedical Sciences, University of Durham, UK.

The first objective of this investigation was to establish growth and maintenance of *Synechocystis* sp. PCC 6803 within the laboratory and to grow reproducible large scale gassed cultures within a strictly controlled environment for experimental purposes. Other objectives of this chapter were to develop cellular breakage, fractionation and protein extraction methodology capable of generating sufficient quantities of protein for subsequent proteomic analysis, to analyse the complexity of soluble and membrane associated protein fractions via 2-DE, and develop the proteomic methodology for the particular samples under study.

3.2 Results

3.2.1 Growth of *Synechocystis* cultures

Synechocystis cultures were initiated from frozen DMSO stocks and grown using BG-11 media (Allen, 1968) (see material and methods). Cells were maintained on agar plates or slopes (Figure 3.1a) and as 100 ml shaking suspension cultures in 500 ml conical flasks (Figure 3.1b), where it was standard practice to subculture every month using the previous suspension culture as the inoculum. Suspension cultures were shaken at 120 rpm using an orbital shaker (Figure 3.1c) The culture environment was sustained at 32°C within a growth room where a series of fluorescent tubes provided constant illumination at approximately 30 μE m^{-2} s^{-1}.

A purpose built cyanobacteria growth apparatus (adapted from Prof. Norio Muarta's design, NIBB Japan) was constructed to grow large scale *Synechocystis* suspension cultures quickly in a strictly controlled environment for experimental purposes (Figure 3.2). Temperature and light intensity could be kept constant or adjusted accordingly and were maintained at 34°C and 70 μE m^{-2} s^{-1} respectively for normal growth. Temperature was maintained through the use of water baths and two independently controllable baths were available for heat shock experimentation. To limit evaporation of water from the baths and therefore accurately maintain culture temperature, plastic balls were floated on the surface of the water. Illumination was provided laterally from a bank of three white fluorescent tubes positioned either side of the culture. Intensity could be adjusted by selectively switching lights on or off and
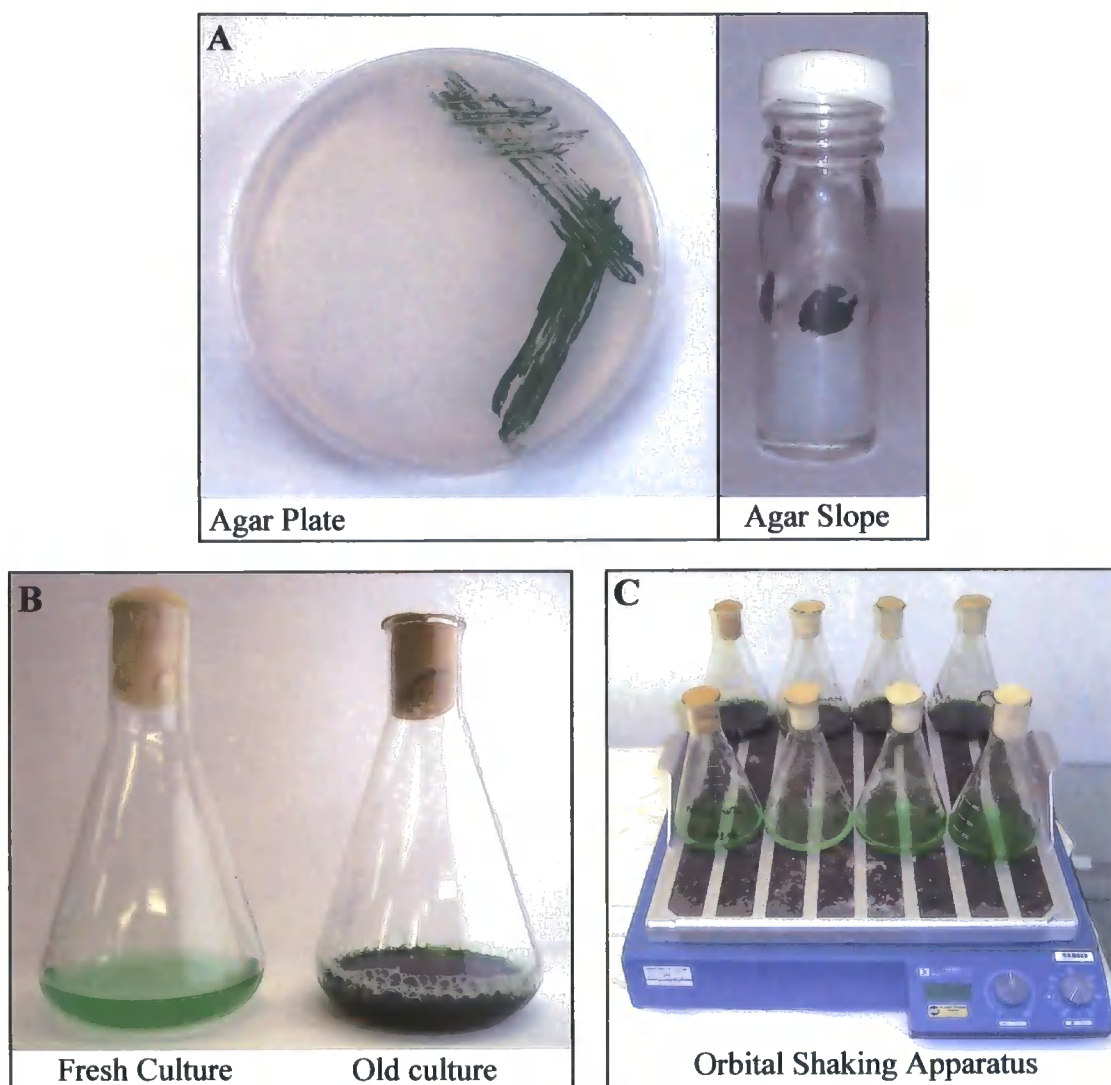
Figure 3.1. Maintenance of *Synechocystis* sp. PCC 6803 cells grown using BG-11 medium on solid agar and as shaking suspension cultures.

Synechocystis cells grown on solid BG-11 media supplemented with 1.5 % (w/v) agar (**A**) and in suspension in 500 ml conical flasks containing 100 ml of liquid BG-11 media (**B**). All cultures were incubated at 32°C under 30 $\mu E\ m^{-2}\ s^{-1}$ light provided by white fluorescent tubes where suspension cultures were continually aerated by shaking at 120 rpm using an orbital shaker (**C**). Growth in this fashion was maintained by inoculating fresh media once a month.

Figure 3.2. Cyanobacterial cell culture system.

A, schematic diagram of the cyanobacterial culture system illustrating aerial and side views. B, Photograph of cyanobacterial culture system. Two water baths were available in the cell culture apparatus, each accommodating a total of 4 test tube cultures and 2 flask cultures (Figure 3.3). Temperature was maintained in each water bath via its own variable heater and could be adjusted accordingly. Water was heated by a heating coil and circulated throughout the bath by an impeller. The presence of two water baths permitted cultures to be grown under normal conditions in one bath and then exposed to elevated temperature in the second bath. For normal growth, temperature was maintained at 34°C. Cultures were illuminated through the use of two banks of three white fluorescent tubes, the intensity from which in the centre of the water bath was adjusted to 70 μE m^{-2} s^{-1} of PAR. Cultures were aerated with moistened 1 % CO_2 in air through a glass delivery tube (Figure 3.3). This gas mix was moistened by being bubbled through sterilised dd.H_2O in order to reduce evaporation from cultures, a side effect of aeration. The gas flow rate could be regulated independently for each *Synechocystis* culture through the use of taps.

A

Key :
- Light Switch
- Culture Vessel Grips
- Variable Water Heater
- Heating Coil & Impeller
- White Fluorescent Tubes
- Gas bubbled through dd. H_2O

Aerial view -

GAS

Air Outlets

Water Baths

Gas Taps

Fans

Side View -

GAS

B

1 % CO_2 in air bubbled through dd. H_2O

Water Baths

Variable Water Heater

Culture Vessel Grips

Air Taps

Culture Vessel

Light Switch
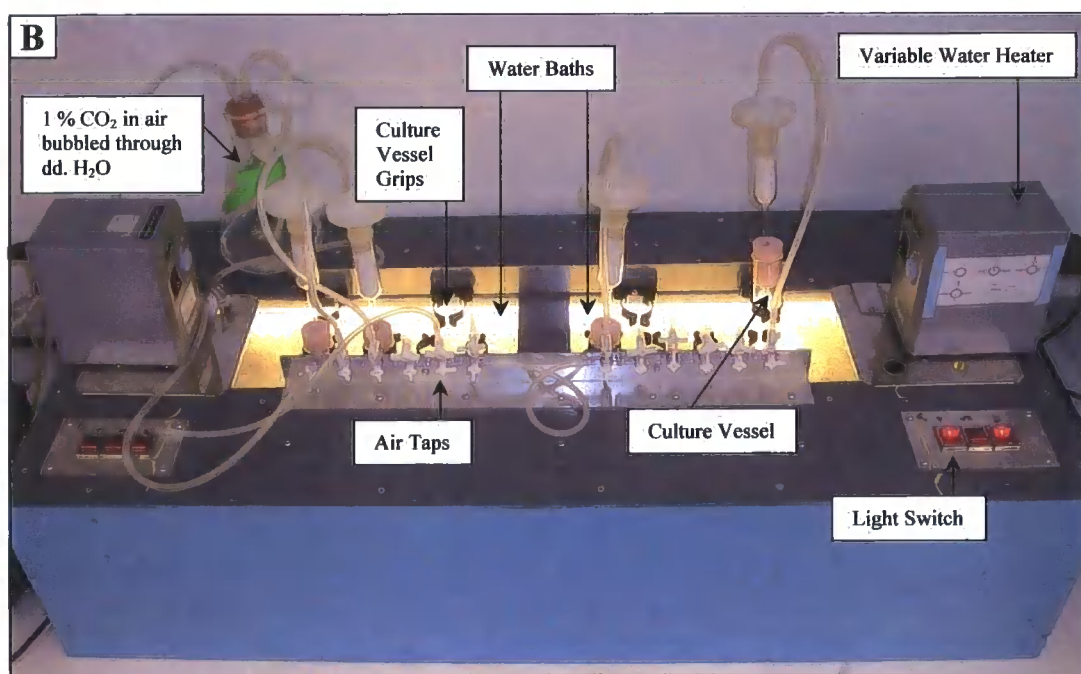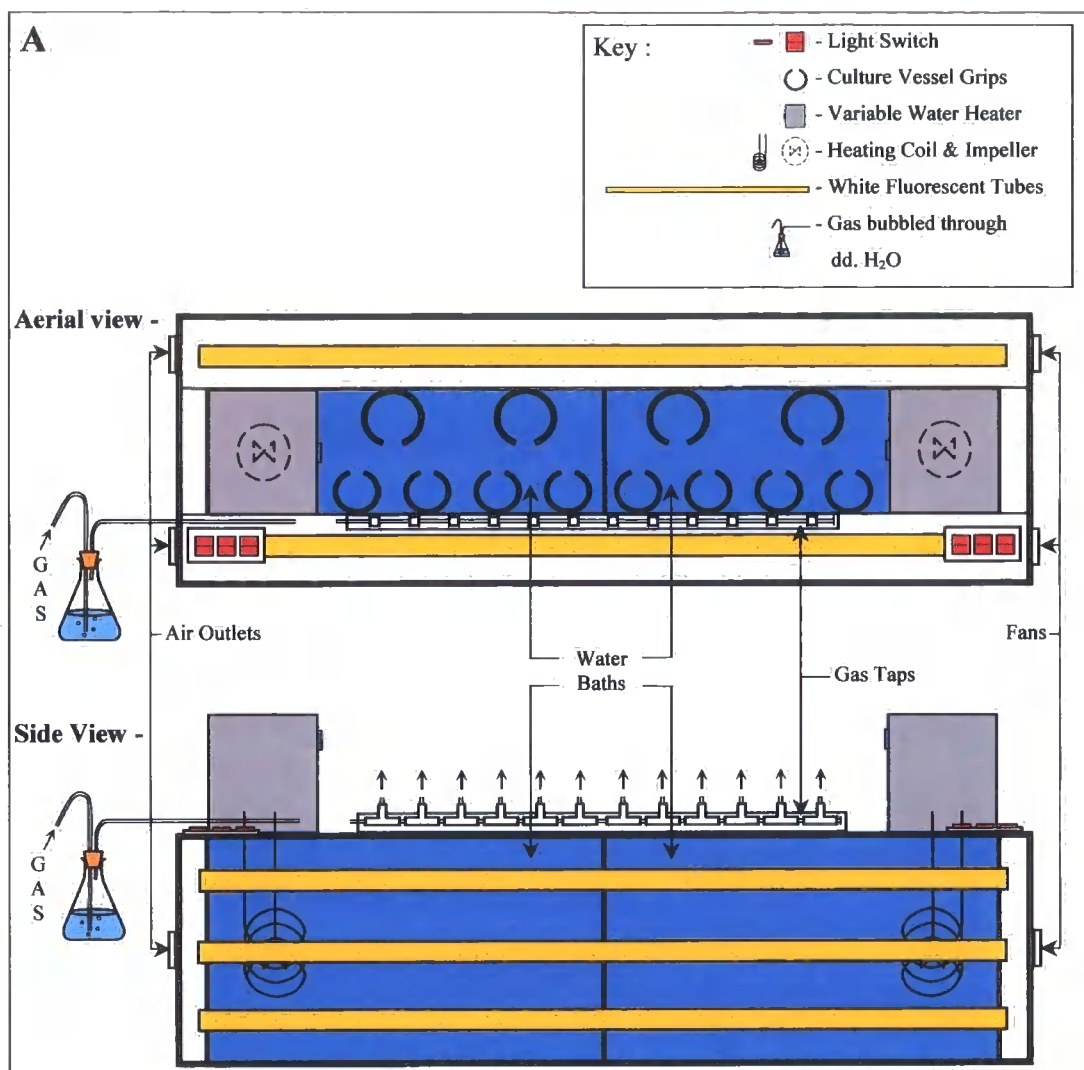
for normal growth, top and bottom fluorescent tubes on both sides of the culture were used. Cultures were grown using 125ml test tubes and 1 litre flasks (Figure 3.3) which were held securely in the water baths by plastic grips and were continuously gassed through a sterile glass tube (Figure 3.3) with 1% (v/v) CO_2 in air for rapid division and as a result were named "gassed cultures". This gas mix was moistened before being introduced into the culture to reduce the extent of evaporation and sterilised by passing through a 50 μm filter. Gas flow rate could be regulated independently for each *Synechocystis* culture through the use of taps. As a general rule the correct gas flow rate was judged to be when approximately 3 bubbles of gas were seen on the surface of the culture at any one time.

The vessels employed for *Synechocystis* growth within this growth apparatus were also purposely designed (Figure 3.3). Culture volumes of 20 – 100 ml could be grown within the 125 ml cultures tubes and large scale 200 ml – 1 litre cultures could be grown in the 1 litre culture vessels (VWR international Ltd, Merck House, Poole, Dorset, BH15 1TD, UK) (Figure 3.3). The latter were adapted by Durham University's glass blowing facility to have a curved base and an extended neck. The curved base was created to facilitate the circulation of cells within the vessel and thus preventing cells from precipitating. The neck of the flask was extended to accommodate the porous bung which supported the gas delivery tube and allowed gas to escape from the culture flask.

Cell growth of *Synechocystis* suspension cultures was monitored by following the change in Absorbance A_{730nm}. Growth of *Synechocystis* gassed cultures followed a classical sigmoid pattern and the exponential growth rate of these cultures

- 135 -
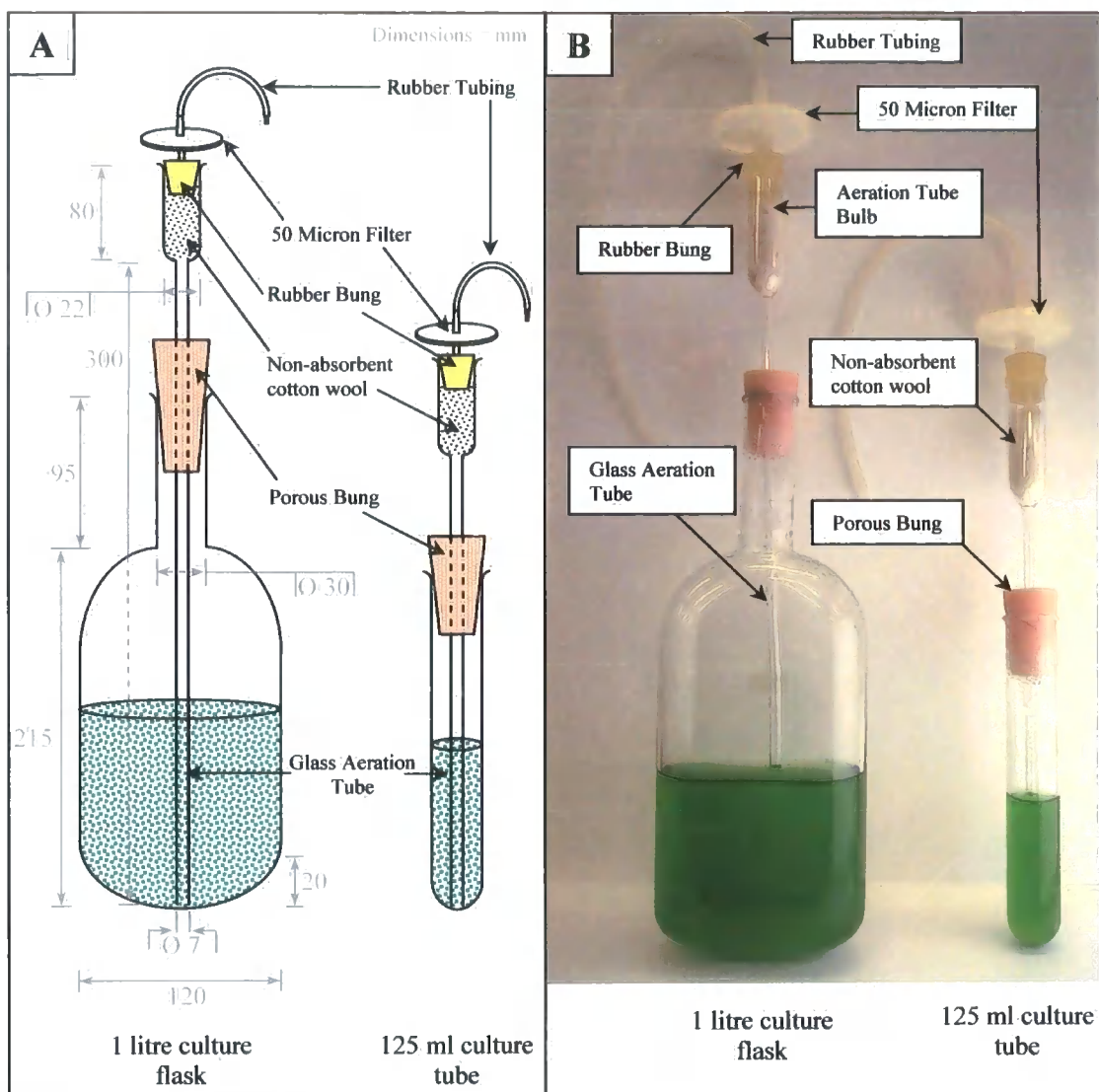
Figure 3.3. *Synechocystis* **aerated suspension cultures.**

A, a schematic diagram of the culture vessels and aeration delivery system used to grow gassed *Synechocystis* suspension cultures. **B**, photograph of the culture vessels and aeration system. *Synechocystis* cells were routinely grown in suspension in 1 litre glass flasks and 125 ml glass test tubes typically containing 500 ml and 50 ml of sterilised BG-ll media, respectively. These cultures were aerated with 1 % CO_2 in air, transported through rubber tubing and introduced into the culture through a sterilised glass tube. This aeration tube was positioned within the vessel so that gas entered at the bottom of the culture which, together with the rounded base of the vessels, circulated the culture and prevented cells from precipitating. Before gas entered the vessel it passed through a double filter system, composed of first a 50 μm filter positioned into the neck of the aeration tube via a rubber bung and second a bung of non-absorbent cotton wool lodged into the aeration tube bulb. The 50 μm filters were sterilised before use and the cotton wool bung was sterilised in position together with the glass aeration tube. The gas bubbled through the culture escaped through a porous bung at the neck of the vessel, which was also sterilised in position with the glass aeration tube.

was far quicker than that of shaking cultures, over 9 times faster (Figure 3.4). Furthermore, higher cell yields could be achieved with gassed cultures with A_{730} exceeding 10.0, where as shaking suspension cultures reached an A_{730} of approximately 6.0, almost half that of gassed cultures (data not shown). *Synechocystis* gassed cultures, upon subculturing, entered a short lag phase for approximately 24 hours, after which time the cultures maintained exponential division for about 4 days. Following this period, the rate of cell growth decreased and the cultures entered stationary growth. In contrast, shaking cultures demonstrated a lag phase for approximately 48 hours, after which they continued to grow exponentially for over 2 weeks. Both culture types displayed minimal variation between replicates, as indicated by the narrow standard error of means. In conclusion, *Synechocystis* cultures demonstrated highly reproducible growth rates. Furthermore, higher cell densities and quicker growth rates could be obtained if cells were grown within the growth apparatus where cultures were continually gassed with 1% (v/v) CO_2 in air.

3.2.2   Cellular breakage

Having established the growth pattern of *Synechocystis* cells (see section 3.2.1), it was important to determine the efficiency and quantity of sample which could be prepared from exponentially growing cultures following cellular disruption. Various techniques exist for cell breakage (for a comprehensive description see Berkelman and Stenstedt, 2001) and have to be optimised as certain techniques are far more efficient than others. This is significant because quantity of sample ultimately determines the extent of the proteomic investigation which can be performed. With a system where sample
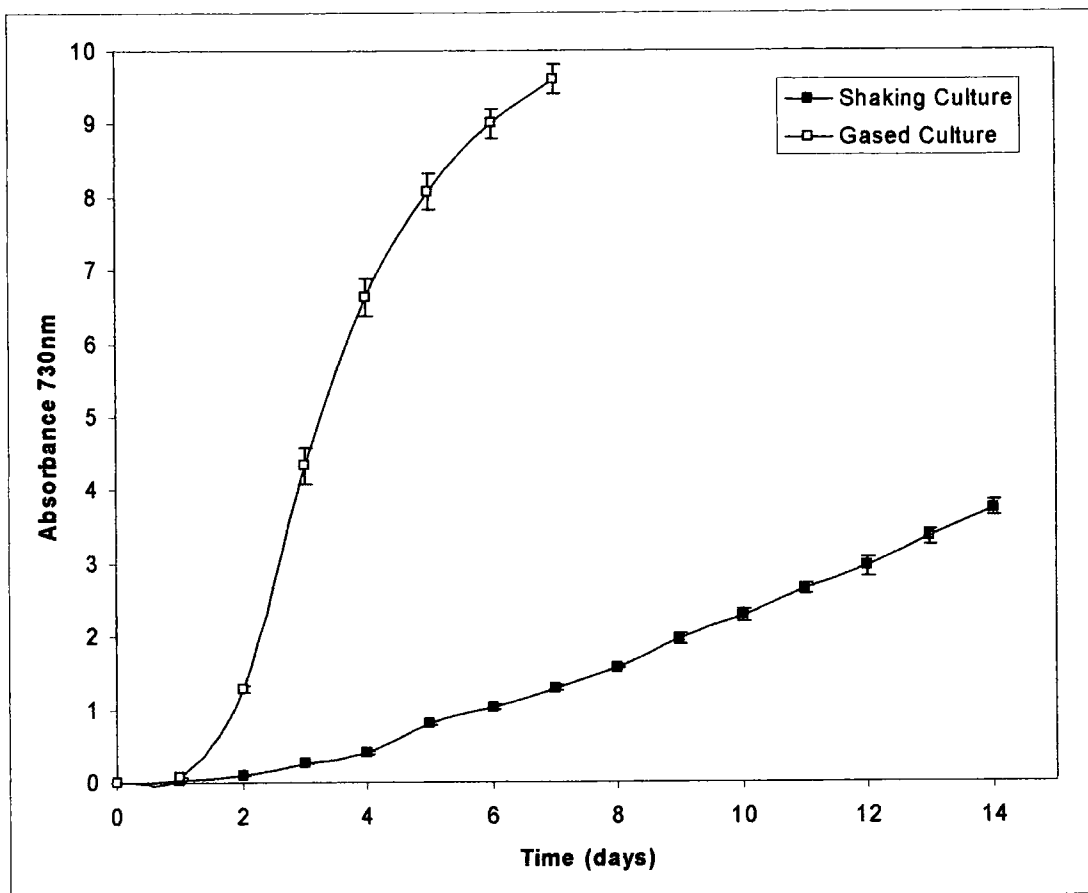
Figure 3.4. Growth of *Synechocystis* cells as shaking and gassed cultures.

Four gassed cultures and four shaking cultures were prepared. Each culture contained 100 ml of sterilised BG-11 media and was inoculated with *Synechocystis* cells from a previous shaking suspension culture to a starting A_{730} of ~ 0.001. Shaking cultures were incubated in a growth room at 32°C under fluorescent tubes providing ~ 70 µE m^{-2} s^{-1} PAR. Gassed cultures were grown in the cyanobacterial growth apparatus at 32°C where they were continuously gassed with moistened 1% CO_2 in air and illuminated with fluorescent tubes providing ~ 70 µE m^{-2} s^{-1} PAR. Growth of these cultures was monitored in terms of turbidity by measuring the absorbance at 730 nm at the times indicated. The plots are representative of the average data obtained from the four replicate cultures for each growth method and error bars indicate standard error of mean.

preparation is complicated and quantity is sparse, proteomics experimentation is difficult and without scope for improvement or development.

Synechocystis is a gram negative prokaryote and therefore possesses a complex cell wall. The cell wall acts as a rigid barrier and functions to provide protection against osmotic pressure and cell lysis. Consequently basic cell breakage techniques such as freeze-thaw are inefficient when extracting internal cellular components. In order to rupture these cells more abrasive methodologies were employed i.e. glass bead and French press techniques. To determine the efficiency of *Synechocystis* cell breakage using these two techniques, liberated protein and chlorophyll quantities were measured and compared. *Synechocystis* cells were harvested from an exponentially growing (A_{730} 1.130) 500 ml aerated culture generating a wet pellet mass of 2.23 g and were re-suspended in 20 ml of ice cold extraction buffer (20 mM Tris-HCl pH 8.0, 1 mM EDTA, 2 mM DTT). This ice cold extraction buffer functioned to prevent protease action during cell lysis. Half of the cells were broken using glass bead shearing where 10 ml of the cell suspension was transferred to a pre-chilled 50 ml glass test tube containing 10 ml of pre washed glassed beads (106 μm in diameter). This cell/glass bead suspension was vortexed in 30 second bursts for a total of 10 minuets. After each vortex burst the broken cell slurry was put on ice, an aliquot removed and analysed for protein and chlorophyll content (Figure 3.5a). Protein concentration was determined via Bradford assay and chlorophyll content was determined spectrophotometrically (A_{418}). The remaining half of the cell suspension was broken via French press technique using a Basic Z Cell Disrupter (Constant Systems Ltd.), where 10 ml of suspended cells in ice cold extraction buffer were twice passed through the machine at 24.5 KPSI and the protein content of the
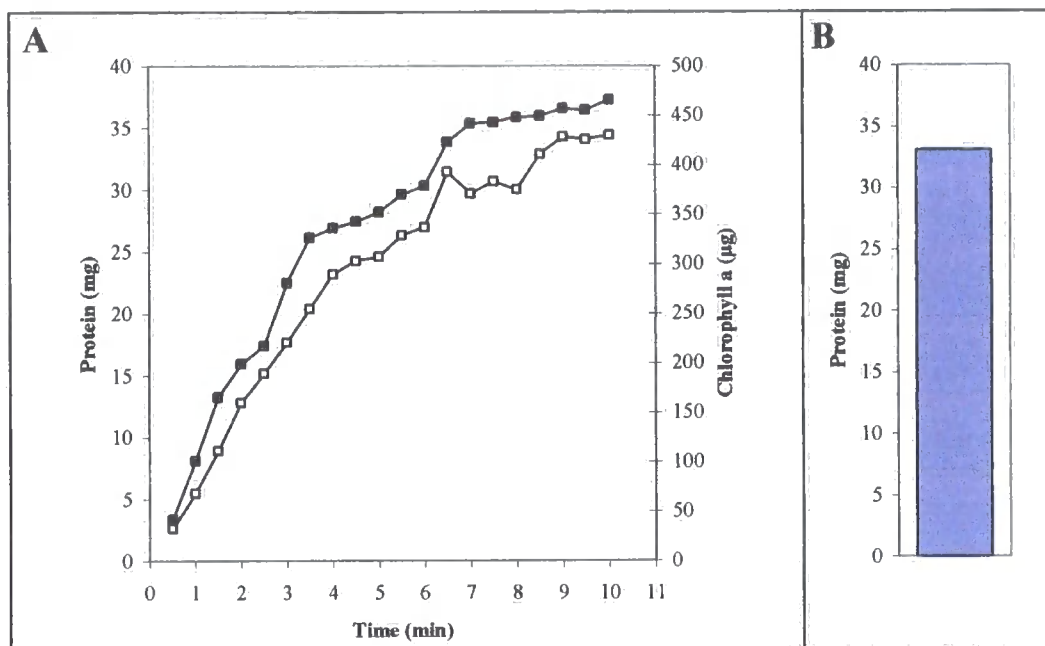
Figure 3.5. Liberation of total soluble protein (TSP) from *Synechocystis* cells via glass bead breakage and French press techniques.

Synechocystis cells from a 500 ml culture with an A_{730} of 1.13 were harvested via centrifugation giving a wet pellet mass of 2.23 g. Half of the cells were broken with glass beads (106 μm in diameter) for a total of 10 minuets. In 30 second intervals, protein and chlorophyll content was analysed (**A**). Protein concentration was determined via Bradford assay (■) and chlorophyll content was determined spectrophotometrically (Abs λ_{418}) (□). The remaining half of the cell suspension was broken using French press, where suspended cells in extraction buffer were twice passed through the machine at 24.5 KPSI and the protein content of the resultant suspension was determined via Bradford assay (**B**).

resultant suspension determined via Bradford assay (Figure 3.5b). The quantity of protein and chlorophyll liberated by the glass bead method increased linearly for approximately 6-7 minutes before levelling off, signifying that optimal breakage had been achieved after approximately 7 minutes. In comparison, the French press method liberated a quantity of protein comparable to that released after 6.5 minuets of glass bead shearing, indicating that the French press technique was highly efficient at lysing the cells.

Although the French press technique was quick and efficient, it could only be used when breaking cells from large culture volumes. This was because the internal piston cavity volume of the Basic Z Cell Disrupter was 10ml and must be filled to avoid damaging the system. Standard cell breakage technique involves concentrating the harvested cells 10 fold before shearing and therefore only cells from cultures with volumes greater than 100 ml could be broken using French press. As a result, cells from cultures with volumes less than 100 ml were broken using glass beads and where sheared for a total of 6 minutes. Most documented glass bead breakage methods for cyanobacteria involve shearing cells for a total of 3 minutes. This amount of time is not sufficient to obtain maximum cell breakage as shown by the glass bead breakage experiment (Figure 3.5a).

Quantity and availably of sample is an important issue in any analysis as it can be a limiting factor. In this case it is not so as milligram quantities of protein were extracted easy and efficiently, as shown by the plots of protein liberation from glass bead and French press broken cells (Figure 3.5), and fresh samples could be generated in a matter of days.

3.2.3   Subcellular fractionation and biological uniformity

Growth of *Synechocystis* was discovered to be highly reproducible from one culture to the next (3.2.2). However, it was important to establish whether the cells between different cultures were in fact uniform at the molecular level. To investigate this, both total soluble and membrane fractions were isolated from the cell lysate of multiple cell cultures and analysed by SDS-polyacrylamide gel electrophoresis (SDS-PAGE) (Figure. 3.6c). Cells were harvested from four different 50 ml exponentially dividing gassed cultures grown on different occasions and broken with glass beads (see materials and methods). Broken cells samples were subsequently fractionated using ultracentrifugation into soluble and membrane extracts (see materials and methods). The protein concentration of the soluble and membrane fractions was determined by Bradford (Figure. 3.6a) and TCA Lowry assay (Figure. 3.6b), respectively, and 50 μg of protein from each sample were loaded onto 12 % polyacrylamide resolving gels. SDS-PAGE revealed that the soluble and membrane protein fractions have distinct profiles and different degrees of complexity, with the membrane fraction appearing to have a less complex nature. In addition, both fractions were reproducible between different preparations, grown under the same conditions.

A (graph: Absorbance @ 595 nm vs BSA (µg))

Sample	Mean Abs @ 595nm	Protein (µg)	[Protein] (µg/µl)	Total Protein (mg)
1	0.558	14.33	1.43	7.15
2	0.611	15.71	1.57	7.85
3	0.528	13.57	1.36	6.80
4	0.564	14.49	1.45	7.25

B (graph: Absorbance @ 750 nm vs BSA (µg))

Sample	Mean Abs @ 750nm	Protein (µg)	[Protein] (µg/µl)	Total Protein (mg)
1	0.089	7.02	2.81	1.41
2	0.097	7.66	3.06	1.53
3	0.088	6.94	2.78	1.39
4	0.088	6.98	2.79	1.40
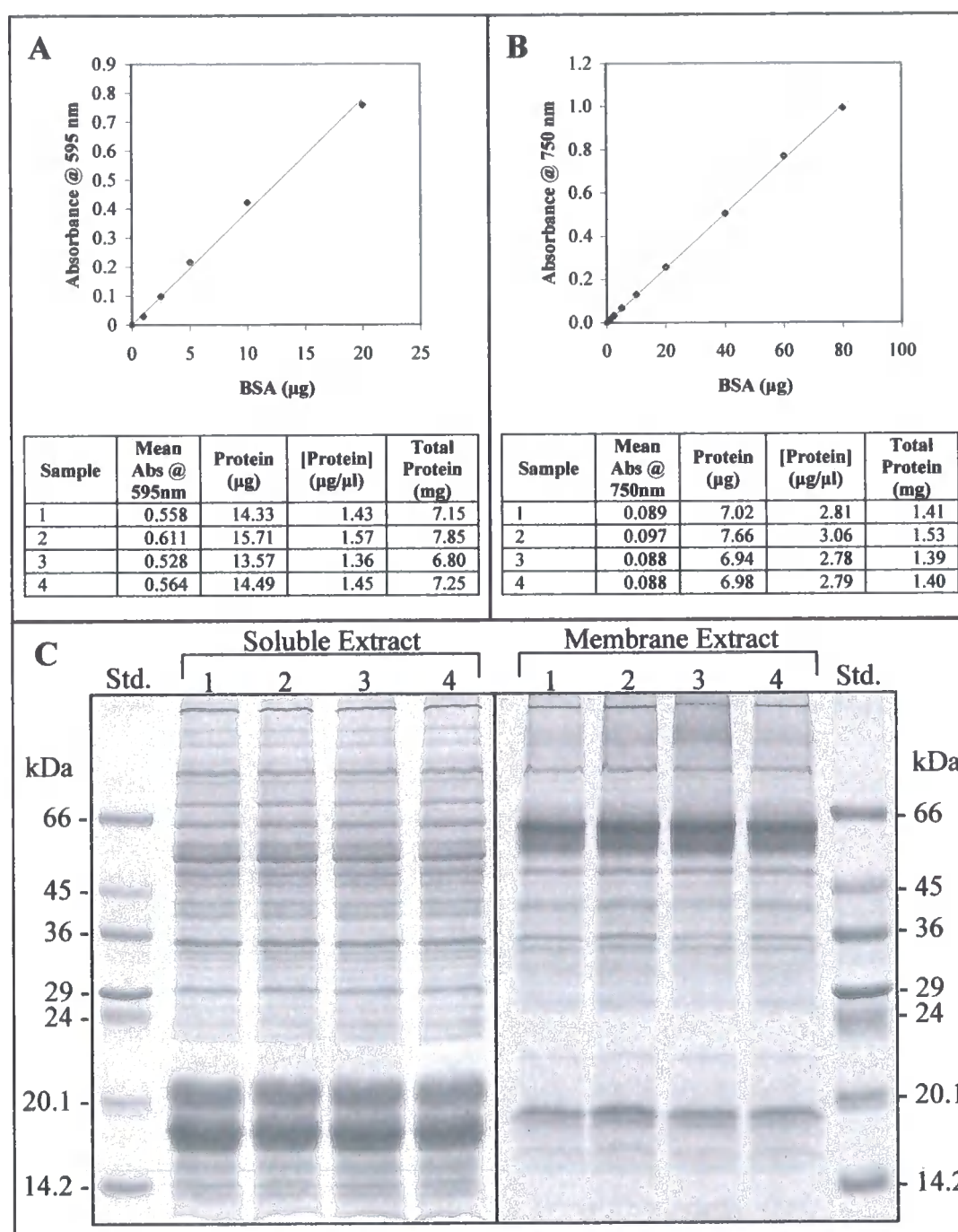
Figure 3.6. Evaluation of reproducibility and solubility of soluble and membrane protein extracts from exponentially growing *Synechocystis* cells.

Soluble and membrane fractions were isolated from *Synechocystis* cells harvested from four different 50 ml exponential dividing gassed cultures (A_{730} ~1.0) grown on different occasions. Protein concentration from both soluble and membrane fractions was determined via Bradford assay (**A**) and TCA Lowry assay (**B**), respectively. 50 µg of protein from all soluble and membrane samples were resolved via SDS-PAGE using 12 % polyacrylamide gels and the resolved proteins bands were visualised by staining with Coomassie Blue (**C**).

3.2.4 Two-dimensional gel electrophoresis (2-DE) of *Synechocystis* soluble proteins, analysis of sample complexity and optimisation of 2-DE technique.

3.2.4.1 Sample preparation for 2-DE

Having established sample preparation and determined biological uniformity, the next requirement was to extract and separate *Synechocystis* soluble and membrane proteins via two-dimensional gel electrophoresis (2-DE). The methodology behind 2-DE is fundamentally sample dependent and therefore it was important to optimise for each sample. The following section describes the experimentation performed for optimisation of 2-DE for resolution of the soluble protein fraction. This was attempted first as it is well known that soluble proteins resolve far more successfully on 2D gels than membrane associated proteins due to there hydrophilic nature.

2-DE separates a mixture of proteins by two physical factors, pH and molecular weight. Before separation, extracted *Synechocystis* soluble proteins were precipitated with 80 % acetone, re-solubilised in a urea based buffer denoted lysis buffer (9M urea, 2M thiourea, 4 % (w/v) CHAPS) and their concentration determined via a modified Bradford assay (see materials and methods section). The precipitation step removes any components from the soluble protein extract that may interfere with protein separation, such as salts and nucleic acids. It was therefore important to determine whether any proteins were lost as a result of the precipitation and re-solubilisation steps. To investigate this, the direct soluble lysate and lysis buffer solubilised protein profiles were compared via SDS-PAGE (Figure 3.7). This result proved that the soluble lysate and lysis buffer solubilised protein profiles were
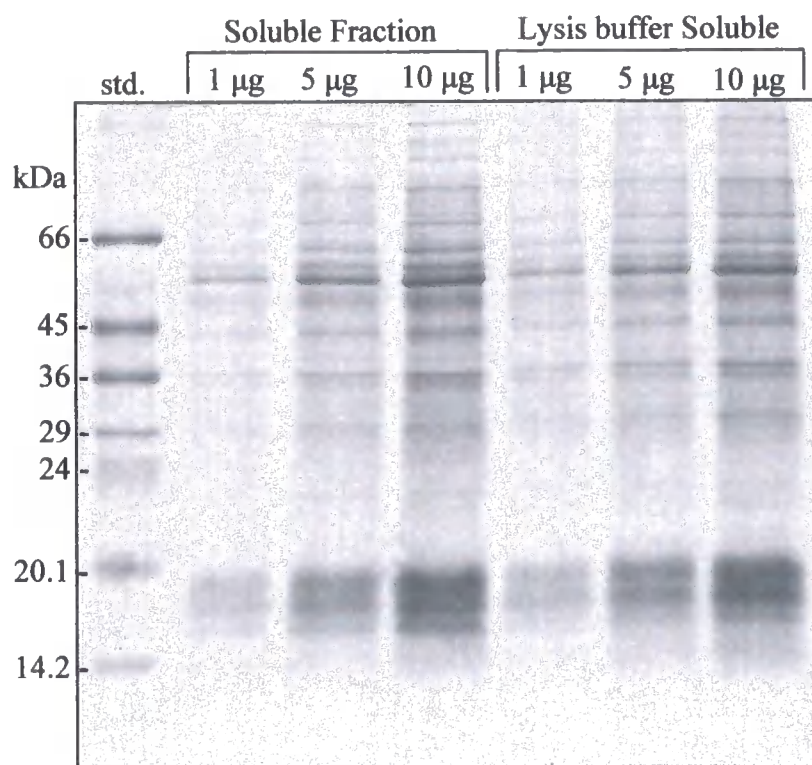
Figure 3.7. Comparison of the protein diversity present in the isolated soluble fraction from *Synechocystis* and that soluble by lysis buffer.

Soluble protein fractionated from broken *Synechocystis* cells was precipitated with ice cold 80 % acetone and solubilised in lysis buffer (9 M urea, 2 M thiourea, 4 % (w/v) CHAPS). Any insoluble material was removed by centrifugation and the protein concentration of the supernatant determined via modified Bradford assay. Lysis buffer solubilised protein was re-precipitated with 80 % ice cold acetone and 50 mM and Tris-HCL pH 8.8. The precipitated protein was solubilised in 1 x SDS loading buffer and aliquots containing 1, 5 and 10 μg of total protein, calculated from the modified Bradford assay, were resolved via SDS PAGE along with 1, 5 and 10 μg aliquots of protein from the initial isolated soluble fraction.

identical and that no visible protein constituents of the soluble fraction were differentially lost as a result of the precipitation and re-solubilisation process.

3.2.4.2   Analysis of 2D gel reproducibility

Within the 2-DE methodology, solubilised proteins are initially subjected to iso-electric focusing (IEF), which separates the proteins by pH. In this process, proteins are loaded onto an immobilised pH gradient (IPG) strip through which a current is passed; this causes the individual proteins to migrate to their intrinsic pH. There are a variety of IPG strips available that differ in size and pH range and therefore their use can be adjusted for the particular sample under study and for the type of analysis conducted. Depending on the size of the IPG strip together with the visualisation stain used, different quantities of protein were loaded onto the 2D gels (Table 3.1). In this study I have used small (7 cm) and large (18 cm) IPG strips in combination with a variety of stains, including Coomassie, Silver Nitrate and SYPRO Ruby. Small (7 cm) broad range (pH 3-10) IPG strips with conventional mini 12 % polyacrylamide gels were routinely used as an analytical tool for testing sample solubility and 2D gel reproducibility (Figure 3.8). These "mini" 2D gels were usually stained with disruptive silver and therefore 20 μg of *Synechocystis* soluble protein was loaded via in-gel rehydration (IGR) into each IPG strip and subjected to mini 2-DE (see material and methods). Results demonstrated that 2D gel profiles were reproducible across multiple samples whether they were prepared and run on the same day or on different days. Such analysis can be completed in a day and was, as a rule, conducted on any sample before performing large format 2-DE analysis. This is because; large format

Table 3.1. Protein loadings routinely used for different IPG strip sizes with different protein visualisation stains.

2D gel size	IPG strip size	Staining Method	Protein Loading (µg)
Mini	7 cm	Coomassie Brilliant Blue	200
		Silver	20
		SYPRO Ruby	50
Large	18 cm	Coomassie Brilliant Blue	1000
		Silver	200
		SYPRO Ruby	200
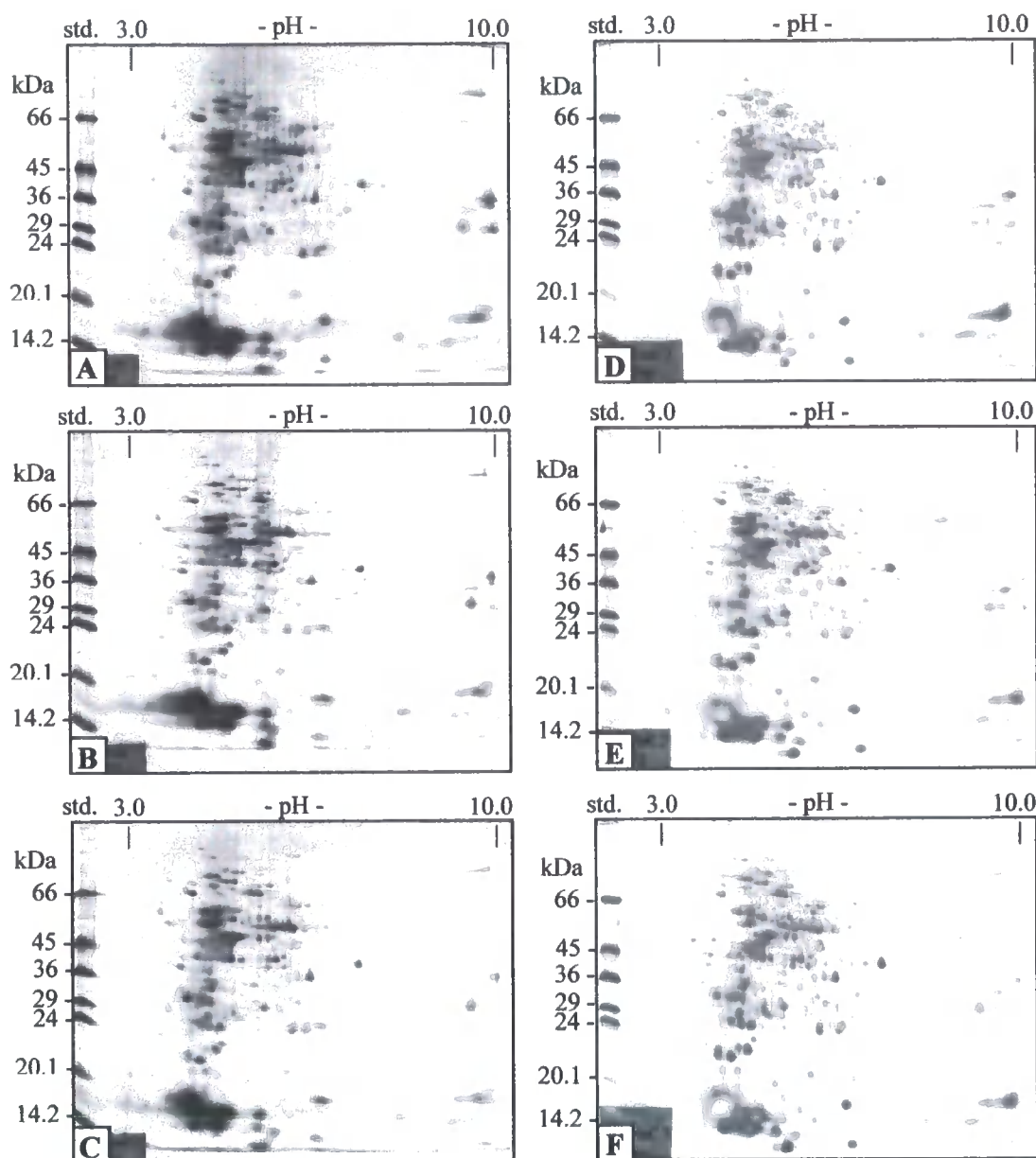
Figure 3.8. 'Mini' pH 3-10 two-dimension gel electrophoresis of *Synechocystis* soluble proteins performed on two different days.

Soluble protein isolated from 6 different *Synechocystis* cultures was acetone precipitated, re-solubilised in lysis buffer and the protein concentration determined via modified Bradford assay. 20 μg of protein from each culture was loaded via in gel rehydration (IGR) into 7 cm pH 3-10 dry immobilised pH gradient (IPG) strips. Proteins were resolved in the 1st dimension (horizontal) via isoelectric focusing (IEF) and in the second dimension (vertical) via mini SDS PAGE using 12 % acrylamide resolving gels. The resolved protein spots were visualised with disruptive silver staining and imaged. 2-DE and staining of these 6 samples was performed on 2 different days, Gels A, B and C were electrophoresed and stained together one day and gels D, E and F were processed together on a separate day.

gels require a significant amount of expensive resources and take a considerable amount of time to perform, approximately 3-4 days.

3.2.4.3 Improving the resolution of *Synechocystis* soluble proteins by the use of narrow pH Isoelectric Focusing (pH 4-7 and pH 4.5-5.5)

Studying mini 2D gels of *Synechocystis* soluble proteins revealed that protein separation was good and little if no streaking was evident. However, when examining the overall spot profile it was clear that the majority of soluble proteins were acidic and resolved within the pH range 4-7. As a result, the majority of protein spots had merged together because of the lack of resolving area. This was a major concern, as one of the sources of artefacts in protein identification via 2-DE and peptide mass fingerprinting is the possibility of two or more proteins migrating to the exact same position on the 2D gel. Proteins do this because they share similar isoelectric point (pI) and molecular weight (MW) properties. To improve the 2D gel profile and minimise the possibility of more than one spot migrating to the same position, narrow range IPG strips with pH ranges 4-7 and 4.5-5.5 were employed (Figure 3.9). 200 µg of *Synechocystis* soluble protein was loaded via IGR over night into the 18 cm IPG strips and subsequently focused using a MultiPhor™ II IEF system (Amersham Biosciences). Following IEF, IPG strips were equilibrated and layered on top of large format 12 % polyacrylamide gels and electrophoresed using a Hoefer DALT system (Amersham Biosciences). Resolved spots were stained with SYPRO Ruby fluorescent stain (Genomic Solutions) and imaged using a ProXPRESS imager (Genomic Solutions). This analysis illustrated the improved resolution obtained when using narrow range IPG strips, as spots seen on the pH 3-10 gels were further separated into

- 149 -

Figure 3.9. Improving the resolution of *Synechocystis* soluble proteins by the use of zoom 2D gels.

A, 20µg of protein was loaded via in gel rehydration (IGR) into a 7 cm pH 3-10 dry immobilised pH gradient (IPG) strip. Proteins were resolved in the 1st dimension (horizontal) via isoelectric focusing (IEF) and in the second dimension (vertical) mini SDS PAGE using mini 12 % acrylamide resolving gels. The resolved protein spots were visualised with disruptive silver staining and imaged. B & C, 200 µg of protein was loaded via IGR into separate 18 cm dry IPG strips, pH 4-7 (B) and pH 4.5-5.5 (C). Proteins were resolved in the 1st dimension (horizontal) via isoelectric focusing (IEF) and in the second dimension (vertical) via SDS PAGE using large format 12 % acrylamide resolving gels. Resolved protein spots were visualised via SYPRO Ruby staining and imaged.
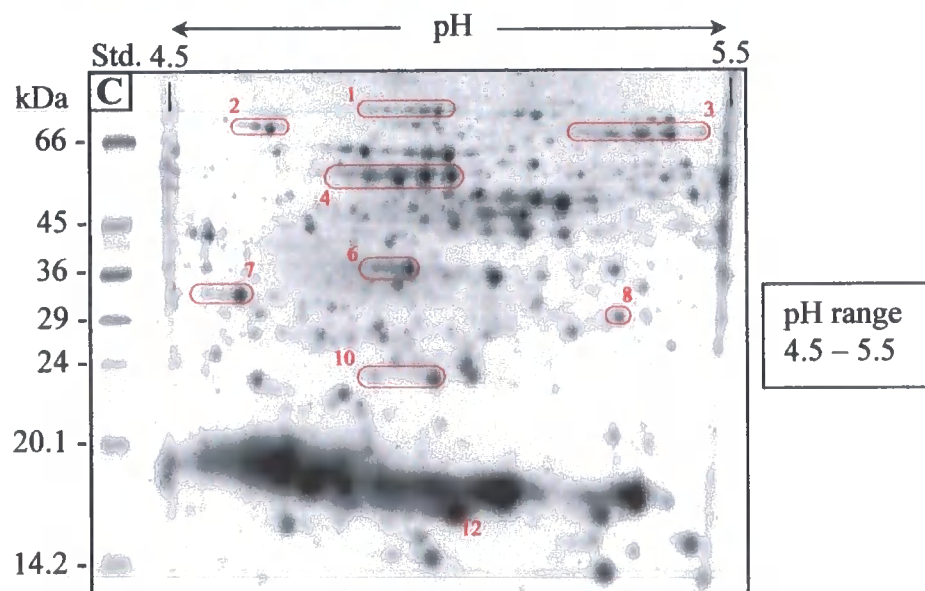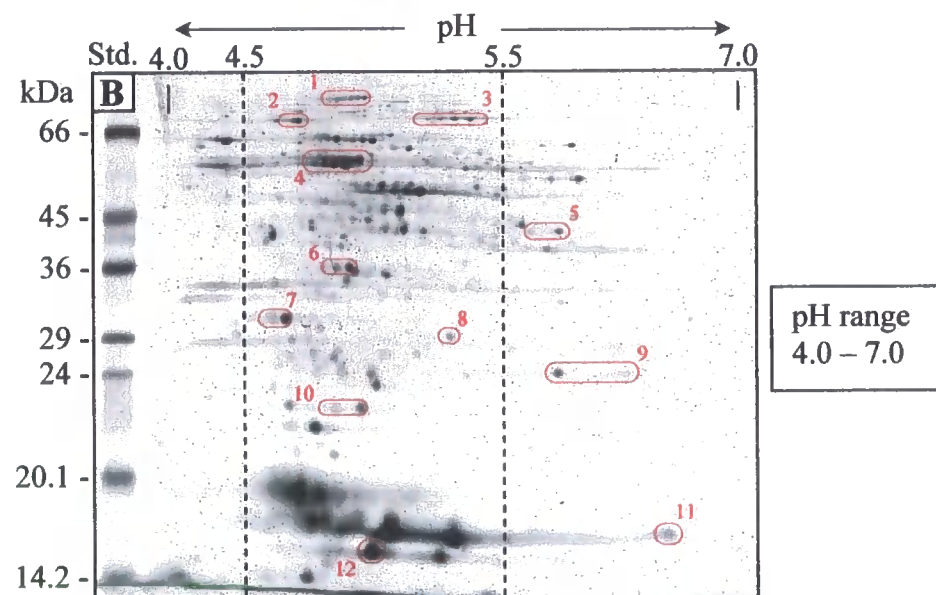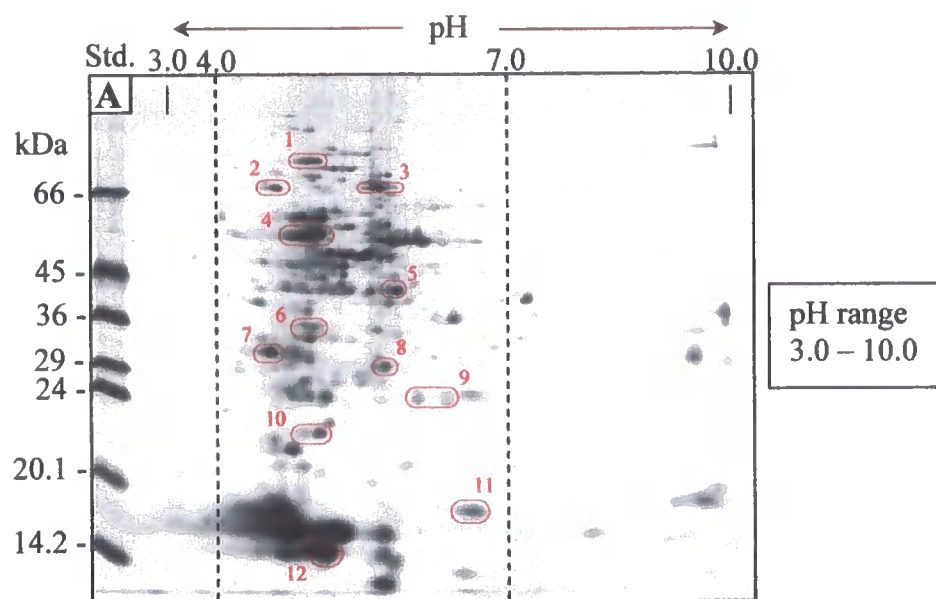
multiple clearly defined spots on the pH 4-7 and pH 4.5-5.5 gels. Examples of such improved resolution have been labelled in Figure 3.9, notably spots 1, 2, 3 and 4 on the pH 3-10 gel have been separated into multiple spots on the pH 4.5-5.5 gel.

3.2.4.4 Different protein loading methods into IPG strips ultimately effects protein resolution

Protein sample can be applied into IPG strips either during rehydration, called in-gel rehydration (IGR) (Rabilloud *et al.*, 1994; Sanchez *et al.*, 1997), or by directly applying to the rehydrated IPG strip via sample cups, called cup loading (Görg *et al.*, 1999, 2000; as used by Sazuka *et al.*, 1997, 2000). In both cases the IPG strips, which are purchased in a dehydrated form, are rehydrated over night with rehydration buffer (9 M urea, 2 M thiourea, 4 % (w/v) CHAPS, 1 % (w/v) DTT, 2 % (v/v) Pharmalyte, 0.002 % (w/v) bromophenol blue). With IGR loading the protein sample itself is dissolved in the rehydration buffer. Cup loading, on the other hand, involved separately rehydrating the IPG strips and then applying the protein sample, also solubilised in rehyrdation buffer, into the anodic end of the IPG strips via a small plastic cup during IEF. Therefore, it was important to compare these two methods to identify which gave the best separation. It is important to note that protein samples can also be cup loaded at the cathode; however, because the majority of *Synechocystis* soluble proteins are acidic, anodic loading was preferred.

Protein loading methods were compared using pH 4-7 18 cm IPG strips focused using an IPGphor™ IEF system (Amersham Biosciences) and subjected to SDS-PAGE using an Ettan™ DALT*twelve* unit (Amersham Biosciences) with large format 12 %

polyacrylamide resolving gels. Resolved spots were subsequently visualised with silver staining. These gels were chosen as they separated a large number of proteins with high quality resolution and sensitivity. Different amounts of protein loaded into IPG strips were also compared to identify if certain loading methods managed better with higher protein quantities than others. This was an important question to answer for two reasons. Firstly, different gels have different purposes and therefore require different quantities of protein. For example, it is only necessary to have small quantities of protein on analytical gels, enough to be able to visualise the resolved protein spots. In contrast, preparative picking gels require much higher protein loads to generate enough material per protein spot for identifying via PMF. Secondly, because protein spots responding to a treatment are discovered on analytical gels and are subsequently excised from preparative gels for identification, these two separate gels must be comparable. This is necessary in order to be confident that the spots being excised correspond to those that have been discovered to change in abundance, and are therefore correctly identified.

Results comparing the two protein loading methods (Figure 3.10) showed that the resolution achieved with cup loading was far greater than with IGR across all protein loading quantities. This is contradictory to previous comparisons (Rabilloud *et al.*, 1994). Reasons for this may be due to the presence of salts in the protein sample which migrate through the entire strip with IGR but not with anodic cup loading, or due to the dominance of acidic proteins in the *Synechocystis* soluble protein fraction which therefore do not have to travel as far distances with anodic cup loading. Also, low abundant spots were less visible on high loaded gels. This is a problem of silver staining, as on higher loaded gels more abundant protein spots will converge the more

Figure 3.10. Comparison of the resolution quality of *Synechocystis* soluble proteins achieved by cup and in gel rehydration (IGR) protein loading methods into IPG strips.

Synechocystis soluble protein was loaded into 18 cm pH 4-7 IPG strips via cup loading using 200 µg (A), 400 µg (B) and 800 µg (C) of protein and in gel rehydration (IGR) also using 200 µg (D), 400 µg (E) and 800 µg (F) of protein. Proteins were resolved via IEF and large format 12 % SDS-PAGE and visualised via disruptive silver staining.
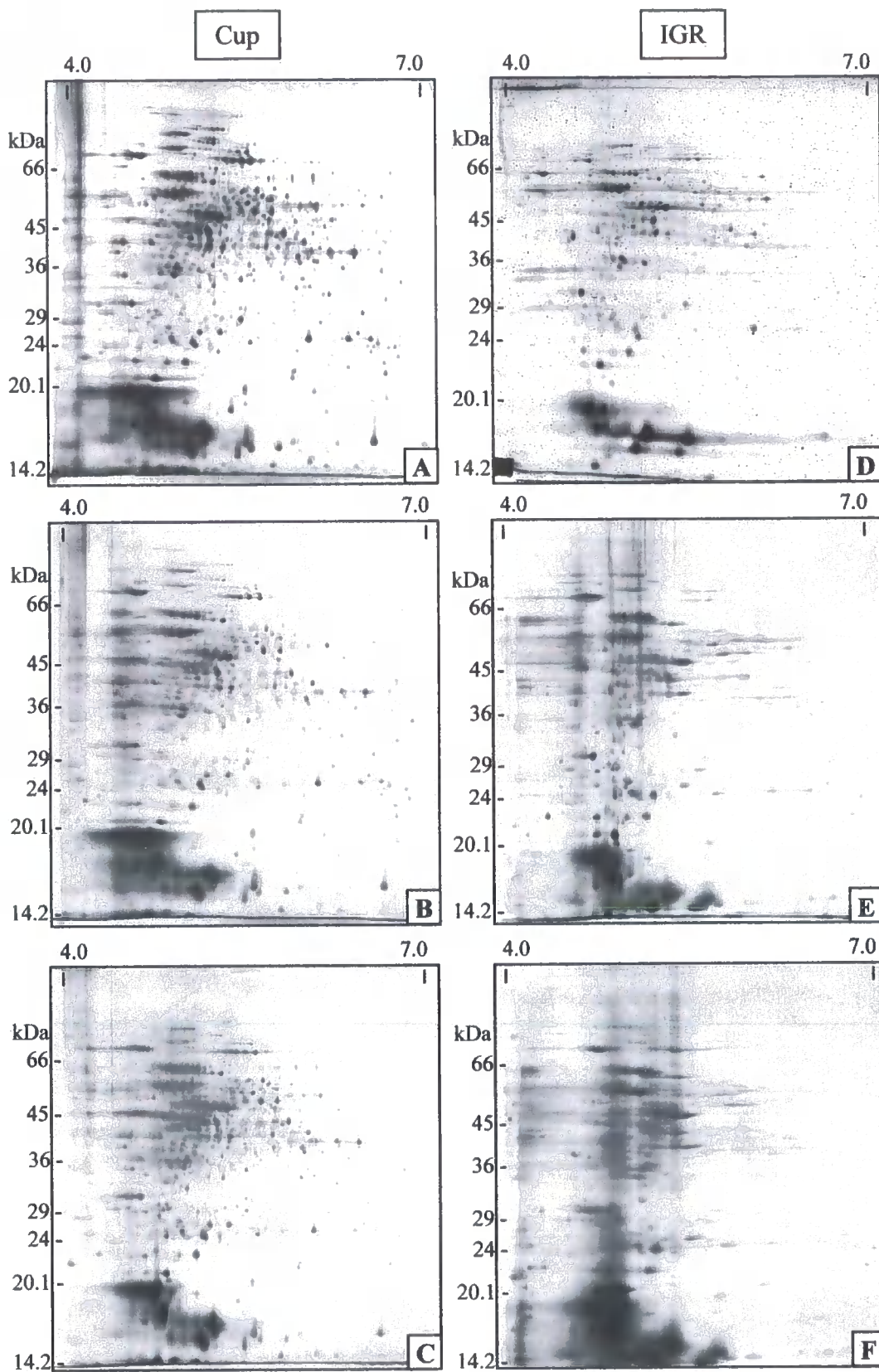
the gel is developed. Therefore gels are usually underdeveloped, leaving low abundant spots less visible than possible. However, resolution of cup loaded 200 μg and 400 μg of protein were sufficiently comparable allowing their use for analytical and picking gels, respectively. Cup loading was therefore obviously the preferred method for protein loading as this gave far better resolution. However, this effected the required concentrations of protein samples for generation of preparative picking gels as the maximum protein sample volume applied via cup loading was restricted to approximately 100 μl (Berkelman and Stenstedt, 2001). Consequently, in order to load in excess of 400 μg of protein into an IPG strip using cup loading, a realistic quantity of protein required for obtaining successful spot identifications, the concentration of the protein sample must be over 4 μg μl^{-1}. This is not an issue when loading via IGR, as rehydration solution volumes for large (18 cm) IPG strips may be up to 450 μl, meaning sample concentrations could be as low as 1.8 μg μl^{-1}.

3.2.4.5 Different Acrylamide concentrations utilised in second dimension separation affects the resolvable molecular weight range

Polyacrylamide is the medium through which proteins are separated by MW and due its physiochemical properties, the concentration of acrylamide can be adjusted to allow the separation of different molecular weight ranges. High concentrations (15-20 %) increase the area of separation for low MW proteins and low concentrations (10-12 %) increase the area of separation for high MW proteins. However, by increasing the area of separation for one you reduce the area of separation for other. Often, increasing acrylamide concentration causes high molecular weight proteins to

converge and decreasing the acrylamide concentration causes low molecular weight proteins to remain in the dye front.

I have routinely used 12 % polyacrylamide resolving gels in my analyses for both 1D (SDS-PAGE) and 2D gels. However, when examining the large format 12 % polyacrylamide 2D gels of *Synechocystis* soluble proteins it was clear that some proteins remained in the dye front (Figure 3.11a). Therefore, analysis of 2D protein resolution using 15 % polyacrylamide resolving gels was conducted (Figure 3.11b) and compared to that achieved using 12 % polyacrylamide resolving gels. In this analysis, 200 μg of *Synechocystis* soluble protein was cup loaded into two pre-hydrated 18 cm pH 4-7 IPG strips, focussed using an IPGphor™ IEF system (Amersham Biosciences), subsequently electrophoresed using an Ettan™ DALT*twelve* unit (Amersham Biosciences) and resolved proteins were stained with disruptive silver. This result revealed that over 50 additional proteins spots were resolved above the dye front using 15 % polyacrylamide resolving gels not previously seen on 12 % polyacrylamide gels. However, separation of higher MW proteins throughout the rest of the gel had been reduced. In conclusion any proteomic investigation using 2D gels would require an analysis at both 12 % and 15 % acrylamide concentrations.

3.2.4.6   Testing of Duracryl, a high tensile strength acrylamide alternative

One of the problems of large format polyacrylamide gels is their tendency to tear due to their size and weight, which can cause difficulties when moving, staining and picking proteins spots. Consequently, it was important to look for a possible

Figure 3.11. Analysis of the resolvable molecular weight range of *Synechocystis* soluble protein using 12% and 15% large format acrylamide gels.

200 µg of *Synechocystis* soluble protein was cup loaded into two 18 cm pH 4-7 pre-hydrated IPG strips and resolved via IEF in the 1st dimension and large format SDS PAGE using 12 % (**A**) and 15 % (**B**) polyacrylamide gels. Resolved protein spots were visualised via disruptive silver staining and imaged.
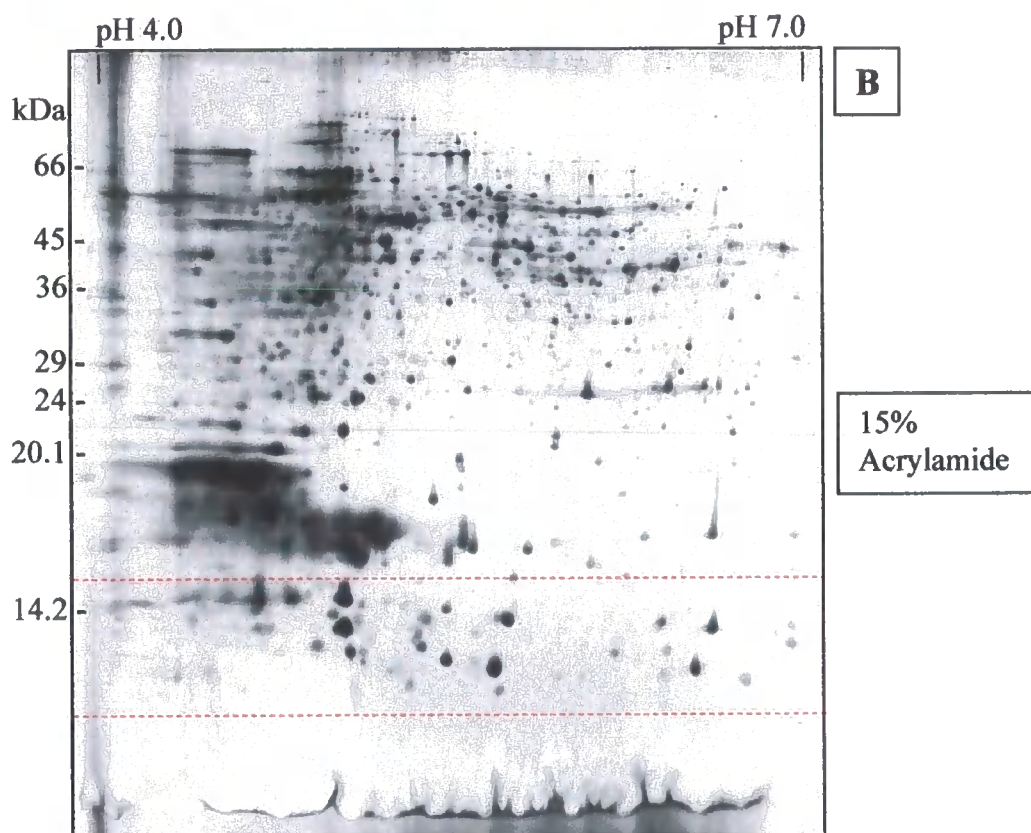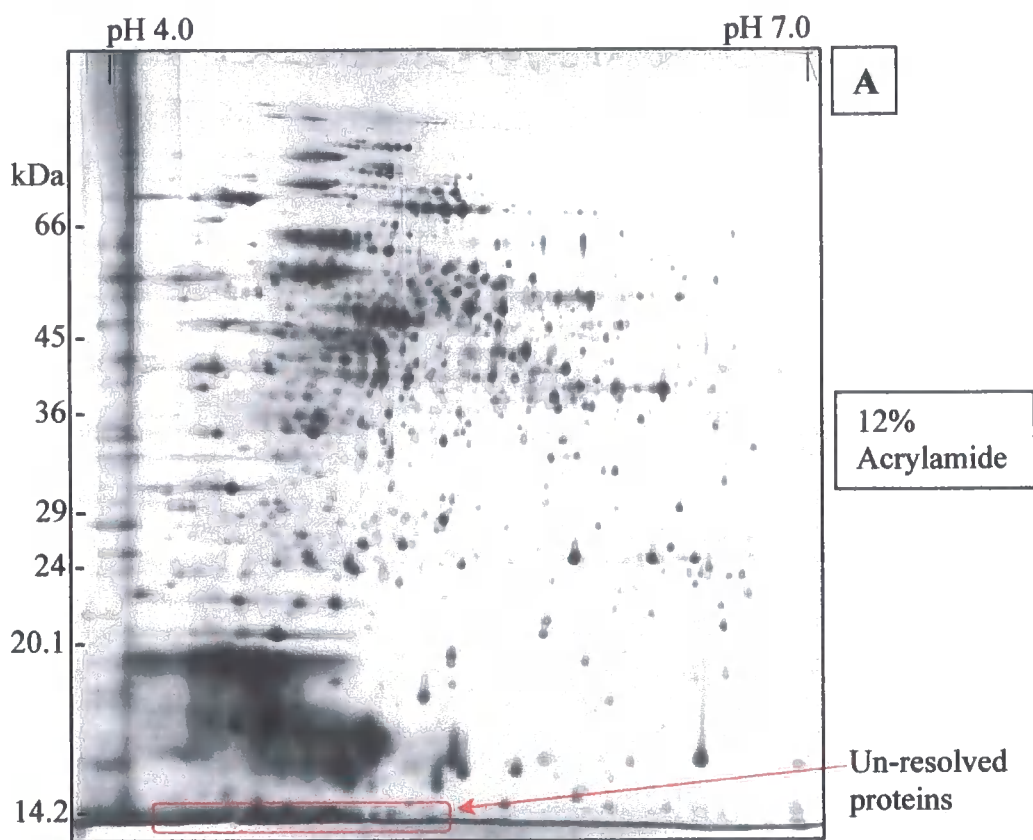
alternative. One such alternative tested in this investigation was Duracryl™ (Genomic Solutions) (Patton *et al.*, 1991), a high tensile strength acrylamide substitute that is easily handled without fear of tearing. Before Duracryl™ was put to use in a real experiment, its ability to separate proteins on 1D and 2D gel formats was analysed and compared to that of conventional acrylamide. Comparison of *Synechocystis* soluble protein resolution via 12 % acrylamide and Duracryl™ SDS-PAGE demonstrated that the acrylamide and Duracryl™ 1D protein profiles are different, especially in the high molecular weight range (Figure 3.12). To determine whether or not this difference had an effect on the overall 2D profile, 200 µg of *Synechocystis* soluble protein was cup loaded into 18 cm pH 4-7 IPG strips, focused using an IPGphor™ unit and subsequently subjected to large format SDS-PAGE performed through both 12 % acrylamide (Figure 3.13a) and 12 % Duracryl™ (Figure 3.13b) resolving gels using an Ettan™ DALT*twelve* system. Resolved spots were stained with SYPRO ruby fluorescent stain (Genomic Solutions) and visualised using Typhoon imager (Amersham Biosciences) in fluorescence acquisition mode. This result showed that although overall protein resolution with Duracryl™ was good, as seen with conventional acrylamide, high molecular weight proteins resolved as tear drop shaped spots rather than spherical shaped spots. When the abundance of individual protein spots was high or when spots had similar molecular weights, this tear drop artefact caused them to converge. Evidence of this artefact was more prominent with increased protein loading (data not shown). Consequently, when attempting to attain identification of converged spots there is a possibility of miss-characterisation due to the presence of contaminating protein. It was therefore concluded that Duracryl™ was an unsuitable solution to the tearing problem of polyacrylamide gels in this particular study.
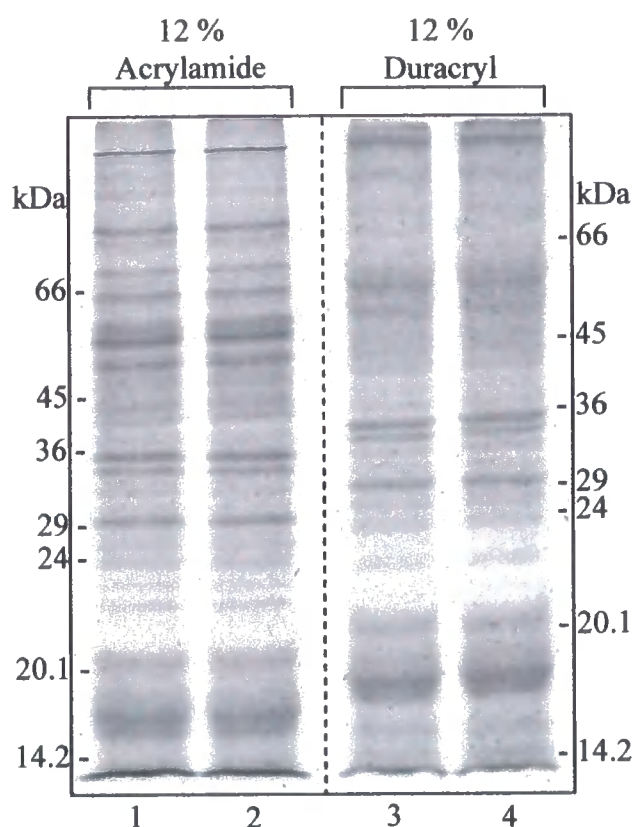
Figure 3.12. Comparison of *Synechocystis* soluble protein separation via SDS PAGE using 12% acrylamide and 12% Duracryl™ resolving gels.

Synechocystis soluble protein was separated via SDS PAGE using a 12 % acrylamide resolving gel (**Lanes 1 & 2**) and a 12 % Duracryl™ resolving gel (**Lanes 3 & 4**). Each lane containing 5 µg of protein. Separated bands were stained with SYPRO™ Ruby and visualised via fluorescence imaging.

Figure 3.13. Comparison of the 2D resolution of *Synechocystis* soluble proteins using acrylamide and Duracryl™ 2nd dimension resolving gels.

200µg of *Synechocystis* soluble protein was cup loaded into two pre-hydrated pH 4-7 IPG strips and resolved via IEF in the first dimension and large format SDS PAGE in the second dimension using 12 % acrylamide (**A**) and 12 % Duracryl™ (**B**) resolving gels. Resolved protein spots were stained via SYPRO™ Ruby and imaged.
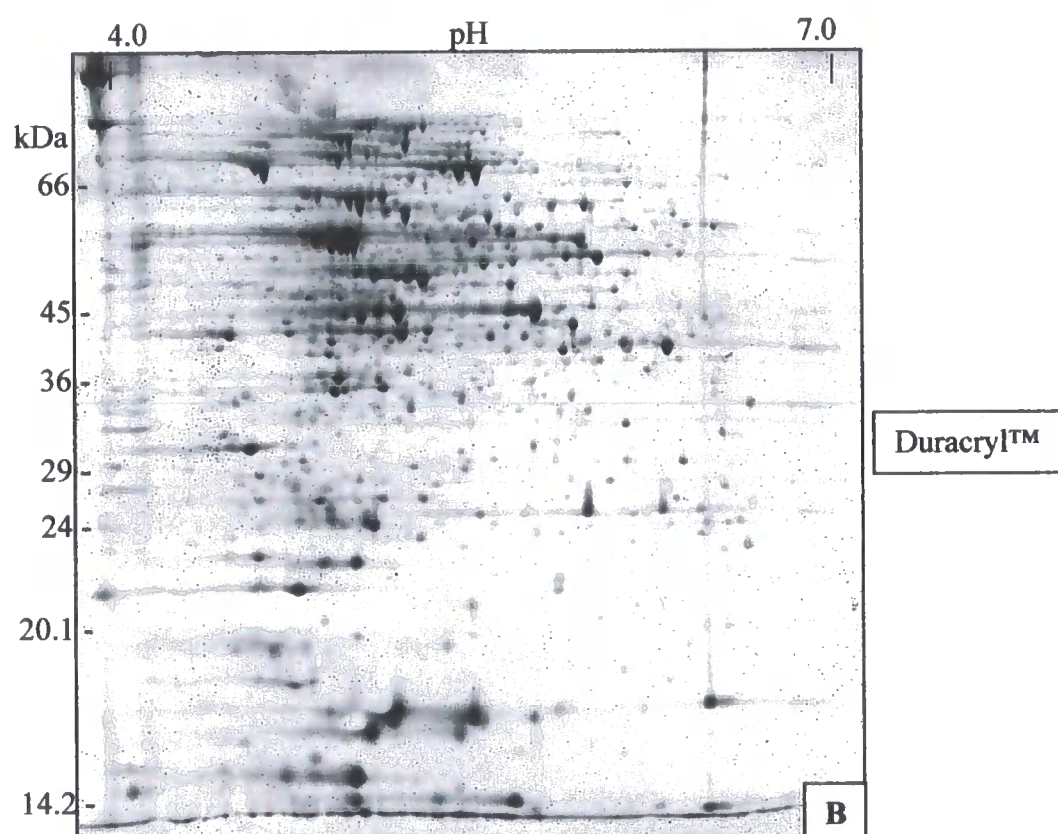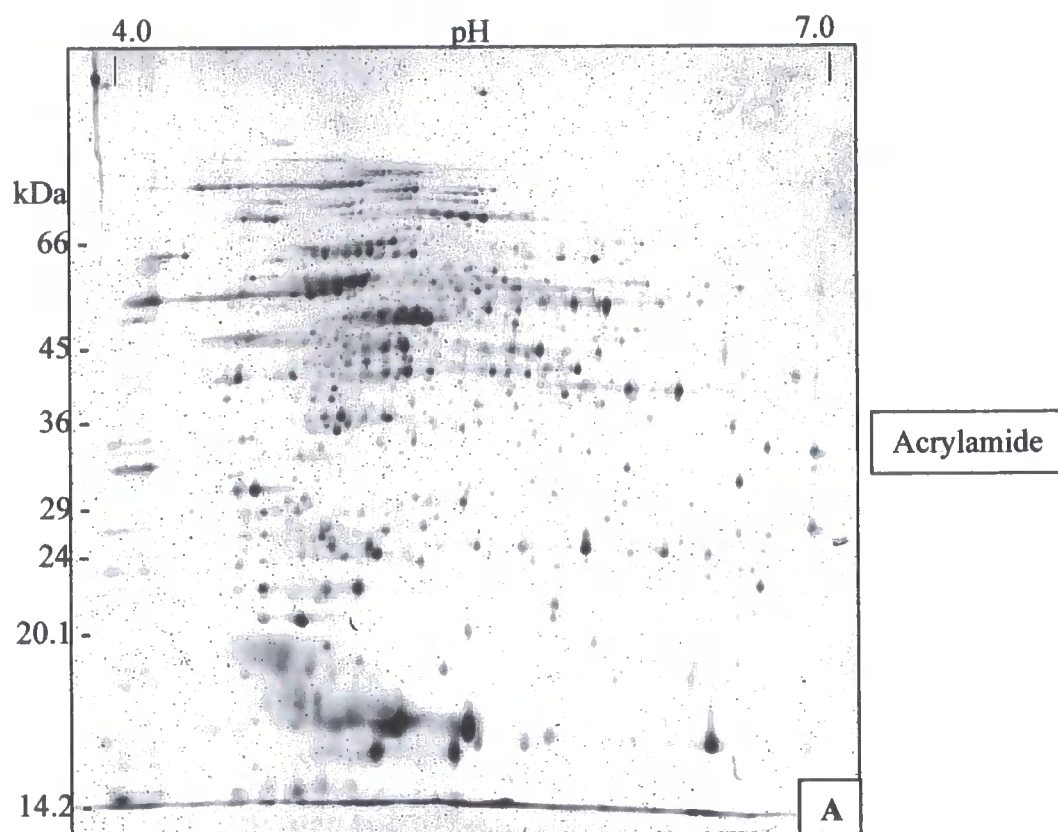
Although the use of Duracryl™ as a high tensile strength alternative to acrylamide had not been plausible, other solutions were available. One such solution used was to fix gels onto low fluorescence glass plates using PlusOne Bind-Silane (Amersham Pharmacia Biotech). These "backed" gels, once electrophoresed, were stained with SYPRO Ruby and scanned using a Typhoon florescence imager attached to the glass plate. This type of scanner is able to scan backed gels as it focuses the excitation laser above the plain of the glass plate and onto the surface of the gel itself. This solution was adequate for analytical gels, but not suitable for preparative gels as excision of spots from backed gels using the in house ProPick robot spot picker (Genomic Solutions) was not possible at the time of study. This is however now possible. Consequently, in order to increase the strength of conventional acrylamide gels intended for spot picking, the thickness of the gels were increased from 1 mm to 1.5 mm. This additional 50 % provided sufficient strength to the gel allowing successfully staining, imaging and picking without tearing. However, one draw back of increasing the thickness of preparative 2D gels is that you increase the quantity of acrylamide in excised spots. The greater the amount of acrylamide in an excised spot the lower the efficiency of tryptic digestion and thus the lower the number of tryptic peptides for PMF identification.

3.2.4.7 The presence of series of spots with similar molecular weight but different p*I* on 2D gels, a result of re-oxidation or real biological isoforms?

All previous 2-DE analysis of *Synechocystis* soluble proteins has shown some protein spots to resolve in "trains" as a series of spots with similar molecular weights but different pI's. It was therefore important to determine if spots within the same train

were in fact isoforms of the same protein and, if they were, ascertain the cause of their formation. One such known reason for the formation of "trains" is carbamylation of proteins by amidated urea in the lysis buffer used to solubilise the protein sample. However, it is unlikely that this is the cause as you would expect to see all or most of the proteins on a 2D gel suffering from the effects of carbamylation and, in the case of *Synechocystis* soluble proteins, only a select few show multiple isoforms. Another cause of their formation may be a result of proteins re-oxidising during the IEF dimension as proteins are not reductively alkylated until after IEF. Although DTT is present in the IPG strip during IEF to maintain protein reduction, it migrates towards the anode away from the proteins due to its charge. This therefore generates an environment in which proteins are able to oxidise. A final possibility for their presence in the 2D gel profile is that they are in fact real biological isoforms.

In order to determine whether the protein "trains" were a result of re-oxidation during IEF or in fact real biological isoforms, pre-IEF reductively alkylated soluble protein was analysed via 2-DE and compared to the 2D profile of post-IEF reductively alkylated soluble protein (Figure 3.14). Protein samples were reductively alkylated pre-IEF immediately after acetone precipitation by solubilising the protein precipitate in lysis buffer containing 100 mM Tri-butylphosphine for 2 hours and then adding lysis buffer containing 100 mM iodoacetamide to a final concentration of 50 mM and incubating of 30 minutes. Following this, 200µg of reductively alkylated and non-modified *Synechocystis* soluble protein samples were cup loaded into two separate pre-hydrated 18 cm pH 4-7 IPG strips and focused using an IPGphor IEF system (Amersham Biosciences). Strips were subsequently equilibrated where only the non-modified sample was reductively alkylated according to standard 2-DE methodology

Figure 3.14. Effect of pre- and post-IEF reductive alkylation methods on the resolution of *Synechocystis* soluble protein isoforms.

A, 200 µg of *Synechocystis* soluble protein, cup loaded into an 18 cm pH 4-7 pre-swelled IPG strip, focused via IEF and subsequently equilibrated in equilibration solution with 1 % (w/v) DTT followed by 4.8 % (w/v) iodoacetamide. B, 200 µg of *Synechocystis* soluble protein reductively alkylated with 100 mM Tri butylphosphine and 50 mM iodoacetamide, cup loaded into an 18 cm pH 4-7 pre-swelled IPG strip, resolved via IEF and equilibrated in equilibration solution only. Both strips were electrophoresed using large format 12% acrylamide resolving gels backed to a glass plate. Resolved proteins were visualised by staining with SYPRO™ Ruby and imaged using a Typhoon scanner.
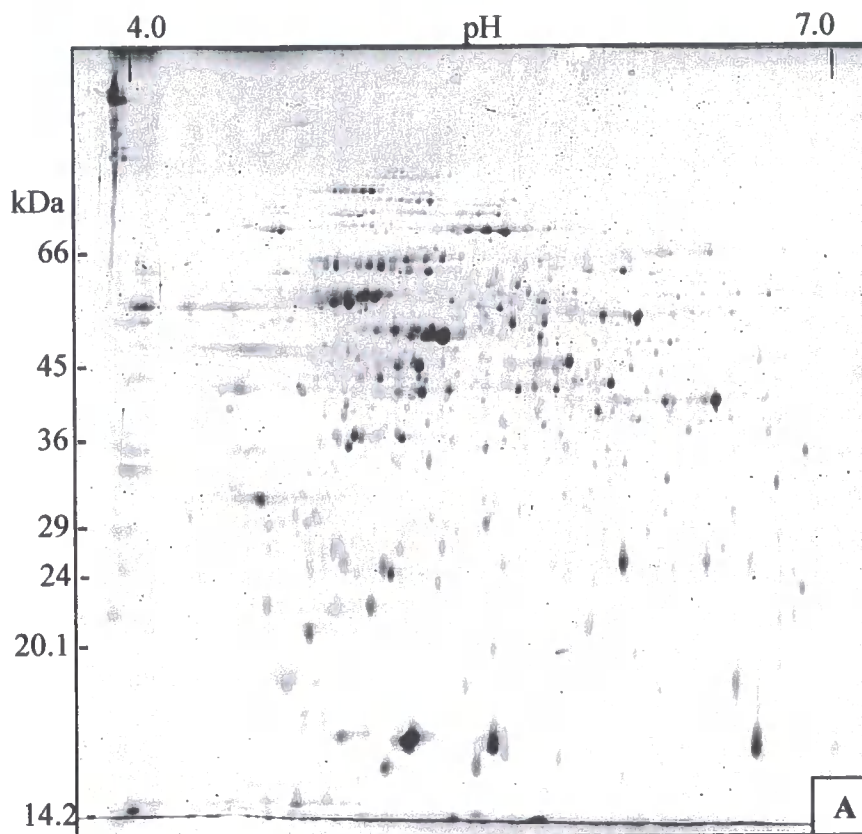
Figure showing two 2D gel electrophoresis images. Panel A labeled "Post-IEF Reductive Alkylation" and Panel B labeled "Pre-IEF Reductive Alkylation". Both panels have pH gradient from 4.0 to 7.0 on the horizontal axis and kDa molecular weight markers (66, 45, 36, 29, 24, 20.1, 14.2) on the vertical axis.
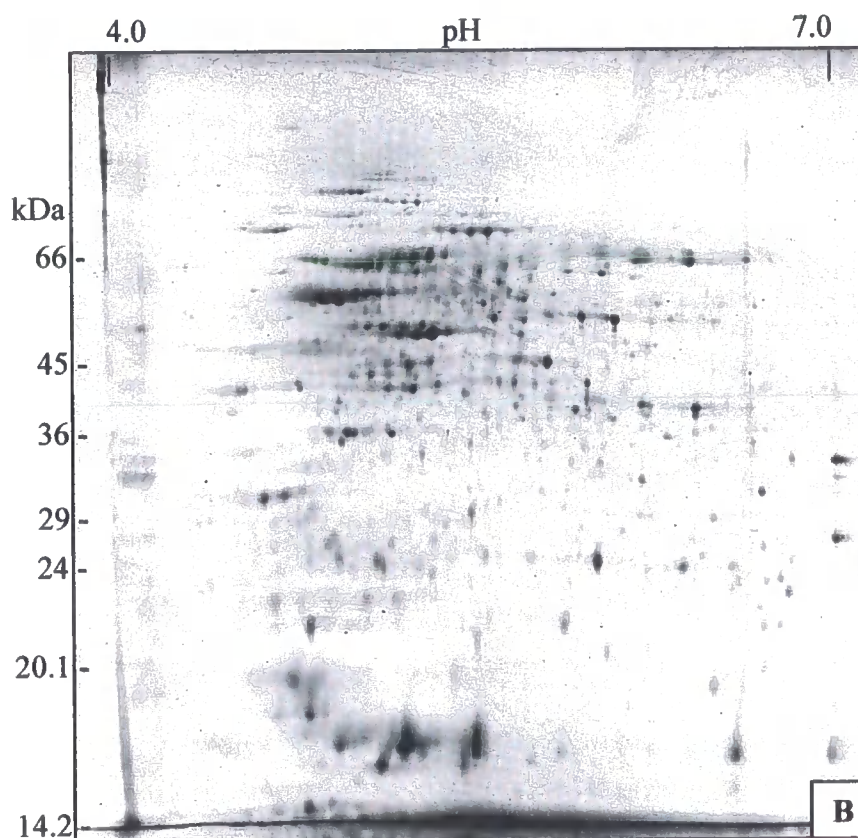
(see material an methods) and the pre-alkylated sample was incubated in equilibration solution (6 M urea, 30 % (v/v) glycerol, 2 % (w/v) SDS, 50 mM Tris-HCl pH 8.8, 0.002 % (w/v) bromophenol blue) for 30 minutes. Equilibrated strips were loaded onto large format 12 % polyacrylamide backed gels and subjected to electrophoresis using an Ettan™ DALT*twelve* system (Amersham Biosciences). Resolved spots were stained with SYPRO Ruby (Genomic Solutions) and visualised using a Typhoon fluorescence imager (Amersham Biosciences) attached to the low fluorescence glass plate.

Comparing pre- and post-IEF reductively alkylated soluble protein samples via 2-DE showed that there is no difference in the protein spot profiles between the two different reductive alkylation techniques. It was therefore concluded that trains of multiple protein spots with the same MW but different p*I* were in fact intrinsic to the biological sample. Consequently conventional reductive alkylation post-IEF remained as the method of choice.

3.2.5   Analysis of *Synechocystis* membrane associated proteins

3.2.5.1   Membrane subfractionation

Proteins are associated with bio-membranes at different locations within the lipid bilayer. This can be used to classify a protein as either peripheral or integral. Peripheral proteins are usually soluble cytosolic proteins that interact with the surface of the membrane of which there are many mechanisms for their attachment. For example: (i) via the covalent addition of a fatty acyl or prenyl group (Johnson *et al.*,

1994; Clarke, 1992), (ii) through the noncovalent interaction with other membrane proteins, or (iii) via a glycosyl phosphatidyl inositol (GPI) anchor (Doering *et al.*, 1990). Integral membrane proteins on the other hand, contain regions of amino acid sequence largely composed of residues with nonpolar side chains which commonly form α-helical structures (Engelman *et al.*, 1986; Popot, 1993) or less frequently a closed β-sheets (e.g. porins) (Schulz, 1993) as they transverse the lipid bilayer. Different integral membrane proteins differ in their topologies. Some transverse the lipid bilayer only once where as others, termed mutipass membrane proteins, transverse the lipid bilayer several times, some as much as seven times (e.g. rhodopsin). The location of a protein within the bilayer usually determines its function, for example peripheral proteins function as receptors and adhesins where as integral membrane proteins function as membrane channels and pores. Also, by their nature, membrane proteins are hydrophobic and integral membrane proteins are more hydrophobic than peripheral proteins. Therefore it is important to incorporate membrane subfractionation methodology to separate these two functionally and hydrophobic variant protein classes. In addition to this, subfractionation will allow the simplification of gel profiles by enriching for specific subsets of proteins. Enrichment is also important where a relatively small number of highly abundant, possibly 'housekeeping', components account for a significant proportion of total protein. Without subfractionation gel loadings determined by estimation of total protein content may render some of the more 'interesting' lower abundance proteins undetectable.

To develop the subfractionation methodology, experiments were conducted on a micro (100 μg) scale in order to preserve material. Fractionated *Synechocystis*

membranes were sequentially treated with 300 µl of extraction buffer (20mM Tris pH 8.0, 1mM EDTA, 2mM DTT), 300 µl of 500 mM NaCl and 300 µl of 100 mM Na_2CO_3 (pH 12.0). All extractions involved a 5 minute homogenisation step preceded by a 30 minute incubation period on ice before re-harvesting the membranes by ultracentrifugation (see material and methods). The first buffer wash step removed any soluble protein contaminants. The following 0.5 M NaCl and 100 mM Na_2CO_3 treatments extracted peripheral proteins situated on the external and luminal faces of the *Synechocystis* microsomes respectively, leaving behind the integral membrane proteins in the pellet (Figure 3.15a). Extracted proteins from each treatment were precipitated with ice cold 50 % (w/v) TCA in acetone at a final concentration of 10 % TCA/20 % acetone. Protein precipitates were harvested by centrifugation and washed sequentially twice with 80 % (v/v) acetone and once with absolute acetone. Following this, protein precipitates and the remaining membrane pellet were solubilised in 1 X SDS loading buffer and subsequently centrifuged to remove any insoluble material. These samples along with 50 µg of total membrane extract were subjected to mini SDS-PAGE using a 12 % polyacrylamide resolving gel and resolved bands were stained with Coomassie blue (Figure 3.15b).

This analysis demonstrated that different subsets of proteins were extracted by different treatments and that all protein bands present in each fraction could be traced back to the original total membrane fraction. However several other observations could also be deduced. Firstly, the quantity of proteins removed from the *Synechocystis* total membrane fraction using extraction buffer indicated that the crude membrane fraction was contaminated with soluble proteins and therefore it was essential that all future membrane preparations were extensively washed before any

Figure 3.15. Subfractionation of peripheral and integral *Synechocystis* membrane proteins.

A, diagram illustrating the sequential removal of locationally different membrane proteins by washing with extraction buffer (20mM Tris-HCl pH 8.0, 1mM EDTA, 2mM DTT), 0.5 M NaCl and 100 mM Na_2CO_3. B, 100 μg of *Synechocystis* membranes was sequentially washed with extraction buffer, 0.5 M NaCl and 100 mM Na_2CO_3. Total protein from all generated fractions was subjected to mini SDS PAGE analysis along with 50 μg of total membrane extract at 25 μg of purified membranes using 12 % acrylamide resolving gels. The resolved protein bands were visualised by staining with Coomassie brilliant blue and imaged. Lane 1; standards, lane 2; total membrane fraction, lane 3; buffer extracted proteins (soluble contaminants), lane 4; purified membrane fraction after removal of soluble contaminants, lane 5; 0.5 M NaCl extracted proteins (extrinsic peripheral proteins), lane 6; 100 mM Na_2CO_3 extracted proteins (luminal peripheral proteins), lane 7; remaining membrane pellet after all extractions (integral membrane proteins).
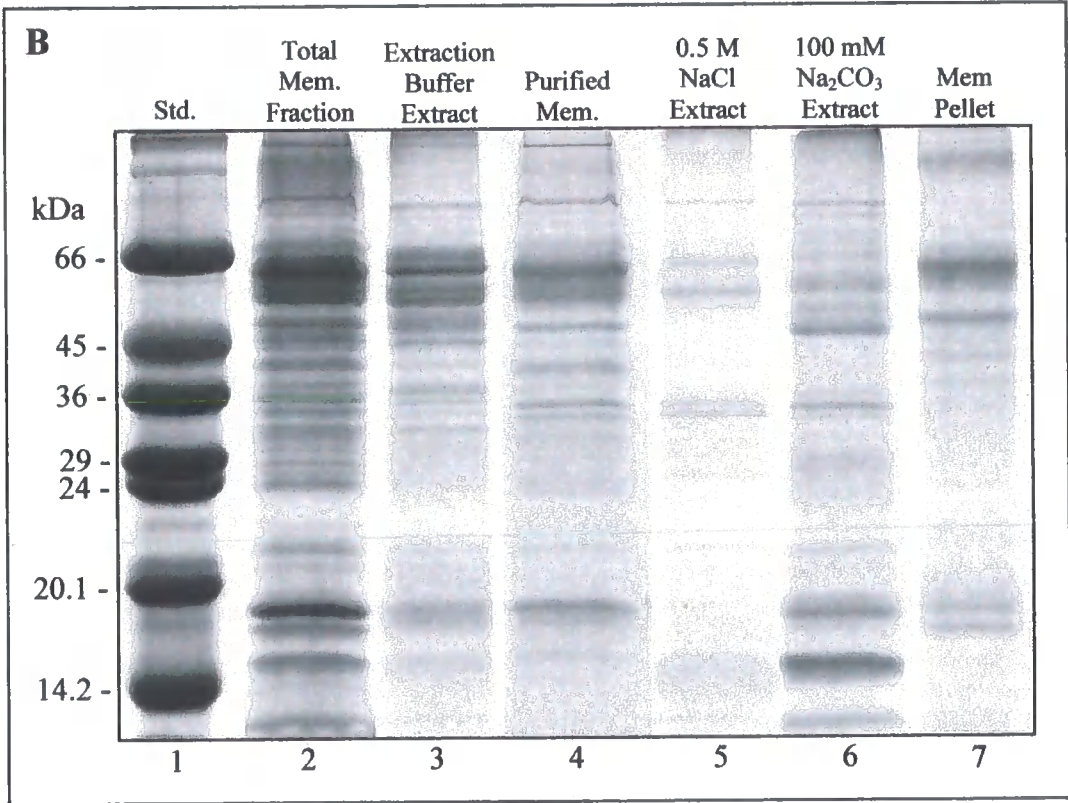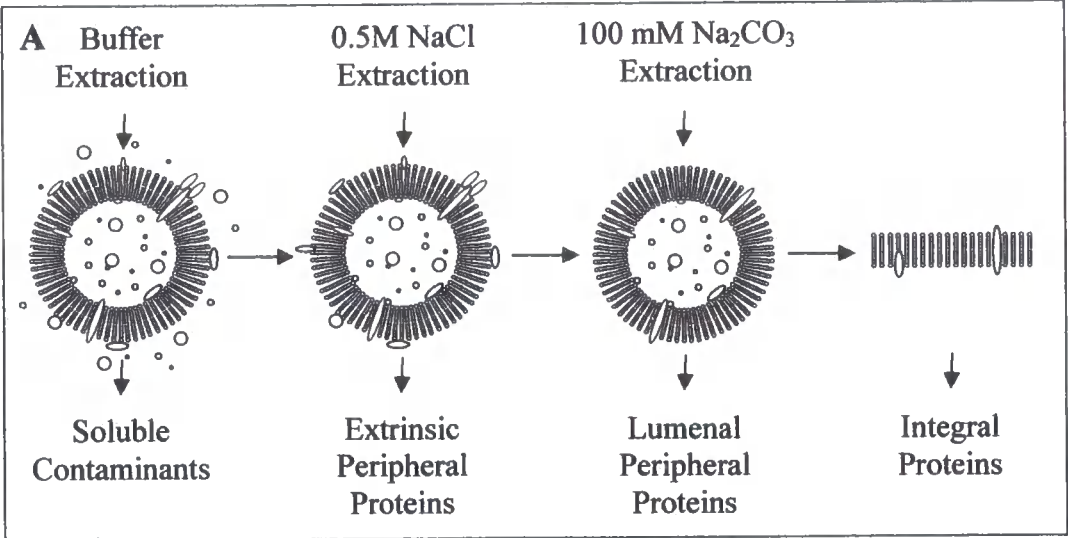
experimentation. Secondly, because membranes by their nature vesicularise and because 0.5 M NaCl and 100 mM Na_2CO_3 treatments both act to remove peripheral membrane proteins it was expected that both treatments would extract the same subset of proteins. However, it was evident that although the Na_2CO_3 extract contained the same protein bands as those seen in the NaCl extract, it did in fact contain a number of extra protein bands not present in the NaCl extract. One explanation for the presence of these additional proteins seen in the Na_2CO_3 fraction may be that they are soluble proteins trapped inside the membrane vesicles which are released by the vesicular inversion action of the Na_2CO_3 (Fujiki *et al.*, 1982). Another explanation for the presence of these additional proteins in the Na_2CO_3 extract may be because Na_2CO_3 actually extracts a different subset of proteins than NaCl.

These experiments demonstrate the efficient implementation of a reagent-based membrane subfractionation technique at a micro-scale level, able to effectively enrich for specific subsets of proteins and suitable for transfer to large scale experimentation.

3.2.5.2   2-DE analysis of fractionated membrane proteins

Having established successful subfractionation of *Synechocystis* membrane proteins, it was important to determine the solubility and complexity of these fractionated proteins on 2D gels. In order to generate sufficient material for 2D analysis, subfractionation was conducted on 1 mg of total membranes using 3 ml of each extraction reagent (see material and methods). Large format pH 3-10 2-DE was performed using 200 µg of protein from each fraction (i.e. buffer extract, 0.5 M NaCl extract, 100 mM Na_2CO_3 extract and the remaining membrane pellet) where protein

samples were IGR into 18 cm IPG strips and focused using a Multiphor™ II IEF unit (Amersham Biosciences). Focused strips were subsequently equilibrated and layered onto 12 % polyacrylamide resolving gels and electrophoresed using a Hoefer DALT™ system (Amersham Biosciences). The resultant separated proteins were visualised with silver staining (Figure 3.16).

These results demonstrated that a number of membrane associated proteins resolved well on 2D gels and confirmed that *Synechocystis* membranes have been successfully fractionated due to the distinct differences in 2D gel profiles. Furthermore, by comparing the buffer extracted and NaCl extracted 2D protein profiles, it is evident that these two treatments may have extracted some of the same proteins, as several spots with a p*I* of approximately 4.5 and masses between 45-66 kDa are present in both 2D gels. The probable reason for this is that these proteins are soluble contaminants and that they have not been completely removed by a single buffer washing step. To remove all soluble contaminants, a more realistic method would be to buffer wash the membranes at least twice. The majority of proteins removed by the Na_2CO_3 extract appear to be specific for this treatment as there are little similarities when comparing this to the 2D gel profiles of proteins removed by both the buffer and NaCl treatments and also the proteins remaining in the membrane pellet. However, there are some protein spots in the Na_2CO_3 extract that do match by there location on the 2D gel with spots present in the buffer extract sample. This observation supports the prediction that soluble proteins are trapped inside the membrane vesicles and they are released by the vesicular inversion action of Na_2CO_3 (section 3.2.5.1).
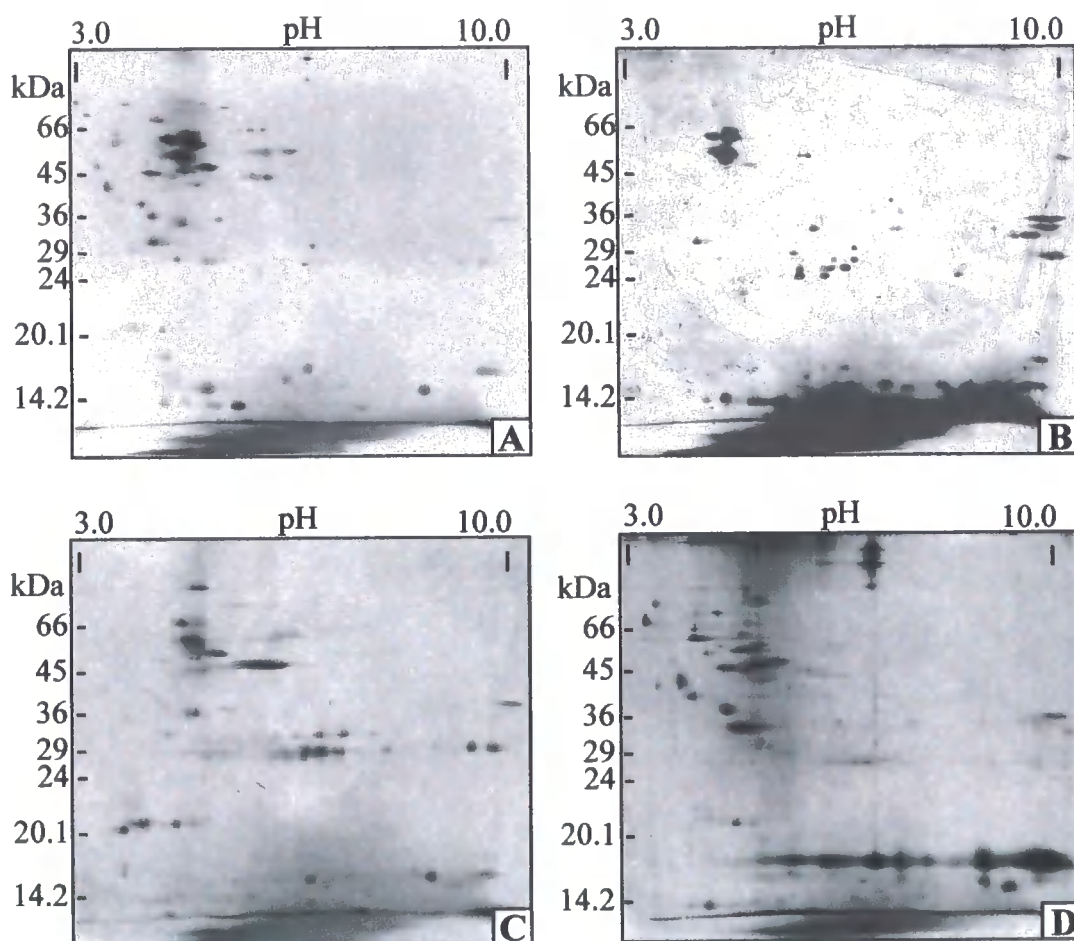
Figure 3.16. Large format pH 3-10 2-DE of subfractionated *Synechocystis* **membrane proteins.**

Synechocystis membranes containing 1 mg of protein were sequentially washed with extraction buffer (20 mM Tris-HCl pH 8.0, 1 mM EDTA, 2 mM DTT), 0.5 M NaCl and 100 mM NaCO₃. These treatments extracted contaminating soluble proteins (A), extrinsic peripheral proteins (B) and luminal peripheral proteins (C), respectively, leaving the integral membrane proteins within the membrane pellet (D). 200 μg of protein from each fraction was loaded via IGR into 18 cm pH 3-10 IPG strips. Proteins were resolved via IEF in the first dimension and large format SDS PAGE in the second dimension using 12 % acrylamide resolving gels. Resolved protein spots were visualised via disruptive silver staining.

One third of *Synechocystis* proteins are believed to be membrane associated which, with 3168 genes, indicates that there are approximately 1000 membrane associated proteins. The number of membrane proteins extracted and visualised via 2-DE (Figure 3.16) is difficult to determine due to the broad pH 3-10 range used and the fact that single gene products are often represented by multiple protein spots. As some membrane associated proteins may be lost into the soluble fraction during cell lysis and that some cytosolic proteins may be contaminating the membrane protein 2D gels this also complicates the prediction. However, it is certain that 1000 gene products are not represented on these 2D gels. Although, it is important to remember that proteins have different abundances within the cell and low abundant proteins will not be detectable on 2D gels. Also, not all genes are constitutively expressed within the cell all the time and due to their intrinsic hydrophobicity some membrane proteins are not resolvable by 2-DE (Wilkins *et al.*, 1998). Recent advancement have improved the separation of membrane associated proteins on 2D gels, such as the development of zwitterionic detergents (Santoni *et al.*, 1999, 2000), the application of cationic 16-BAC/SDS-PAGE 2-DE (Hartinger *et al.*, 1996), and organic solvent extraction (Seigneurin-Berny *et al.*, 1999; Ferro *et al.*, 2000).

3.2.6 Characterisation of 2-DE resolved *Synechocystis* soluble proteins via peptide mass fingerprinting

Characterisation of resolved proteins via peptide mass fingerprinting is fundamental to any proteomic investigation. It was therefore imperative to first establish this technology for the specific sample under study and ascertain the level of success for identifying proteins of interest. To determine this, 192 protein spots were robotically

excised using a ProPick robot (Genomic solutions) from a large format pH 4.5-5.5

Coomassie stained 2D gel containing 1.5 mg of *Synechocystis* soluble protein,

generated using a MultiPhor™ electrophoresis unit (Amersham Biosciences) for IEF

and a Hoefer™ DALT system (Amersham Biosciences) for large format SDS-PAGE

(Figure 3.17). The picked protein spots were proteolysed with trypsin and the

resultant peptide mixtures analysed via MALDI-ToF PMF using a Voyager-DE™

STR Biospectrometry workstation (Applied Biosystems, Warrington, Cheshire, UK).

Generated mass spectra were acquired, peak de-isotoped and calibrated in a fully

automated mode and the resultant calibrated peak masses were used to interrogate, in

real time mode, all entries in the NCBInr database (October 2001). First pass searches

were carried out at 150 ppm mass accuracy and based on the mass errors of the

identifications (hits) from this search, the data was recalibrated using the INTELICAL

feature of the PS1 (Proteome Systems 1) software (Applied Biosystems) and re-

submitted for a second search pass at 50 ppm mass accuracy. Of the 192 analysed

peptide mixtures, positive identifications with MOWSE scores greater than 10^3 were

obtained for 105 of the proteins (Appendix 1), a hit rate of 55 %. Of these 105

proteins, 74 were unique proteins and at the time of analysis 37 were novel, not

previously mapped via two-dimensional gel electrophoresis (Appendix 1 bold text)

and thus stating their existence in the soluble proteome of *Synechocystis* growing

under non-stressed conditions. Also, of the 74 proteins 19 were hypothetical, assigned

from predicted ORF analysis of the genomic sequence data, 10 of which were not

previously mapped via 2-DE and therefore confirming their existence as soluble

proteins and their location on a 2D gel. BLAST searches were performed using the

NCBI BLASTP online software program (Altschul *et al.*, 1997) on these 19

hypothetical proteins to attempt to ascertain their function by sequence homology

- 177 -
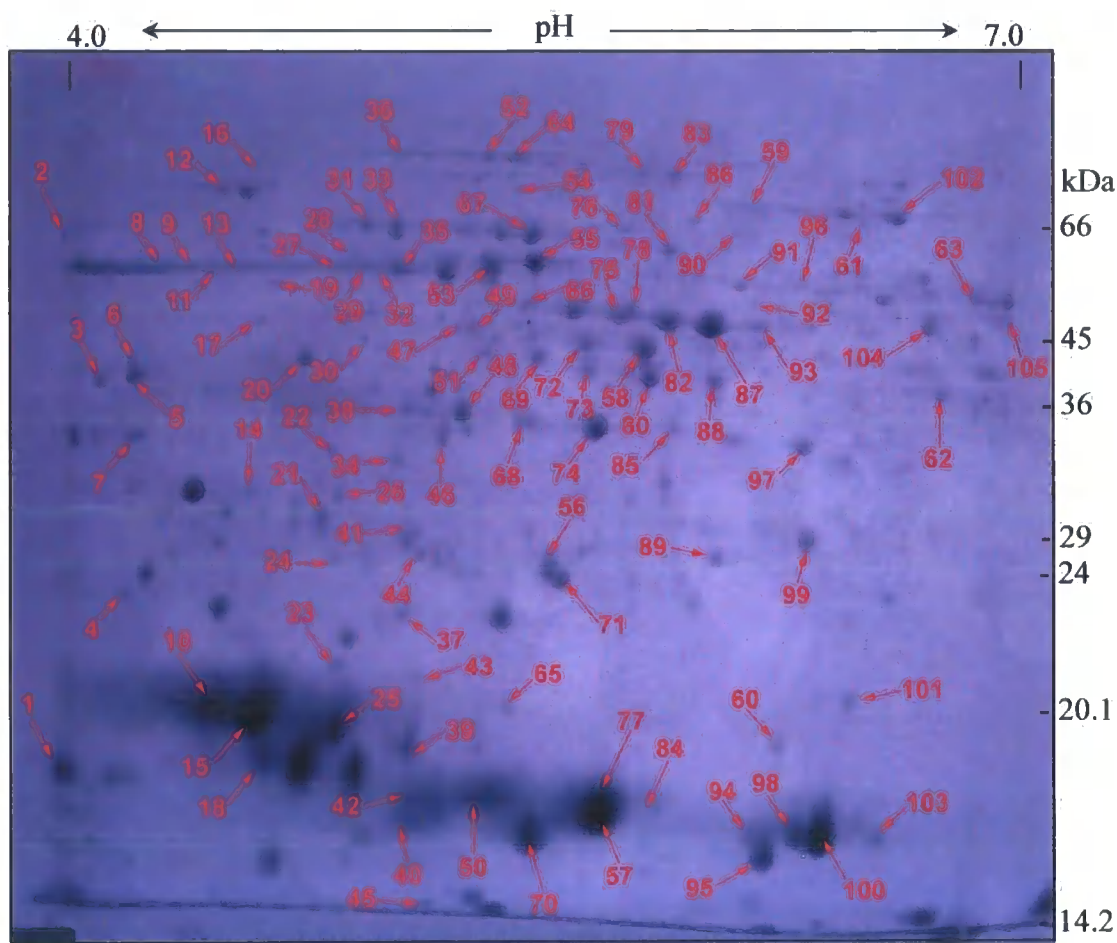
Figure 3.17. Annotated Coomassie stained zoom gel (pH 4.4-5.5) of 105 MALDI-PMF characterised *Synechocystis* soluble proteins.

1.5 mg of *Synechocystis* soluble protein IGR into a pH 4.5-5.5 IPG strip was resolved via IEF and large format SDS-PAGE at 12 % polyacrylamide concentration. Resolved spots were stained with Coomassie blue and 192 were excised for MALDI-PMF identification. Annotated spots are the 105 (55%) for which positive identifications with MOWSE scores $> 10^3$ were obtained (Table 3.2) which represented 74 unique proteins.

with proteins from other organisms. Of the 19 proteins analysed, matches other than hypothetical were obtained for 13 and of these, 6 matches had a > 50 % level of identity (Table 3.2).

The 74 proteins identified included representatives from the majority of cellular processes (Table 3.3); in fact there are representatives of 14 functional classes. For example, six are involved in amino acid biosynthesis, six in energy metabolism, four are involved in protein modification and five in nucleotide biosynthesis.

Of the 74 characterised proteins, 19 were found to be represented by two or more positively identified individual protein spots. Such identifications include the subunits of phycocyanin, ATP synthase, chaperones and Rubisco and their position on the 2D gel is such that the spots with the same identification share similar MW but different pI. As discussed previously in section 3.2.4.7, the presence of these spots is not due to sample handling and suggests that gene products are present as isoforms with post translational modifications, although, this can only be proved by analysis of amino acid sequence. This observation is supported by the findings of other *Synechocystis* proteomic analyses where as high as 23 % of identified proteins were found as isoforms with different pI's but similar MW's (Fulda *et al*, 2000; Sazuka *et al*, 1999; Wang *et al*, 2000). To examine the effects of PTM on proteins, pI and MW values calculated from the 2D gel using protein standards and apparent pI and MW values predicted by PEDANT (http://pedant.gsf.de) (Frishman *et al.*, 2001) from sequence data were compared (Appendix 1). This analysis demonstrated that in comparison to the theoretical values some proteins displayed a similar MW but reduced pI on the 2D gel (e.g. Rubisco large subunit and Phycobilicome LCM), others showed a similar pI

Table 3.2. Hypothetical protein sequence homologies with proteins from other organisms.

Annotation No.[a]	ORF No.[b]	Accession No.[c]	NCBI BLASTP Search (nr database)	E-value[d]	Identities (%)	Positives (%)
3	sll0408	gi|22298363	Peptidyl-prolyl cis-trans isomerase [*Thermosynechococcus elongatus BP-1*]	1×10^{-112}	60	76
21	slr1854	gi|23042503	COG0693: Putative intracellular protease/amidase [*Trichodesmium erythraeum IMS101*]	3×10^{-84}	74	85
28	sll0887	gi|45525630	COG0312: Predicted Zn-dependent proteases and their inactivated homologs [*Crocosphaera watsonii WH 8501*]	1×10^{-166}	66	82
30	sll0245	gi|46119556	COG0012: Predicted GTPase, probable translation factor [*Crocosphaera watsonii WH 8501*]	1×10^{-146}	74	84
34	slr0848	gi|45525736	COG3599: Cell division initiation protein [*Crocosphaera watsonii WH 8501*]	4×10^{-20}	29	60
45	slr0923	gi|27923871	Probable 30S ribosomal protein PSRP-3 (Ycf65-like protein)	2×10^{-32}	68	85
46	slr1963	gi|28373616	Crystal Structure Of Orange Carotenoid Protein	1×10^{-152}	82	89
58	sll1582	gi|29349512	DNA helicase [*Bacteroides thetaiotaomicron VPI-5482*]	9×10^{-80}	28	48

Table 3.2 continued

Annotation No.[a]	ORF No.[b]	Accession No.[c]	NCBI BLASTP Search (non-redundant database)	E-value[d]	Identities (%)	Positives (%)
58	slr0104	gi|46129489	COG1480: Predicted membrane-associated HD superfamily hydrolase [*Synechococcus elongatus* sp. PCC 7942]	1×10^{-163}	44	60
		gi|23129382	COG2202: FOG: PAS/PAC domain [*Nostoc punctiforme*]	0	47	65
61	slr0359	gi|46107119	COG5001: Predicted signal transduction protein containing a membrane domain, an EAL and a GGDEF domain [*Rubrobacter xylanophilus DSM 9941*]	1×10^{-138}	47	65
62	sll1424	gi|45523399	COG4372: Uncharacterized protein conserved in bacteria with the myosin-like domain [*Crocosphaera watsonii WH 8501*]	2×10^{-96}	47	69
62	slr1968	gi|23127516	COG4995: Uncharacterized protein conserved in bacteria [*Nostoc punctiforme*]	1×10^{-138}	38	58
105	sll1135	gi|45523229	COG3380: Predicted NAD/FAD-dependent oxidoreductase [*Crocosphaera watsonii WH 8501*]	3×10^{-59}	41	57

NCBI BLASTP (Altschul *et al.*, 1997) ver. 2.2.8 (Jan 05 2004) was used to compare the identified hypothetical protein sequences against the NCBI non-redundant database (April 23 2004). The highest scoring matches with assigned function are tabulated.
[a] Annotation number of protein excised from pH 4.5-5.5 Coomassie stained gel (Figure 3.17). [b] Hypothetical protein ORF, [c] NCBI accession number, [d] Expect value – probability that the matched sequence is not a result of a random event (lower the score, higher the probability).

Table 3.3. Functional categories of identified *Synechocystis* soluble proteins.

(A) Photosynthesis and Respiration

Annotation No.	Gene Product Name	Function
53	ATP synthase α subunit	ATP synthase
27, 29, 32, 35	ATP synthase β subunit	
80	Phosphoribulokinase	CO$_2$ fixation
8, 9, 11, 13, 27	Ribulose bisphosphate carboxylase large subunit	
18	Allophycocyanin α chain	Phycobilisome
40, 42, 70, 94, 95	Allophycocyanin β chain	
42, 50, 51, 57, 77, 84, 98	Phycocyanin α subunit	
10, 15, 23, 25, 39, 43	Phycocyanin β subunit	
36, 52	Phycobilisome LCM core-membrane linker polypeptide	
1	Cytochrome c$_{550}$	Photosystem II

(B) Cellular processes

Annotation No.	Gene Product Name	Function
67	60kD chaperonin 1	Chaperones
31, 33	60kD chaperonin 2	
12, 14	DnaK protein	
7	Heat shock protein GrpE	
97	Methyl accepting chemotaxis protein	Chemotaxis
92	Sec A	Protein and peptide secretion
2	Trigger Factor	

Table 3.3 continued

(C) Transcription

Annotation No.	Gene Product Name	Function
79,83	Polyribonucleotide nucleotidyltransferase	RNA synthesis, modification, and DNA transcription
20	RNA polymerase alpha subunit	
63	RNA polymerase beta prime subunit	

(D) Translation

Annotation No.	Gene Product Name	Function
5, 6	30S ribosomal protein S1	Ribosomal proteins: synthesis and modification
24	ATP dependant Clp protease proteolytic subunuit	Degradation of proteins, peptides, and glycopeptides
20	Carboxyl-terminal protease	
54,60,61,63	ClpB protein	
52, 64	Elongation factor EF-G	Protein modification and translation factors
75,82,87,93	Protein synthesis elongation factor Tu	
99	Elongation factor TS	
86	Aspartyl-tRNA synthase	Aminoacyl tRNA synthetases and tRNA modification
36	Phenylalanyl-tRNA synthase	

(E) Biosynthesis of cofactors, prosthetic groups, and carriers

Annotation No.	Gene Product Name	Function
47,49	Molybdopterin biosynthesis MoeB protein	Molybdopterin

Table 3.3 continued

(F) Amino acid biosynthesis

Annotation No.	Gene Product Name	Function
96	2-isoproplylmalate synthase	
6	3-isopropylmalate dehydrogenase	Branched chain family
81	Dihydroxyacid dehydratase	
38,48	Ketol-acid reductoisomerase (acetohydroxy-acid isomerase)	
78	Argininosuccinate synthase	Glutamate family/Nitrogen assimilation
53,55	Glutamate-ammonia ligase	

(G) Purines, pyrimidines, nucleosides, and nucleotides

Annotation No.	Gene Product Name	Function
16	Phosphoribosylformyl glycinamidine synthetase II	
88	IMP dehydrogenase subunit	Purine ribonucleotide biosynthesis
91	Phosphoribosyl aminoimidazole carboxy formyl fomyltransferase	
101	Adenylate Kinase	

(H) DNA replication, restriction, modification, recombination, and repair

Annotation No.	Gene Product Name	Function
19	DNA polymerase III beta subunit	-
58,63,103	DNA mismatch repair protein	-
61,62	Primosomal protein N	-
92	DNA topoisomerase	-
103	DNA helicase	-

Table 3.3 continued

(I) Energy metabolism

Annotation No.	Gene Product Name	Function
82	6-phosphogluconate dehydrogenase	
89	Pentose-5-phosphate-3-epimerase	
17	Putative Oxppcycle Protein Opac	Pentose phosphate pathway
41	Ribose 5-phosphate isomerse	
59,102	Transketolase	
66,73	Enolase	Glycolysis
69	Phosphoglycerate kinase	
62,90	Aspartate kinase	Amino acids and amines
100,104	S-adenosylhomocysteine hydrolase	

(J) Central intermediary metabolism

Annotation No.	Gene Product Name	Function
62	Glycogen phosphorylase	Polysaccharides & glycoproteins

(K) Cell envelope

Annotation No.	Gene Product Name	Function
105	Soluble lytic transglycosylase	Murein sacculus & peptidoglycan

(L) Transport and binding proteins

Annotation No.	Gene Product Name	Function
68,74,85	Periplasmic iron-binding protein	-

Table 3.3 continued

(M) Regulatory functions

Annotation No.	Gene Product Name	Function
26	Regulatory components of sensory transduction system	-
58	Sensory transduction histidine kinase (Hik6)	-

(N) Other

Annotation No.	Gene Product Name	Function
37	Membrane protein	-
56	Rehydrin	-
65	GCPE	-
72	GlpX protein	-

Functional categories for identified proteins were obtained from the Cyanobase web site 2002 (www.kazusa.or.jp/cyano/cyano.html) (Nakamura *et al.*, 1998).
Database identifiers for the proteins quoted in this table are available in Appendix 1.

but increased MW (e.g. 60 kDa chaperonin 2 and Polyribonucleotide nucleotidyltransferase) and finally certain spots had a similar p*I* but reduced MW (e.g. ClpB protein). This supports the evidence for extensive post translational modification of proteins and recent advancements in MS have enabled the identification of protein PTM sites including *O*-glycosylation and phosphorylation (Annan and Carr, 1997; Jensen, 2004).

These results have been obtained in a fully automated mass spec mode, demonstrating that identification of a large number of protein samples can be obtained quickly. The use of a narrow pH range gel, which allows for the separation of proteins as individual spots, has probably aided this process. Further identification of protein spots will require other technologies, such as MS-MS sequencing, however; this proteomic study has provided an ideal platform for identifying stress responsive changes in the proteome of *Synechocystis*, leading to the characterisation of stress perception and signal transduction genes.

3.3 Discussion and Conclusion

3.3.1 Maintenance of *Synechocystis* cells

Synechocystis is an ideal experimental organism for proteomic and transcriptomic studies due to the simplicity of its genome. It therefore presents an attractive system to study the response of photosynthetic organisms to elevated temperature. However, before cultures could be used in this way the growth and maintenance of *Synechocystis* was established within the laboratory. Cells were grown and maintained as shaking liquid cultures and on solid agar medium within a separate algal growth room maintaining temperature and light constant. They were routinely sub-cultured every month using the previous culture as the inoculum and initiated every six months from frozen DMSO stocks to maintain genetic integrity.

3.3.2 Establishment of rapid growth and large scale cultures

In order to exploit the advantages offered by *Synechocystis*, rapid and reproducible growth of *Synechocystis* had to be established providing a sizeable and unlimited source of material. Although shaking suspension cultures could be grown on a relatively large scale, as the only limiting factor was the size of the culture flask, cultures grew slowly with a doubling time of three days. Furthermore, with the intension of performing an investigation into the response of *Synechocystis* to elevated temperatures, two separate growth environments were required, one for normal growth and one for growth at elevated temperature. As shaking suspension cultures were grown within a communal growth room and a second growth room was

unavailable for use, an alternative growth system had to be found. To overcome these problems associated with shaking suspension cultures a specialised cyanoabacterial growth apparatus was constructed. Its design was adapted from a Japanese design (Prof. Norio Murata, NIBB, Okasaki, Japan) which allowed rapid reproducible growth of large scale cyanobacterial cultures and had been extensively used to generate biological material for a variety of stress investigations. This apparatus maintained culture temperature through the use of temperature controllable water baths and two separate water baths were available, the temperature of which could be independently adjusted, ideal for investigating high temperature stress/acclimatisation. Cultures were illuminated through fluorescent tubes and light intensity was stringently maintained constant for both water baths. *Synechocystis* suspension cultures grown within this apparatus were also continually gassed with moistened 1 % (v/v) CO_2 in air. This constant CO_2 bubbling was responsible for faster growth and higher cell yields compared to that of shaking suspension cultures (Stanier *et al* 1971), where gassed cultures displayed an exponential doubling time of approximately 8 hours and possible culture densities at A_{730} of up to 11.0. Exponentially growing cultures for experimentation could be generated from freshly inoculated media in 24 hours and with volumes of up to 1 litre. This explosive growth and high cell culture volumes coupled with optimised glass bead and French press cell breakage methods enabled milligram quantities ($\sim$ 30 mg from a 500 ml culture) of protein material to be generated in short periods of time, making this system ideal for proteomic experimentation providing that cultures were reproducible.

3.3.3 Uniformity of cell growth and proteome

To determine the reproducibility of gassed *Synechocystis* suspension cultures, both their growth and protein composition was studied across different cultures. Growth of *Synechocystis* followed a classical sigmoidal growth pattern common to batch cultures, in which three distinct phases of growth; lag phase, exponential phase and stationary phase were clearly visible. Batch cultures are grown in a closed vessel with a single batch of medium, because no fresh medium is provided during growth, nutrient concentrations decline and concentration of waste increases, thus slowing the growth rate of the cultured cells. Analysis of the growth pattern of three separate cultures by measuring density over time provided a good indication that *Synechocystis* growth within gassed suspension cultures was reproducible from one culture to the next. This was demonstrated by the narrow variation around the mean average data.

Proteome uniformity was analysed in two major prokaryote cell compartments, the soluble (cytosolic) and total membrane (both plasma and thylakoid) fractions. These two fractions were extracted from four independent exponentially growing cultures and analysis via mini SDS-PAGE did not provide any evidence of differences in protein composition in either soluble or total membrane isolates across all four cultures. This, together with the evidence for reproducible growth, demonstrated that *Synechocystis* gassed suspension cultures were suitable for generation of biological material for proteomic studies.

3.3.4   Preparation of *Synechocystis* protein samples for 2-DE

The first requirement for proteomic analysis is the separation of complex mixtures of proteins containing as many as several thousand individual species. Although, with recent advancements in technology there are several protein separation methods employable, such as chip based technologies (Nelson *et al.*, 2000), the use of affinity tags such a ICAT and TAP (Gygi *et al.*, 1999a; Rigaut *et al.*, 1999) and the direct analysis of protein complexes using MS (Link *et al.*, 1999), two dimension gel electrophoresis still remains the platform technology for the majority of proteomic investigations. This is due to its unparalleled ability to simultaneously separate several thousand proteins, up to 10,000 (Klose *et al.*, 1999), and the relative ease with which protein spots can be identified using MS based methods. However, 2-DE is an extremely sample dependent technique and methods had to be developed for the specific samples under study, especially at the level of protein sample preparation and IEF.

Cell breakage methodology was optimised to extract maximum quantities of protein; however it was important to ensure protein isolates were representative of the cell sate they were extracted from and had not undergone post cell lysis modification. Such modifications usually arise from the action of proteases, which are co-liberated in the protein extract and cause great complication to the analysis of 2-DE results. This is because their activity, post cellular disruption, is not representative of the biological system being studied and can result in artefactual spots. To inhibit the action of protease enzymes in this experimentation, cell samples and extracts were always kept on ice and tris base and EDTA were included in the extraction buffer (Berkelman and

Stenstedt, 2001), whereas other proteomic investigations have included protease inhibitor cocktails in the extraction solution (Granier, 1988). However, protease inhibitors modify the proteins upon which they act, which may lead to charge artefacts on the 2D gel (Dunn and Görg, 2001) and some inhibitors are small peptides and may therefore appear on the 2D gel.

Although *Synechocystis* has only 3168 genes and 2-DE can simultaneously resolve several thousand individual proteins, PTM's generating multiple isoforms of the same protein and the high dynamic range of proteins expressed in biological systems, as many as 9000 different protein moieties could exist. Therefore, total cell lysates were fractionated into membrane and soluble protein fractions using ultracentrifugation to reduce sample complexity and enrich for low copy number proteins. This also allowed the independent development of 2-DE methodology for both soluble and membrane protein fractions which differ greatly in their solubility and thus 2D resolution.

Fractionated cell lysates containing proteins for analysis also contain other biological material such as salts, lipids and nucleic acids all which can interfere with the 2-DE process (Dunn and Görg, 2001). In order to remove these contaminants *Synechocystis* soluble proteins fractionated from broken cells were precipitated with 80 % (v/v) acetone and subsequently resolubilsed in 2D lysis buffer. However, no precipitation technique is 100 % efficient and some proteins can be selectively lost as a result of refusing to resolubilise following precipitation (Berkelman and Stenstedt, 2001). In order to determine if the precipitation process and subsequent solubilisation in 2D lysis buffer greatly altered the *Synechocystis* soluble protein complement, direct soluble extracts and precipitated soluble protein samples solubilised in 2D lysis buffer

were compared via SDS-PAGE, which revealed no evidence of differential loss of proteins following precipitation and subsequent resolubilisation.

3.3.5   Optimisation of 2-DE for resolution of *Synechocystis* soluble proteins

Due to the relative ease with which soluble proteins are resolvable via 2-DE, the methodology was first optimised for the *Synechocystis* soluble protein fraction. It was initially important to establish reproducible two dimensional separation of soluble protein samples and analysis of six different samples via mini pH 3-10 2-DE, performed on two separate occasions, demonstrated this. However, this analysis also showed that the majority of *Synechocystis* soluble protein spots focused within the pH 4-7 range. Although wide linear range pH 3-10 IEF gels provide a good initial analysis of a new sample type (Görg *et al.*, 1999) these 2D gels often suffer from a lack of resolution. In other proteomic investigations this has been overcome by using nonlinear pH 3.5-10 IPG IEF gels (Bjellqvist *et al.*, 1993) in which the pH 4-7 range contains a must broader distance for separation. However, greater resolution has been achieved by using narrow range (zoom) IPG IEF gels (Görg *et al.*, 2000), and in this analysis 2-DE employing pH 4-7 and pH 4.5-5.5 zoom gels resulted in far greater resolution of *Synechocystis* soluble protein spots, although this does sacrifice the separation of basic proteins. Image analysis of the pH 4-7 and pH 4.5-5.5 zoom gels used in this investigation demonstrated that the number of individual resolved spots increased from 200 in the min pH 3-10 gels to 400 and 600 resolved by the pH 4-7 and 4.5-5.5 large format gels, respectively. In some investigations multiple, overlapping narrow range IEF gels spanning 1-1.5 pH units have been utilised to successfully increase the resolution across the entire pH range (Wildgruber *et al.*,

2000) or IEF gels with extended separation distances of up to 24 cm (Görg et al., 1999, 2000). By increasing the resolution of protein samples you increase the separation of proteins as individual spots and thus the probability of obtaining a positive identification.

Development of IEF methodology in this investigation was extended further to test protein loading methods into IPG IEF gels. There are currently three different methods for this, these being, in-gel rehydration (IGR), cup loading and paper bridge. The latter is specifically suited for the separation of basic proteins and high sample quantities can be applied promoting its use in preparative gels (Sabounchi-Schütt, et al., 2000). Cup loading and IGR on the other hand are virtually universal, being used across all pH ranges and for both analytical and preparative gels, with IGR being a simpler method and preferred for generation of preparative gels due to the greater capacity for protein loading (Sanchez et al., 1997; Rabilloud et al., 1994). Experiments, analysing both cup and IGR loading methods determined that cup loaded 2D gels had far greater resolution than IGR loaded gels across a variety of protein loadings. This was unexpected as it has been reported that IGR provides better resolution than cup loading, due to the tendency for precipitates to occur during IEF at the point of application (Rabilloud et al., 1994). Also, a good level of comparability was attained between low loaded analytical gels and high loaded preparative gel using cup loading, an important consideration for accurate picking spots from preparative gels selected for identification on analytical gels. Furthermore, by using cup loading the possibility of proteolysis and protein modification during over night IGR is removed.

Second dimension SDS-PAGE was also optimised during this investigation as the lack of resolution of low molecular weight proteins using 12 % polyacrylamide gels was evident. Resolution of low MW proteins was dramatically improved using 15 % polyacrylamide gels, however this did sacrifice the separation of high MW proteins which tended to converge using these gels due to the reduced distance for separation. Therefore, it was concluded that both 12 % and 15 % polyacrylamide gels would be required for comprehensive proteomic investigations. The use of polyacrylamide concentration gradient gels have been employed in other investigations which also extend the range over which proteins of different molecular weight are separated (reviewed by Dunn, 1987).

Large format 2D gels have a tendency to tear whilst handling which has great repercussions on image analysis and spot picking and several techniques were tried and tested to avoid this. One such method was the use of Duracryl™, a high tensile strength alternative to acrylamide (Patton et al, 1991). Although gels were much stronger, Duracryl had a marked effect on the resolution of high MW proteins, causing closely migrating individual protein spots to merge together. This effect was exaggerated with higher loaded gels. Consequently, Duracryl was not applicable to this investigation due to the obvious problems of comparability between low loaded analytical gels and high loaded preparative gels, and also due to the inability to separate proteins as individual spots which would complicate accurate protein identification. However, Duracryl, has been used in other investigations to successfully resolve different protein samples (Patton et al, 1991). Other methods were therefore developed to prevent tearing of large format gels, these being the backing of gels to low fluoresce glass plates which allowed staining and subsequent

visualisation using SYPRO Ruby florescent stain. Unfortunately, at the time of investigation spots could not be excised from backed gels, and therefore only analytical gels could be generated using this technique. Therefore, preparative gel thickness was increased to 1.5 mm from 1 mm, which improved the strength of the gel and also gels were handled using a nylon mesh which helped support the entire gel while being lifted out of the staining tray and onto glass plates for imaging and picking. Since this time, a compound called Rhinohide™ developed by Molecular Probes which can be added to acrylamide gel solutions to increase the rigidity of the gel and which does not cause merging of high molecular weight proteins similar to that seen in Duracryl™ gels (Schulenberg et al., 2003).

3.3.6 Subfractionaction of *Synechocystis* membrane proteins and resolution via 2-DE

A reagent-based subfractionation methodology was successfully employed in this investigation able to enrich for specific subsets of membrane proteins, simplify 2D gel profiles and increase abundance of low copy number proteins. Other reported methods for the subfractionation of membrane proteins include the differential solubilisation in varying chloroform/methanol mixtures as a function of their hydrophobisity (Seigneurin-Berny et al., 1999; Ferro et al., 2000) and the sequential extraction on the basis of their solubility in a series of detergent based buffers with increasing solubilising power (Molloy et al., 1998). Such methods provide a good platform for proteomic analysis of *Synechocystis* membrane proteins. However, the independent analysis of thylakoid and plasma membrane protein fractions would generate more biologically accurate data and with the development of aqueous polymer two phase

partitioning methodology able to prepare pure plasma and thylakoid membranes from *Synechocystis* cells (Norling *et al.*, 1998) such analysis is possible. Several proteomics investigations of *Synechocystis* membrane fractions have already been under taken, including total thylakoid membranes extracts (Sazuka *et al.*, 1999), peripheral thylakoid proteins (Wang, *et al.*, 2000), and also isolation and identification of functional membrane complexes and their subunits using 2-D blue native/SDS-PAGE (Herranen *et al.*, 2004).

3.3.7 Establishing MALDI-ToF PMF methodology for the identification of *Synechocystis* proteins

The development of MS based technologies has been fundamental in the formation of the field of proteomics as they provide the means by which proteins can be identified from predicted sequence data. In this study MALDI-ToF PMF technology has been successful applied in identification of *Synechocystis* soluble proteins. A rapid methodology was established with a relatively high hit rate providing the ideal starting point for characterisation of proteins in future proteomic studies although LC MS-MS may have to be subsequently employed to generate further identifications. The success of protein identification using MALDI-Tof PMF was probably increased due to the application of narrow range pH gradient 2D gels, indicating their importance in future 2-DE analysis. This analysis also demonstrated that 18 % of the *Synechocystis* proteins identified were represented as multiple spots on the 2D gel, indicating that gene products are present as multiple protein isomforms with PTM. Analysis of post IEF protein reductive alkylation demonstrated that these isoforms were not a result of re-oxidation during IEF and that they were probably real

biological isoforms. The data obtained from this proteomic study of *Synechocystis* soluble proteins was subsequently published in Proteomics: (Simon. *et al.*, 2002).

3.3.8   Concluding remarks

Synechocystis sp. PCC 6803 has been demonstrated as an ideal model organism for proteomic analysis and also for the investigation of stress induced responses, due to its ease of growth, the availability of the entire genome sequence (Nakamura *et al.*, 1998) and the ease of transformation (Dzelzkalns and Bogorad, 1986) generating several mutant strains many with mutations in stress responsive and signal perception genes. In particular gene knockouts of histidine kinase (*hik*) (Suzuki *et al.*, 2000a) and response regulators (*rre*) genes, involved in the two-component signal transduction mechanisms have been created. Investigations using these strains have identified Hiks involved in signal perception and transduction of a variety of stimuli/stresses. These include, cold stress (Suzuki *et al.*, 2000a and 2001; Inaba *et al.*, 2003), salt stress (Marin *et al.*, 2003), heat shock (Suzuki *et al.*, 2003) high light (Hsiao *et al.*, 2004) adaptation to light-dark transitions (Garcia-Dominguez *et al.*, 2000, Park *et al.*, 2000) phosphate ion sensing (Hirani *et al.*, 2001, Suzuki *et al.*, 2004) manganese ion sensing (Yamaguchi *et al.*, 2002, Ogawa *et al.*, 2003) and photoinhibition (Mikami *et al.*, 2003). DNA microarrays containing 95 % of the *Synechocystis* genes have allowed stimuli/stress responses to be studied at the level of gene expression in this organism. Such investigations to date include the acclimation to high light (Hihara *et al.*, 2001), the response to salt and osmotic stress (Kanesaki *et al.*, 2002), the response to cold stress (Suzuki *et al.*, 2001) and phosphate sensing (Susuki *et al.*, 2004).

Although a number of proteomic investigations, aimed at mapping the proteome of *Synechocystis* have been performed at thylakoid (Wang *et al.*, 2000, Herranen *et al.*, 2004) soluble (Sazuka *et al.*, 1997, 1999) periplasmic (Fulda *et al.*, 2000) and plasma membrane (Huang *et al.*, 2002) levels, only two have been performed analysing the stress/stimuli responses of *Synechocystis*, these being salt stress (Fulda *et al.*, 2000) and light induction (Choi *et al.*, 2000). Consequently little is known about the adaptive and stress changes in the proteome. With the establishment of large scale rapid reproducible growth generating adequate biological material, cellular fractionation methodology for enrichment of specific subset of proteins and reduced 2D complexity, and also high resolution 2-DE coupled to MALDI-ToF PMF mass spectrometry, a technology base has been developed geared to identifying time specific changes in the proteome of *Synechocystis* following stress treatment.

CHAPTER 4

Characterisation of the Heat Shock Response and

Identification of an Upstream Heat Sensor in *Synechocystis*

4.1   Introduction

Upon exposure to elevated temperature all cells respond by transiently inducing the expression of the heat shock genes, essentially encoding molecular chaperones and proteases, which function to re-fold and degrade denatured and aggregated proteins, an effect of the increased ambient temperature (Georgopoulos and Welch, 1994; Hendrick and Hartl, 1993; Ellis, 2001).

Extracellular signals are perceived by and transduced into cells via signal transduction pathways, the major mechanism of which is reversible protein phosphorylation and is catalysed by kinase enzymes (Hunter, 1995). In eukaryotic cells, multiple kinase enzymes take part in phorphorylation cascades, where each kinase phosphorylates another sequentially. This eventually leads to the activation of transcription factors that catalyse the transcription of relevant mRNAs and results in the production of stimuli related polypeptides. The most common sites for phosphorylation on proteins in eukaryotic cells are serine, threonine and tyrosine amino acid residues. In contrast, a much simpler signal transduction system exists in prokaryotes (Appleby *at al.*, 1996). Referred to as the two-component signal transduction mechanism, proteins are phosphorylated on histidine residues (histidine kinases, hiks) and this phosphoryl group is subsequently transferred to an aspartyl group on a response regulator (Rre) protein which in turn catalyses the transcription of relevant mRNAs (Saito, 2001). Two-component signalling mechanisms were once believed to be specific to prokaryotic cells, however, recent findings have proved this to be incorrect as hiks have been found within the cytosol and plasma membrane of various eukaryotes, including yeast (Maeda *et al.*, 1994) and plants (Chang *et al.*, 1993; Kakimoto, 1996).

Analysis of the *Synechocystis* genome sequence has identified 43 putative genes for

hiks (Mizuno *et al.*, 1996). Since the protein products of these genes have been

shown, in many cases, to be sensors or components of signal-transducing mechanisms

(Appleby *at al.*, 1996; Mizuno *et al.*, 1996) some of the *hik* genes in *Synechocystis*

may also have similar functions. The functions of some 30 hiks have been determined

in *E.coli* (Mizuno *et al.*, 1996), however there are no obvious homologues of these

enzymes in *Synechocystis* and therefore it is not possible to deduce the function of the

Synechocystis hik genes by comparing their primary structure.

Despite numerous studies aimed at investigating how cells perceive and transduce

extracellular stress, little is known about the nature of sensors and signal transduction

participating in the heat shock response. There are two groups of mechanisms by

which prokaryotes sense and regulate the heat shock response. One is the positive

regulation through the action of transcriptional initiation σ-factors which have been

observed in *E.coli* (Yura and Nakahigashi, 1999), *B. subtilis* (Hecker and Voelker,

1998) and *S. coeliclor* (Kormanec *et al.*, 1999). Aditionally, heat shock genes have

been shown to undergo negative regulation through the action of a transcriptional

repressor, such as HrcA in *B. subtilis* (Mogk *et al.*, 1997) and *Streptomyces* sp.

(Servant and Mazodier, 2001) and HspR and RheA also in *Streptomyces* sp. (Servant

and Mazodier, 2001). In cyanobacteria less information is known. A novel heat shock

gene repressor has been shown to regulate the expression of the *hspA* gene (sHsp) in

Synechococcus vulcanus (Roy *et al.*, 1999). This is a similar mechanism to that

observed in *S. albus* where the *hsp18* gene in under the control of the RheA repressor

(Servant and Mazodier, 2001). Also a positive regulator of the *groESL* operon was

identified in *Synechococcus* sp. PCC 7942 (Nakamoto *et al.*, 2001) and in

Synechocystis sp. PCC 6803, a CIRCE element has been identified upstream of the *groESL* operon and mutagenesis of the hrcA *gene* has demonstrated depression (Nakamoto *et al.*, 2002).

To attempt to elucidate the functions of the *hik* genes in *Synechocystis* and thus their role in the perception and transduction of stimuli/stress, systematic gene knockouts of all 43 hiks have been created (Suzuki *et al,.* 2000a). This work was done by members of Prof. Norio Murata's Lab. Using these mutant strains of *Synechocystis, hiks* involved in sensing and signal transduction of a variety of external stimuli have been identified, such as cold stress (Suzuki *et al,.* 2000a, 2001), manganese sensing (Yamaguchi *et al,.* 2002), osmotic stress (Marin *et al.*, 2003) and phosphate sensing (Suzuki *et al.*, 2004). Unpublished work by Iwane Susuki in Prof, Murata's Lab (personal communication) has identified a Hik in *Synechocystis*, Hik34, as a candidate heat sensor. This work was done by screening a *Synechocystis* knockout library of all *hik* genes for expression of heat shock genes via DNA microarray. These results showed that under normal growth conditions expression of heat shock genes, such as *groESL, hspA, htrA* and *groEL-2,* were greatly elevated in Δ*hik34* cells in comparison to wild type cells. Also, the heat inducibility of these heat shock genes was decreased in Δ*hik34* cells. Additional work analysing the survival of *hik* mutant *Synechocystis* strains at high temperature demonstrated that Δ*hik34* cells were shown to be more heat tolerant than wild type cells and any of the other *hik* gene knockout mutants. Moreover, analysis of the phosphorylation activity of Hik34 *in vitro* showed that it was maximal at normal growth temperature and reduced at higher temperatures, to the extent that it was almost completely inactive under heat shock conditions. These findings suggested that under normal growth conditions Hik34 is active and functions

to repress the expression of heat shock genes. Under heat shock conditions it ceases to be active releasing this repression and thereby allowing the expression of heat shock inducible genes. This negative regulatory mechanism is very similar to that of the HrcA repressor mechanism in *B. subtilis* (Mogk *et al.*, 1997).

Despite what is known about the role Hik34 and other prokaryotic gene expression regulatory mechanisms in the heat shock response and also about the genes that are induced/repressed by heat shock, very little in known about the effects of heat shock and the role of transcriptional regulation on protein steady state levels in *Synechocystis*. This is an important consideration as proteins carry out cellular function and there is little correlation between protein and mRNA levels has been observed (Haynes *et al.*, 1998, Gygi *et al.*, 1999b; Pennington & Dunn 2001). Also, the biological activity of a mature protein is regulated at several levels above the transcription of its corresponding gene. For example post translational modifications (PTMs) can greatly affect the activity and cellular localisation of the protein they modify and one gene can give rise to multiple protein products possessing different PTMs. Such information is not accessible from analysis at the mRNA level, but examination of the proteins will provide a more accurate description of the activity and function of the cell under the particular stress being studied.

The aims of this research were to, firstly, apply a proteomic approach to characterise the heat shock response in *Synechocystis* and, secondly, to quantify and compare the heat shocked induced changes in protein steady state levels between wild type and Δ*hik34 Synechocystis* cells. The optimised 2D-E method (as described in chapter 3) was used to separate individual proteins, and 2D DIGE technology was employed to

accurately quantify and compare individual spot abundances between control and heat treated samples. This data would be subsequently compared to the changes in gene expression studied by Iwane Susuki in Prof. Norio Murata's Lab and to determine the extent of correlation between the protein and mRNA data sets. It was the intention that this proteomic analysis would give a global picture of the proteins actively induced under heat shock conditions and also support the theory that Hik34 functions as a negative regulator of the heat shock response. Key to the approach which is being used in proteomics is the consideration of biological variation and a rigorous statistical analysis of the data. This should allow one to identify changes as small as 10 % at the 95 % confidence limit and also potentially identify any changes in the diversity of post-translational products arising from the initial mRNA translations. Furthermore, this analysis will also allow the identification of changes which occur not only in the known heat shock proteins but also in the components of other cellular processes, such as metabolism.

4.2   Results

4.2.1   Effect of heat shock on soluble protein steady state levels in wild type *Synechocystis*

The effects of a stress are not immediately noticeable at the protein level following application of the stress. Transcription and translation, post translational modification and translocation all take time. Therefore, before proceeding into an extensive investigation of the heat shock response in *Synechocystis* and function of Hik34, it was necessary to establish a suitable time window in which this stress response would be studied. To investigate this, a 500 ml exponentially dividing wild type culture (A_{730} ~ 1.0) was heat shocked by shifting the growth temperature from 34°C to 44°C, heat shock conditions for this organism. Cells were incubated at 44°C for 8 hours, during which time 50 ml aliquots of culture were removed at specific time points and immediately placed on ice. Cells were collected, broken using glass beads (ø ~ 106 μm) and the soluble protein isolated. Aliquots of crude *Synechocystis* soluble fractions from each time point containing 20 μg of protein were analysed via SDS PAGE (Figure 4.1). This revealed 5 obvious protein bands that increased in abundance in response to heat shock with time. These bands, labelled a-e, had molecular weights of 70.1, 67.5, 61.0, 47.7 and 16.1 kDa, although the first of these two bands are outside the molecular weight range of the standards used, and their increased abundance was obvious after 90 minutes. However, because this analysis presented no clear indication of the time frame for heat shock induced changes in protein synthesis, the more sensitive and specific technique of *in vivo* protein radiolabelling was employed. This investigation would highlight only those proteins *de novo* synthesised under heat
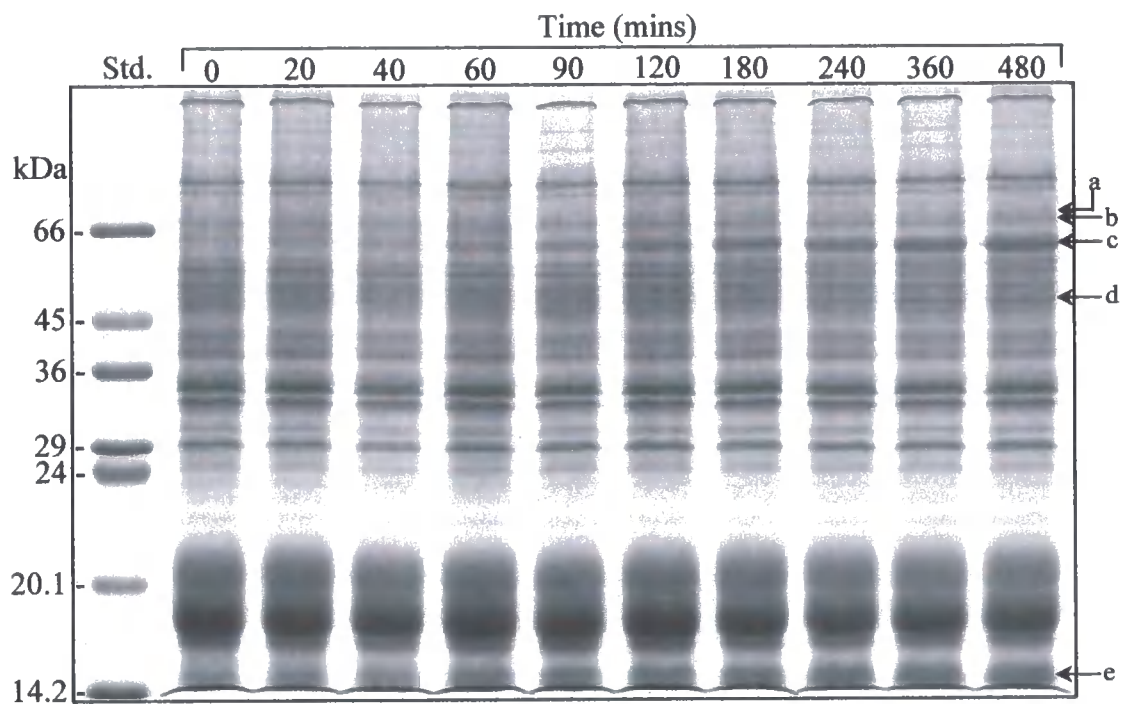
Figure 4.1. SDS PAGE of soluble protein fractionated from wild type *Synechocystis* cells subjected to a time course of heat shock (0-8 hours).

An exponentially growing *Synechocystis* culture was exposed to heat shock conditions (44°C) and at set time points over an 8 hour period cells were removed. Soluble protein was fractionated from these cells, resolved via SDS PAGE (20 µg per lane) and visualised with Coomassie Brilliant Blue. Arrows on the right of the gel indicate protein bands that have increased in abundance from steady state levels in response to heat shock.

shock and also allow a comparison of *de novo* protein synthesis in cells grown under normal conditions and those under heat shock. This would gain further insight into the heat shock response and facilitate the identification of an ideal time window in which to study the cellular heat shock response at the protein level.

4.2.2 ^{35}S radiolabelling of *de novo* synthesised *Synechocystis* proteins

Before conducting an *in vivo* radiolabelling experiment during heat shock, the efficiency of labelling was investigated and safe radiochemical procedures were established. A 50 ml exponentially growing wild type culture was incubated under normal growth conditions with 125 µCi of Redivue™ PRO-MIX™ L-[^{35}S] *in vitro* Cell Labelling Mix (Amersham Biosciences). This radiolabelling reagent contains both L-[^{35}S]-methionine and L-[^{35}S]-cysteine at a ratio of 70:30. The presence of both methionine and cysteine compensates for mature polypeptides that may not contain one of these amino acids and therefore ensures the majority of *de novo* synthesised proteins are labelled. Cells were labelled for 1 hour after which time they were harvested and broken with glass beads (ø ~ 106 µm). The crude soluble protein fraction was precipitated with 80 % acetone (see material and methods) and resolved via both mini SDS PAGE and mini 2D-E (Figure 4.2). Total protein was visualised with Coomassie Brilliant Blue staining and radiolabelled proteins were detected by autoradiography. These results demonstrated that *de novo* synthesised proteins were successfully radiolabelled using this method and could therefore be adopted to analyse *de novo* protein synthesis under heat shock conditions.
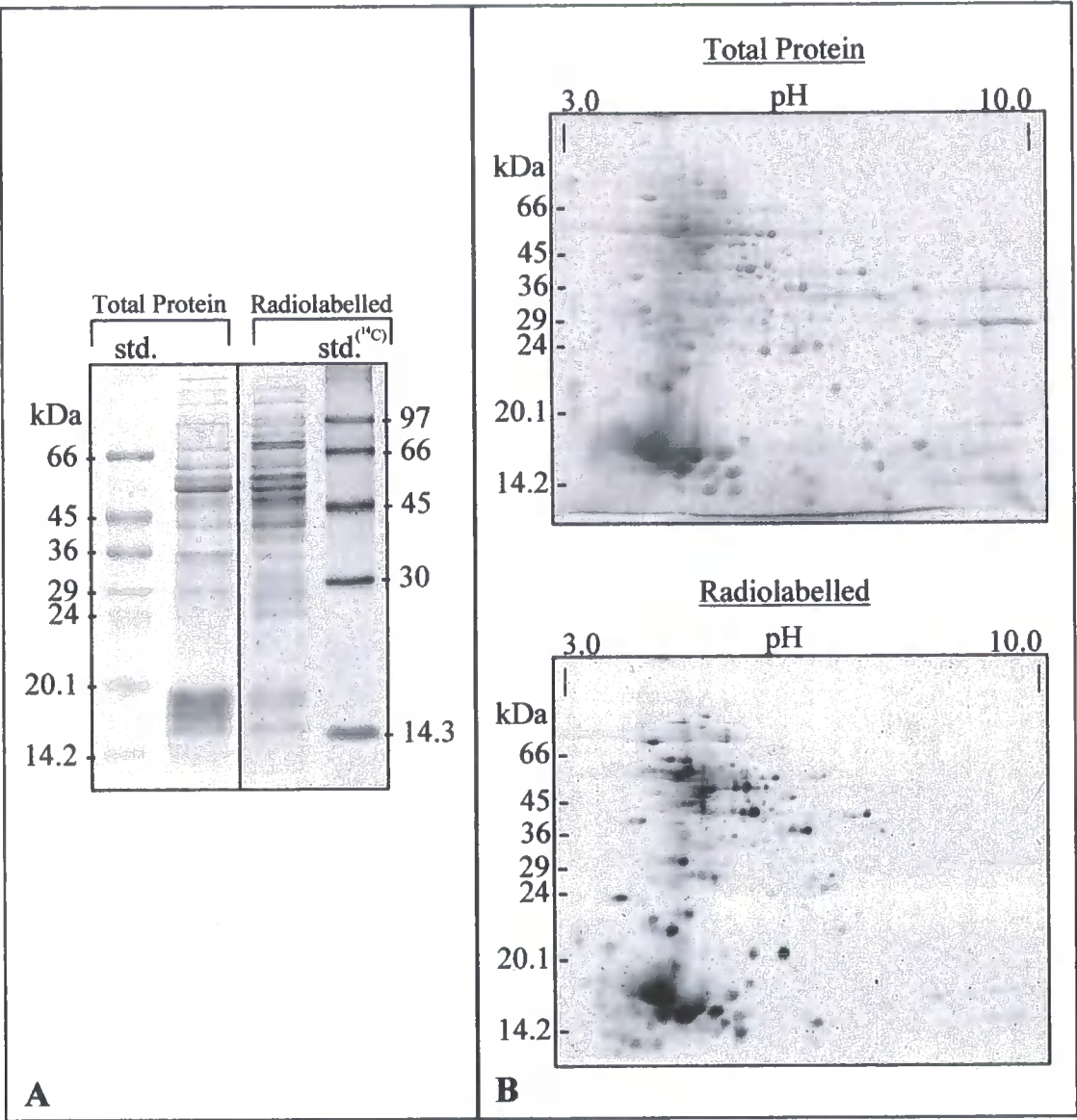
Figure 4.2. SDS PAGE and mini 2D-E of radiolabelled soluble proteins fractionated from exponentially growing *Synechocystis* cells.

Synechocystis cells were grown in the presence of L-[^{35}S]-methionine/cysteine (70:30) for 1 hour. Radiolabelled soluble proteins were isolated and 10 µg resolved via SDS PAGE (A) and 200 µg resolved by 2D-E (B). Total protein was visualised by Coomassie staining and radiolabelled protein detected by autoradiography.

4.2.3 ^{35}S radiolabelling of *de novo* synthesised *Synechocystis* proteins under heat shock conditions.

De novo protein synthesis in wild type *Synechocystis* cells grown under both normal (34°C) and heat shock (44°C) conditions was compared using ^{35}S radiolabelling. A 100 ml *Synechocystis* gassed culture (A.$_{730}$ ~ 1.0) was divided equally into two 125 ml glass culture tubes. These two 50 ml cultures were allowed to re-equilibrate to normal growth conditions for 4 hours before addition of ^{35}S radiolabel (as described in section 4.2.2). Following this, one culture was maintained at normal growth temperature (34°C), while the second culture was immediately transferred to 44°C. At set time points of 20, 40, 60, 120 and 340 minutes, 10 ml aliquots of were removed from both cultures and immediately placed on ice. Cells were harvested by centrifugation and radioactivity in the resultant culture media supernatants quantified by measuring 10μl and 20μl aliquots via scintillation counting. The loss of radioactivity from the culture media over time was plotted as a percentage of the original quantity of ^{35}S added (Figure 4.3). This was done to give an indication of the amount of radioactivity incorporated into cells as time progressed and to determine if incorporation differed between normal (34°C) and heat shock (44°C) cells. The loss of radioactivity from the media was similar under both normal and heat shock conditions and that during the first 40 minutes of labelling, ~ 30 % of the ^{35}S radioactivity was taken up by the cells, however after this time the rate of loss slowed.

Harvested cells from each time point grown under both control and heat shock conditions were broken with glass beads and the soluble protein fractionated. 50 μg of protein from each sample was subjected to SDS PAGE and resolved bands were
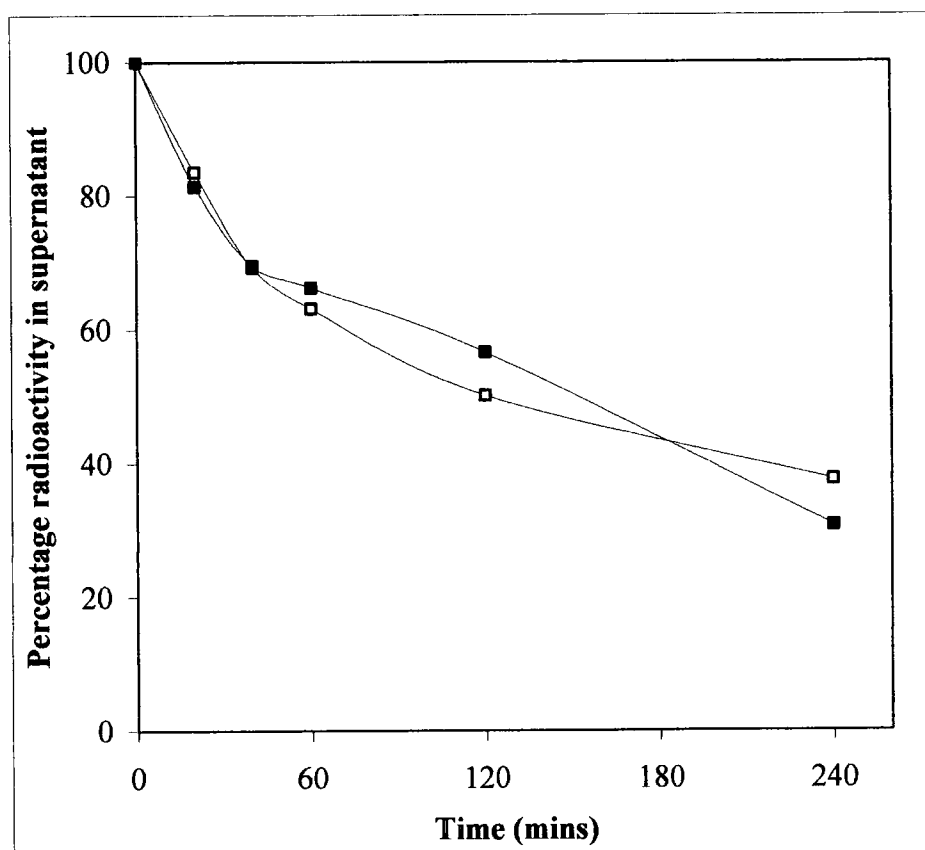
Figure 4.3. Loss of [35]**S radioactivity from** *Synechocystis* **culture media during cellular growth under normal (34°C) and heat shock (44°C) conditions.**

Exponentially dividing *Synechocystis* cells were incubated with 125 μCi of L-[35S]-methionine/cysteine under normal (34°C, □) and heat shock (44°C, ■) temperatures for 4 hours. At set time points of 20, 40, 60, 120 and 240 minuets, 10 ml aliquots of culture were removed and the cells harvested by centrifugation. Radioactivity in the resultant supernatants was quantified and the loss from the culture media calculated as a percentage of the original quantity of radioactivity added.

stained with Coomassie Blue. Radiolabelled bands were detected by autoradiography and the resultant autroradiogram was scanned along with the Coomassie gels using an Image Master scanner (Amersham Biosciences). The Coomassie stained gel and autroradiogram for both control and heat shock time courses are shown in Figure 4.4. Individual autoradiogram band volumes were quantified using Phoretix ID Advance software (Nonlinear Dynamics, Newcastle) using "valley to valley" background subtraction and normalised against the total band volume of the corresponding lane on the Coomassie stained gel to account for any variation in protein loading. These total bands volumes were pre-normalised for any variation in background staining by dividing the lane pixel volume by the background volume/area. Quantified volumes for corresponding protein bands in control and heat shocked samples were compared graphically. Figure 4.5a, Figure 4.5b and Figure 4.6 display a selection of protein bands with increased (bands & a-g) and decreased (bands u-z) *de novo* protein synthesis rates in response to heat shock, respectively. This analysis showed that an increase in the quantity of *de novo* synthesised protein was responsible for at least some if not all of the increased abundance identified for the 5 heat shock responsive bands (labelled a-e) highlighted in the initial 8 hour time course (Figure 4.1). Moreover, an additional two protein bands displayed increased *de novo* synthesis (labelled f and g) under heat shock conditions. In the majority of cases, with the exception of band d, there is a dramatic increase in synthesis over the first 1-2 hours of heat shock, after which it levels off and with certain bands synthesis starts to decrease, as with bands e and f. This levelling off indicates that for those particular protein bands, protein turnover is at equilibrium where protein is synthesised and degraded at equal rates. Where the level of *de novo* synthesised protein starts to decrease, the rate of degradation has exceeded the rate of synthesis. This analysis has

- 212 -

Figure 4.4. Time course of *de novo* protein synthesis in *Synechocystis* cells grown under normal growth conditions and following a shift in growth temperature to 44°C.

De novo synthesised proteins in *Synechocystis* cells grown under normal (A) and heat shock conditions (B) were ^{35}S radiolabelled *in vivo* for 4 hours. At specific time intervals of 20, 40, 60, 120 and 240 min, aliquots of cells were removed from both cultures and the soluble protein extracted. Protein was precipitated from an aliquot of each crude soluble fraction containing 50 µg of protein and resolved via SDS PAGE. Protein bands were visualised with Coomassie staining (C lanes) and rabiolabelled proteins were detected by autoradiography (A lanes). Bands marked with blue and red arrows are those which display a decreased or increased quantity of *de novo* synthesis, respectively. Bands labelled with a green arrow are those synthesised under normal growth temperature but not under heat shock conditions.
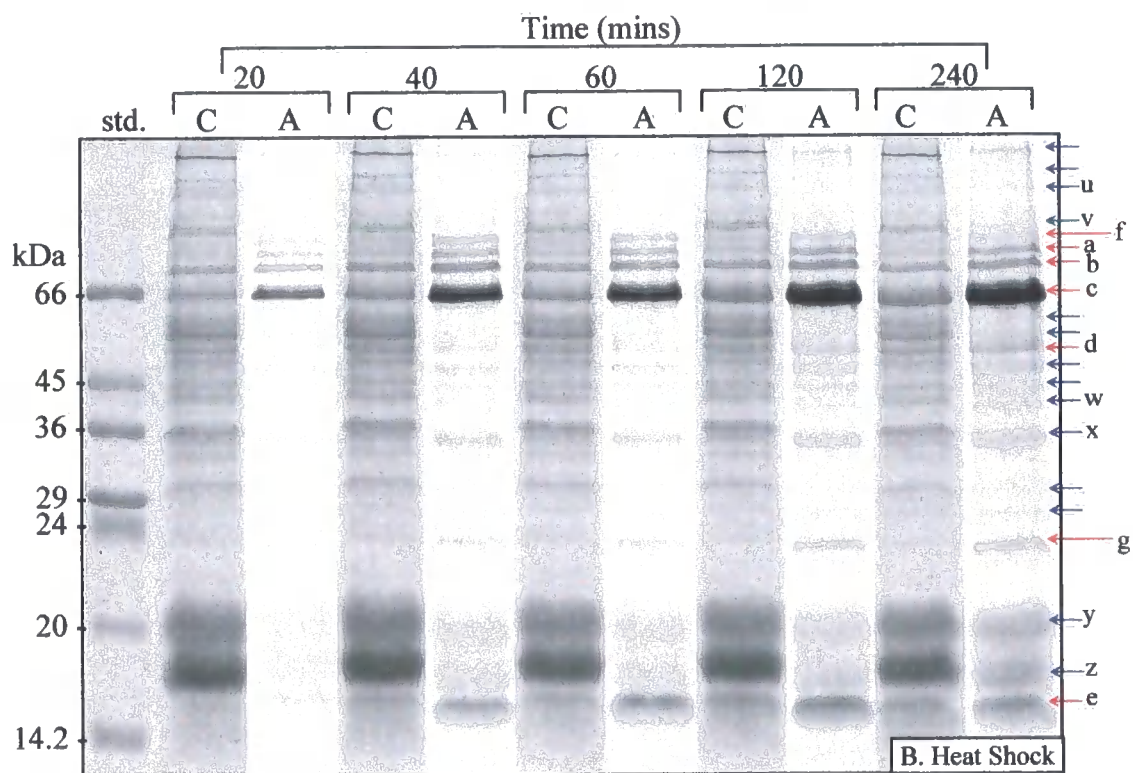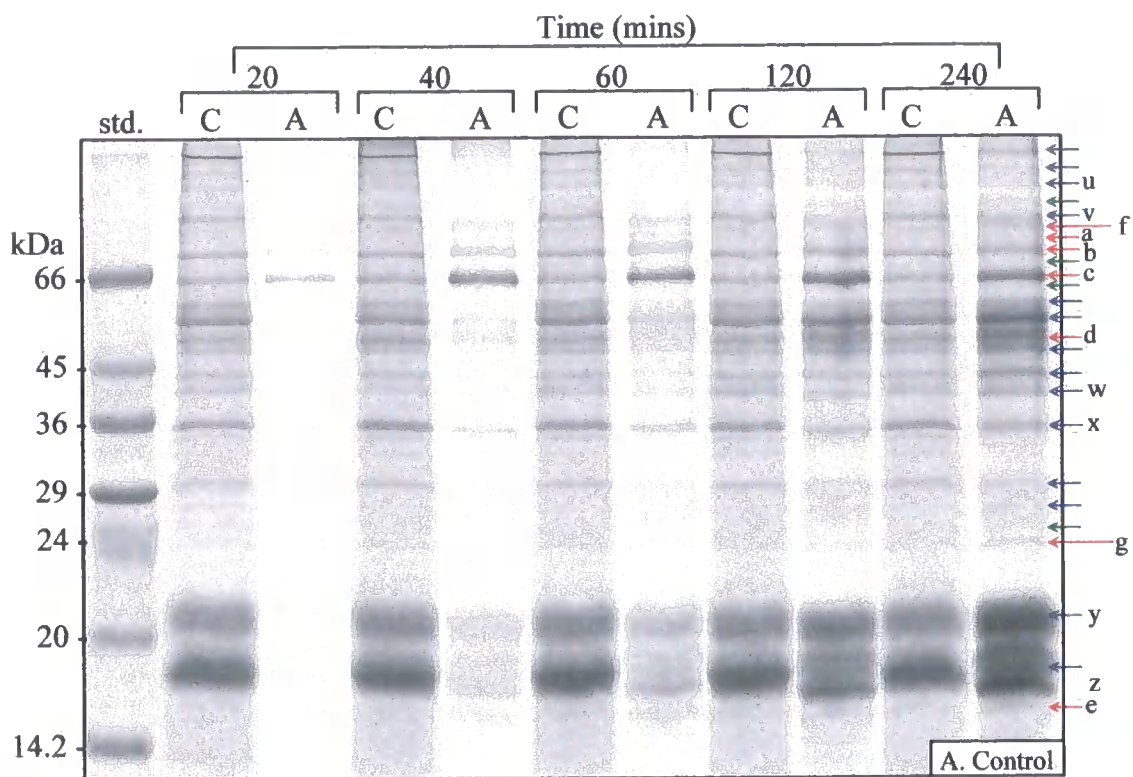
Figure 4.5a. Heat shock induced increased quantity of *de novo* protein synthesis for specific protein bands over time in *Synechocystis*.

Autoradiogram band volumes (Figure 4.4) were measured and normalised against the related lane volume on the Coomassie Blue stained gel. The values obtained for corresponding bands from control (■) and heat shock (●) time courses were plotted. Graphs labels relate to the band annotations in Figure 4.4.
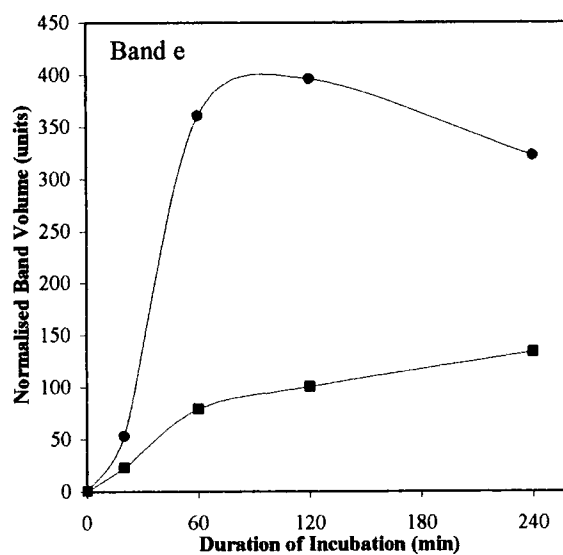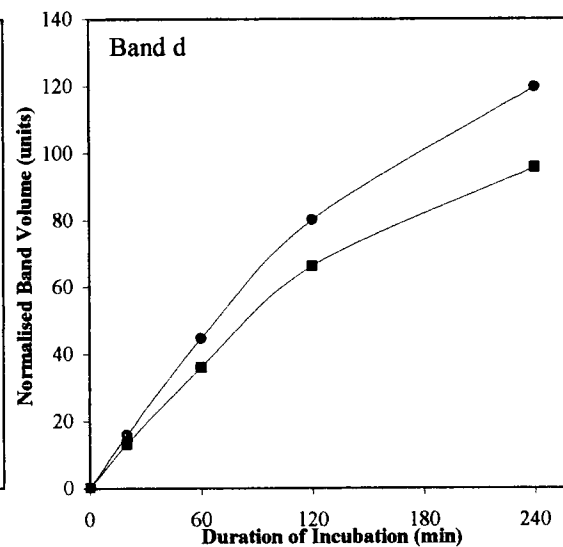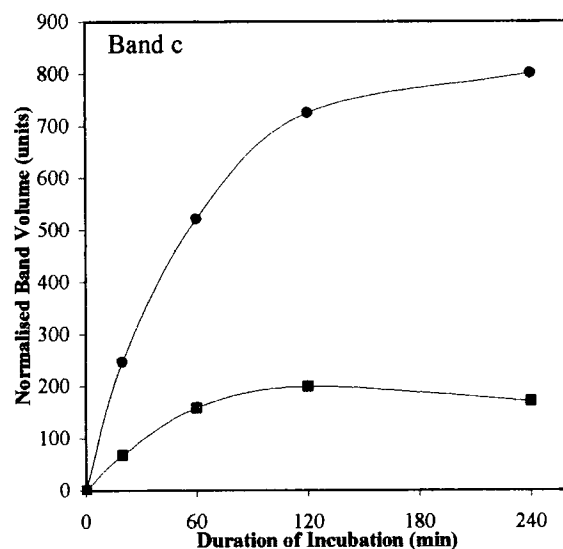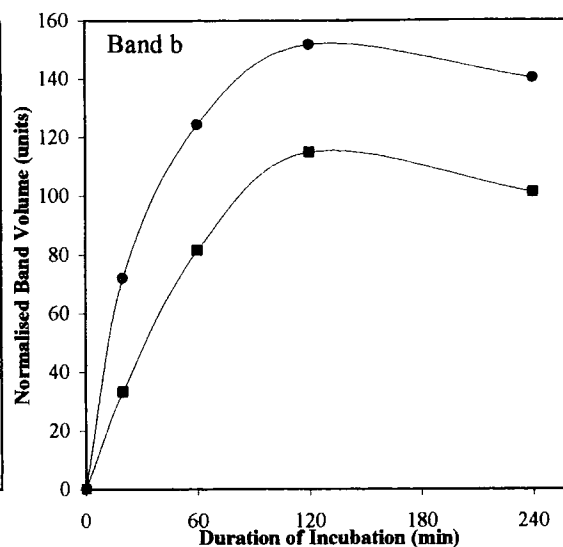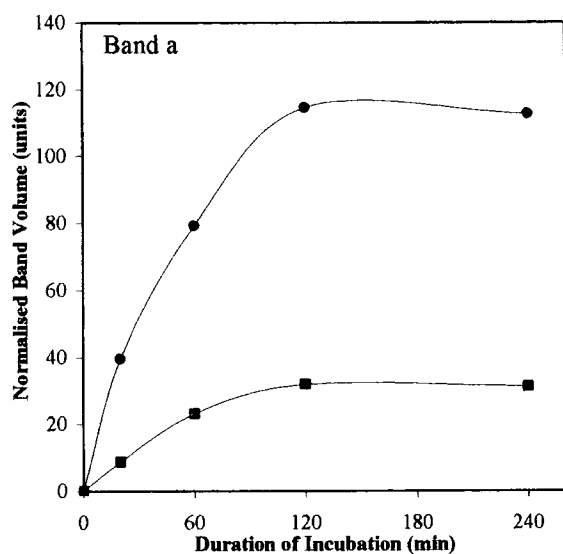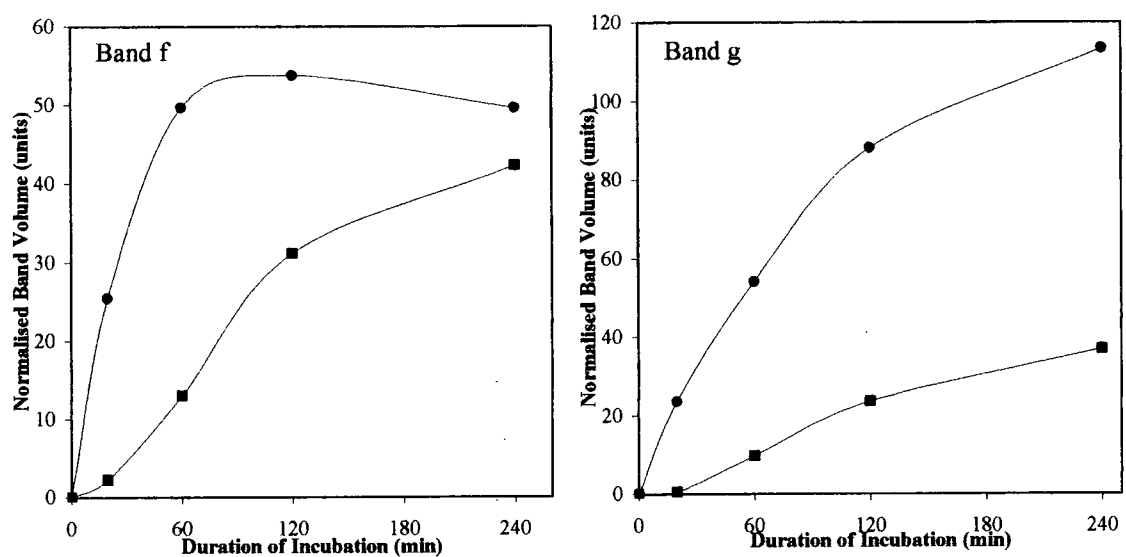
Figure 4.5b. Heat shock induced increased quantity of *de novo* protein synthesis for specific protein bands over time in *Synechocystis*.

Autoradiogram band volumes (Figure 4.4) were measured and normalised against the related lane volume on the Coomassie Blue stained gel. The values obtained for corresponding bands from control (■) and heat shock (●) time courses were plotted. Graphs labels relate to the band annotations in Figure 4.4.

Figure 4.6. Decreased quantity in *de novo* protein synthesis over time for specific protein bands in *Synechocystis* following heat shock.

Autoradiogram band volumes (Figure 4.4) were measured and normalised against the related lane volume on the Coomassie Blue stained gel. The values obtained for corresponding bands from control (■) and heat shock (◉) time courses were plotted. Graphs labels relate to the band annotations in Figure 4.4.
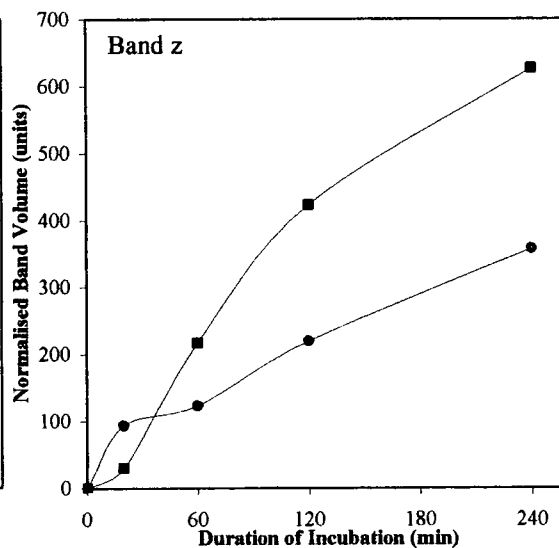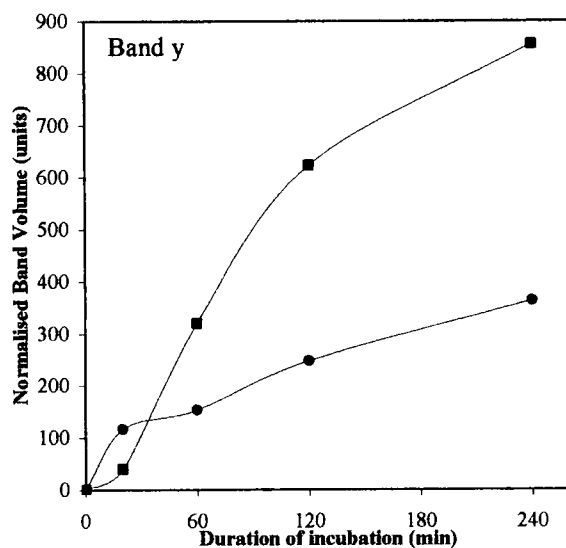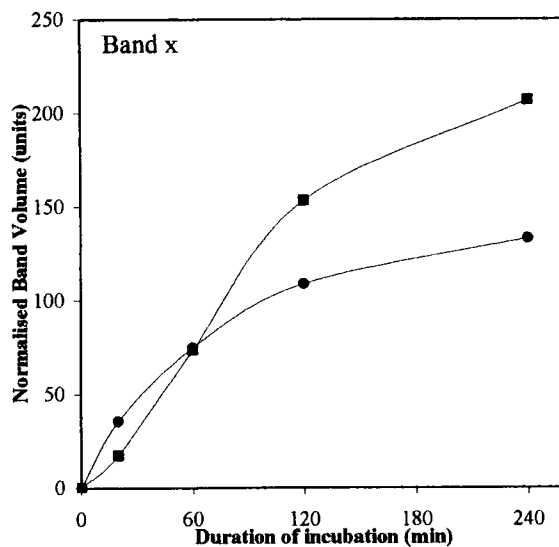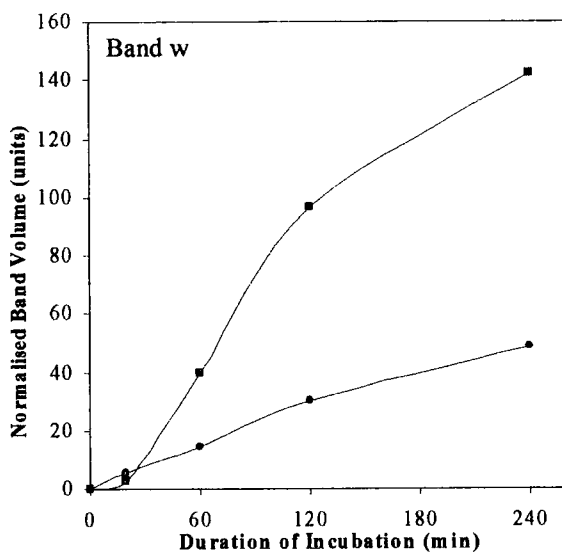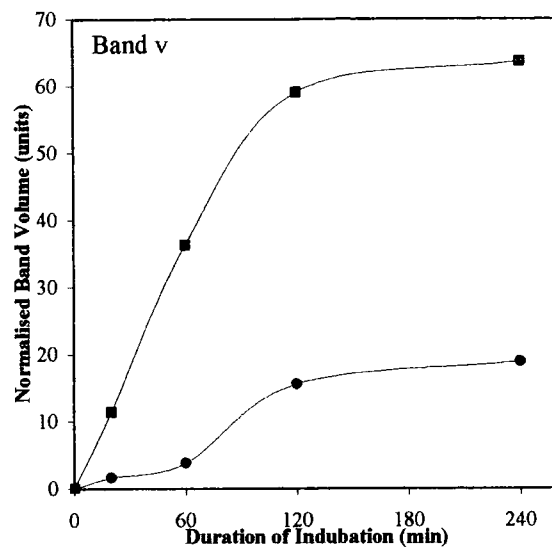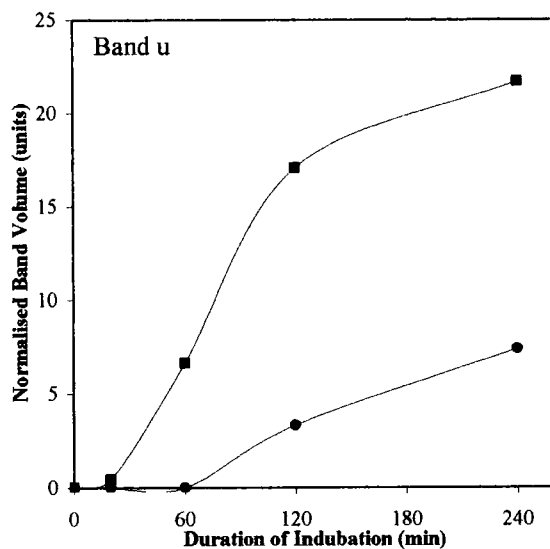
also demonstrated that 14 proteins bands, labelled with blue arrows in Figure 4.4, are synthesised during heat shock but at lower levels when compared to the control. Therefore the *de novo* protein synthesis of these 14 protein bands is reduced under heat shock conditions. However, some of these bands, i.e. bands x, y and z, show an initial heat shock induced level of synthesis greater than in cells grown under normal temperature, which subsequently declines. Bands y and z are the low molecular weight constituents of the phycobilisome proteins characteristic in cyanobacterial soluble protein preparations. In the later stages of the heat shock time course, *de novo* protein synthesis of these two bands is over two fold less than in cells grown under normal conditions. Band x is more noteworthy, as although protein synthesis is decreased in latter stages of the time course, after 60 minutes of heat shock it is one of the most abundant radiolabelled bands and the level of protein expression is slightly greater than in control cells. This indicates that this protein is important to the survival of *Synechocystis* cells under heat shock conditions. Finally, there are a number of protein bands synthesised under normal growth conditions that are not synthesised during heat shock, these are labelled with green arrows in Figure 4.4, and are obviously not essential to the cell for survival under heat shock conditions.

It is likely that the most important changes to the cells biochemistry and physiology will occur early on during the response. Therefore the earliest time window showing the widest variety of changes should be chosen for future analysis. When taking a broad look at the heat responsive protein bands, it is evident that for all but one band the difference in the level of *de novo* protein synthesis between control and heat shock samples is not the same across all time points, the exception being band b. However, the majority of bands do display a clear difference in the level of protein synthesis

after 1 hour. Consequently the 1 hour heat shock time point was chosen as the window in which the response to this stress would be studied.

4.2.4   Mini 2D-E of 1 hour ^{35}S radiolabelled soluble proteins from wild type *Synechocystis* cells grown under control and heat shock conditions.

There is no certainty that the compared radiolabelled bands from control and heat shock samples are the same protein(s), they may be different proteins with similar molecular weights. In order to investigate this, 200 μg of soluble protein isolated from 1 hour radiolabelled cells grown under both normal and heat shock conditions was analysed via mini 2D-E. Both pH 4-7 (Figure 4.7) and pH 6-11 (Figure 4.8) IPG strips were used in order to resolve the entire spectrum of proteins. The resolved spots were visualised by staining with Coomassie Blue and radiolabelled proteins were detected by autoradiography. The 7 protein bands showing an increased level of *de novo* protein synthesis in response to heat shock (a-g), when analysed via 1D SDS PAGE (Figure 4.4), were again seen to display this response and resolve as multiple spots with similar MW but different p*I* on the pH 4-7 min 2D gel (Figure 4.7). Moreover, band C appears to be composed of 2 different proteins, as 2 separate spot trains are clearly visible on this gel (labelled c and h). In addition to this, 5 more protein spots were discovered on the pH 4-7 min 2D gel (Figure 4.7), which display heat shock induced increased protein synthesis (labelled i-m). Both these observations demonstrate the increased resolution achieved by 2D gels in comparison to 1D gels. Also, it is evident from this analysis that protein "x" is a major constituent of the total *de novo* protein synthesis during heat shock, although its synthesis does not appear to be greatly elevated from steady state levels. This was seen on the mini 1D gel
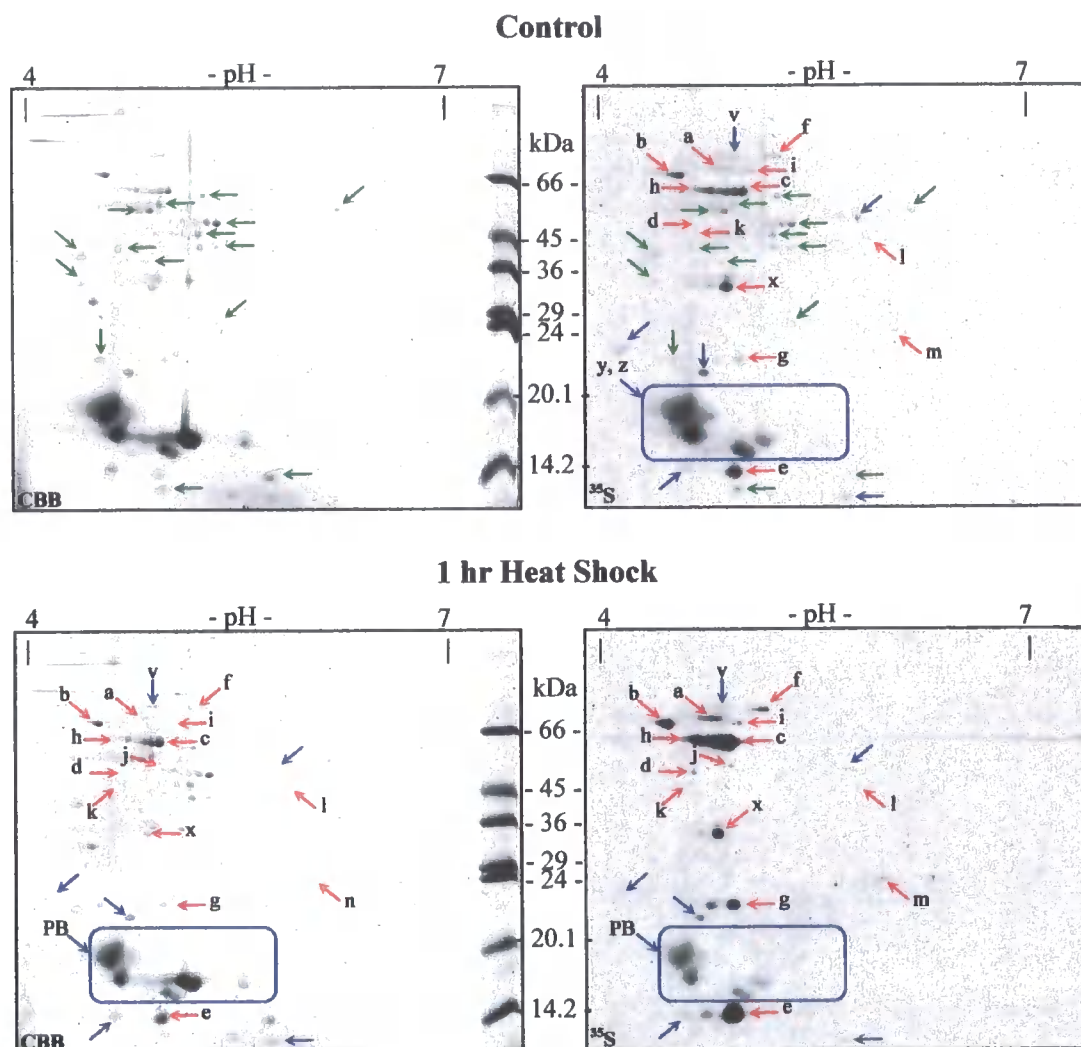
Figure 4.7. Mini pH 4-7 two-dimensional gel electrophoresis of *de novo* synthesised proteins during a 1 hour time window in *Synechocystis* cells grown under normal (34°C) and heat shock (44°C) conditions.

Soluble protein was fractionated from 1 hour radiolabelled *Synechocystis* cells grown under normal and heat shock conditions and 200 µg of protein from each sample was subjected to mini pH 4-7 2D-E. The resultant protein spots were visualised with Coomassie Brilliant Blue staining (**CBB**) and the radiolabelled proteins detected by autoradiography (^{35}S). Spots labelled with blue and red arrows are those which display decreased and increased *de novo* synthesis respectively, in response to heat shock. Green arrows indicate those spots synthesised under normal growth temperature but not in cells when heat shocked. (PB = phycobilsiome protein constituents).

Control
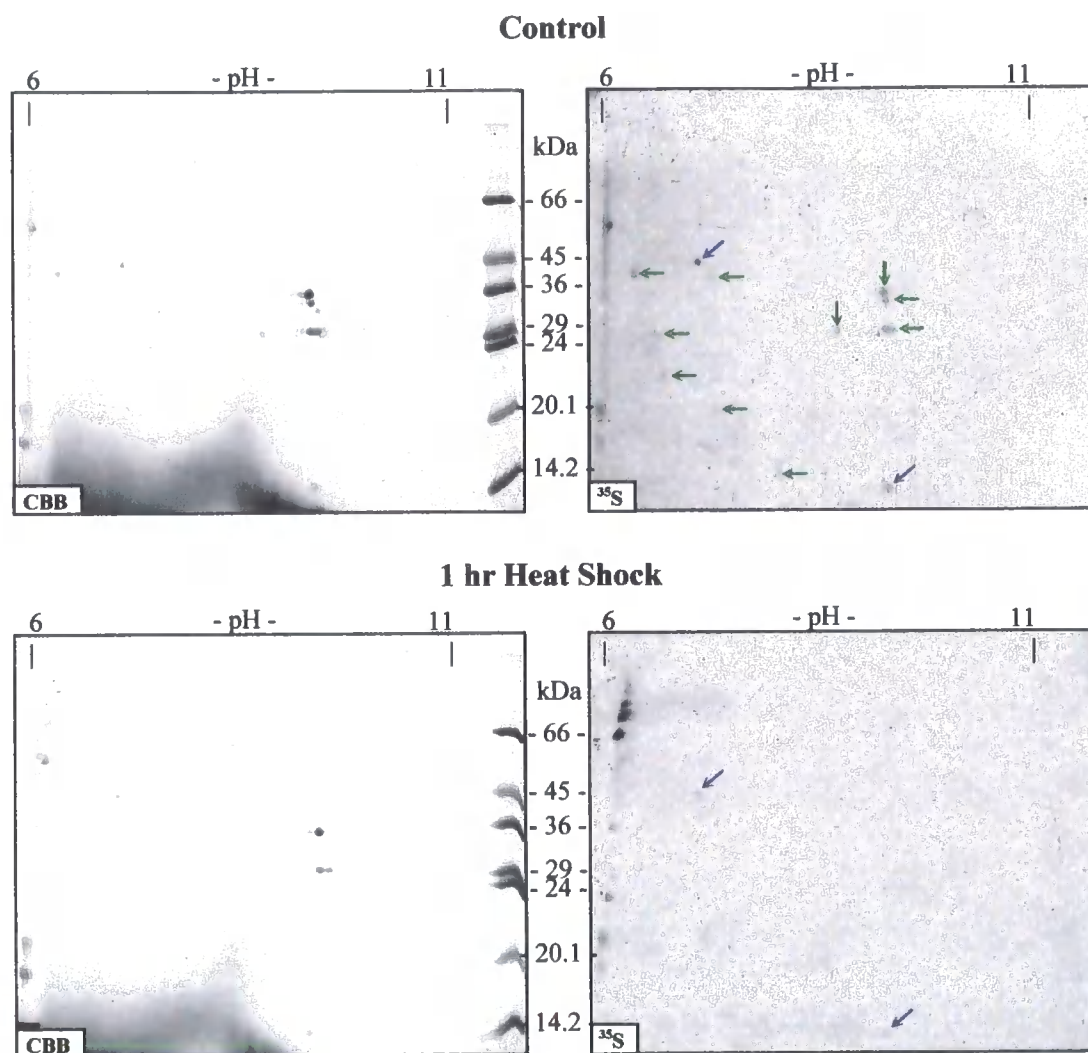
1 hr Heat Shock

Figure 4.8. Mini pH 6-11 two-dimensional gel electrophoresis of *de novo* synthesised proteins during a 1 hour time window in *Synechocystis* cells grown under normal (34°C) and heat shock (44°C) conditions.

Soluble protein was fractionated from 1 hour radiolabelled *Synechocystis* cells grown under normal and heat shock conditions and 200 µg of protein from each sample was subjected to mini pH 6-11 2D-E. The resultant protein spots were visualised with Coomassie Brilliant Blue staining (**CBB**) and the radiolabelled proteins detected by autoradiography (^{35}S). Spots labelled with blue and green arrows are those which display decreased or no *de novo* synthesis in response to heat shock, respectively.

(Figure 4.4) and confirms the prediction that this protein is probably an integral part of the cells survival mechanism under heat shock. The decreased *de novo* synthesis of phycobilisome constituents is further reinforced in this study (labelled PB on Figure 4.6). In addition, other protein spots displaying decreased or undetectable levels of protein synthesis under heat shock in comparison to levels in cells grown under normal temperature are evident in both pH 4-7 (Figure 4.7) and pH 6-11 (Figure 4.8) mini 2D gels. However there are no protein spots that show increased synthesis during heat shock on the pH 6-11 gel. For this reason pH 4-7 2D gels were used for all future analysis of the effects of heat shock on the soluble protein steady state levels. Finally, when comparing the levels of *de novo* synthesised protein with the abundance on the Coomassie stained gel, it is noticeable that although many proteins are reasonably abundant, there are many that are barley detectable with Coomassie staining. Because it is not possible to characterise very low abundant spots due to the quantity of protein available, this is an important issue to consider when the main intension of this study is to identify these proteins.

4.2.5   Large format 2D-E analysis of the effect of heat shock on soluble protein steady state levels in *Synechocystis*.

Having established a suitable time window in which to study the heat shock response in *Synechocystis*, the next phase of this investigation was to perform a large format 2D-E based comparison of control and heat shock soluble protein samples. Multiple repeats are essential to allow for statistical validation.

Four 500 ml exponentially dividing cultures grown under normal conditions were heat shocked at 44°C for 1 hour. Prior to heat shock half of the culture was removed and the cells immediately harvested. The remaining culture was shifted to 44°C for 1 hour before collecting the cells. Cells were broken with French press (see materials and methods for details) and the crude soluble protein fraction isolated. These crude extracts were precipitated with acetone and the protein complexities from repeat control and heat shock cells were visualised and compared using SDS PAGE (data not shown). The repeat protein extracts from both control and heat shocked samples were revealed to be highly reproducible and the obvious differences previously detected were visible. Aliquots of lysis buffer solubilsed protein from the four repeat control and heat shocked samples (totalling 8 samples) containing 200 µg of protein were cup loaded onto individual pre-hydrated 18 cm pH 4-7 IPG strips. These strips were focused using an Ettan IPGphor IEF System (Amersham Biosciences) for ~ 70 kVh and subsequently electrophoresed through SDS 12 % polyacrylamide resolving gels (26 x 20 cm), backed onto low fluorescence glass plates, using an Ettan DALT*twelve* Large Format Vertical Electrophoresis System (Amersham Biosciences). The resultant gels were stained attached to the glass plate each with 400 ml of SYPRO Ruby stain and visualised using a Typhoon Variable Mode Imager. High resolution scans at 100 µm were obtained for quantitative analysis. An example of each control and heat shock protein sample analysed in this fashion is displayed in Figure 4.9. The lack of detection of the Phycobilisome protein constituents using fluorescence imaging was immediately obvious and was deemed to be a result of the conflict between the wavelength of their intrinsic fluorescence and the emission wavelength of the SYPRO Ruby stain (see section 4.2.6). Protein abundance levels were quantified using Phoretix Evolution software (Nonlinear Dynamics). The corresponding ".gel"

Figure 4.9. SYPRO™ Ruby stained large format pH 4-7 2D gels of soluble protein isolated from *Synechocystis* cells grown normal (34°C) and heat shock (44°C) temperatures.

Soluble proteins were isolated from *Synechocystis* cells grown under normal (**A**) and heat shock (**B**) conditions and 200 μg from each cell sample were subjected to large format pH 4-7 2D-E. Resolved spots were visualised with SYPRO Ruby staining and imaging using a Typhoon Variable Mode Imager. Proteins detected by Phoretix Evolution analysis which increase in abundance are indicated in red. The area of interest (AI), highlighted with a blue square, encircling these proteins is enlarged in Figure 4.10. Phycobilisome proteins (PB), highlighted with a green square, are masked due to the conflict between the wavelength of their intrinsic fluorescence and the SYPRO Ruby emission wavelength.
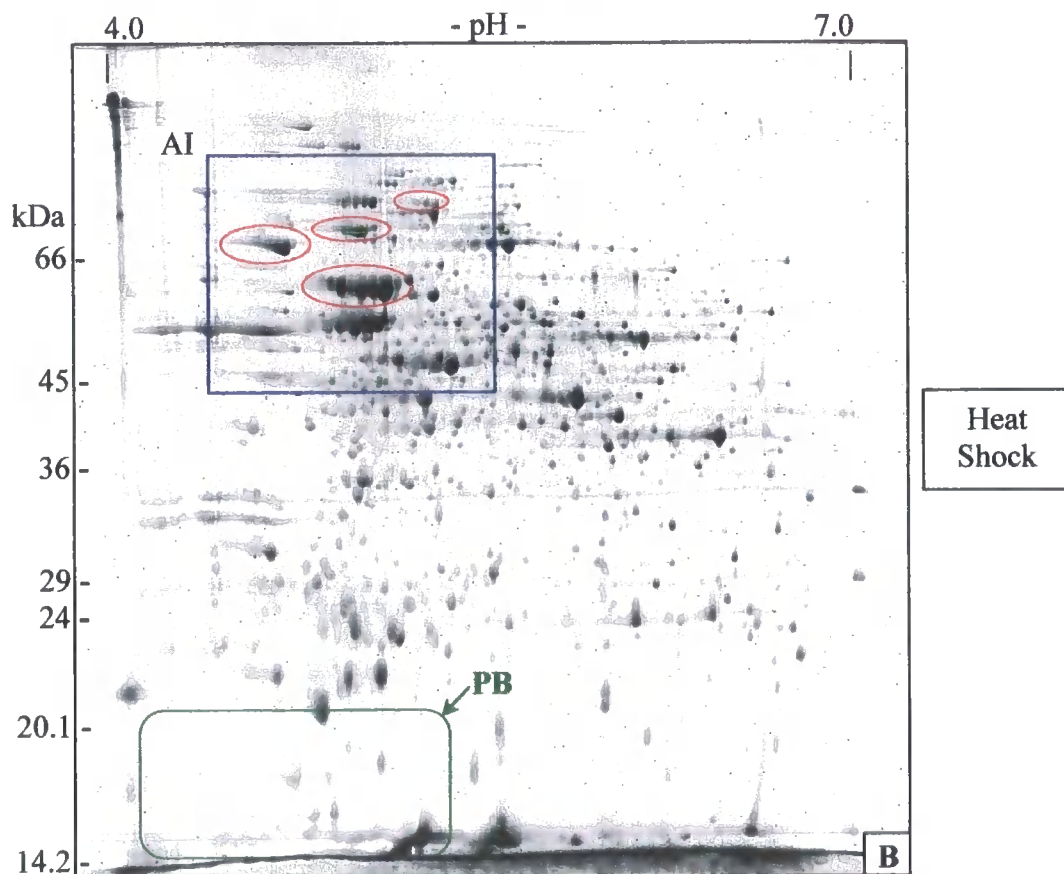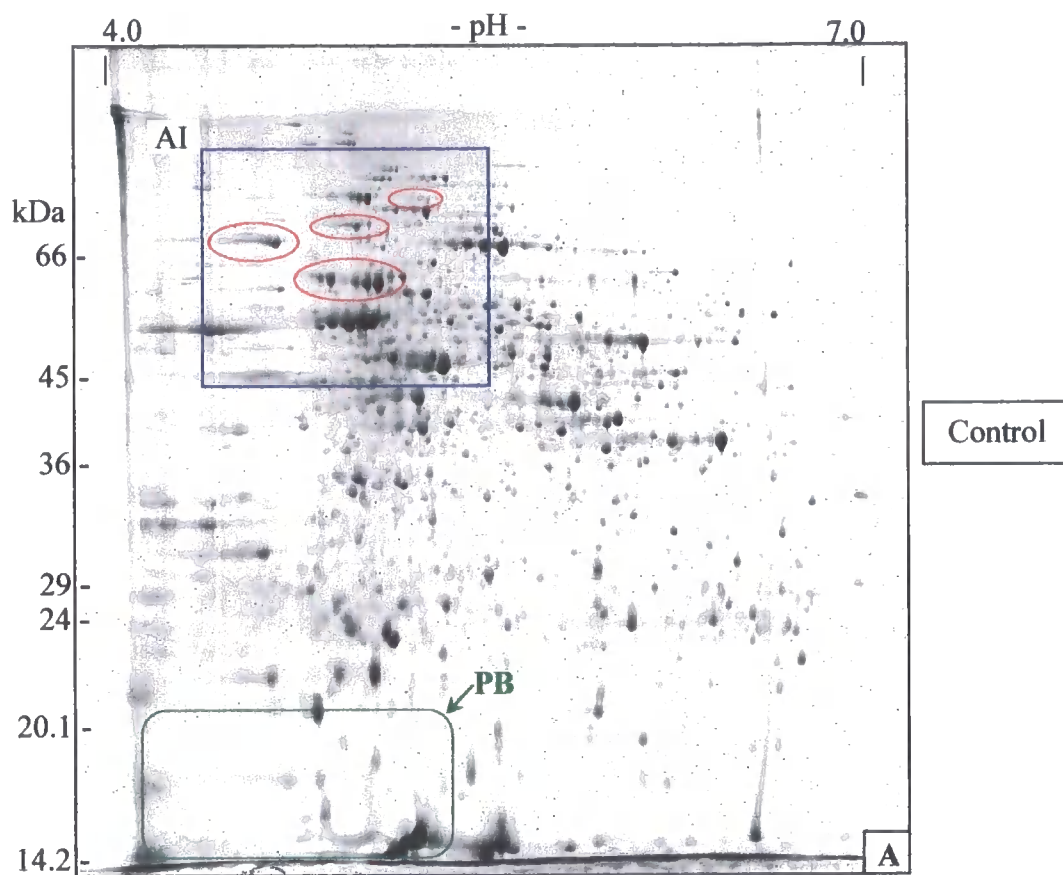
Control

Heat
Shock

image files for each control and heat shock sample were cropped using ImageQuant Tools (Amersham Biosciences) and directly imported into the Evolution software. Spots were automatically detected and matched with manual confirmation of the matched spots before the background staining was subtracted using the mode of non-spot algorithm and the quantified spot volumes were normalised against the total spot volume. Average gels for each control and heat shock sample set were created which contain only those spots that are matched in each sample set (i.e. control and heat shock) and the abundance of each spot is averaged across all replicates. Comparison of the averaged data generated 18 protein spots (Figure 4.10) which displayed a greater than 1.4 fold increase in abundance, 13 of which demonstrated a greater than 95 % statistical confidence (Table 4.1). These statistics were calculated using a 2 tailed paired t-test, which was chosen because it is able to measure the variance for two related sets of mean data and also take in to account the possibility of bidirectionality in the relationship between the two data sets (i.e. in terms of protein spot abundance, an increase or decrease). The 18 protein spots were manually excised from a SYPRO™ stained un-backed large format 2D gel containing 400 μg of protein and analysed via peptide mass fingerprinting using MALDI ToF MS performed on a Voyager DE-STR Biospectrometry workstation (Applied Biosystems). The obtained MS data was used to interrogate all entries in the NCBI database (http://www.ncbi.nlm.nih.gov) using Protein Prospector (http://prospector. ucsf.edu/) (Clauser *et al.*, 1999) and the validity of these identifications were confirmed using the MOWSE statistical test (Pappin *et al* 1993). This test states, that for an identification to be considered accurate a certain percentage of the protein sequence must be covered. Positive identifications with a MOWSE > 10^3 were attained for 15 of the 18 picked proteins spots (Table 4.1). These 15 different protein spots equate to

Figure 4.10. Protein spots identified via Phoretix Evolution analysis as increasing in abundance in response to heat shock.

Highlighted area of interest (AI) of large format SYPRO Ruby stained pH 4-7 2D gels (Figure 4.9) containing 18 protein spots displaying increased abundance in response to heat shock. 3D profile extracted directly from Phoretix Evolution software (Nonlinear Dynamics) displaying the increased abundance of spots 11-18. Specking artefact of SYPRO Ruby staining, which effects accurate quantification of spot volumes is also highlighted.

Control

Heat Shock

SYPRO
Speckling

- AI Gel Section

- 3D Profile

- AI Gel Section

- 3D Profile
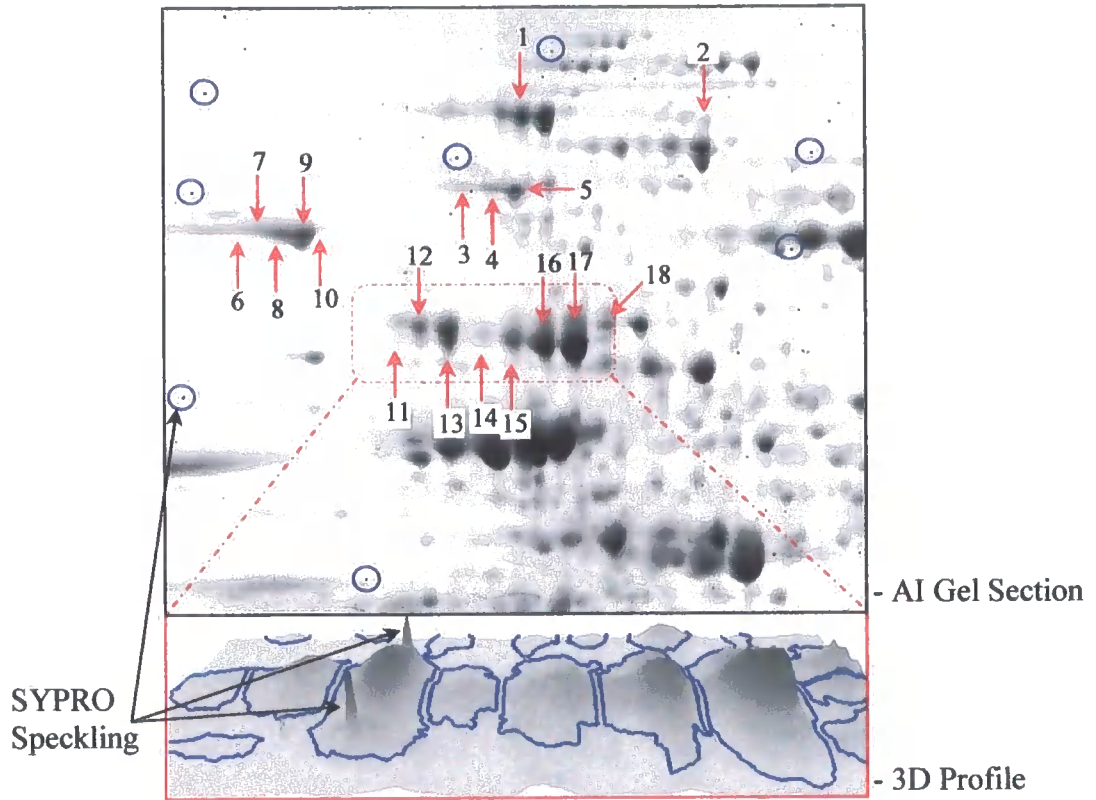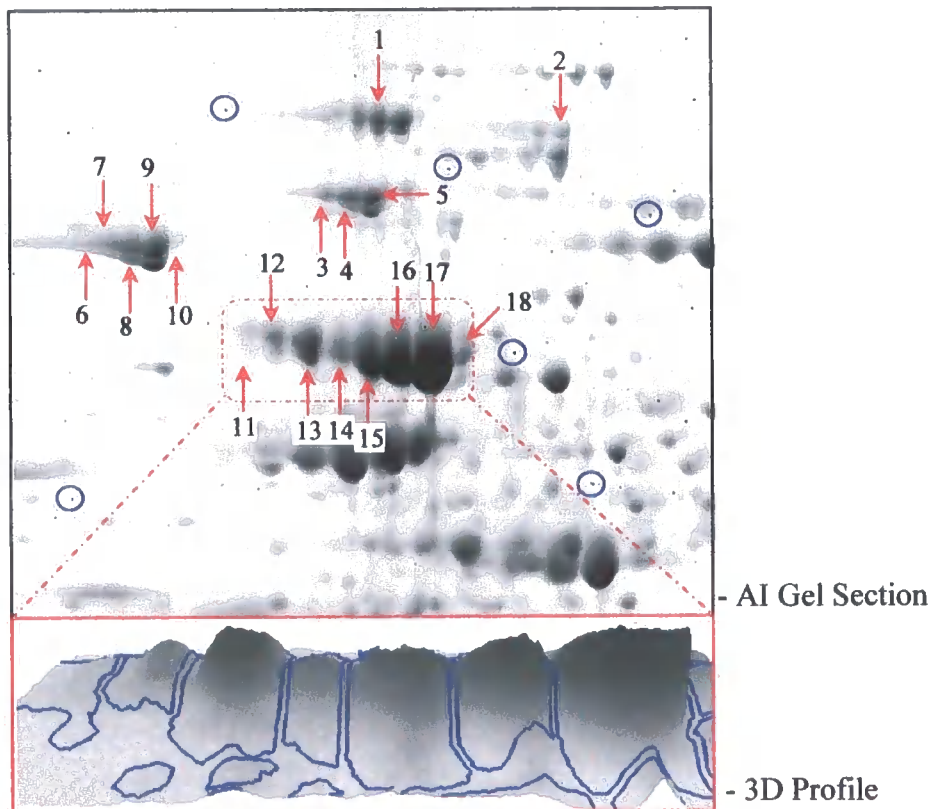
Table 4.1. Identified *Synechocystis* soluble proteins demonstrating increased abundance under heat shock.

Spot No.	Control Ave. Spot Vol.	S.D.	Heat Shock Ave. Spot Vol.	S.D.	Paired T-test: 2 tailed	Protein Abundance Difference	Protein I.D.	NCBI Accession No.	MOWSE Score
1	0.099	0.020	0.144	0.030	1.13E-01	1.45	Elongation Factor EF-G 1	gi|16332123	8.3E+03
2	0.038	0.012	0.083	0.029	9.71E-02	2.18	ClpB protein	gi|16331048	3.3E+06
3	0.049	0.009	0.148	0.022	6.55E-03	3.03	DnaK protein 2, hsp 70	gi|16331261	1.43E+09
4	0.070	0.010	0.141	0.060	1.28E-01	2.01	DnaK protein 2, hsp 70	gi|16331261	8.7E+06
5	0.118	0.029	0.245	0.084	1.08E-01	2.07	DnaK protein 2, hsp 70	gi|16331261	1.2E+03
6	0.258	0.074	0.512	0.094	4.44E-02	1.99	DnaK protein 2, hsp 70	gi|16331261	1.1E+07
7	0.015	0.003	0.048	0.004	1.98E-04	3.25	Same spot "train" as DnaK protein 2		
8	0.055	0.018	0.118	0.041	5.16E-02	2.14	HtpG, hsp 90	gi|16332281	3.2E+03
9	0.081	0.029	0.210	0.044	1.35E-02	2.59	HtpG, hsp 90	gi|16332281	9.6E+02
10	0.197	0.011	0.426	0.072	9.97E-03	2.17	HtpG, hsp 90	gi|16332281	4.5E+03
11	0.048	0.027	0.143	0.019	1.26E-02	2.97	Same spot "train" as GroEL 2		

Table 4.1 continued

Spot No.	Control Ave. Spot Vol.	Control S.D.	Heat Shock Ave. Spot Vol.	Heat Shock S.D.	Paired T-test: 2 tailed	Protein Abundance Difference	Protein I.D.	NCBI Accession No.	MOWSE Score
12	0.106	0.022	0.245	0.051	3.93E-03	2.30	Same spot "train" as GroEL 2		
13	0.252	0.068	0.598	0.250	4.16E-02	2.37	60kD chaperonin 2, GroEL 2	gi|16331442	2.3E+03
14	0.058	0.020	0.280	0.072	3.87E-03	4.83	60kD chaperonin 1, GroEL 1	gi|16330003	3.3E+03
15	0.176	0.078	0.775	0.230	8.02E-03	4.40	60kD chaperonin 1, GroEL 1	gi|16330003	1.0E+08
16	0.318	0.149	1.054	0.375	8.56E-03	3.32	60kD chaperonin 1, GroEL 1	gi|16330003	1.7E+04
17	0.595	0.293	1.956	0.512	8.25E-03	3.29	60kD chaperonin 1, GroEL 1	gi|16330003	3.8E+06
18	0.034	0.012	0.097	0.008	4.67E-03	2.87	60kD chaperonin 1, GroEL 1	gi|16330003	1.2E+03

Underlined protein identifications were not obtained via PMF MS and are predicted to be the same protein as the positively identified neighbouring spots.

6 unique proteins and again it is evident that these 6 proteins are resolving in "trains" of multiple protein spots with similar MW put different p*I*. The identifications of the 3 unidentified protein spots can therefore be predicted to be the same as the other neighbouring identified spots. This is shown in Table 4.1. The six identifications obtained account to five classical heat shock proteins/chaperones two 60 kDa in size and the others 70, 90 and 100 kDa in size and an elongation factor.

A specking artefact of SYPRO Ruby staining, not known to exist at the time of this analysis, is clearly evident in these gels (Figure 4.10). This artefact can occur inside a protein spot and thus affects the calculated volume, as is shown by the spot 3D profile. Consequently the quantitative data obtained in this investigation for spots containing these speckles is inaccurate and may also be reason for the lack of heat shock responsive protein spots with good statistical values. Furthermore because each protein sample has to be resolved via individual 2D gels there is inherent gel to gel system variation, adding to the difficulty of obtaining good statistical data. Therefore, 2D Difference In Gel Electrophoresis (DIGE) technology was employed for further 2-DE based analysis of the heat shock response. This system has been developed by Amersham Biosciences (Tonge *et al.*, 2001) and is based on the differential labelling of two different protein samples with separate Cyanine dyes possessing distinct fluorescence properties (Unlu *et al.*, 1997; Tonge *et al.*, 2001). This allows both control and treated samples for an individual experiment to be co-resolved in the same 2D gel, thus reducing the extent of system variability. Cyanine Dye labelling is as sensitive as SYPRO and doesn't have a speckling problem. This technology also incorporates the ability to co-resolve a third protein sample in each gel, usually a

mixture of all experimental samples (Alban *et al.*, 2003), this third sample functions as an internal standard in each 2D gel, further reducing gel to gel system variability and ensuring accurate quantification and matching of resolved spots in later software analyses.

4.2.6   Optimisation of the 2D DIGE technology for *Synechocystis* soluble proteins

Cyanine dyes used in DIGE technology are expensive, and because of this, the effect of reducing the amount of labelled protein loaded into 2D gels on the extent of protein detection was investigated. Standard Amersham DIGE protocol suggests subjecting 50 μg of each Cy-Dye labelled sample to 2D-E. To test this 100 μg of *Synechocystis* soluble protein was labelled with Cy5 (see materials and methods) and 12.5μg, 25μg and 50μg quantities of Cy5 labelled sample were cup loaded on to independent large format pH 4-7 12 % polyacrylamide 2-D gels and visualised (Figure 4.11) using a Typhoon 9200 imager (Amersham Biosciences). Although the required intensity of excitation (photon multiplier tube value, PMT) increased for lower protein loadings, the detection of low abundant protein spots was not compromised. Therefore, preceding DIGE experiments were conducted using 12.5μg of each Cy-Dye labelled sample and became standard protocol within the laboratory.

Synechocystis is a photosynthetic bacterium and contains light harvesting protein complexes known as phycobilisomes. The constituents of these complexes dominate the soluble protein fraction and are the most abundant proteins seen on a 2D gel. These proteins have intrinsic fluorescence and therefore it was predicted that they

Figure 4.11. Detection of different quantities of Cy5 labelled *Synechocystis* soluble protein.

12.5 µg (A), 25 µg (B) and 50 µg (C) of Cy5 labelled *Synechocystis* soluble protein was cup loaded into separate pre-hydrated 18 cm pH 4-7 IPG strips and subjected to 2-D gel electrophoresis. The resolved spots were detected using a Typhoon 9200 variable mode imager in fluorescence acquisition mode varying the PMT value so each gel obtained a maximum pixel intensity between 70,000 and 90,000.

12.5 µg -
PMT – 580 V

25 µg -
PMT – 545 V
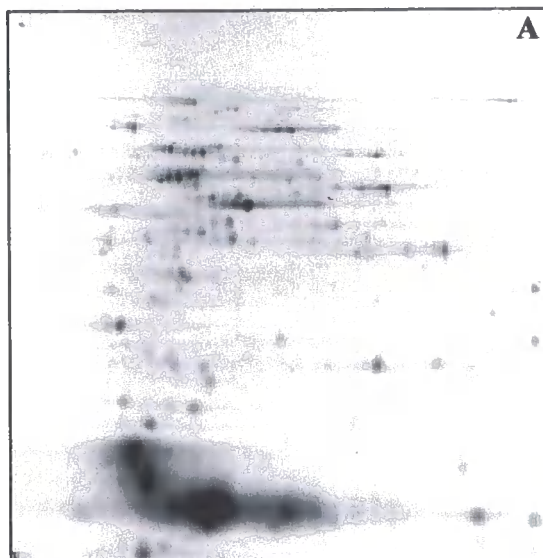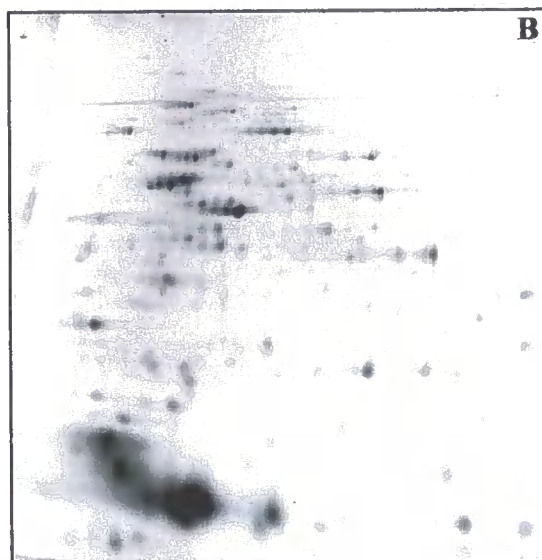
50 µg -
PMT – 500 V
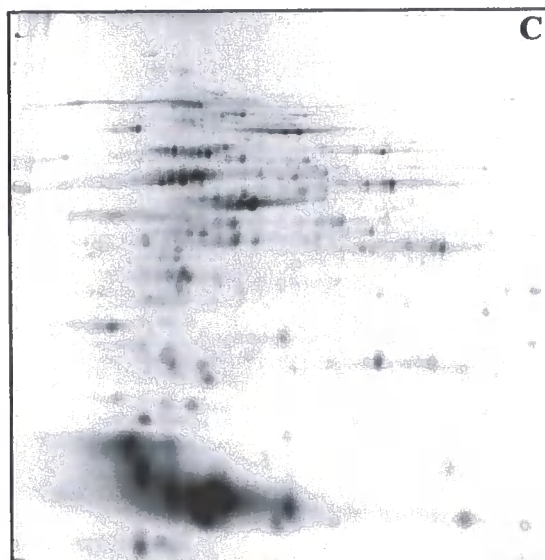
would be excited and their emission detectable during visualisation of Cy-Dye labelled samples. The excitation and emission wavelengths used to detect the three Cy-Dyes are shown in Table 4.2a which are compared to the emission maxima wavelength for the various phycobilisome constituents shown in Table 4.2b. In order to test this hypothesis 200 µg of non-Cy labelled *Synechocystis* soluble protein was two dimensionally separated (large format, pH 4-7 and 12% polyacrylamide). The resultant gel was imaged directly, without any staining, using a Typhoon 9200 variable mode imager (Amersham Biosciences) and the recommended excitation and emission parameters for all three Cy-Dyes (Figure 4.12). This analysis revealed the detectable intrinsic fluoresce of phycobilisome constituents C-phycocyanin, allophycocyanin and the core membrane linker (L_{cm}) (phycobilisome rod linkers do not have intrinsic fluorescence), which were previously identified via MALDI-PMF. Furthermore, it was evident that other proteins within the soluble protein fraction also possessed intrinsic fluorescence (Figure 4.12), one of which was subsequently identified by MALDI-PMF as being succinate dehydrogenase flavoprotein. The other fluorescent proteins detected were too low abundant to obtain identification but some are most likely to be the low MW phycobilisome linkers which also possess intrinsic fluorescence.

This data is important to the DIGE investigation because the detected intrinsic fluorescence of these proteins may be additive to the intensity of their Cy-Dye signal and also therefore to their abundance. Consequently abundance quantification for proteins with intrinsic fluorescence will be calculated erroneously and as a result these proteins have been omitted from further DIGE analysis.

Cy-dye	Excitation λ	Emission man λ	Bandwidth
Cy2	488 nm	520 nm	40
Cy3	532 nm	580 nm	30
Cy5	622 nm	670 nm	30

Table 4.2a. Cyanine dye optimal detection parameters.

PBS subunits - protein (gene name)	Emission	Size kDa*	pI*
C-Phycocyanin (cpcA & cpcB)	640 nm	17.6/18.1	5.3/5.0
Allophycocyanin (apcA & apcB)	660 nm	17.4/17.2	4.9/5.4
Allophycocyanin-B (apcD)	670 nm	18.0	5.4
Core membrane linker (apcE)	670-680 nm	100.3	9.2

Table 4.2b. Fluorescence emission maxima for phycobilisome constituents excited at 570 nm.

*Molecular weights and pI's are taken directly from the PEDANT database (http://pedant.gsf.de/) (Frishman *et al.*, 2001, 2003) and are theoretically predicted from sequence information. Fluorescence emission maxima obtained from Sidler (1994). Note: *Synechocystis* sp. PCC 6803 does not contain a gene for phycoerythrin (Kaneko *et al.*, 1996).

Figure 4.12. Intrinsic fluorescence of *Synechocystis* soluble proteins visualised using cyanine dye excitation and emission parameters.

200 µg of *Synechocystis* soluble protein was cup loaded into an 18 cm pH 4-7 IPG strip and subjected to large format 2D-E. The resultant gel was directly scanned using a Typhoon 9200 variable made imager in fluorescence acquisition mode and all three Cy-dye excitation and emission detection parameters (Table 4.2a).

Succinate
dehydrogenase
flavoprotein
subunit

C-Phycocyanin &
Allophycocyanin

Phycobilisome core membrane
linker

SYPRO

Cy2

Cy3

Cy5
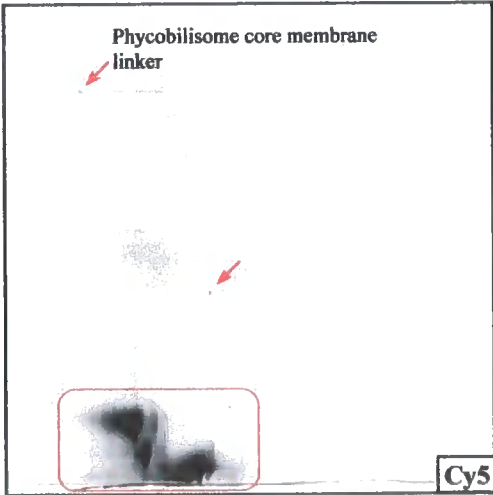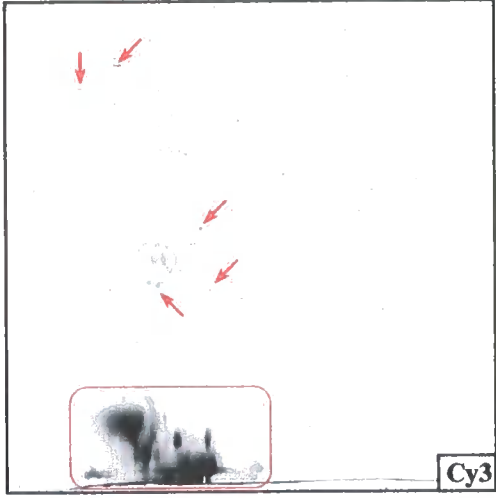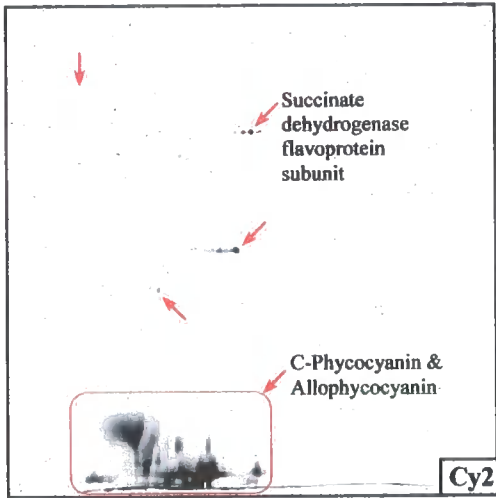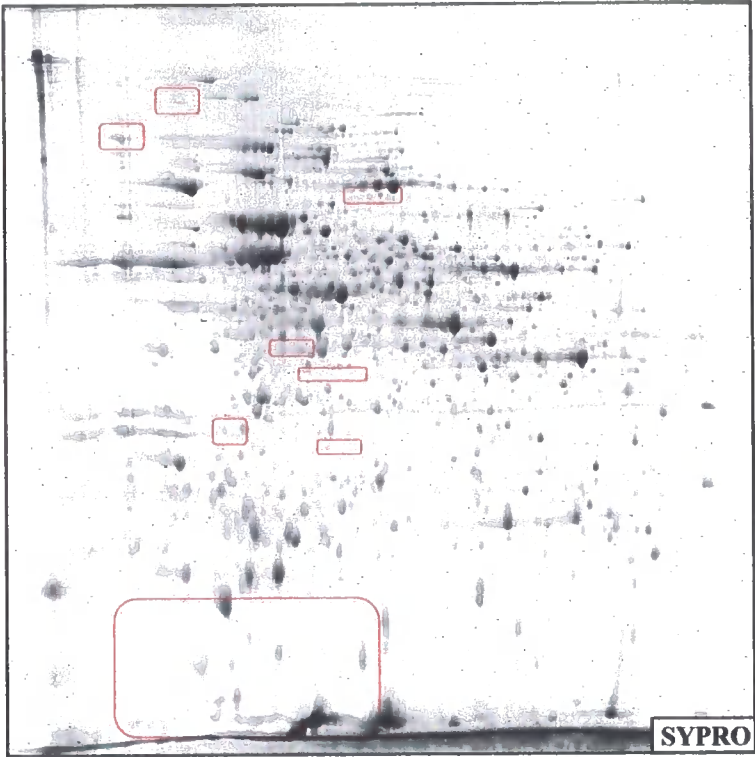
4.2.7 Two Dimensional Differential Gel Electrophoresis (2D DIGE) analysis, revealing changes in *Synechocystis* soluble protein steady state levels following heat shock for 1 hour.

Amersham DIGE protocol stresses the importance of biological replicates which guarantee the measurement of bona fide biological changes in response to a treatment above the inherent background biological variation. A large number of biological replicates ensure a greater account for inherent biological variation and thus increases the confidence that the results are representative of the genuine biological response. Thus, six repeat heat shock experiments were conducted on different days using 500 ml *Synechocystis* gassed cultures grown under normal conditions (34°C, 70 μE m^{-2} s^{-1}) until reaching an A$_{730}$ of ~ 1.0. In each experiment half of the culture (250 ml) was removed prior to heat shock exposure, generating a control cell sample, while the remaining half was transferred to heat shock conditions (44°C) for 1 hour. Cells from both control and heat shock populations were harvested by centrifugation and broken using French press, from which the soluble protein was fractionated and precipitated (see materials and methods). This experimentation generated six control and six 1 hour heat shock soluble protein extracts and their reproducibility was confirmed via both SDS PAGE and mini pH 3-10 2-DE (data not shown).

Having generated sufficient repeat material for DIGE analyses and established that it was reproducible; a proportion (approximately 200 μg) of each protein sample was solubilised in Lysis buffer and prepared for Cy Dye labelling (see material and methods). Following this a 50 μg aliquot from each sample was Cy labelled using the minimal dye labelling method with 400 pmol of dye at a protein concentration of 2.5

μg/μl and (see materials and methods for details). This method limits the extent of labelling to only 1 % of all lysine residues. All six control samples were Cy3 labelled, all six heat shocked samples were Cy5 labelled and 25 μg aliquots from each control and heat shocked sample were pooled together and labelled with Cy2 (generating the internal standard). The success of Cy-Dye labelling was confirmed by visualisation of 2.5μg of each sample on SDS PAGE (data not shown), which also demonstrated that samples were equally loaded.

On establishing successful Cy labelling, large format pH 4-7, 12 % polyacrylamide 2-DE was performed. Here equal 12.5 μg quantities of Cy labelled control and heat shocked samples from the same experiment were mixed with the same quantity of pooled internal standard. To these six sample mixes, lysis buffer (9 M urea, 2 M thiourea, 4 % (w/v) CHAPS), DTT (50 % w/v in lysis buffer) and Pharmalytes (pH 4-7) were added to a final volume of 70 μl and a final concentration of DTT and Pharmalyte of 1% (w/v) and 2 % (v/v), respectively. These samples were subsequently cup loaded (at the anode) into 18 cm, pH 4-7 IPG strips (Amersham Biosciences) pre-hydrated over night with reswelling buffer (9 M urea, 2 M thiourea, 4 % (w/v) CHAPS, 1% (w/v) DTT, 2% (v/v) Pharmalytes (pH 4-7), 0.002 % (w/v) bromophenol blue). Strips were focused overnight for 70 kVh using an IPGphor IEF system (Amersham Biosciences) (see materials and methods for details) and subsequently equilibrated before loading on large format 12 % polyacrylamide gels (260 x 200 x 1 mm) cast within Ettan DALT low fluorescence glass cassettes (Amersham Biosciences). Gels were electrophoresed using the discontinuous buffer system of Laemmli (Laemmli, 1970) and an Ettan DALT*twelve* Large Format Vertical System (Amersham Biosciences) at 5 W/gel for 30 minutes followed by 17

W/gel until the dye front had reached the bottom of the gel. All six gels were immediately visualised via fluorescence imaging using a Typhoon 9200 variable mode imager (Amersham Biosciences) detecting all three Cy images, i.e. Cy2, Cy3 and Cy5, simultaneously and obtaining a maximum pixel intensity above 60,000 but bellow 100,000 (saturation) for each image by selecting appropriate photon multiplier tube (PMT) values (see materials and methods). Fluorescence images for each DIGE gel can be viewed either as individual Cy flours or as a triple overlay image (Figure 4.13). The triple overlay image of all three Cy flours does give some indication of the spots which change in abundance, predominantly red spots decrease in abundance, whereas green spots are those showing an increase in abundance. However this kind of information is not quantitative as spot abundance has not been normalised at this stage.

Having obtained all the images for all six 2D DIGE gels it was evident that one of the gels had not acceptably resolved and was therefore not carried forward for software analysis, thus reducing the number of replicate gels to five. Before analysis the images from these five gels were cropped, selecting only the area of the gel within which proteins had resolved. These cropped images were subsequently imported into DeCyder Batch Processor software (Amersham Biosciences) where spots were automatically detected and matched and their volume (i.e. their abundance) normalised and quantified. The DeCyder Batch Processor software is able to detect all resolved protein spots in each gel through the use of a pre-determined number given by the user before the process is started. A total estimated spot number of 3,000 was given which achieved detection of all resolved spot in all gels, this number was determined from previous DeCyder Differential In-gel Analysis (DIA) software

Figure 4.13. 2-D DIGE analysis of changes in *Synechocystis* soluble protein abundance following exposure to heat shock conditions for 1 hour.

Equal 12.5 µg quantities of control (Cy3 labelled), heat shock (Cy5 labelled) and pooled internal standard (Cy2 labelled) samples were co-resolved through large format pH 4-7 12 % acrylamide 2-D gels. Labelled proteins were visualised immediately after electrophoresis detecting all three labelled samples. Each Cy image, i.e. Cy2, Cy3 and Cy5, can be viewed individually (panels A, B and C), or all 3 Cy images can be viewed on top of one another as an overlay (D). Using this overlay image proteins having an increased or decreased abundance can be seen as green and red spots, respectively. Red circle indicates a green coloured spot resolved in the dye front.

A) Cy3

B) Cy5

C) Cy2

- pH -

4.0

7.0

kDa

66

45

36

29

24

20.1

14.2

D) Triple overlay
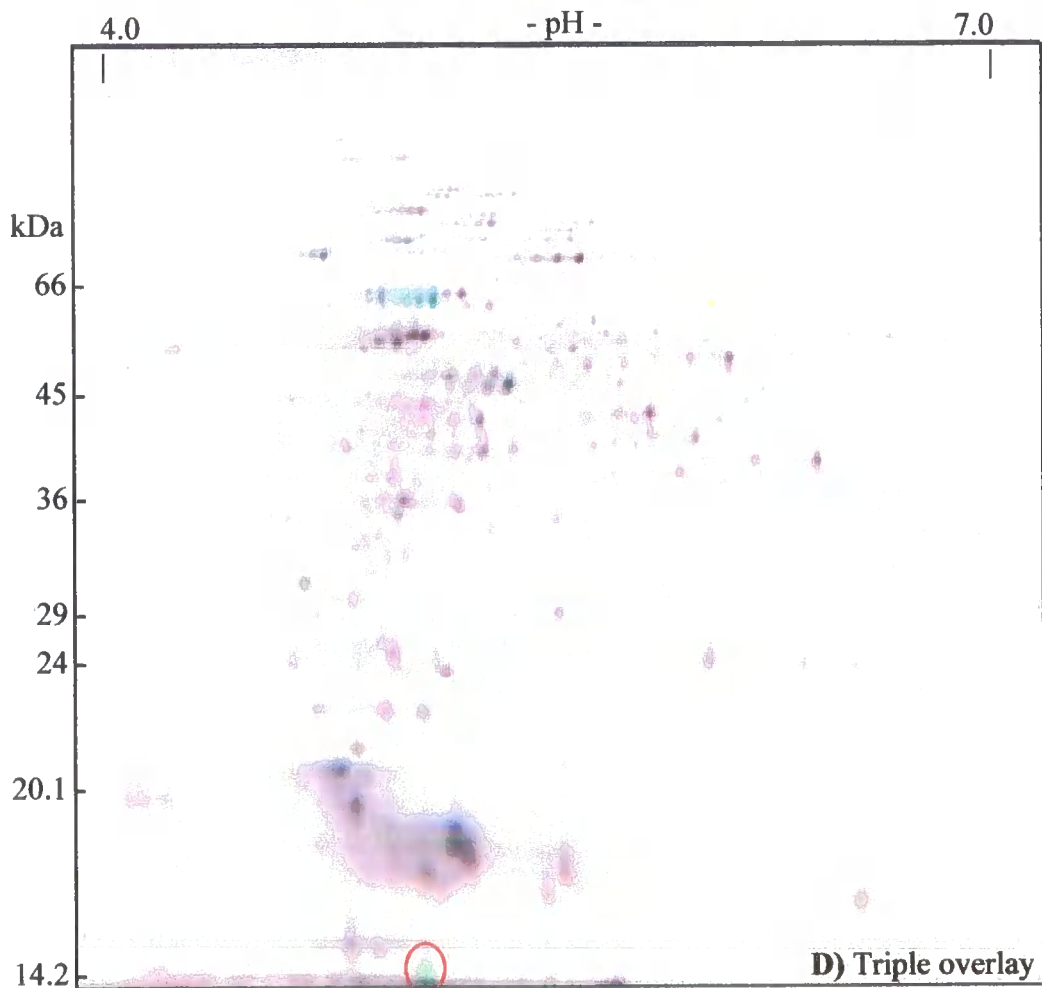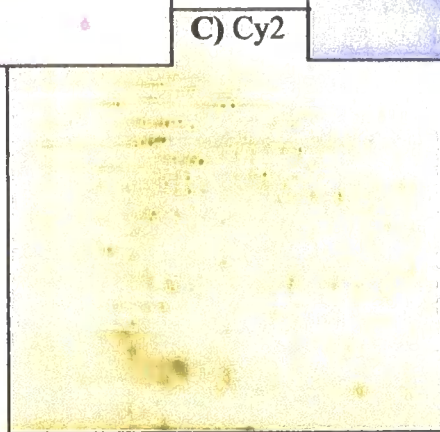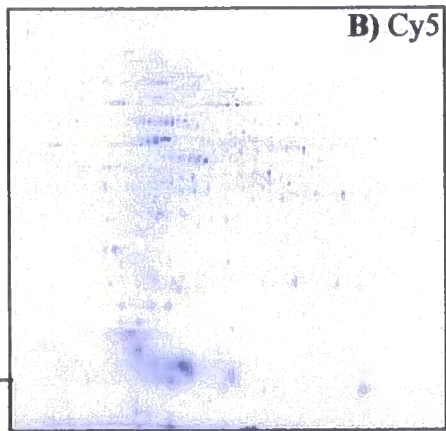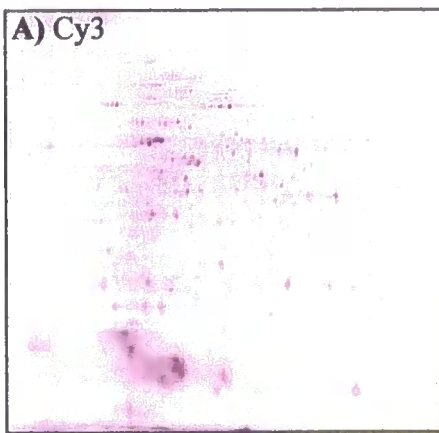
analysis. All spot detection and matching was performed using the Cy2 image from each DIGE gel, as was normalisation and quantification of spot abundance. The data generated from this process was viewed using DeCyder Biological Variation Analysis (BVA) software (Amersham Biosciences). This automatically matched all spots across all 5 gels, which were manually checked and altered if necessary. DeCyder BVA software was subsequently used to determine the average change in protein abundance across all 5 gels for each protein spot between the control (Cy3) and heat shocked (Cy5) samples. The software also concurrently calculated the variance for each set of average data, expressed through a paired T-test, and was used to determine the reproducibility and validity of the replicate data. Protein spots having a greater than +/-10 % change in abundance in response to heat shock across all 5 repeat experiments and also a statistical confidence above 95 % were manually selected for MALDI-TOF PMF identification. The basis for this statistical significance was that an event is significant if it is expected to occur at random with a frequency of less than 5%. In application of the criteria a total of 210 spots were selected for MS characterisation, 169 of which demonstrated an increase in abundance and 41 displayed a decrease. However, those spots which resolved in the same MW train as a spot(s) which displayed a statistically valid change in abundance but themselves did not display a statistically valid change were also selected for identification. These proteins spots did display a greater than 10 % change in abundance but were slightly outside the statistical cut off. This added 5 addition spots to the investigation. Therefore in total 215 spots were selected for identification. Of these 215, 22 spots displayed a statistically valid change in abundance but only across four of the five repeat experiments. These spots were either missing from one of the gels due to slight differences in resolution or were so low abundant that they were not detected.

Because of this these proteins were still selected for identification as reproducibility across 4 repeat experiments is still a valid result.

Before these proteins spots were identified by PMF, analysis of the heat shock response in the *Δhik34* mutant cells was conducted and which is described in the following section. See section 4.2.10 for characterisation of the 215 selected protein spots.

4.2.8 Comparison of soluble protein extracted from wild type and *Δhik34* *Synechocystis* cells grown under normal and heat shock conditions.

One of the main objectives of this chapter was to study the function of the *Synechocystis* histidine kinase, Hik34, in the cellular heat shock response using a *hik34* gene knockout *Synechocystis* strain, namely *Δhik34*. Transcript expression analyses via DNA microarray technology and other studies performed by Prof. Norio Murata's Lab have suggested that Hik34 functions as a heat sensor and a suppressor of Hsp expression under normal growth conditions.

Having established a suitable time window in which to study the effect of heat shock on protein steady state levels and also established a suitable technology capable of generating quantitative data, the next stage of this investigation was to compare protein complements from wild type and *Δhik34* cells grown under both normal and heat shock conditions using this technology. However, before any extensive investigation of repeat heat shock experiments was undertaken, soluble protein extracts from 50 ml gassed wild type and *Δhik34* cultures grown under both normal

(34°C) and heat shock (44°C) conditions were compared via both SDS-PAGE and min 2-DE. This was done to see if there were any obvious differences in soluble protein extracts from wild type and *Δhik34* mutant cells and to determine if the heat shock responsive proteins likely to be chaperones (seen in Figures 4.1, 4.4 and 4.7) do increase in abundance as a result of the *hik34* knockout, as indicated by analysis of mRNA expression (see introduction).

Cells, both wild type and *Δhik34*, were grown as 50 ml gassed cultures under normal conditions (34°C, 70 µE m^{-2} s^{-1}) until they reached an A_{730} of ~1.0. At this point half of both cultures were removed, generating the control cell samples, and the remaining halves were transferred to heat shock conditions (44°C) for 1 hour. Cells from all four samples were harvested by centrifugation, broken using glass beads and the soluble protein extracted (see materials and methods for details). This experimentation was repeated, thus generating duplicate samples for each sample type. Subsequently, 20 µg of protein from each sample was subjected to SDS-PAGE using 12 % polyacrylamide resolving gels and the resolved bands were visualised with Coomassie blue (Figure 4.14). This analysis demonstrated that when comparing wild type and *Δhik34* mutant *Synechocystis* cells grown under normal conditions a slight elevation in abundance could be detected for some of the high molecular weight heat shock responsive bands. Moreover, four of the heat shock responsive bands did show an obvious elevation in abundance in the *Δhik34* mutant cells grown under heat shock conditions when compared to wild type cells subjected to the same environment. These observations support the theory previously demonstrated from mRNA analysis that Hik34 functions as a heat sensor and a repressor of Hsp expression (Iwane Suzuki, NIBB, Japan – personal communication).
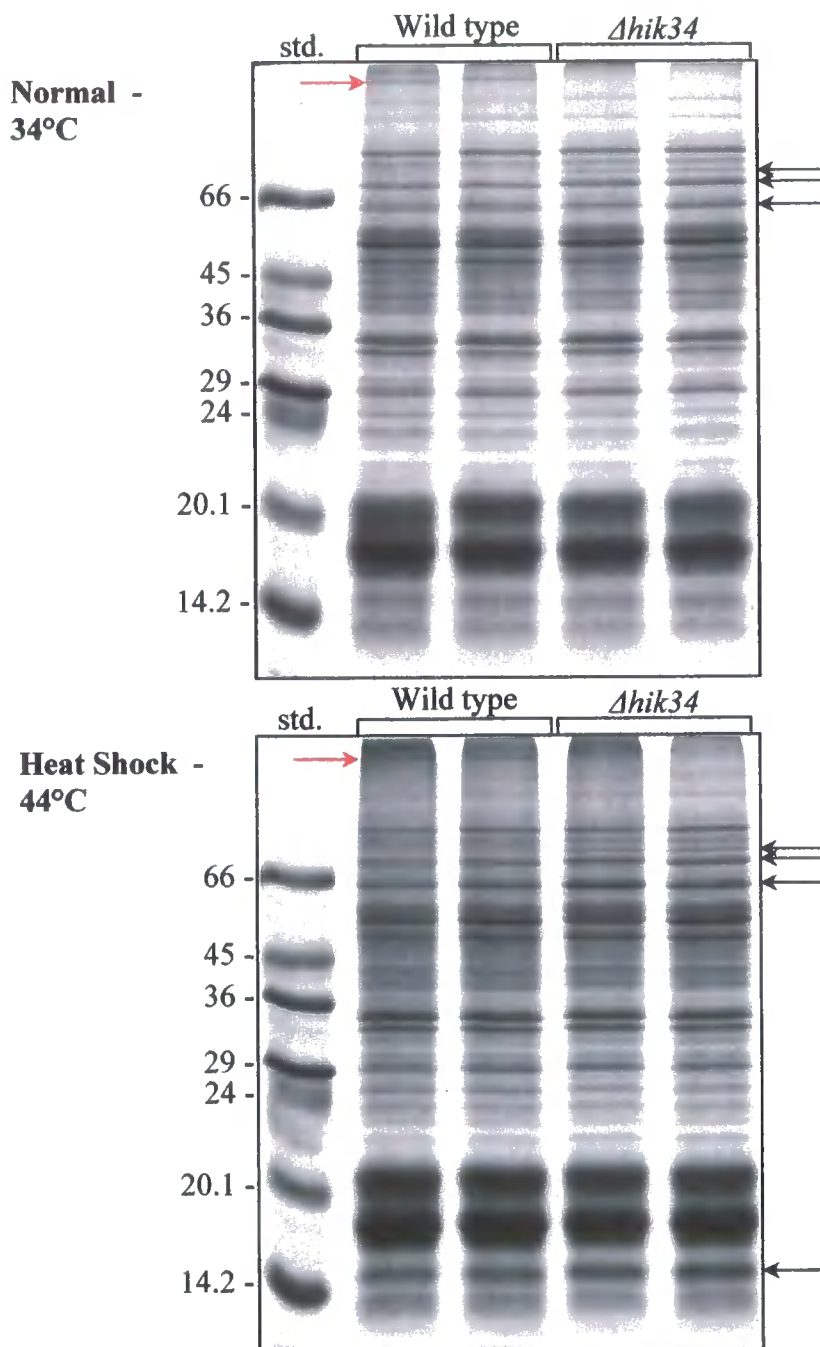
Figure 4.14. SDS-PAGE analysis comparing soluble protein extracted from wild type and *Δhik34 Synechocystis* cells grown under normal (34°C) and heat shock (44°C) conditions.

Soluble protein was fractionated from duplicate wild type and *Δhik34 Synechocystis* cells populations grown under normal and 1 hour heat shock conditions. An aliquot of each sample containing 20 μg was subjected to SDS-PAGE using 12 % acrylamide resolving gels and resolved protein bands were visualised via Coomassie blue. Black arrows indicate bands showing an increase in abundance as a result of the *Δhik34* knockout mutation in both normal and heat shock samples. Red arrow highlights the loss of a protein band in the soluble protein fraction of *Δhik34* cells.

The SDS-PAGE study also demonstrated that a high molecular weight protein present in the soluble protein fraction of wild type *Synechocystis* cells was reproducibly absent in the same protein fraction of *Δhik34* mutant cells (Figure 4.14). This protein could not be Hik34 due to it size and therefore in order to determine the identity of this protein and perhaps help elude to the function of Hik34, 200 μg of total soluble protein fractionated from both wild type and *Δhik34 Synechocystis* cells was resolved via mini pH 4-7 2-DE. The resolved spots were visualised with Coomassie blue and again the absentness of the high molecular weight protein from the *Δhik34* soluble fraction was evident (Figure 4.15). This protein was manually excised from the gel, digested with trypsin and the harvested tryptic peptides were analysed via ESI tandem MS. Fragment ion mass spectra was obtained for one peptide (Figure 4.16a) which was used together with the mass of its parent ion to interrogate the NCBI non redundant database against all organisms using the MASCOT search engine (http://www.matrixscience.com) (Perkins *et al.*, 1999) and a mass accuracy of 50 ppm. Using this technology the protein was positively identified as a hemolysin-like protein (HLP) with a MOWSE score of 75 (Figure 4.16b) and indicates that Hik34 is involved in the expression of the *hlp* gene due to its absence from the soluble/cytosolic protein fraction of *Δhik34 Synechocystis* mutant. This protein in *E. coli* (Suttorp *et al.*, 1990) and *S. aureus* (Song *et al.*, 1996) is a secreted toxin which functions to lyse the cells of infected tissues by forming small beta-barrel membrane spanning pores through which small molecules and ions can traverse the membrane. However, in *Synechocystis* sp. PCC6803, HLP is exclusively localised at the surface layer and lacks hemolytic activity (Nagai *et al.*, 2001). The physiological function of HLP is currently unknown although a link with cell motility has been proposed (Bhaya *et al.*, 1999).
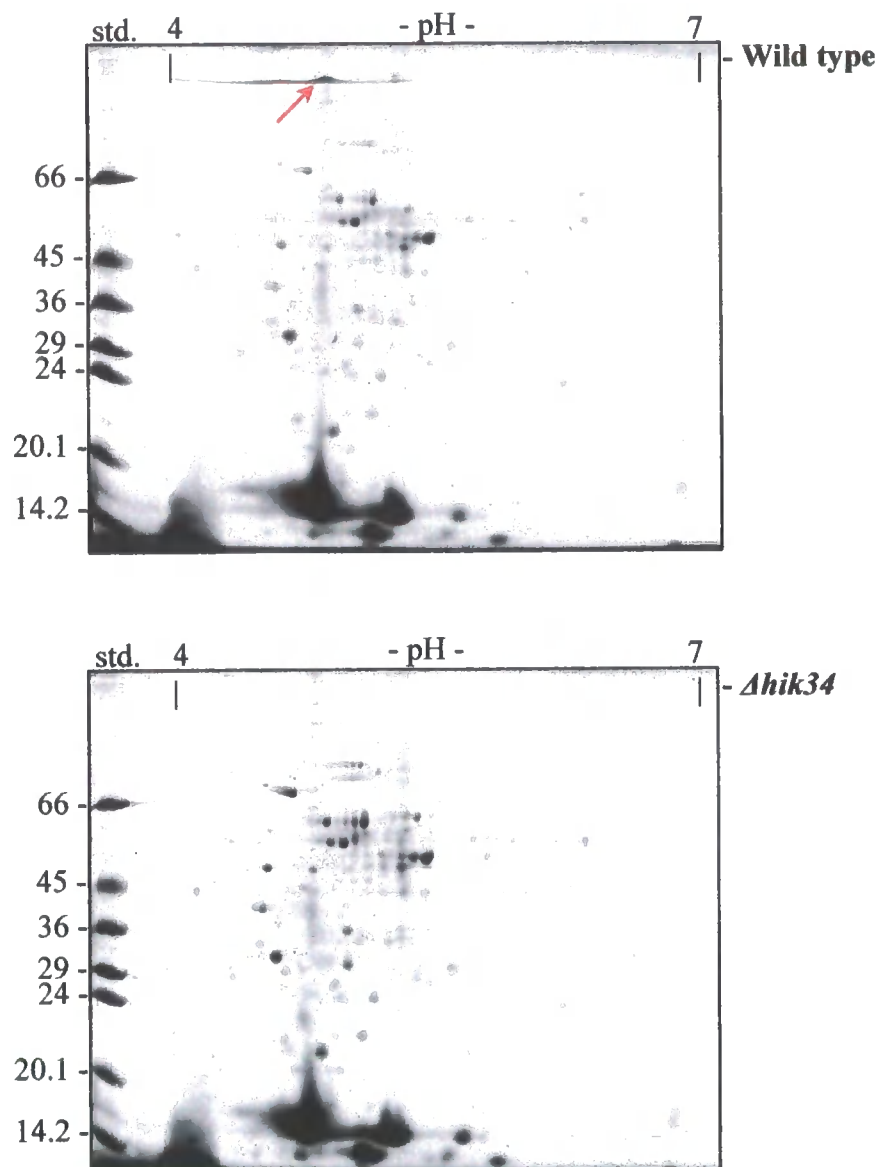
Figure 4.15. Mini pH 4-7 2-DE showing the loss of a high molecular weight protein from the soluble protein fraction of *Δhik34* mutant *Synechocystis* cells.

Soluble protein was fractionated from exponentially dividing wild type and *Δhik34 Synechocystis* cells. Aliquots from both samples containing 200 μg of protein were subjected to mini pH 4-7 2-DE and the resolved spots were visualised with Coomassie blue. Red arrow indicates the high molecular weight protein present in the wild type soluble protein sample but absent from the *Δhik34* sample.
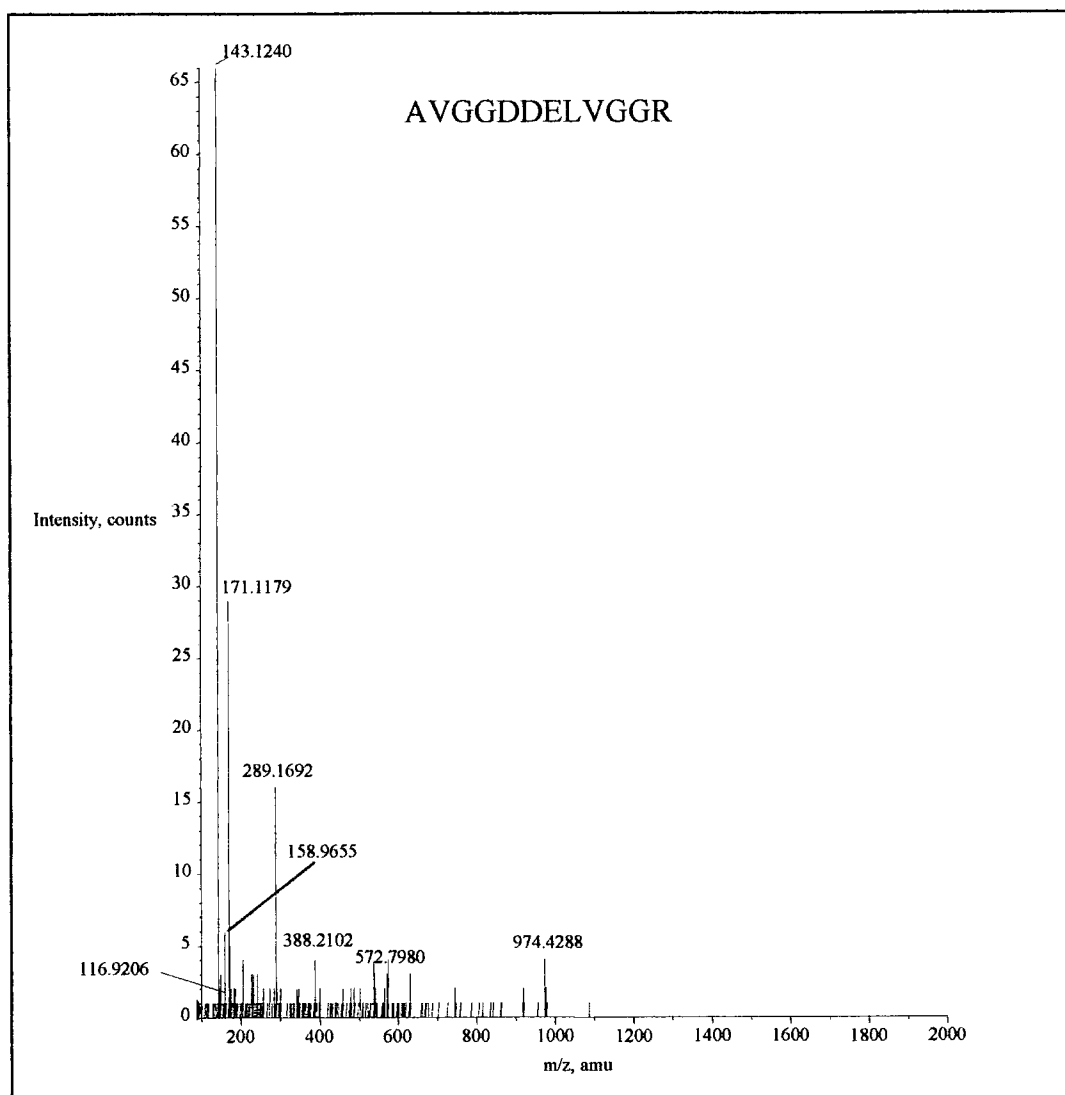
Figure 4.16a. MS-MS spectrum for hemolysin peptide ion.

Doubly charged peptide ion of 1143.55 m/z was further fragmented in the second quadrupole of a Q-TOF MS. Analysis of the generated *y* and *b* ions determined the sequence of the parent ion to be AVGGDDELVGGR.

```
   1 MALSPNVIAA LQIMYTGRGV SASDLNWWAT DGANITYAEA VALFASSPDA
  51 AIKYPFFQAP QTADKRQYVA QVFANLYNID INDTSLVPTE ELDYWINWLS
 101 LSPDNYLDFP NALNNASAAA GLTDRLEALT NKADVSLSYT EALSTAGVNT
 151 FTEAQYAEAA GIIATVDDTN ASVLAAEAQI VEIAASLSVF TIAQAQATPN
 201 LPPAYTISDT ADNLIAGADD PVVTGANNVI ANQSPAAPLS VEDANILLAT
 251 ADELAAGVTW DILDTAADVL AGGAAVSGAA SVGITDIVDV ATASQLLALG
 301 NFDGVYAIAD TSANIVADPG VSGGATAITL SDPDVPVSVA SATFLQGLGI
 351 PVGPSYIVED TSANILAALS TPAIVNAAEV IVNNTDVPLS VAQAEDLLSL
 401 PNLNAGFTYI IADTLDNLSA APSTLLDGAV SYSLTNTNPD LGVITEAEAV
 451 IVNGATNASD FNFLVADVIL TPQADIRSGN SFLSVAVVEG GSIFNTLNSN
 501 DRLTGTGEDP TLSLTWQEAT FGNINTIFPV LDGIETLVAT LIENDLTLVS
 551 NDFDVVGQGF ITGLKNVAAS GTKGGDLELI NLQTALETVS VTNYFFGDDV
 601 SFSIADPELA GDNDLLLLTV DQVTEDGPDV TSIKISDFSG NGGYETLGLT
 651 SGVTTSSKGN TNTVDIEGIV AVESIGITGI ENLTLSTSLI GSVVKVDATG
 701 SALIPEFEGR EVFTGDLKAF FDDRPGGDIT FLSGSGNDEI SIARDAFTLS
 751 EDLKDVISKG HILDGGAGND ELTITGDAFS DTDAGHTVIG GEGNDSILLT
 801 GVAEGPIAGH VVNSFDLINE VGGAGDDDIN ISGDAIGDSA GHVVFGGAGE
 851 DDIFIGFDKT LAVSGNGAAL GVDLAGHVVF AGDDDDTVRI TGDSFTSDSA
 901 NGSGHSVEGG TGDDLIEISG DALTADPDSE TIANPFFDDS EPSDLDLFIA
 951 ADQPIPTTEE QYQVLLAQLG LPADYNPRNF IRGVAAISGA HTVRGGEGND
1001 VILFGPIAGE PGNGDGQHLA FGDEGDDFIE MTGIGSVEFN GGAGDDTLVG
1051 GDGDPILGFG NDILNGDEGN DFLFGGKGND NLQGGEGDDI MSGGEGDDFF
1101 FVDAGFDVIE DLGDANSETG DQFQVSEDAE AEIRVVQDWE ATGLTFNLGI
1151 ATLTIENPGG GSVDLSASNV PPNTNGYTVI GNIGDDEIIG SRDDDSIFGG
1201 RGEDSIAGLG GDDIIEGNDD DDFISGDSLL LPLLPLEEIL PFGNDDIDAG
1251 SGNDVIAGDL LVVTGDDIDL NLFNGGKDTI EAGLGSDITV GDWSIGAFGD
1301 IDLNASLERT AIGGDDTITT KQGDNGIVFP IGQVAIDNFL VGDLAAAVDG
1351 VGNDIFLTET LTVIGGDDTM TGADGLDVIV GDVGLFGFEF NDSEINLTNF
1401 KLGQVNGSTV SAGDDSITGE GGNDILVGDL FVGVINNNGI IIDGGKGFQL
1451 GKDGTTSFIG GDDSISGGDG NDFLAGDFVL VDQLSAPFDP LDPNDWTFVN
1501 PYATLQGQAG DSKAQAAQAA INLAQLRLEF RAVGGDDELV GGRGNDTFYG
1551 GLGADTIDIG NDVTVGGVGV NGANEIWYMN GAFENAAVNG ANVDNITGFN
1601 VNNDKFVFAA GANNFLSGDA TSGLAVQRVL NLQAGNTVFN LNDPILNASA
1651 NNINDVFLAV NADNSVGASL SFSLLPGLPS LVEMQQINVS SGALAGREFL
1701 FINNGVAAVS SQDDFLVELT GISGTFGLDL TPNFEVREFY A
```

Figure 4.16b. Sequence coverage obtained for the positive identification of hemolysin.

The peptide sequence obtained (Figure 4.16a) was used to search the NCBInr database using the MASCOT search engine (http://www.marrixscience.com). A positive identification of hemolysin with a MOWSE probability score of 75 was obtained. The position of the sequenced peptide is shown in bold.

4.2.9 2D DIGE analysis, revealing changes in *Synechocystis* soluble protein steady state levels following heat shock for 1 hour and the role of Hik34 in their expression.

Initial correspondence with Prof. Murata laboratory revealed their primary studies investigating the role of Hik34 in the heat shock response were conducted using a different set of growth and heat shock temperatures to those previously used in the initial proteomic investigations described in this chapter. The temperatures employed for all proteomic analyses were 34°C for normal growth and 44°C for heat shock, however mRNA expression analyses were conducted on cells grown at 30°C and heat shocked at 42°C. Consequently in order to compare proteomic and transcriptomic data accurately a new set of protein samples were generated from both wild type and *Δhik34 Synechocystis* cells exposed to the same temperature regimes as used in the mRNA expression study. Here 500 ml gassed wild type and *Δhik34 Synechocystis* cultures grown under normal conditions (30°C, 70 μE m^{-2} s^{-1}) until they reach an A$_{730}$ of ~1.0. At this point half of the cultures were removed, generating the control samples, and the remaining halves were transferred to heat shock conditions (42°C, 70 μE m^{-2} s^{-1}) for 1 hour (samples were continually gassed under heat shock conditions). This experimentation generated 16 samples, 4 of each type, these being wild type control, wild type heat shock, *Δhik34* control, and *Δhik34* heat shock. Cells were harvested by centrifugation and broken using French press before the soluble protein was fractionated and precipitated with acetone (see materials and methods for details). Before proceeding into Cy labelling and 2D DIGE analysis of these samples, the reproducibility and solubility of all soluble protein extracts were assessed via SDS PAGE and min pH 4-7 2-DE (data not shown).

Samples were prepared for Cy labelling and labelled as previously described (see section 4.2.7) so that 50 µg aliquots from all 8 control samples and all 8 heat shocked samples were Cy3 and Cy5 labelled, respectively. Also, 25 µg aliquots from each control and heat shocked sample were pooled together and labelled with Cy2, generating the pooled internal standard. The success of each Cy-dye labelling was confirmed by visualisation on SDS PAGE (Figure 4.17).

Having established successful labelling, the next stage of this investigation was to perform large format pH 4-7 2-D DIGE. This was conducted using the same protein loadings (12.5 µg per sample) and sample pairing system (i.e. control and heat shock samples from the same cell type and heat shock experiment were co-resolved with the same quantity pooled standard) as described previously, (see section 4.2.7). 2-DE and imaging of the resolved Cy labelled protein spots was also performed as described in section 4.2.7 using the same electrophoresis and scanning equipment. As seen in the previous heat shock 2-D DIGE investigation there was a protein resolving in the dye front which appeared to quite dramatically increase in abundance (see Figure 4.13). A protein of similar molecular weight has also been seen in the several 1D SDS-PAGE analyses (Figures 4.1, 4.4 and 4.14) and also in the mini 2-DE analysis of radiolabelled protein (Figure 4.7). As this protein appears to be a significant constituent of the heat shock response it is important to include it in the 2-D DIGE analysis. Because this protein does not seem to resolve out of the dye front on large format gels when using 12 % polyacrylamide, both 12 % and 15 % polyacrylamide large format gels have been used in this 2-D DIGE investigation. Figure 4.18 clearly shows the resolution of low molecular weight proteins achieved by using 15 % polyacrylamide. However, it was still a requirement to also use 12 % polyacrylamide
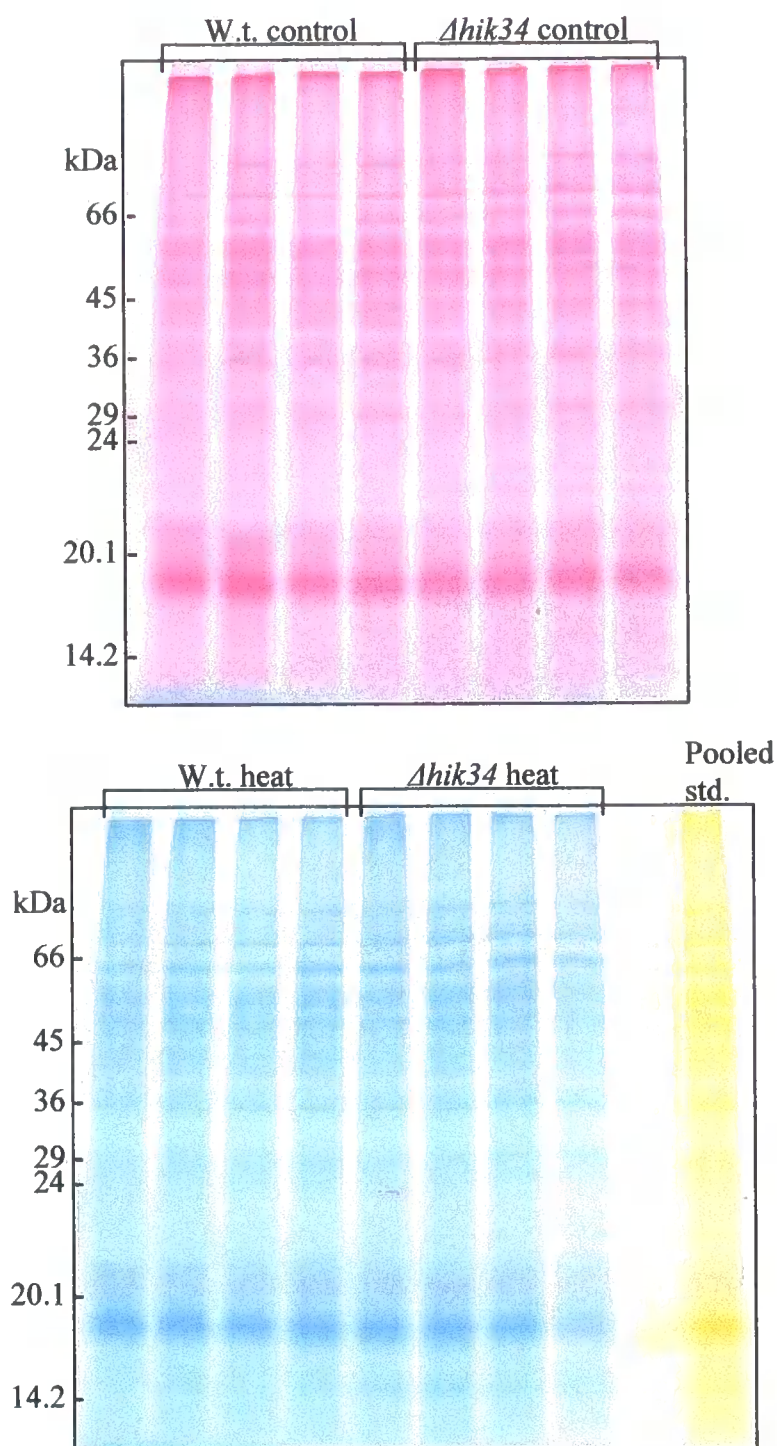
Figure 4.17. Cy labelled soluble protein extracted from wild type and *Δhik34 Synechocystis* cells grown under both normal (30°C) and 1 hour heat shock (42°C) conditions.

A 1 µl aliquot from each Cy labeled sample containing 2.5 µg protein was subjected to SDS-PAGE using 12 % acrylamide resolving gels. Following electrophoresis, labeled bands were visualised using fluorescence imaging and the corresponding Cy-dye excitation and emission parameters.

Figure 4.18. Application of both 12 % and 15 % acrylamide resolving gels to the 2-D DIGE analysis of changes in soluble protein steady state levels following exposure of wild type and *Δhik34 Synechocystis* cells to 1 hour heat shock conditions.

Equal 12.5 μg quantities of control (Cy3 labelled), heat shock (Cy5 labelled) and pooled internal standard (Cy2 labelled) samples were co-resolved through large format pH 4-7 12 % and 15 % acrylamide 2-D gels. Labelled proteins were visualised immediately after electrophoresis detecting all three labelled samples. Cy images, i.e. Cy2, Cy3 and Cy5, were overlaid and using this overlay image proteins having an increased or decreased abundance can be seen as blue/green and red spots, respectively. The extra resolution achieved for the low molecular weight proteins is clearly visible.

12 % Acrylamide
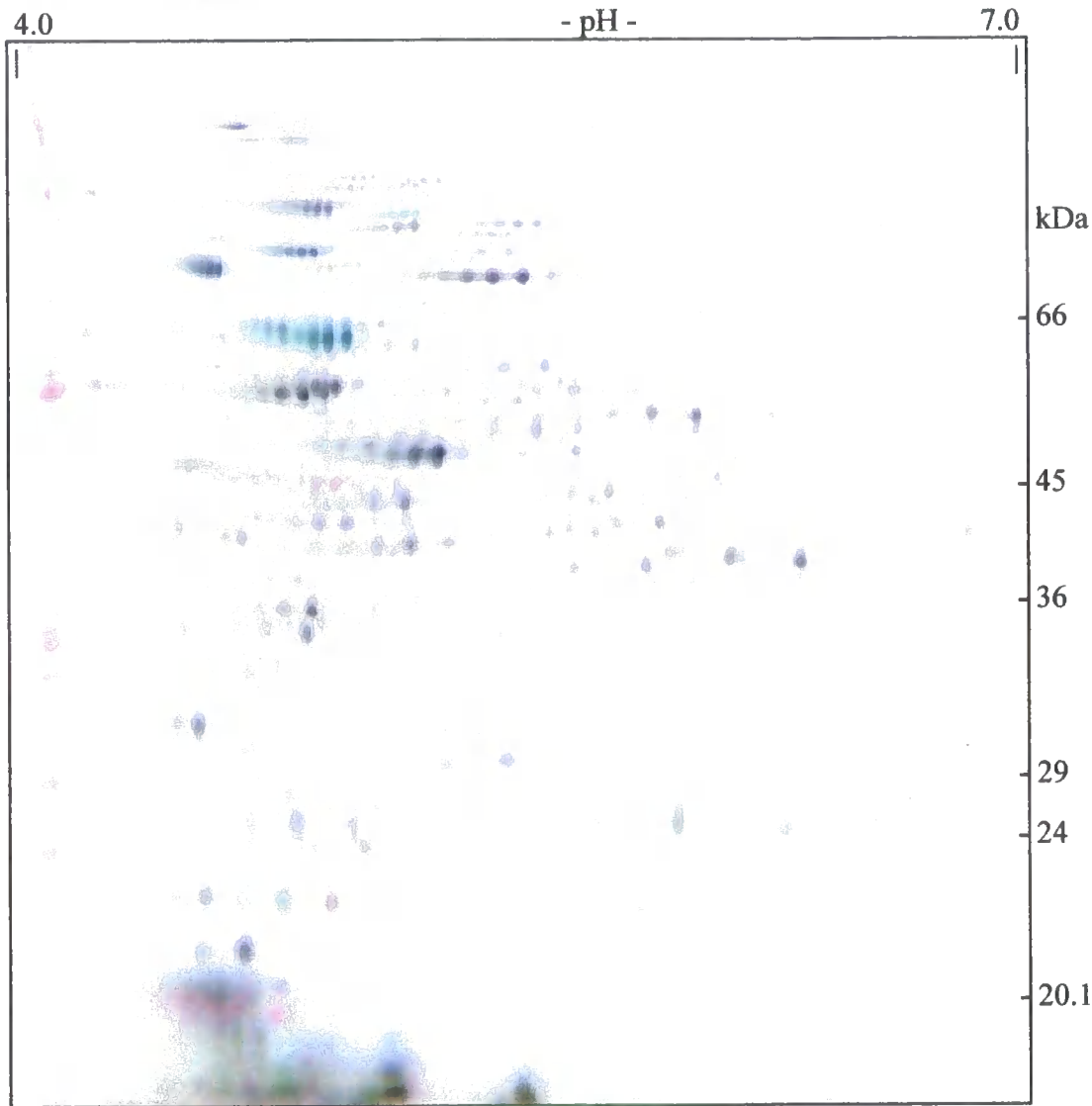
15 % Acrylamide
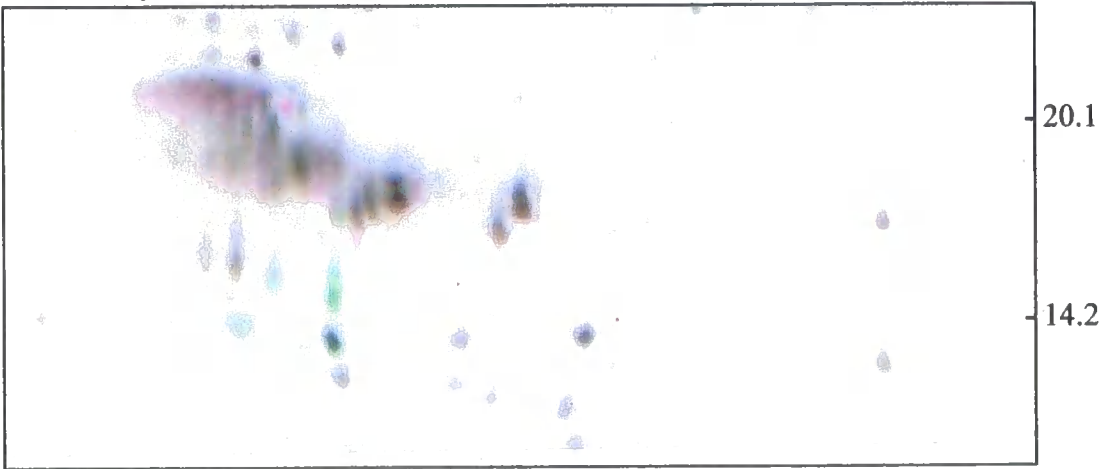
gels, as resolution of high molecular weight proteins is reduced at higher acrylamide concentrations.

Having obtained all the images for all eight 2-D DIGE gels at both 12 % and 15 % polyacrylamide concentrations, it was evident that one of the four 12 % acrylamide wild type gels had not acceptably resolved and was therefore not carried forward for software analysis. This therefore reduced the number of replicate wild type 12 % polyacrylamide experiments to three. The remaining 2-D DIGE gels were cropped and processed via DeCyder Batch processor software (Amersham Biosciences) as previously described in section 4.2.7 where 12 % and 15 % polyacrylamide gels were processed separately. Again all spot matching across all gels was manually checked and altered if necessary in DeCyder BVA software (Amersham Biosciences) before using this software to automatically determine the average change in protein abundance across all replicate gels for each protein spot between all four sample types. This was between (i) wild type control and wild type heat shock samples, (ii) *Δhik34* control and *Δhik34* heat shock samples, (iii) wild type control and *Δhik34* control samples, and (iv) wild type heat shock and *Δhik34* heat shock samples. As before the software also calculated the variance for each set of average data using a paired T-test. This type of analysis asks the questions (a) which protein spots change in abundance as a result of heat shock, (b) which proteins change in abundance as a result of the *Δhik34* mutation, and (c) what effect does the mutation have on the heat shock responsive proteins. Those protein spots displaying a greater than +/-10 % change in abundance in response to heat shock or as a result of the *Δhik34* mutation, across all repeat experiments and also having a statistical confidence above 95 % were selected for MALDI-TOF PMF identification. The total number of spots selected for

identification equalled 321, 251 of which demonstrated an elevated abundance and 70 a decreased abundance. In many cases the same protein spot was selected for identification across all four sample comparisons, however in other cases a particular spot may only have statistically valid data from only one of the sample comparisons. Of the 321 spots selected for identification the 15 % polyacrylamide DIGE analysis contributed 20 additional spots which met the selection criteria.

4.2.10 MALDI-TOF PMF identification of *Synechocystis* soluble proteins which display a change in abundance following exposure of *Synechocystis* cells to heat shock conditions and as a result of the *Δhik34* gene knockout mutation.

In each 2-D DIGE analytical gel there were only 37.5 μg (3 x 12.5 μg) of total protein loaded, this means that if an average protein mass of 30,000 Da and a total of 3,000 *Synechocystis* soluble protein spots are assumed, there is only 0.42 pmoles of protein per spot. This is insufficient material to obtain identification via the MALDI-TOF PMF technique. Therefore, three higher loaded 2-D gels each containing 400 μg of total soluble protein were generated. The same 2-D methodology that was performed to generate the DIGE analytical gels, i.e. pH 4-7 18 cm IEF, anodic cup loading and large format electrophoresis, was employed to generate these higher loaded preparative picking gels where two of the gels were at 12 % polyacrylamide concentration and one was at 15 % concentration. The resolved spots were visualised with MS compatible silver staining and scanned using a Proxpress imager (Genomic Solutions). Spots selected for identification from all three heat shock 2-D DIGE analyses, (including the initial 34°C – 44°C 12 % polyacrylamide analysis and both 12 % and 15 % polyacrylamide analysis of the 30°C – 42°C heat shock study), were

manually matched to the same spots on the silver stained preparative gels. Upon examination of the preparative gel it was evident that several of the spots selected for identification were very low abundant. Because the likelihood of obtaining identification for these low abundant spots is remote and because MALDI-TOF PMF is very expensive, these spots were omitted from the analyses. Consequently the most abundant 288 spots (3 microtitre plates worth) were manually picked (see materials and methods for details) from the gels into 96-well microtitre plate (Genomic Solutions) where selected spots from the 12 % DIGE analyses were picked from both 12 % preparative gels into the same well of the microtitre plate. It was interesting to note that the majority of proteins which displayed a low abundance were proteins that also demonstrated a decrease from steady state levels following heat shock. The picked spots were proteolysed with trypsin using a Progest autodigestion robot (Genomic Solutions) and the resultant tryptic peptides were analysed via MALDI-ToF MS. The mass spectra generated by the MALDI-ToF were used to interrogate, in manual mode, all entries in the NCBI non redundant database using the MASCOT search engine (http://www.matrixscience. com) (Perkins *et al.*, 1999). This resulted in 168 of the 288 spots being positively identified having a MOWSE (MOlecular Weight SEarch) score greater that the statistically valid threshold of 64. This score was used as the statistically valid threshold because it equated to a greater than 95% confidence that the probability of an observed match was not a random event. Furthermore, there is also a high degree of confidence in the identifications obtained because of the high probability that each protein spot on the 2D gel is a single protein species due to the small genome size of *Synechocystis*. For all identifications listed, a protein from *Synechocystis* PCC 6803 was the highest scoring hit. Other protein identification criteria which could have been applied include the University of Washington's

SEQUEST algorithm (http://fields.scripps.edu/sequest/index.html), Rockefeller University's ProFound algorithm (prowl.rockefeller.edu/PROWL/prowl.html) and Expasy's PeptIdent algorithm (www.expasy.ch/tools/peptident.html). Identifications from *Synechocystis* were generated for a further 8 protein spots which had MOWSE scores slightly below the threshold score of 64. However, because a neighbouring protein in the same molecular weight train had the same identification, these identifications have also been included in the data set and considered accurate. Therefore 176 proteins were identified from the original 288 picked, this is a hit rate of 61 %. All 176 identified proteins are tabulated along with the corresponding DIGE data and their location on the silver stained 2-D gel is indicated in Figure 4.19. Table 4.3 lists all identified proteins seen to change in abundance in response to heat shock in both wild type and *Δhik34* mutant cells. Table 4.4 list all identified proteins seen to change in abundance as a result of the *Δhik34* knockout mutation.

In Table 4.3 three protein spots numbered 143, 144 and 145 are of particular interest. All three spots resolved in the same molecular weight train and all contained the same few peptides in their MALDI-Tof mass spectra, but only a low probability identification as manganese stabilising polypeptide was attained. To attempt to generate a positive identification, the two major peptides in the mass spectra of 1240.69 amu and 2128.06 amu were sequenced by ESI tandem MS. The mass spectra generated were again used to search all entries in the NCBI non redundant database using the MASCOT search engine (http://www.matrixscience.com) (Perkins *et al.*, 1999) and a positive match for manganese stabilising polypeptide was obtained (Figure 4.20).

Figure 4.19. Annotated silver stained preparative gel of identified *Synechocystis* soluble protein spots which show a change in steady state levels following exposure of cells to heat shock conditions or as a result of the *Δhik34* knockout mutation.

Synechocystis soluble protein was fractionated from wild type cells grown under heat shock conditions for 1 hour. Aliquots containing 400 μg of protein were subjected to large format pH 4-7 2-DE using both 12 % and 15 % acrylamide resolving gels and the resolved protein spots were stained with MS compatible silver stain. Annotated spots are those shown to change in abundance following heat shock or as a result of the *Δhik34* mutation and have been successfully identified via MALDI-ToF MS or ESI tandem MS (see Tables 4.3 & 4.4). Spots labelled with a blue arrow are only present in Table 4.4.

12% acrylamide
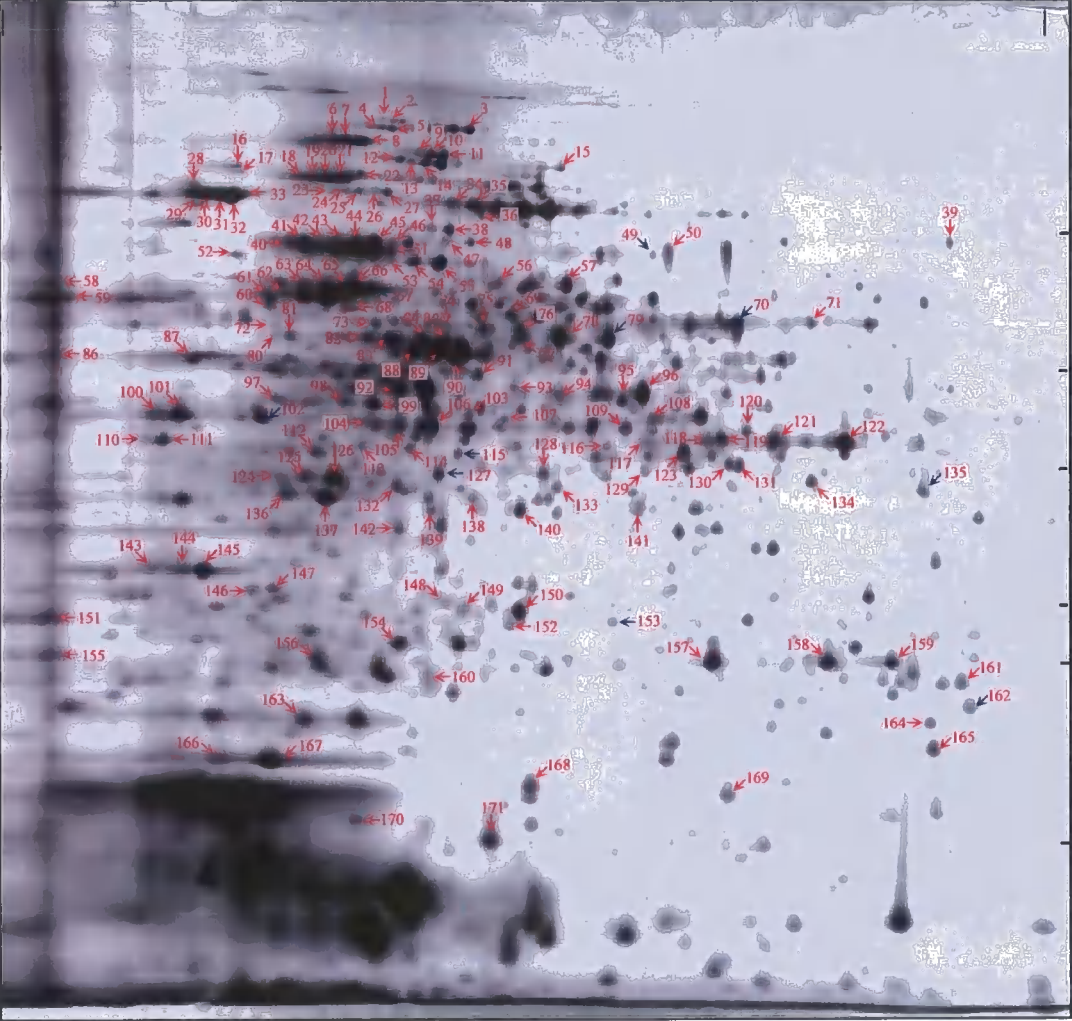
15% acrylamide
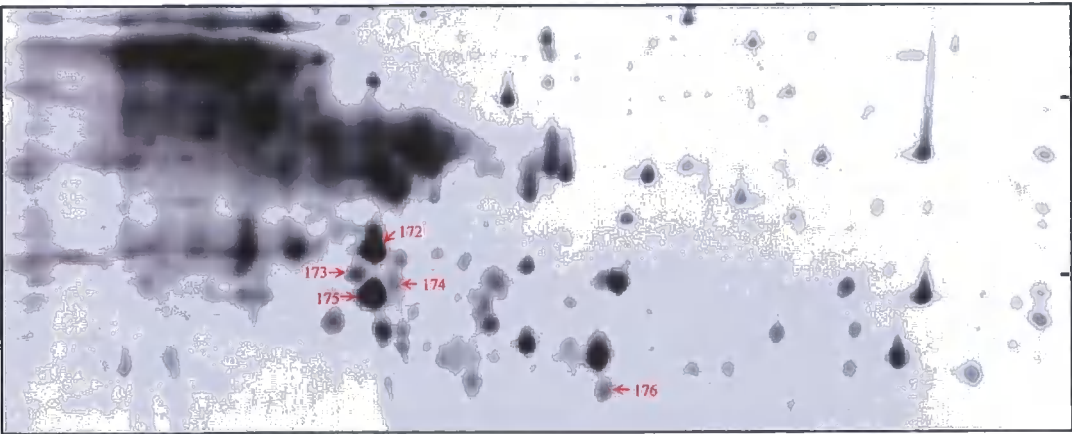
Table 4.3. *Synechocystis* soluble proteins which display a change in abundance following exposure of W.T. and *Δhik34* cells to heat shock temperatures.

Spot No.	Protein I.D (gene)	MOWSE score	ORF/ Accession No.[c]	Protein Abundance Difference		
				W.T. 34-44°C	W.T. 30-42°C	Δhik34 30-42°C
1	preprotein translocase SecA subunit (*secA*)	77	sll0616 gi|16331549	1.33[b]	1.34	1.17
2	preprotein translocase SecA subunit (*secA*)	172		1.29[b]	1.29	1.22
3	aconitate hydratase (*acnB*)	169	slr0665 gi|16332149	-	1.13	1.34
4	valyl-tRNA synthetase (*valS*)	127	slr0557 gi|16332082	-	1.17	1.23
5	valyl-tRNA synthetase (*valS*)	50[a]		-	1.21	1.19
6	elongation factor EF-G 1 (*fusA, fus*)	151	slr1463 gi|16332123	1.32	1.64	1.39
7	elongation factor EF-G 1 (*fusA, fus*)	155		1.28	1.6	1.46
8	elongation factor EF-G 1 (*fusA, fus*)	132		1.28	1.59	1.49
9	ClpB protein (*clpB1*)	291	slr1641 gi|16331048	4.57	2.48	3.55
10	ClpB protein (*clpB1*)	200		5.77	2.57	3.95
11	ClpB protein (*clpB1*)	269		5.13	2.32	3.15

Table 4.3 continued.

Spot No.	Protein I.D (gene)	MOWSE score	ORF/ Accession No.[c]	Protein Abundance Difference		
				W.T. 34-44°C	W.T. 30-42°C	Δhik34 30-42°C
12	DNA ligase (*lig, ligA*)	131	sll1583 gi|16329814	1.33	1.41	1.2
13	polyribonucleotide nucleotidyltransferase (*pnp*)	174	sll1043 gi|16329253	1.59	1.32	1.2
14	polyribonucleotide nucleotidyltransferase (*pnp*)	120		1.59	1.22	1.26
15	ATP-dependent Clp protease ATPase subunit (*clpC*)	112	sll0020 gi|16331384	1.46	1.38	1.5
16	phosphoribosylformylglycinamidine synthase II (*purL, purI*)	132	sll1056 gi|14916653	1.43	-	-
17	glycyl-tRNA synthase beta chain (*glyS*)	86	shr0220 gi|16331421	1.7 [b]	-	-
18	HtpG, heat shock protein 90, molecular chaperone (*htpG*)	64		2.56	2.42	1.74
19	HtpG, heat shock protein 90, molecular chaperone (*htpG*)	93	sll0430 gi|16332281	2.75	2.4	1.87
20	HtpG, heat shock protein 90, molecular chaperone (*htpG*)	106		2.76	2.27	1.99

Table 4.3 continued.

Spot No.	Protein I.D (gene)	MOWSE score	ORF/ Accession No.[c]	Protein Abundance Difference		
				W.T. 34-44°C	W.T. 30-42°C	Δhik34 30-42°C
21	HtpG, heat shock protein 90, molecular chaperone (*htpG*)	195	sll0430 gi|16332281	2.68	2.1	2
22	elongation Factor EF-G 2 (*fusB, fus*)	79	sll1098 gi|16330914	1.68	1.33	1.39
23	oligopeptidase A (*prlC, opdA*)	66		1.69	1.61	1.74
24	oligopeptidase A (*prlC, opdA*)	58[a]	slr0659 gi|16332138	1.76	1.49	1.73
25	oligopeptidase A (*prlC, opdA*)	96		1.44[b]	1.27	1.63
26	ClpB protein (*clpB1*)	167	slr1641 gi|16331048	3.31	1.92	2.67
27	ClpB protein (*clpB1*)	160		4.03	2.07	2.75
28	DnaK protein 2, heat shock protein 70, molecular chaperone (*dnaK2*)	136		2.36	-	-
29	DnaK protein 2, heat shock protein 70, molecular chaperone (*dnaK2*)	148	sll0170 gi|16331261	2.99[b]	-	-
30	DnaK protein 2, heat shock protein 70, molecular chaperone (*dnaK2*)	125		2.85	2.45	1.82

Table 4.3 continued.

Spot No.	Protein I.D (gene)	MOWSE score	ORF/ Accession No.[c]	Protein Abundance Difference		
				W.T. 34-44°C	W.T. 30-42°C	Δhik34 30-42°C
31	DnaK protein 2, heat shock protein 70, molecular chaperone (*dnaK2*)	233		2.75	2.26	1.95
32	DnaK protein 2, heat shock protein 70, molecular chaperone (*dnaK2*)	132	sll0170 gi|16331261	2.63	2.06	2.03
33	DnaK protein 2, heat shock protein 70, molecular chaperone (*dnaK2*)	93		2.64	1.98	1.84
34	transketolase (*tktA*)	112	sll1070 gi|16329902	1.36[b]	1.29	1.06
35	transketolase (*tktA*)	171		1.2	1.33	1.1
36	hypothetical protein - probable peptidase	79	slr0825 gi|16331709	-	-1.14	-1.08
37	aspartyl-tRNA synthase (*asps*)	99	slr1720 gi|16330502	1.19	1.37	1.31
38	aspartyl-tRNA synthase (*asps*)	135		1.2	1.25	1.33
39	pyruvate kinase 2 (*pyk2*)	140	sll1275 gi|16330166	1.23[b]	1.14	1.42
40	60 kDa chaperonin 2, GroEL2, molecular chaperone (*groEL2, cpn60-2*)	73	sll0416 gi|16331442	2.55	3.31	2.3

Table 4.3 continued.

Spot No.	Protein I.D (gene)	MOWSE score	ORF/ Accession No.[c]	Protein Abundance Difference		
				W.T. 34-44°C	W.T. 30-42°C	Δhik34 30-42°C
41	60 kDa chaperonin 2, GroEL2, molecular chaperone (*groEL2, cpn60-2*)	97	sll0416 gi|16331442	3.65	4	2.53
42	60 kDa chaperonin 1, GroEL1, molecular chaperone (*groEL1, cpn60-1*)	189		6.15	5.25	3.01
43	60 kDa chaperonin 1, GroEL1, molecular chaperone (*groEL1, cpn60-1*)	54[a]		7.17	5.25	3.47
44	60 kDa chaperonin 1, GroEL1, molecular chaperone (*groEL1, cpn60-1*)	77	slr2076 gi|16330003	6.82	5.18	3.78
45	60 kDa chaperonin 1, GroEL1, molecular chaperone (*groEL1, cpn60-1*)	82		5.81	4.08	3.56
46	60 kDa chaperonin 1, GroEL1, molecular chaperone (*groEL1, cpn60-1*)	84		1.48	1.26	1.43
47	aspartate kinase (*lysC*)	103	slr0657 gi|16332136	1.48	1.39	1.16
48	aspartate kinase (*lysC*)	111		1.56	1.51	1.37

Table 4.3 continued.

Spot No.	Protein I.D (gene)	MOWSE score	ORF/ Accession No.c	Protein Abundance Difference		
				W.T. 34-44°C	W.T. 30-42°C	Δhik34 30-42°C
50	pyruvate dehydrogenase dihydrolipoamide acetyltransferase component E2 (*odhB, citM*)	64	sll1841 gi|16331208	1.39	1.2	1.23
51	60 kDa chaperonin 1, GroEL1, molecular chaperone (*groEL1, cpn60-1*)	77	slr2076 gi|16330003	-	3.11	2.92
52	N utilisation substance protein (*nusA*)	199	slr0743 gi|16329287	1.54	1.35	1.27
53	60 kDa chaperonin 1, GroEL1, molecular chaperone (*groEL1, cpn60-1*)	214	slr2076 gi|16330003	1.59	1.4	1.55
54	dihydroxyacid dehydratase (*ilvD*)	96	slr0452 gi|16332267	1.28	1.21	1.25
55	dihydroxyacid dehydratase (*ilvD*)	98		1.28	1.12	1.23
56	D-3-phosphoglycerate dehydrogenase (*serA*)	87	sll1908 gi|16330470	-	1.47	1.28
57	D-3-phosphoglycerate dehydrogenase (*serA*)	135		1.54	1.63	1.45
58	glutamate--ammonia ligase, glutamine synthetase type I (*glnA*)	125	slr1756 gi|2494751	-	-1.99	-2.11

Table 4.3 continued.

Spot No.	Protein I.D (gene)	MOWSE score	ORF/ Accession No.[c]	Protein Abundance Difference		
				W.T. 34-44°C	W.T. 30-42°C	Δhik34 30-42°C
59	ribulose bisphosphate carboxylase large subunit (*rbcL*)	131	slr0009 gi|16331392	-2.13	-1.73	-1.87
60	60 kDa chaperonin 2, GroEL2, molecular chaperone (*groEL2, cpn60-2*)	68	sll0416 gi|16331442	1.22	1.42	1.28 [b]
61	60 kDa chaperonin 2, GroEL2, molecular chaperone (*groEL2, cpn60-2*)	58 [a]		1.27	1.4	1.28
62	ATP synthase beta chain of CF1 (*atpB*)	58 [a]	slr1329 gi|16330679	1.24	1.34	1.21
63	ATP synthase beta chain of CF1 (*atpB*)	76		1.25	1.32	1.22
64	ATP synthase beta chain of CF1 (*atpB*)	130		1.21	1.27	1.19
65	S-adenosylmethionine synthetase (*metX*)	96	sll0927 gi|16329479	1.17 [b]	1.19	1.18
66	ATP synthase alpha subunit (*atpA*)	84	sll1326 gi|16329327	1.26 [b]	1.37	1.29 [b]
68	ATP synthase alpha subunit (*atpA*)	80		1.45	1.59	1.37
69	Dihydrolipoyl dehydrogenase (*phdD, lpd*)	84	slr1096 gi|6166120	-	1.18	1.23

Table 4.3 continued.

Spot No.	Protein I.D (gene)	MOWSE score	ORF/ Accession No. [c]	Protein Abundance Difference		
				W.T. 34-44°C	W.T. 30-42°C	Δhik34 30-42°C
71	glucose-1-phosphate adenylyltransferase (*glgC*, *agp*)	86	slr1176 gi|16332282	-	1.16	1.21
72	hypothetical protein	85	sll1693 gi|16330344	1.31	1.3	1.16
73	60 kDa chaperonin 1, GroEL1, molecular chaperone (*groEL1*, *cpn60-1*)	168	slr2076 gi|16330003	1.43	1.95	1.51
74	thiamine-phosphate pyrophosphorylase (*thiE*)	75	sll0635 gi|41019543	1.38	1.41	1.19
75	malic enzyme (*me*)	70	slr0721 gi|16329255	-	1.25	1.15
76	glutamyl-tRNA synthetase (*gltX*)	75	sll0179 gi|16331631	-	1.21	1.1
77	S-adenosylhomocysteine hydrolase (*ahcY*)	108	sll1234	-	1.17	1.25
78	S-adenosylhomocysteine hydrolase (*ahcY*)	115	gi|16330671	1.13	1.15	1.24
80	60 kDa chaperonin 1, GroEL1, molecular chaperone (*groEL1*, *cpn60-1*)	86	slr2076	1.56	1.57	1.64
81	60 kDa chaperonin 1, GroEL1, molecular chaperone (*groEL1*, *cpn60-1*)	42 [a]	gi|16330003	1.37	1.6	1.53

Table 4.3 continued.

Spot No.	Protein I.D (gene)	MOWSE score	ORF/ Accession No. [c]	Protein Abundance Difference		
				W.T. 34-44°C	W.T. 30-42°C	Δhik34 30-42°C
82	hypothetical protein	70	slr0863 gi|16330398	1.2	1.56	1.23
83	enolase (*eno*)	76	slr0752 gi|16332209	1.21	1.53	1.25
84	argininosuccinate synthetase (*argG*)	77	slr0585 gi|16332301	1.22	1.55	1.25
85	6-phosphogluconate dehydrogenase, decarboxylating (*gnd*)	88	sll0329 gi|16331307	1.18	1.4	1.21
86	carbon dioxide concentrating mechanism protein, putative carboxysome structural protein (*ccmM*)	132	sll1031 gi|16329365	-1.53	-1.58	-1.85
87	periplasmic protein, ABC-type urea transport system substrate-binding protein (*urtA, amiC*)	78	slr0447 gi|16331081	-1.36	1	1.07
88	protein synthesis elongation factor Tu (*tufA, tuf*)	77		1.43	1.75	1.34
89	protein synthesis elongation factor Tu (*tufA, tuf*)	84	sll1099 gi|16330913	1.42	1.76	1.44
90	protein synthesis elongation factor Tu (*tufA, tuf*)	90		1.57	1.76	1.5
91	adenylosuccinate synthetase (IMP--aspartate ligase) (*purA, adeK*)	89	sll1823 gi|2500024	-	1.49	1.37

Table 4.3 continued.

Spot No.	Protein I.D (gene)	MOWSE score	ORF/ Accession No. [c]	Protein Abundance Difference		
				W.T. 34-44°C	W.T. 30-42°C	Δhik34 30-42°C
92	fructose-1,6-/sedoheptulose-1,7-bisphosphatase (fbpI, glpX)	75	slr2094 gi|16330580	1.17	1.46	1.24
93	hypothetical protein	65	sll0103 gi|16331837	1.35	1.4	1.32
94	fructose-bisphosphate aldolase, class II (cbbA, cfxA, fbaA, fda)	58[a]	sll0018 gi|16331386	-	1.48	1.7
95	3-oxoacyl-[acyl-carrier-protein] synthase II (fabF, fabJ)	107	sll1069 gi|16329903	-	1.18	1.32
96	fructose-bisphosphate aldolase, class II (cbbA, cfxA, fbaA, fda)	166	sll0018 gi|16331386	-	1.31	2.15
97	hypothetical protein - probable GTP binding protein	107	sll0245 gi|16330542	-	1.31	1.24
98	phosphoglycerate kinase (pgk)	77	slr0394	1.29	1.39	1.21
99	phosphoglycerate kinase (pgk)	105	gi|2499503	1.47	1.43	1.27
100	30S ribosomal protein S1 (rps1, rps1a)	56[a]	slr1356 gi|16330162	1.27	1.37	1.09

Table 4.3 continued.

Spot No.	Protein I.D (gene)	MOWSE score	ORF/ Accession No.[c]	Protein Abundance Difference		
				W.T. 34-44°C	W.T. 30-42°C	Δhik34 30-42°C
101	30S ribosomal protein S1 (*rps1, rps1a*)	78	slr1356 gi|16330162	1.46	1.25	1.18
103	RecA gene product (*recA*)	113	sll0569 gi|16332317	-	1.18	1.12
104	phosphoribulokinase (*prk, ptk*)	91		-	1.19	1.17
105	phosphoribulokinase (*prk, ptk*)	75	sll1525 gi|585368	-	1.21	1.23
106	phosphoribulokinase (*prk, ptk*)	84		-	1.17	1.24
107	hypothetical protein	141	sll0102 gi|16331838	-	1.27	1.22
108	sulfolipid biosynthesis protein; (*sqdB*)	154	slr1020 gi|16329746	-	1.06	1.19
109	coproporphyrinogen III oxidase, aerobic (oxygen-dependent) (*hemF*)	105	sll1185 gi|16329455	-	-1.15	-1.1
110	hypothetical protein - peptidyl-prolyl cis-trans isomerase	129	sll0408	1.5	1.61	1.31
111	hypothetical protein - peptidyl-prolyl cis-trans isomerase	84	gi|16331452	1.59	1.44	1.28
112	porphobilinogen synthase (5-aminolevulinate dehydratase) (*hemB*)	98	sll1994 gi|16330659	-	1.18	1.16

Table 4.3 continued.

Spot No.	Protein I.D (gene)	MOWSE score	ORF/ Accession No.[c]	Protein Abundance Difference		
				W.T. 34-44°C	W.T. 30-42°C	Δhik34 30-42°C
113	MRP protein homolog (MRP)	77	slr0067 gi|16331499	-	1.37	1.41
114	hypothetical protein	117	sll1961 gi|16330450	1.21	1.5	1.3
116	periplasmic protease HhoA (hhoA)	122	sll1679 gi|16329387	1.24	1.28	1.23
117	NAD(P)-dependent glyceraldehyde-3-phosphate dehydrogenase (gap2)	75	sll1342 gi|16332093	1.28	1.5	1.29
118	NAD(P)-dependent glyceraldehyde-3-phosphate dehydrogenase (gap2)	113	sll1342 gi|16332093	1.18	1.44	1.3
119	aspartate beta-semialdehyde dehydrogenese (asd)	94	slr0549 gi|16332070	-	1.34	1.34
119	tryptophanyl-tRNA synthetase (trpS)	79	slr1884 gi|8039807	-	1.34	1.34
120	chorismate synthase (aroC)	136	sll1747 gi|16330007	-	1.17	1.26[b]
121	NAD(P)-dependent glyceraldehyde-3-phosphate dehydrogenase (gap2)	128	sll1342 gi|16332093	-	1.31	1.37
122	NAD(P)-dependent glyceraldehyde-3-phosphate dehydrogenase (gap2)	147	sll1342 gi|16332093	-	1.08	1.3

Table 4.3 continued.

Spot No.	Protein I.D (gene)	MOWSE score	ORF/ Accession No.[c]	Protein Abundance Difference		
				W.T. 34-44°C	W.T. 30-42°C	Δhik34 30-42°C
123	uroporphyrinogen decarboxylase (*hemE*)	92	slr0536 gi|16332025	-	1.3	1.14
124	ketol-acid-reductoisomerase (*ilvC*)	84		1.31	1.28	1.09
125	ketol-acid-reductoisomerase (*ilvC*)	137	sll1363 gi|2506910	1.24	1.25	1.18
126	ketol-acid-reductoisomerase (*ilvC*)	106		1.21	1.26	1.11
128	fructose-bisphosphate aldolase, class II (*cbbA, cfxA, fbaA, fda*)	64	sll0018 gi|16331386	1.22	1.2	1.09
129	LysR family transcriptional regulator (*ycf30*)	207	sll0998 gi|16329741	-	1.24	1.2
130	phenylalanyl-tRNA synthetase alpha chain (*pheS*)	158	sll0454 gi|16331530	-	1.22	1.15
131	hypothetical protein - NADP-thioredoxin reductase	78	slr0600 gi|16332326	-	1.13	1.19
132	pyruvate dehydrogenase E1 component, α subunit	79	slr1934 gi|16331186	-	1.04	1.1
133	ornithine carbamoyltransferase chain f (*argF*)	96	sll0902 gi|16332048	-	1.52	1.38

Table 4.3 continued.

Spot No.	Protein I.D (gene)	MOWSE score	ORF/ Accession No.[c]	Protein Abundance Difference		
				W.T. 34-44°C	W.T. 30-42°C	Δhik34 30-42°C
134	hypothetical protein - probable anion transporting ATPase	190	slr1794 gi|16329406	1.19	1.13	1.13
136	water-soluble carotenoid protein	69	slr1963 gi|16330780	1.4	1.38	1.28
137	water-soluble carotenoid protein	66		1.48	1.44	1.3
138	hypothetical protein	109	slr1438 gi|16330136	-	1.23	1.19
138	cysteine synthase (cysM)	82	sll0712 gi|16329256	-	1.23	1.19
139	hypothetical protein	88	slr0635 gi|16331555	-	1.31	1.13
140	pyruvate dehydrogenase E1 component, β subunit (pdhB)	148	sll1721 gi|16330037	-	1.16	1.2
141	hypothetical protein - GDP-fucose synthetase	77	sll1213 gi|16329176	-	1.15	1.14
142	60 kDa chaperonin 1, GroEL1, molecular chaperone (groEL1, cpn60-1)	106	slr2076 gi|16330003	-	1.42	1.32
143	PSII manganese-stabilising polypeptide (psbO)	92*	sll0427 gi|16331068	1.44	1.72	1.2

Table 4.3 continued.

Spot No.	Protein I.D (gene)	MOWSE score	ORF/ Accession No. [c]	Protein Abundance Difference		
				W.T. 34-44°C	W.T. 30-42°C	Δhik34 30-42°C
144	PSII manganese-stabilising polypeptide (psbO)	92*	sll0427	1.66	1.59	1.27
145	PSII manganese-stabilising polypeptide (psbO)	92*	gi|16331068	1.83	1.47	1.26
146	diaminopimelate epimerase (dapF)	81	slr1665 gi|16332245	-	1.15	1.19
147	response regulator for energy transfer from phycobilisomes to photosystems (rpaB, ycf27, rre26)	83	slr0947 gi|23039836	1.25	1.18	1.17
148	6-phosphogluconolactonase, 6PGL	119	sll1479 gi|2829619	-	1.31	1.30
149	hypothetical protein	70	sll0069 gi|16331474	1.26	1.31	1.44
150	elongation factor TS (tsf)	108	sll1261 gi|16330738	1.31	1.28	1.64
151	phycobilisome rod-core linker polypeptide (cpcG1)	167	slr2051 gi|16329710	-2.03	-1.84	-2.14
152	septum site-determining protein; MinD (minD)	100	sll0289 gi|16331864	-	1.24	1.31
154	triosephosphate isomerase (tpiA, tpi)	73	slr0783 gi|16331347	-	1.21	1.10
155	light repressed protein A homolog (lrtA)	111	sll0947 gi|16331216	-	-1.58	-1.92

Table 4.3 continued.

Spot No.	Protein I.D (gene)	MOWSE score	ORF/ Accession No.[c]	Protein Abundance Difference		
				W.T. 34-44°C	W.T. 30-42°C	Δhik34 30-42°C
156	hypothetical protein	138	slr0552 gi|16332073	1.24[b]	1.27	1.22
157	SOS function regulatory protein - LexA repressor (*lexA*)	79		1.45	1.40	1.46
158	SOS function regulatory protein - LexA repressor (*lexA*)	64	sll1626 gi|16330362	1.42	1.69	1.76
159	SOS function regulatory protein - LexA repressor (*lexA*)	120		1.26	1.31	1.4
160	60 kDa chaperonin 1, GroEL1, molecular chaperone (*groEL1, cpn60-1*)	83	slr2076 gi|16330003	2.29	1.96	2.04
161	PHA-specific acetoacetyl-CoA reductase (*phaB, fabG2*)	84	slr1994 gi|16330475	-	1.07	1.17
163	AhpC/TSA family protein (membrane protein)	81	sll1621 gi|16330368	-	1.3	1.28
164	orotate phosphoribosyltransferase (*umpS*)	115	slr0185 gi|16331279	1.14	-1.1	1.1
165	two-component response regulator CheY subfamily (*rrel3*)	63	slr2024 gi|16329862	1.18	1.24	1.17

Table 4.3 continued.

Spot No.	Protein I.D (gene)	MOWSE score	ORF/ Accession No. [c]	Protein Abundance Difference		
				W.T. 34-44°C	W.T. 30-42°C	Δhik34 30-42°C
166	50S ribosomal protein L6 (*rplF*, *rpl6*)	80	sll1810 gi|16329927	1.24	1.29	1.17
167	50S ribosomal protein L6 (*rplF*, *rpl6*)	67		1.12	1.15	1.11
168	adenylate kinase (*adk*)	71	sll1815 gi|6647539	1.18	1.20	1.16
169	adenylylsulfate 3-phosphotransferase (*cysC*)	150	slr0676 gi|16329549	-	1.16	1.20
170	hypothetical protein	73	slr0001 gi|16331382	1.22	1.37	1.27
171	peptidyl-prolyl cis-trans isomerase (*cyp*, *rot1*)	88	slr1251 gi|16330433	-1.26	-1.16	-1.22
172	16.6 kDa small heat shock protein, molecular chaperone (*hspA*, *hsp17*)	118	sll1514 gi|16329588	-	19.92	21.95
173	photosystem II reaction center 13 kDa protein (*psb28*, *psbW*, *psb13*, *ycf79*)	68	sll1398 gi|16329210	-	2.17	1.75
174	ribulose bisphosphate caboxylase small subunit (*rbcS*)	108	slr0012 gi|16331394	-	1.54	1.47
175	10 kDa chaperone (*groES*)	136	slr2075 gi|1461732	-	3.24	2.58

Table 4.3 continued.

Spot No.	Protein I.D (gene)	MOWSE score	ORF/ Accession No. [c]	Protein Abundance Difference		
				W.T. 34-44°C	W.T. 30-42°C	Δhik34 30-42°C
176	photosystem I subunit VII (*psaC*)	102	ssl0563 gi|16331238	-	1.33	1.21

Changes in protein abundance are represented as a fold change and negative values indicate a decreased abundance, for example a value of -1.33 indicates this protein decreases in abundance from steady stage levels by 1.33 fold or by 33%.

* Proteins identified via ESI MS/MS.

[a] MOWSE scores just bellow the significant threshold (64).

[b] Average data calculated with one missing replicate from the corresponding experiment.

Average data in black is above the 95 % statistical threshold (data was rounded up, i.e. including and above 94.5 %), blue indicates borderline statistical data (between 94.4 – 92.5 %), red indicates statistically invalid data (bellow 92.5 %).

[c] Accession no. is that for the NCBI database.

Table 4.4. *Synechocystis* soluble proteins which display a change in abundance at both normal and heat shock conditions at a result of the *hik34* knockout mutation.

Spot No.	Protein I.D. (gene)	MOWSE score	ORF/ Accession No. [c]	Protein Difference	
				Δhik34/W.T. 30°C	*Δhik34*/W.T. 42°C
9	ClpB protein (*clpB1*)	291		1.48	2.05
10	ClpB protein (*clpB1*)	200	slr1641 gi|16331048	1.65	2.41
11	ClpB protein (*clpB1*)	269		1.77	2.31
15	ATP-dependent Clp protease ATPase subunit (*clpC*)	112	sll0020 gi|16331384	1.82	1.97
18	HtpG, hsp90 molecular chaperone (*htpG*)	64		3.48	2.53
19	HtpG, hsp90 molecular chaperone (*htpG*)	93	sll0430 gi|16332281	3.79	2.9
20	HtpG, hsp90 molecular chaperone (*htpG*)	106		3.82	3.17
21	HtpG, hsp90 molecular chaperone (*htpG*)	195		3.7	3.3
22	elongation Factor EF-G 2 (*fusB, fus*)	79	sll1098 gi|16330914	1.37	1.46
23	oligopeptidase A (*prlC, opdA*)	96		1.38	1.46
24	oligopeptidase A (*prlC, opdA*)	66	slr0659 gi|16332138	1.13	1.28
25	oligopeptidase A (*prlC, opdA*)	58 [a]		1.08	1.38

Table 4.4. continued.

Spot No.	Protein I.D. (gene)	MOWSE score	ORF/ Accession No.[c]	Protein Difference	
				Δhik34/W.T. 30°C	Δhik34/W.T. 42°C
26	ClpB protein (*clpB1*)	167	slr1641 gi|16331048	1.6	2.17
27	ClpB protein (*clpB1*)	160		1.76	2.27
30	DnaK protein 2, hsp70 molecular chaperone (*dnaK2*)	125		2.37	1.75
31	DnaK protein 2, hsp70 molecular chaperone (*dnaK2*)	233	sll0170 gi|16331261	2.73	2.31
32	DnaK protein 2, hsp70 molecular chaperone (*dnaK2*)	132		2.78	2.65
33	DnaK protein 2, hsp70 molecular chaperone (*dnaK2*)	93		2.43	2.25
34	transketolase (*tktA*)	112	sll1070 gi|16329902	-1.05	-1.28
35	transketolase (*tktA*)	171		-1.19	-1.5
40	60 kDa chaperonin 2, hsp60 (*groEL2, cpn60-2*)	73	sll0416 gi|16331442	1.74	1.38
41	60 kDa chaperonin 2, hsp60 (*groEL2, cpn60-2*)	97		1.95	1.45
42	60 kDa chaperonin 1, hsp60 (*groEL1, cpn60-1*)	189	slr2076 gi|16330003	2.27	1.53
43	60 kDa chaperonin 1, hsp60 (*groEL1, cpn60-1*)	54[a]		2.22	1.71

Table 4.4. continued.

Spot No.	Protein I.D. (gene)	MOWSE score	ORF/ Accession No.[c]	Protein Difference	
				Δhik34/W.T. 30°C	Δhik34/W.T. 42°C
44	60 kDa chaperonin 1, hsp60 (groEL1, cpn60-1)	77		2.46	2.1
45	60 kDa chaperonin 1, hsp60 (groEL1, cpn60-1)	82	slr2076 gi|16330003	2.27	2.1
51	60 kDa chaperonin 1, hsp60 (groEL1, cpn60-1)	77		1.75	1.67
49	hypothetical protein	57[a]	sll1913 gi|16329869	1.08	1.18
53	60 kDa chaperonin 1, hsp60 (groEL1, cpn60-1)	214	slr2076 gi|16330003	1.06	1.17
62	ATP synthase beta chain of CF1 (atpB)	58[a]		1.24	1.12
63	ATP synthase beta chain of CF1 (atpB)	76	slr1329 gi|16330679	1.24	1.15
64	ATP synthase beta chain of CF1 (atpB)	130		1.29	1.21
67	glutamate--ammonia ligase, glutamine synthetase type I (glnA)	75	slr1756 gi|16329647	1.28	1.33
70	ferredoxin-NADP oxidoreductase (petH)	84	slr1643 gi|16331051	1.36	1.42
72	hypothetical protein	85	sll1693 gi|16330344	1.46	1.3

Table 4.4. continued.

Spot No.	Protein I.D. (gene)	MOWSE score	ORF/ Accession No. [c]	Protein Difference	
				Δhik34/W.T. 30°C	Δhik34/W.T. 42°C
77	S-adenosylhomocysteine hydrolase (*ahcY*)	108	sll1234 gi|16330671	1.12	1.18
79	S-adenosylhomocysteine hydrolase (*ahcY*)	115	sll1234 gi|16330671	1.27	1.29
81	60 kDa chaperonin 1, hsp60 (*groEL1, cpn60-1*)	42 [a]	slr2076 gi|16330003	1.5	1.46
86	carbon dioxide concentrating mechanism protein (*ccmM*)	132	sll1031 gi|16329365	-1.25	-1.35
87	periplasmic protein, ABC-type urea transport system substrate binding protein (*urtA, amiC*)	78	slr0447 gi|16331081	-1.39	-1.29
94	fructose-1,6-bisphosphate aldolase (*cbbA, cfxA, fbaA, fda*)	58 [a]	sll0018 gi|16331386	-1.36	-1.17
102	RNA polymerase alpha subunit (*rpoA*)	58 [a]	sll1818 gi|16329917	1.14	1.16
108	sulfolipid biosynthesis protein (*sqdB*)	154	slr1020 gi|16329746	1.01	1.13
109	coproporphyrinogen III oxidase (*hemF*)	105	sll1185 gi|16329455	1.37	1.42
115	hypothetical protein	84	slr0624 gi|16331828	1.03	-1.24

Table 4.4. continued.

Spot No.	Protein I.D. (gene)	MOWSE score	ORF/ Accession No.[c]	Protein Difference Δhik34/W.T. 30°C	Δhik34/W.T. 42°C
117	glyceraldehyde-3-phosphate dehydrogenase (NADP+) (phosphorylating) (gap2)	75	sll1342	-1.19	-1.39
118	glyceraldehyde-3-phosphate dehydrogenase (NADP+) (phosphorylating) (gap2)	113	gi|16332093	-1.18	-1.3
120	chorismate synthase (aroC)	136	sll1747 gi|16330007	1.32[b]	1.41[b]
124	ketol-acid-reductoisomerase (ilvC)	84	sll1363	-1.05	-1.25
125	ketol-acid-reductoisomerase (ilvC)	137	gi|2506910	-1.19	-1.24
127	30S ribosomal protein S1 (nbp1, rps1b)	108	slr1984 gi|16330820	1.4	1.39
131	hypothetical protein	78	slr0600 gi|16332326	1.42	1.48
132	pyruvate dehydrogenase E1 component, α subunit	79	slr1934 gi|16331186	1.28	1.36
135	hypothetical protein	65	slr1540 gi|16330056	1.3	1.35
136	water-soluble carotenoid protein	69	slr1963	1.86	1.72
137	water-soluble carotenoid protein	66	gi|16330780	2.31	2.12

Table 4.4. continued.

Spot No.	Protein I.D. (gene)	MOWSE score	ORF/ Accession No. [c]	Protein Difference	
				Δhik34/W.T. 30°C	Δhik34/W.T. 42°C
153	hypothetical protein	159	slr1259 gi|16330445	1.4	1.39
154	triosephosphate isomerase (*tpiA, tpi*)	73	slr0783 gi|16331347	1.17	1.06
161	3-ketoacyl-acyl carrier protein reductase (*phaB, fabG2*)	84	slr1994 gi|16330475	-1.16	-1.06
162	protein DraG (*draG*)	130	slr1719 gi|2499211	-1.22	-1.23
165	CheY subfamily (*rre13*)	63 [a]	slr2024 gi|16329862	1.3	1.24
166	50S ribosomal protein L6 (*rplF, rpl6*)	80	sll1810 gi|16329927	1.59	1.42
167	50S ribosomal protein L6 (*rplF, rpl6*)	102	sll1815 gi|6647539	1.72	1.64
168	adenylate kinase (*adk*)	71	sll1815 gi|6647539	-1.08	-1.13
172	16.6 kDa small heat shock protein, molecular chaperone (*hspA, hsp17*)	118	sll1514 gi|16329588	1.58	1.85
173	PSII reaction centre 13 kDa protein (*psb28, psbW, psb13, ycf79*)	58 [a]	sll1398 gi|16329210	1.54	1.3

Table 4.4. continued.

Spot No.	Protein I.D. (gene)	MOWSE score	ORF/ Accession No. [c]	Protein Difference	
				Δhik34/W.T. 30°C	*Δhik34*/W.T. 42°C
175	10 kDa chaperone (*groES*)	136	slr2075 gi|1461732	1.97	1.57

Changes in protein abundance are represented as a fold change and negative values indicate a decreased abundance, for example a value of -1.33 indicates this protein decreases in abundance from steady stage levels by 1.33 fold or by 33%.

[a] MOWSE scores just bellow the significant threshold (64).

[b] Average data calculated with one missing replicate from the corresponding experiment.

Average data in black is above the 95 % statistical threshold (data was rounded up, i.e. including and above 94.5 %), blue indicates borderline statistical data (between 94.4 – 92.5 %), red indicates statistically invalid data (bellow 92.5 %).

[c] Accession no. is that for the NCBI database.

Figure 4.20. Identification of manganese stabilising polypeptide via MS-MS.

Doubly charged (**A**) and a triply charged (**B**) peptide ions with respective masses of 1240.69 amu and 2128.06 amu were selected for further fragmentation from the tryptic digest of spots 143-145 (Table 4.3) using an ESI Q-TOF MS instrument. Fragmentation spectra and the corresponding sequence obtained are shown for both peptides ions. The sequence coverage achieved for the manganese stabilising polypeptide is also shown (**C**) MOWSE score = 92.

A

GIFYGRVDTDV

B

GLYTGYDNAVALPSAADKFR
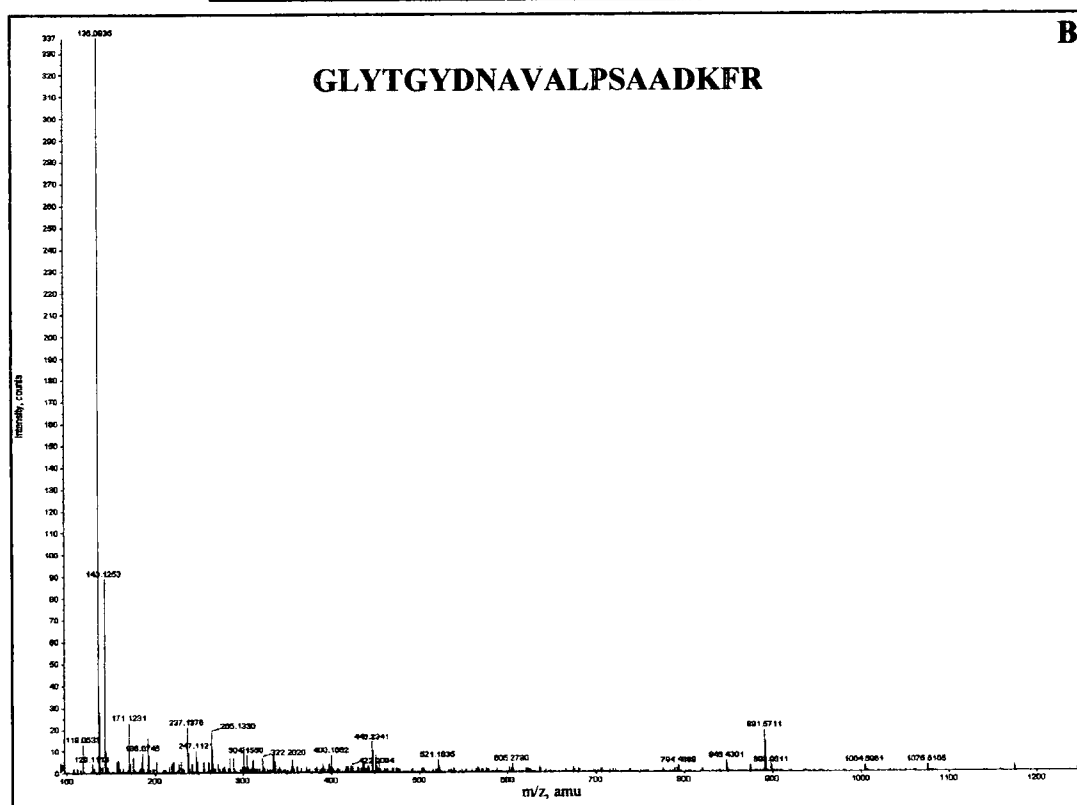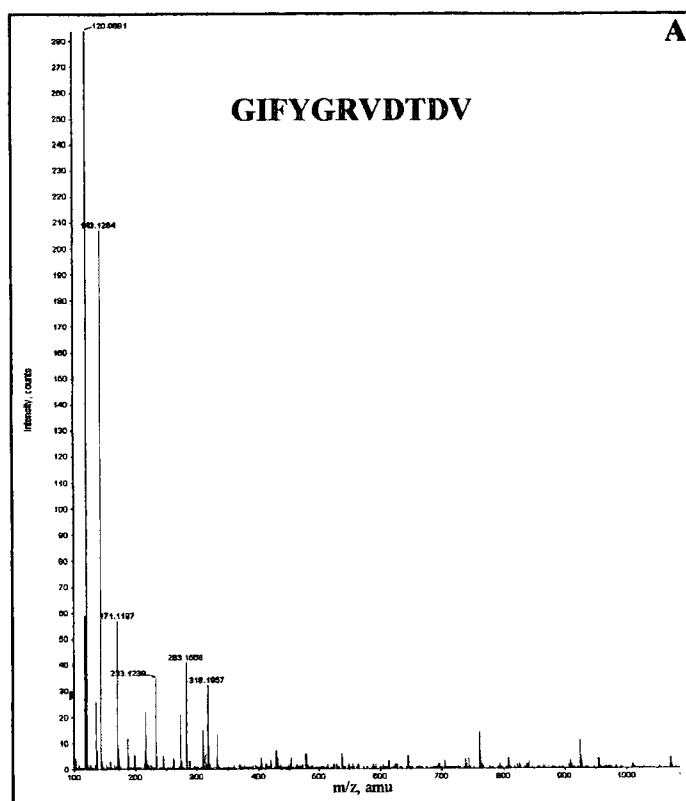
C Manganese stabilising polypeptide sequence

MRFRPSIVALLSVCFGLLTFLYSGSAFAVDKSQLTYDDIVNTGLANVCPEISSFTRGTIE
VEPNTKYFVSDFCMEPQEYFVKEEPVNKRQKAEYVKGKVLTRQTTSLEQIRGSIAVGADG
TLTFKEKDGIDFQPITVLLPGGEEVPFFFTVKNFTGTTEPGFTSINSSTDFVGDFNVPSY
RGAGFLDPKAR**GLYTGYDNAVALPSAADKFR**TNKKETPLGKGTLSLQVTQVDGSTGEIAG
IFESEQPSDTDLGAKEPLDVKVR**GIFYGRVDTDV**

- 291 -

4.2.11 A dramatic increase in environmental temperature results in elevated expression of classical heat shock proteins.

As expected a variety of molecular chaperones have been identified as increasing in abundance from steady state levels in cells exposed to heat shock, including HspA (16.6 kDa sHSP), both GroEL proteins (Hsp60-1 and -2), GroES (Hsp10), ClpB (Hsp100), DnaK-2 (Hsp70) and HtpG (Hsp90). Furthermore, these 7 proteins display the greatest increase in abundance of all heat shock inducible proteins, with HspA having the highest increase of over 19 fold (spot 172, Table 4.3).

The two GroEL proteins have been previously shown in *Synechocystis* to be equally abundant under normal growth at 30°C, however upon exposure to heat shock at 42°C the level of GroEL-1 was greater then that of GroEL-2 (Glatz *et al.*, 1997; Kovács *et al.*, 2001), demonstrating the difference in heat induciblility of the two operons. This also indicates a different expression mechanism, as previously suggested by Lehel *et al* (1993b). This observation has been supported here, where the highest fold change in abundance for GroEL-1 and GroEL-2 protein spots when transferred from 30°C to 42°C were 5.25 (spot 41, Table 4.3) and 4.00 (spot 43, Table 4.3), respectively. Other investigations in cyanobacteria have shown that both GroEL proteins will associate with the thylakoid membrane upon exposure to heat shock (Kovács *et al.*, 1994; Horváth *et al.*, 1998) and that both weak and strong association have be demonstrated via phase-partitioning (Kovács *et al.*, 1994). This indicates that the GroEL proteins may play an important role in stabilisation of the thylakoid membrane upon exposure to heat and may be involved in the refolding of denatured membrane associated proteins. My proteomic investigation also revealed that GroEL-1 and GroEL-2

proteins were represented by more than one protein spot with different p*I*'s and molecular weights (Figure 4.21). Further analysis needs to be performed to investigate the structural differences between these species, although the lower molecular weight proteins were probably truncated forms of the full length proteins and it was the hope that analysis of the PMF sequence coverage would support this. However, because only a few peptides are required to positively identify a protein and due to low sequence coverage attained for the GroE-1 and GroEL-2 proteins this was impossible to confirm. The significance of these proteins is not obvious and the presence of more than one translation initiation site has not been reported for these *groEL* gene transcripts. Of course, these additional low molecular weight proteins may be a result of proteolysis, but whether this has occurred as a response to the elevated temperature or is due to sample handling has still to be determined. However, the latter is less likely due to the use of EDTA in the cell lysis/protein extraction buffer and the maintenance of samples on ice while handling, both function to reduce protease activity. Also, the lysis buffered used to solubilise protein samples fully denatures proteins and thus any protease activity is removed. Perhaps further experimentation would have been desirable to determine whether protease activity was responsible for these additional protein forms, and if it was an actual biological response rather than protease activity post-cell lysis. Such experiments could include the use of protease inhibitor cocktails during cell lysis and sub-cellular fractionation, and the implementation of *in vitro* protease enzyme activity assays of cell lysates from both control and heat shocked material. More recently, bioluminescence imaging based assays have been developed for the evaluation of protease activity *in vivo* (unpublished work www.biophotonics.ucdavis.edu/events/retreat04/Shindes.ppt), and determine if protease activity is an actual biological event.
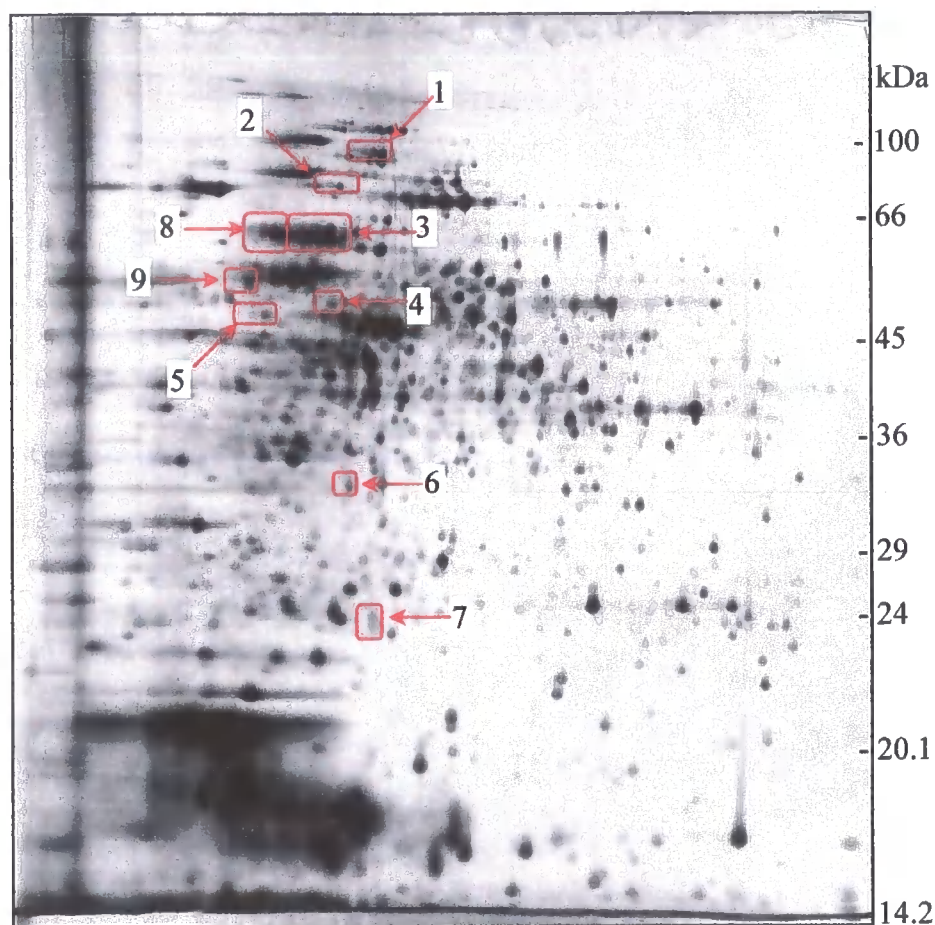
No.	No. of spots	Protein	MW (Da) [a]	Theoretical MW (Da) [b]	Ave. change [c]	Full length/ Truncated
1	3	ClpB	94606.1	98123.0	2.46	FL
2	2		79355.3		2.00	T
3	4		65243.0		4.94	FL
4	1		47298.8		1.95	T
5	2	GroEL-1	46011.8	57652.9	1.6	T
6	1		29588.5		1.42	T
7	1		24139.6		1.96	T
8	2	GroEL-2	65243.0	57774.6	3.66	FL
9	2		50895.1		2.41	T

Figure 4.21. 2D gel localisation and physical properties of full length and truncated forms of major chaperonins in *Synechocystis* seen to display an increased abundance following exposure of cells to heat shock.

[a] Molecular weights calculated from the relative mobility of proteins with known molecular mass.
[b] Theoretical MW obtained from PEDANT database (http://pedant.gsf.de) (Frishman *et al.*, 2001, 2003).
[c] Average change in abundance following transfer of cells from normal growth at 30°C to heat shock at 42°C (see Table 4.3).

In *Synechococcus* sp. PCC 7942 the mRNA levels of the *htpG* gene have been shown to increase over 20 fold when shifting the growth temperature from 30-45°C (Tanaka and Nakamoto *et al.*, 1999). In this investigation protein levels increase as much as 2.76 fold (spot 20, Table 4.3) and 2.42 fold (spot 18, Table 4.3) in the 34-44 °C and 30-42°C temperature regimes, thus supporting the observation that *htpG* expression is elevated upon exposure to heat shock. The difference in the levels of mRNA and protein are obvious and expected. Not only are the temperature regimes slightly different, but these are also different cyanobacterial species. Furthermore, mRNA and protein levels from the same cell sample have been repeatedly shown to have very poor correlation (Gygi *et al.*, 1999b). The fact that they are both elevated under heat shock is good evidence that the expression of this gene is elevated under these conditions and is required for survival. Further analysis of the *htpG* gene in cyanobacteria demonstrated that a mutation did not effect growth at 30°C or 40°C, but at 45°C the mutant was unable to grow, indicating the importance for HtpG in the acquisition of thermotolerance in cyanobacteria (Tanaka and Nakamoto *et al.*, 1999). This is something not previously observed in prokaryotic organisms, where in *B. subtilis* for example *htpG* is not essential for growth at 53°C (Verteeg *et al.*, 1999) and suggests the importance for HtpG in the thermal stress management of photosynthetic organisms.

The prokaryotic Hsp70 homolog DnaK-2 was shown to be elevated in heat stressed cells by 2.99 fold (spot 29, Table 4.3) and 2.45 fold (spot 30, Table 4.3) in the 34-44 °C and 30-42 °C heat regimes investigated, respectively. This is the second *hsp70* gene of three *dnaK* genes in the *Synechocystis* genome and other experimentation indicates that this is the only Hsp70 gene to be transcribed under heat shock

conditions (Varvasovszki *et al.*, 2003). Varvasovszki *et al* also showed that the co-chaperonins of DnaK, DnaJ and GrpE, were also uninduced at the level of transcription in heat shock cells and may explain why these proteins were not seen to increase in abundance in the proteomic investigation reported in this thesis. In *Synechococcus* sp. PCC 7942, gene disruptions in all three *dnaK* genes revealed that *dnak-1* was not essential for normal growth, where as *dnaK-2* and *-3* were (Nimura *et al.*, 2001). However, only the DnaK-2 protein exhibited an increase in abundance following heat shock. DnaK-1 even showed a decrease in abundance. Other analyses revealed the DnaK-3 protein to be associated on the cytosolic side of the thylakoid membrane surface, suggesting this protein may be involved in the correct folding or translocation of thylakoid membrane proteins (Nimura *et al.*, 1996). Together this research demonstrates the different properties and possible cellular functions of the various DnaK proteins in cyanobacteria.

In this proteomic investigation the ClpB (Hsp100) protein was shown to increase in abundance following heat shock, which is consistent with that observed in *Synechococcus* (Eriksson and Clarke, 1996). However, it is evident that two different forms of this protein are present on the 2D gel with molecular weights of approximately 94.6 and 79.4 kDa (Figure 4.21). Both of these forms are heat inducible, where the 94.6 kDa protein increased in abundance as high as 5.77 and 2.57 (spot 10, Table 4.3) in the 34-44 °C and 30-42 °C heat regimes, respectively, and the 79.4 kDa form increased as much as 4.03 and 2.07 (spot 27, Table 4.3) also in the 34-44 °C and 30-42 °C heat regimes, respectively. Analysis of the sequence coverage attained by PMF for these two proteins does show an N-terminal region which is not represented in the fingerprint of ClpB-79.4, which is covered in ClpB-94.6 (Figure

4.22). These results are consistent with previous investigations in *Synechococcus* sp. PCC 7942, where two isoforms of ClpB have also been found in the cytosolic protein fraction, with molecular weights of 93 and 79 kDa (Clarke and Eriksson, 2000). By shifting the growth temperature from 37 to 48.5 °C for 45 minutes the relative level of ClpB-93 and ClpB-79 increased by 6-7 fold and 2-3 fold, respectively. Therefore the ratio of ClpB-93:ClpB-79 abundance under heat shock in *Synechococcus* is approximately 1:3. Clarke and Eriksson also demonstrated that the ClpB-79 protein contributed to one third of the total thermotolerance developed by *Syenchococcus* which is consistent with the quantity of this protein synthesised relative to the ClpB-93 form under heat shock. However; in *Synechocystis* the ratio is approximately 4:5, which may indicate that in this organism the ClpB-79 protein has a greater contribution to thermotolerance than in *Synechococcus*. These two proteins were first identified in *E. coli* (Squires *et al.*, 1991) and actually arise from two separate translation initiation sites in the *clpB* gene transcript, where the ClpB-93 protein is the full length form and the ClpB-79 is the shorter form. There are several other mechanisms in which short versions of full-length polypeptides can be generated by a cell. Once such system is posttranslational proteolysis where terminal parts of a peptide are cut to reveal other functional domains. A good example of this is signal peptides, used in the import of proteins into various cellular compartments and which are removed by protease activity upon protein import. Some peptides targeted to the chloroplast or mitochondria have multiple signal peptides to target them to sub-organellar locations such as the stroma. Another mechanism in eukaryotic organisms which generates short peptide forms is alternative gene splicing. Here different intron combinations are fused together generating in some cases multiple transcripts of

A. ClpB-93

Number of mass values searched: **49**
Number of mass values matched: **30**
Sequence Coverage: **34%**

```
  1 MQPTDPNKFT EKAWEAIAKT PEIAKQHRQQ QIETEHLLSA LLEQNGLATS
 51 IFNKAGASIP RVNDQVNSFI AQQPKLSNPS ESIYLGRSLD KLLDNAEIAK
101 SKYGDDYISI EHLMAAYGQD DRLGKNLYRE IGLTENKLAE IIKQIRGTQK
151 VTDQNPEGKY ESLEKYGRDL TELAREGKLD PVIGRDEEVR RTIQILSRRT
201 KNNPVLIGEP GVGKTAIAEG LAQRIINHDV PESLRDRKLI SLDMGALIAG
251 AKYRGEFEER LKAVLKEVTD SQGQIILFID EIHTVVGAGA TQGAMDAGNL
301 LKPMLARGAL RCIGATTLDE YRKYIEKDAA LERRFQEVLV DEPNVLDTIS
351 ILRGLKERYE VHHGVKIADS ALVAAAMLSN RYISDRFLPD KAIDLVDEAA
401 AKLKMEITSK PEELDEVDRK ILQLEMERLS LQRENDSASK ERLEKLEKEL
451 ADFKEEQSKL NGQWQSEKTV IDQIRTVKET IDQVNLEIQQ AQRDYDYNKA
501 AELQYGKLTD LQRQVEALET QLAEQQTSGK SLLREEVLES DIAEIISKWT
551 GIPISKLVES EKEKLLHLED ELHSRVIGQD EAVTAVAEAI QRSRAGLSDP
601 NRPTASFIFL GPTGVGKTEL AKALAKNLFD TEEALVRIDM SEYMEKHAVS
651 RLMGAPPGYV GYEEGGQLTE AIRRRPYSVI LFDEIEKAHG DVFNVMLQIL
701 DDGRLTDAQG HVVDFKNTII IMTSNLGSQY ILDVAGDDSR YEEMRSRVMD
751 VMRENFRPEF LNRVDETIIF HGLQKSELRS IVQIQIQSLA TRLEEQKLTL
801 KLTDKALDFL AAVGYDPVYG ARPLKRAVQK YLETAIAKGI LRGDYKPGET
851 IVVDETDERL SFTSLRGDLV IV
```

B. ClpB-79

Number of mass values searched: **50**
Number of mass values matched: **24**
Sequence Coverage: **30%**

```
  1 MQPTDPNKFT EKAWEAIAKT PEIAKQHRQQ QIETEHLLSA LLEQNGLATS
 51 IFNKAGASIP RVNDQVNSFI AQQPKLSNPS ESIYLGRSLD KLLDNAEIAK
101 SKYGDDYISI EHLMAAYGQD DRLGKNLYRE IGLTENKLAE IIKQIRGTQK
151 VTDQNPEGKY ESLEKYGRDL TELAREGKLD PVIGRDEEVR RTIQILSRRT
201 KNNPVLIGEP GVGKTAIAEG LAQRIINHDV PESLRDRKLI SLDMGALIAG
251 AKYRGEFEER LKAVLKEVTD SQGQIILFID EIHTVVGAGA TQGAMDAGNL
301 LKPMLARGAL RCIGATTLDE YRKYIEKDAA LERRFQEVLV DEPNVLDTIS
351 ILRGLKERYE VHHGVKIADS ALVAAAMLSN RYISDRFLPD KAIDLVDEAA
401 AKLKMEITSK PEELDEVDRK ILQLEMERLS LQRENDSASK ERLEKLEKEL
451 ADFKEEQSKL NGQWQSEKTV IDQIRTVKET IDQVNLEIQQ AQRDYDYNKA
501 AELQYGKLTD LQRQVEALET QLAEQQTSGK SLLREEVLES DIAEIISKWT
551 GIPISKLVES EKEKLLHLED ELHSRVIGQD EAVTAVAEAI QRSRAGLSDP
601 NRPTASFIFL GPTGVGKTEL AKALAKNLFD TEEALVRIDM SEYMEKHAVS
651 RLMGAPPGYV GYEEGGQLTE AIRRRPYSVI LFDEIEKAHG DVFNVMLQIL
701 DDGRLTDAQG HVVDFKNTII IMTSNLGSQY ILDVAGDDSR YEEMRSRVMD
751 VMRENFRPEF LNRVDETIIF HGLQKSELRS IVQIQIQSLA TRLEEQKLTL
801 KLTDKALDFL AAVGYDPVYG ARPLKRAVQK YLETAIAKGI LRGDYKPGET
851 IVVDETDERL SFTSLRGDLV IV
```

Figure 4.22. Peptide coverage obtained from MALDI-PMF for full length and truncated forms of ClpB.

Amino acid sequence coverage obtained via PMF (**Bold**) of the full length ClpB-93 (**A**) and truncated Clp-79 (**B**) forms of ClpB protein in *Synechocystis*.

varying length. Furthermore, premature termination of translation can generate shorter peptide versions and an example of one such system is rho-dependent termination.

The 16.6 kDa small Hsp, HspA, shows a 19.92 and 21.95 (spot 172, Table 4.3) increase in abundance in the 34-44 °C and 30-42 °C heat shock investigations, respectively. This is the highest increase in abundance for any of the spots detected via 2D-DIGE and therefore this protein may play one of, if not the most important role in the heat shock response and thermal stress management. To support this, the HspA protein was barely detectable at normal growth conditions (both 30 °C and 34 °C), which is unlike both GroEL proteins and the DnaK-2, HtpG and ClpB proteins which are all abundant under normal growth. This indicates that HspA has a specific heat shock-only role and is not required under normal growth. This observation is supported by Roy *et al* (1999) who used *Streptomyces albus* as an experimental system and demonstrated that although large amounts of the sHsp, *hsp18* mRNA were seen under normal growth at 30 °C; the protein was only detectable after exposure of cells to heat shock. HspA has been shown to be unable to refold non-native proteins but instead serves as a reservoir for unfolded protein substrates and subsequently transferring them to the ATP dependent chaperone machines for subsequent refolding (Török *et al.*, 2001). Furthermore, HspA demonstrated an involvement in the stabilisation of the thylakoid membrane under heat shock conditions in both *Synechococcus* and *Synechocystis* cells (Nakamoto *et al.*, 2000; Török *et al.*, 2001). This has been demonstrated through several investigations. Firstly, inactivation of this gene greatly reduced the photosynthetic oxygen evolution in heat stressed cells (Lee *et al.*, 1998, 2000). Secondly, constitutive expression of the HspA protein in *Synechococcus* sp. PCC 7942 resulted in a faster recovery and higher survival rate

when cells were directly shifted from 30°C to a lethal temperature of 50 °C and also greater thermal protection of the photosystem II complex and the light-harvesting phycobilisomes (Nakamoto *et al.*, 2000). Thirdly, HspA demonstrated an ability to increase membrane stability and protect membranes from heat induced decreased physical order (Török *et al.*, 2001), in which the membranes increase in fluidity, become more permeable and proteins are disassociated. This suggests a dual role for HspA in the protection and recovery of thermally stressed cells.

Other proteins expected to display an elevated abundance in response to heat shock are proteases. In this proteomic investigation three were identified and shown to increase from steady state levels in response to heat shock. These being Oligopeptidese A which increased as much as 1.76 fold (spot 24, Table 4.3) and 1.61 fold (spot 23, Table 4.3), the periplasmic protease HboA which increased by 1.24 fold and 1.28 fold (spot 116, Table 4.3) and ClpC the ATPase subunit of the ClpC/ClpP protease which increased by 1.46 fold and 1.38 fold (spot 15, Table 4.3) in the 34-44 °C and 30-42 °C heat shock investigations, respectively. Although no ClpP was found to be up regulated in heat stressed cells, several heat shock responsive proteins discovered from 2D-DIGE analysis were not identified via MS techniques, suggesting ClpP could be responding yet remains to be identified.

4.2.12   Protein constituents of the oxygenic photosynthetic apparatus increase in abundance in response to heat shock.

This proteomic investigation has demonstrated that the photosystem II components, manganese stabilising polypeptide (PsbO) and PsbW, and the photosystem I

component PsaC, increase in abundance following exposure of cells to heat shock. The PsbO protein increases by 1.83 (spot 145, Table 4.3) and 1.72 (spot 143, Table 4.3) in the 34-44 °C and 30-42 °C heat regimes investigated. The PsbW and PsaC proteins increase by 2.17 fold (spot 173, Table 4.3) and 1.33 fold (spot 176, Table 4.3), respectively, in the 30-42 °C heat shock experiment.

The PSII complex and moreover oxygen evolution has been described as being the most heat sensitive component of the photosynthetic machinery (Berry and Bjökman, 1980, Mamedov et al., 1993). High temperatures cause inactivation of the oxygen evolving machinery by disruption of the manganese cluster, the catalytic site for oxygen evolution, and subsequent dissociation of the manganese ions (Nash et al., 1985). However photosynthetic organisms have demonstrated the ability to increase the thermal stability of their photosynthetic machinery (Berry and Bjökman, 1980). Recently in Synechocystis, the manganese stabilising polypeptide (PsbO) located on the thylakoid lumen side of the PSII complex, has been characterised as a protein involved in the maintenance of PSII thermal stability and required for the acclimation to high temperature (Kimura et al., 2002). These investigations have suggested that PsbO is closely associated with the manganese cluster, and prevents dissociation of manganese ions (Shen et al., 1998). Other proteins associated with the manganese cluster have also been characterised and shown to be required for thermal stability and heat acclimation, namely Cyt c_{550} and PsbU (Nishiyama et al., 1994, 1999). However, western blotting analysis of Cyt c_{550} and PsbU protein abundance following exposure of cells to heat has suggested that these proteins are not elevated in abundance under heat shock conditions (Nishiyama et al., 1999). Therefore these proteins may not be involved in the development of increased thermotolerance and other proteins are

responsible. The manganese stabilising polypeptide and the PsbW protein identified are likely candidates for this purpose. Little is known about the PsbW protein itself; however it is reported to contain a single transmembrane domain and insert itself into the thylakoid membrane (Lorkovic *et al.*, 1995) and an investigation using transgenic *Arabidopsis thaliana* displaying low levels of PsbW has suggested its role in the stabilisation of the dimeric PSII supracomplex (Shi *et al.*, 2000).

Much less is known about the effect of heat shock on the stability of PSI than PSII. However, this proteomic investigation has indicated that the PsaC protein may be involved in the stabilisation of this complex. In cyanobacteria, PsaC is associated on the cytosolic side of the thylakoid membrane and contains the penultimate and ultimate redox sites (FA and FB) for the transfer of electrons to ferredoxin (Yu *et al.*, 1997). PsaC is also required for binding of PsaD and PsaE to PSI, which are involved in the binding of ferredoxin to PSI (Yu *et al.*, 1995). Perhaps the biding of ferredoxin to PSI and the subsequent transfer of electrons is particularly susceptible to heat inactivation and therefore requiring protein factors to increase the stability of this association, a function which may be achieved by PsaC.

The α and β subunits of the ATP synthase CF(1) catalytic core complex, located on the cytosolic side of the thylakoid membrane in cyanobacteria, are also elevated in abundance following exposure to heat shock. The α subunit increases in abundance as much as 1.45 fold and 1.59 fold (spot 68, Table 4.3) in the 34-44 °C and 30-40 °C growth temperature regimes, respectively. The β subunit increases as much as 1.25 fold (spot 63, Table 4.3) and 1.34 fold (spot 62, Table 4.3) also in the 34-44 °C and 30-40 °C growth temperature regimes, respectively. The ATP synthase complex

produces ATP in the presence of a proton gradient generated by the flow of electrons form PSII through the b_6f complex and to PSI. The α subunit of this complex has a regulatory function where as the β subunit has a the catalytic function. Perhaps under heat shock conditions these proteins increase the quantity of ATP, demanded by the extra work load of the ATP dependent chaperone machines, i.e. GroEL/GroES and Dnak/DnaJ/GrpE. Or these proteins may fulfil a stabilisation role, like that observed for PsbO. The other subunits of the ATP synthase complex, γ, δ and ϵ, have not been shown to increase in abundance following heat shock. It is likely that because these proteins are directly associated with the thylakoid membrane, and are therefore not present in the soluble fraction, that they are more hydrophobic and consequently do not enter the 2D gel.

4.2.13   Other proteins showing increased abundance following exposure of cells to heat shock.

A global representation of the cellular functions with which the identified proteins displaying a heat induced elevated abundance are involved in is shown in Figure 4.23. The most well represented cellular functions include chaperones and protein folding, translation, amino acid biosynthesis and energy metabolism. Also a number of hypothetical proteins have also been identified. The significance of translation and amino acid biosynthesis indicates the extra requirement for *de novo* protein biosynthesis. Proteins within these groups include 4 elongation factors, 2 ribosomal proteins, 7 different amino-acyl tRNA sythetase enzymes and 10 enzymes associated with amino acid biosynthesis. However, the importance of energy metabolism was surprising and a closer examination revealed that the majority of the proteins involved
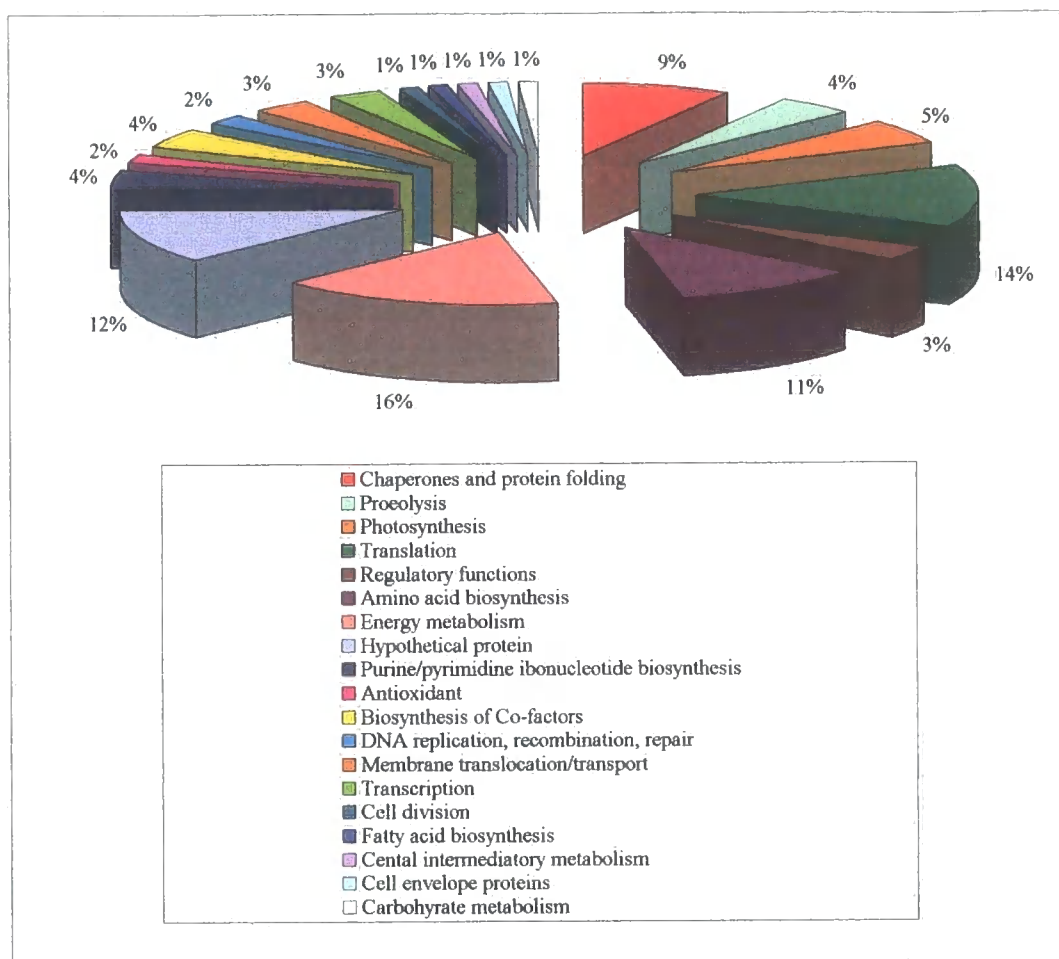
Figure 4.23. Proteins displaying increased abundance in response to heat shock organised by cellular function.

The frequency of representation for each functional category is displayed as a percentage.

in the Calvin cycle were observed to increase in abundance following exposure of cells to heat shock (Figure 4.24). Some of these enzymes are also involved in the pentose phosphate pathway and therefore it may be that it is the pentose phosphate pathway that is elevated under heat shock, however it is known that phosphoribulokinase and sedoheptulose-1,7-bisphosphatase are specific to the Calvin cycle. Unfortunately some of the data obtained for the increased expression of these proteins does not exceed the statistically valid threshold, due to the low number of biological replicates in the 30-42°C heat shock investigation (only 3). However, statistically valid data has been obtained for 6 of these proteins which display an increased level of abundance following heat shock, which is clear cut evidence for the elevation of this system in cyanobacteria under heat shock. To my knowledge there are no other reports which have characterised the increased abundance of Calvin cycle enzymes following heat shock. A possibility for their elevation under heat shock is that these enzymes are not heat stable and therefore newly synthesised protein is required to maintain carbon fixation in heat stress cells.

Other proteins which display a high increase in abundance, above 50 %, include the LexA repressor protein which increases as much as 1.45 fold (spot 157, Table 4.3) and 1.69 fold (spot 158, Table 4.3) and a probable peptidyl prolyl cis-trans isomerase protein which increases as much as 1.59 fold (spot 111, Table 4.3) and 1.61 fold (spot 110, Table 4.3) in the 34-44 °C and 30-42°C heat shock regimes, respectively. In *E. coli* The LexA repressor functions as part of the SOS regulon along with the RecA protein, which incidentally is also shown to be elevated in abundance by 1.18 fold (spot 103) in heat shocked cells. This SOS regulon in *E. coli* functions to repair the effects of stress on DNA denaturisation, in other words it is a DNA repair mechanism
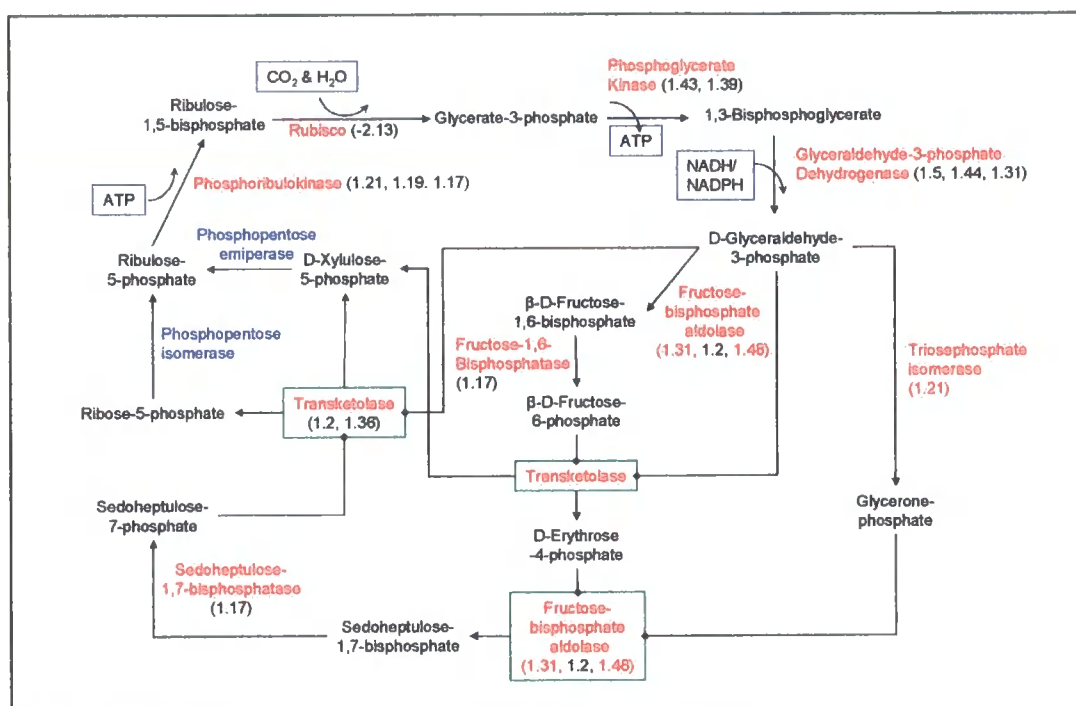
Figure 4.24. Proteins involved in the Calvin cycle which display a heat shock induced change in abundance.

Enzymes which display a change in abundance following heat shock and those which have not been identified as displaying a heat shock induced change are coloured red and blue, respectively. Numbers correspond to the level of change following heat shock; those in red are below the statistical cut off.

(Harmon *et al.*, 1996). However, inactivation of the *lexA* gene in *Synechocystis* sp. PCC 6803 and subsequent analysis of gene expression via DNA microarry has shown that LexA does not operate in a DNA repair mechanism in cyanobacteria, as none of the genes seen to change in abundance are not involved in DNA repair. Instead, the majority of LexA-responsive genes were involved in carbon assimilation or controlled by carbon availability and therefore indicating that LexA is involved in the survival of cells to inorganic carbon starvation (Domain *et al.*, 2004). The LexA-depleted strain was subsequently found to be strongly dependent on the availability of inorganic carbon, supporting this theory (Domain *et al.*, 2004).

Two proteins with reported antioxidant function have also been demonstrated to increase in abundance following exposure of cells to heat shock. These are the water soluble carotenoid protein and the AhpC/TSA family protein or Alkyl hydroperoxide reductase/Thiol specific antioxidant which belong to the peroxiredoxin family of antioxidants. The water soluble carotenoid protein increases as much as 1.48 fold and 1.44 fold (spot 1.37, Table 4.3) in both the 34-44°C and 30-42°C heat shock investigations, respectively. The AhpC/TSA family membrane protein increased 1.3 fold (spot 163, Table 4.3) following transfer of cells form 30°C to 42°C. It is known that photosynthetic organisms generate oxidising molecules under high illumination dude to the excess excitation energy in the chlorophyll protein complexes which exceeds what can be used in photosynthesis (Kerfeld *et al.*, 2003). Excited states of chlorophyll can accumulate and convert to an excited triplet state which can react with oxygen to form singlet oxygen. Singlet oxygen has been demonstrated to destroy the D1 and D2 proteins of the PSII complex through peroxidation reactions (Gotz *et al* 1999); however carotenoids, besides their light harvesting capabilities, have been

demonstrated to de-excite triplet state chlorophyll preventing it from reacting with oxygen (Ort, 2001). Perhaps the generation of reactive oxidising molecules also occurs under heat shock conditions, inducing the expression of the antioxidant genes.

Peptidyl prolyl cis-trans isomerse proteins (PPIases) are chaperone enzymes which alter the peptide bond between a given amino acid and a proline residue, changing it from the cis to the trans conformation and vice versa. This post translational modification can result in dramatic structural modifications which can affect the function of targeted proteins. In addition to this functional activity PPIases have also been reported to have a chaperone activity, for example the *E. coli* trigger factor (TF) was shown to cooperate with the DnaK chaperone machine (Deuerling *et al.*, 1999; Agashe *et al.*, 2004) and in humans the Hsp90 protein was shown to associate with several PPIases (Pirkl and Buchner, 2001). This chaperone function would explain the increased abundance of the cyanobacterial PPIase under heat sock conditions. However, recent studies investigating the eukaryotic Pin1 PPIase have demonstrated that this protein modulates the dephosphorylation of some proteins by allowing trans-specific phosphatases to recognize their target Serine/Threonine-Proline motifs after isomerisation (Smet *et al.*, 2004). This unexpected role might allow regulation of protein activity via peptidyl-prolyl isomerase activity. Perhaps this protein is involved in the dephosphorylation of Hik34 under heat shock conditions leading to the de-repression of *hsp* gene transcription.

Two regulatory proteins, Rre13 and Rre26 have also shown an elevated abundance following heat shock. Rre13 increased by 1.25 fold and 1.18 fold (spot 147, Table 4.3) and Rre26 increased by 1.18 fold and 1.24 fold (spot 165, Table 4.3) in the 34-44

°C 30-42 °C heat shock investigations, respectively. No function of Rre13 has yet been reported although a knockout *rre13* mutant *Synechocystis* strain has been deposited in the Cyanobase database (http://www.kazusa.or.jp/cyano/cyano.html). Rre26 is an OmpR-type DNA-binding response regulator and has been shown to be involved in the regulation of the coupling of phycobilisomes to the photosystem reaction centres (Ashby and Mullineaux, 1999). Reduction in the copy number of this protein in *Synechocystis* sp. PCC 6803 displays a decreased efficiency of energy transfer from the phycobilsiomes to PSII (Ashby and Mullineaux, 1999). Because phycobilisome composition is known to change in response to elevated temperature (MacColl, 1998), this protein may be involved in transcription of genes whose protein products help adapt and stabilise the phycobilisome complex to elevated temperature.

Finally, the SecA protein also increases in abundance following heat shock. SecA protein increases as much as 1.33 fold and 1.34 fold (spot 1, Table 4.3) in the 34-44°C and 30-42°C temperature regimes, respectively. This protein is involved in the translocation of proteins across the cytoplasmic and thylakoid membranes (Nakai *et al.*, 1994), very similar to the Sec61 protein machine in eukaryotic endoplasmic reticulum. Because, thylakoid lumenal proteins such as PsbO have been shown to increase in abundance following heat shock, it would fit that an increased quantity of membrane translocation machinery is required for the insertion of this protein.

4.2.14   Proteins decreased in abundance in response to heat shock

The majority of proteins characterised in this investigation were those which displayed an increase in abundance following exposure to heat. Although less proteins

displaying a decreased abundance were discovered in the 2D DIGE investigation only a small fraction were actually identified via PMF. The reason for this was because, the majority of proteins which decreased in abundance were low abundant on the 2D gel and consequently insufficient material was available for MS analysis. This reflects the general response of the cell to heat shock, in which the expression of high abundant house keeping proteins required for the normal up keep of the cell are elevated and non essential proteins are suppressed. In short, the cell chooses to expresses only the essential proteins which will help it survive.

While the majority of the enzymes involved in carbon fixation are elevated in abundance following heat shock, the Rubisco large subunit decreases more than 2 fold in abundance (spot 59, Table 4.3). The significance of this observation can only be speculated and there are several possible reasons for this. Firstly, the Rubisco large subunit is a very abundant protein in the cell and its synthesis is a drain on the internal amino acid pool. Consequently, because under heat shock conditions cells synthesise several new proteins the synthesis of Rubisco is reduced to allow for this. Secondly, Rubisco is known to be present in the cell in active and inactive forms and an enzyme Rubisco activase functions maintain Rubisco in its active form. Investigations have shown that elevated temperatures decrease the activation state of Rubisco caused by a reduced ability of Rubisco activase at maintaining Rubisco catalytically competent (Eckardt *et al.*, 1997; Salvucci and Crafts-Brandner *et al.*, 2004). Perhaps, the inability of Rubisco activiase to maintain Rubisco in its active form under heat shock, promotes the degradation of Rubisco via proteolytic pathways and thus the reduced abundance of Rubisco in heat stressed cells.

Another protein seen to decrease in abundance following exposure of *Synechocystis* cells to heat shock is the carbon concentrating mechanism protein (CcmM). This protein decreases by -1.53 fold (spot 86, Table 4.3) and is involved in the concentration of inorganic carbon in the carboxysome for subsequent use by Rubisco (Ghoshal and Goyal, 2001). This observation presents another possible reason for the reduced abundance of Rubisco in heat shocked cells. Rubisco activity is known to be regulated by the availability of CO_2, therefore if the reduced abundance of CcmM in the cell results in the reduced availability of CO_2, perhaps Rubisco is reduced because the cell does not require as much. Also, the possibility of reduced carbon availability in heat shock cells as a result of reduced inorganic carbon concentration is supported by the observation that the LexA protein, previously seen to be elevated in abundance in carbon starved cyanobacterial cells (Domain *et al.*, 2004), is also elevated in heat shock cells.

The phycobilisome rod linker polypeptide CpcG1 (spot 151, Table 4.3) is also reduced in abundance in cells exposed to heat shock. This protein is involved in the construction of the phycocyanin billiprotein containing light harvesting rods. Unlike the core membrane linker the rod linker proteins do not possess billins and are therefore not fluorescent, indicating the detected change in abundance is a real response to heat shock. This result is also consistent with the analysis of *de novo* synthesised proteins under heat shock where phycobilisome synthesis was observed to be reduced (section 4.2.4). Phycobilisome rod length has been shown to reduce under a variety of environmental stresses (MacColl, 1998), it is probable this also occurs under heat shock.

4.2.15   The role of Hik34 in the response to heat shock and the regulation of
hsp **gene expression.**

The levels of heat induction/suppression for all heat shock responsive proteins in wild

type and *Δhik34* cells is shown in Table 4.3. This comparison was only performed for

the 30-42°C growth temperature regime. Upon analysis of the data it was apparent

that in *Δhik34* cells, proteins could display either increased or decreased heat

inducibility in comparison to that observed in wild type cells. For example, ClpB-93

(full length form), ClpC, oligopeptidase A, ClpB-79 (truncated form) and HspA all

displayed a higher level of heat inducibily in *Δhik34* cells than in wild type cells.

However, HtpG, DnaK-2, GroEL-1 (native form), GroEL -2, ATP synthase α and β

subunits, PsbO, 50S ribosomal protein L6, water-soluble carotenoid protein, PsbW,

GroES and PsaC all demonstrated a decrease in the level of heat inducibility. This

indicates that Hik34 may be involved in the positive expression of the latter group of

proteins under heat shock conditions, but not for the induced expression of ClpB,

ClpC, oligopeptidase A and HspA proteins. HspA is of particular interest because

under heat shock conditions this protein is elevated over 19 fold (spot 172, Table 4.3)

in both wild type and *Δhik34* cells, however, the *hik34* mutation only results in an

increase in abundance of 1.58 fold and 1.85 fold under normal and heat shock

conditions, respectively (Table 4.4). This indicates that expression of this protein is

not greatly repressed by Hik34 which is different to that observed for other Hsp which

show a nearer equal level of expression following heat shock as with that as a result of

the *hik34* mutation. This also shows that transcription or translation or both is not high

under normal growth conditions, however upon exposure to heat shock cells rapidly

synthesis this proteins. Comparison of the mRNA and protein levels will determine whether the level of regulation is either at transcription or translation.

The comparison of the levels of protein in wild type and *Δhik34* cells grown under both normal (30 °C) and heat shock conditions (42 °C) is shown is Table 4.4. Proteins which show an elevated level under both normal and heat shock conditions in *Δhik34* cells in comparison to that in wild type cells include ClpB-93, HtpG, oligopeptidase A, ClpB-79, DnaK-2, GroEL-2, GroEL-1, ATPase β subunit, water-soluble carotenoid protein, 50S ribosomal protein L6, HspA, PsbW and GroES. This indicates that Hik34 functions as a suppressor of these heat inducible proteins under normal growth conditions. Furthermore, for all these proteins except ClpB, ClpC oligopeptidase A and HspA, Hik34 functions to both suppress their expression under normal growth but also increase their expression under heat shock, as the level of their heat inducibility is reduced in *Δhik34* cells when compared to that in wild type cells (see Table 4.3). The later role may not be a direct function of Hik34, but instead acts through a mechanism in which deactivation of Hik34 upon exposure to heat shock results in the activation of a positive regulator of Hsp expression factor which in turn elevates the expression of the heat shock proteins. Evidence for the presence of a positive regulator is supported through the observation that for all heat shock inducible proteins mentioned, although the loss of Hik34 results in an increase in abundance, the levels of proteins increase further upon exposure of the *Δhik34* cells to heat shock. This indicates that the positive regulator of Hsp expression may be able to act without activation from Hik34 but the activation is faster through this mechanism, or that a second positive regulator is present totally independent of Hik34.

The 50S ribosomal protein L6 (spots 166-167, Table 4.3) and the water-soluble carotenoid protein (spots 136-137, Table 4.3) characterised with in this group of heat inducible proteins are of particular interest. These two proteins although they do show an increase in abundance in response to heat shock, this increase is rather minimal compared to other heat shock responsive proteins. However, their expression is greatly elevated in the *Δhik34* cells grown under normal conditions (Table 4.4), higher than that seen for the elevation under heat shock. This indicates that these proteins are heavily suppressed by Hik34 under normal growth, the opposite to that seen for HspA.

Some of the Calvin cycle proteins appear to be down regulated as a result of the *hik34* gene mutation. Unfortunately some of this data for these proteins is not above the statistically valid threshold; due to the low number of replicates in the 30-42 °C heat shock investigation. However, this does provide an indication that the expression of these proteins may be under the control of Hik34. Only further analysis and an increase of the number of biological replicates will clarify this.

4.3. Discussion

4.3.1 Analysis of the heat shock response - selection of a 1 hour time window and using pH 4-7 2D gels.

Selection of a time window in which to study the heat shock response was an important consideration. Firstly, because transcription, translation and protein translocation all take time and secondly, because responses are not sustained at the same level the entire time a stimulus is present. The latter was previously shown for the heat shock response in *Synechococcus* sp. PCC 6301 (Borbély *et al.*, 1985) and the salt shock response in *Synechocystis* sp. PCC 6803 (Hagemann *et al.*, 1991) where different shock induced protein bands had different rates of synthesis. Consequently it was important to select a time window which would allow the study of the majority of heat induced proteins and also the highest level possible of their heat shock induced response. Radiolabelling and subsequent analysis via SDS-PAGE of the relative amounts of radioactivity incorporated into specific heat shock induced protein bands over time revealed that heat shock for 1 hour provided a global representation of the heart shock induced proteins with the majority of proteins at their highest rate of synthesis. Furthermore, analysis via 2D-E demonstrated that all the 1 hour heat induced proteins were present within the pH gradient 4-7. This pH range was therefore adopted throughout the entire heat shock investigation and although narrower pH gradients would have provided greater resolution, as shown in chapter 3, some of the heat shock inducible proteins would have been lost from the analysis.

4.3.2   2D DIGE – analysis of multiple repeat experiments

2D DIGE has been successfully employed in this investigation to allow the analysis of repeat heat shock experiments. The ability to co-resolve two separate samples in the same 2D gel and the integration of an internal standard through which all spots are quantified has enabled the discovery of statistically valid changes in protein abundance. Without this system very few statistically valid changes would have been identified due to the large amount of system variation incorporated when each protein sample is analysed on a separate 2D gel. As demonstrated by the SYPRO Ruby analysis of the heat shock response. However, the intrinsic fluorescence of certain proteins in cyanobacteria has prevented DIGE analysis of these proteins due to the possibility of increased fluoresce signal and thus incorrect abundance quantification.

4.3.3   The heat shock response

The heat shock response has been characterised in all organisms by the induction of the Hsps, predominantly molecular chaperones and proteases, for the stabilisation, re-folding and removal of heat denatured proteins. This analysis has clearly demonstrated that this same response occurs in *Synechocystis* where the proteins which show the highest level of heat induction are a variety of molecular chaperones and proteases. Some of these molecular chaperones, i.e. GroEL and HspA, have been previously reported to have a possible dual function in cells under heat shock conditions, providing stabilisation and refolding of both soluble and membrane bound proteins (Kovács *et al.*, 1994; Nakamoto *et al.*, 2000). Other proteins which increase in abundance in response to heat shock and function to protect against protein

denaturation include a peptidyl prolyl cis-trans isomerse which has been reported to have a protein refolding function (Deuerling *et al.*, 1999; Agashe *et al.*, 2004) and two antioxidants which function to remove reactive oxidative species (Kerfeld *et al.*, 2003).

In addition to the classical Hsps, proteins from a variety of other cellular processes have been identified in this investigation as being involved in the cyanobacterial heat shock response. These include several proteins of the photosynthetic machinery such as the manganese stabilising polypeptide, previously shown to be involved in the thermal stability of the oxygen evolving machinery of PSII (Kimura *et al.*, 2002), but not previously shown to increase in abundance following heat shock. This supports current research indicating its role in the acquisition of thermal tolerance of PSII in cyanobacteria (Kimura *et al.*, 2002). The PsbW protein of the PSII complex and PsaC protein of the PSI complex have also been shown to be involved in the heat shock response. To my knowledge this is the fist time these proteins have been associated with such a response in cyanobacteria and suggests a role in the thermal stabilisation of their respective complexes. The light harvesting phycobilisome proteins were observed to decrease in the level of *de novo* synthesis under heat shock conditions as were some of the linker components. This suggests a rearrangement of the light harvesting complex under heat shock similar to that observed under high light (MacColl, 1998) and was supported by the observation that a DNA-binding response regulator (Rre26), involved in the regulation of the coupling of phycobilisomes to the photosystem reaction centres (Ashby and Mullineaux, 1999), was seen to be elevated in heat shocked cells. Other cellular process shown to be represented by proteins involved in the heat shock response include carbon fixation, although the exact role of

this is unknown, and transcription, translation and amino acid biosynthesis, probably required for the increased rate of Hsp synthesis. Also, a change in abundance was observed for the large Rubisco subunit (decrease), CcmM (decrease) and LexA protein (increase) and these responses may be linked through the availability of CO_2.

Recently, DNA microarray analysis of the genes induced by exposure to high light was performed (Hihara *et al.*, 2001). Comparison of the high light induced changes with those identified in this proteomic analysis of the heat shock response has revealed that several of the induced genes/proteins are the same in both stresses. For example the α and β ATP synthase genes, the *clpB*, *htpG*, *dnaK-2*, *GroEL-1*, *GroEL-2* and *hspA* genes and the elongation factor TS gene are all induced, and the phycocyanin and allophycocyanin genes are repressed. Also, analysis of light induced proteins revealed that the Glyceraldehyde 3-phosphate dehydrogenase, Fructose 1,6-bisphosphatase aldolase, manganese stabilising polypeptide and the alkyl hydroperoxide reductase/thiol specific antioxidant were also shown to increase in abundance (Choi *et al.*, 2000) . Furthermore, in the proteomic investigation reported in this thesis a protein characterised as being light-repressed was shown to decrease in abundance following heat shock (spot 155, Table 4.3). These observations may indicate that some of the regulatory mechanisms which control gene expression under high light and heat shock conditions are the same and that the cell possibly perceives the heat shock and high light stresses as similar.

4.3.4   Hik34 – possible regulation of the heat shock response

At physiological temperature, the *Δhik34* mutant *Synechocystis* strain displayed increased abundance of all the chaperones and other heat shock induced proteins including oligopeptidase A, ATPase β subunit, water-soluble carotenoid protein, 50S ribosomal protein L6 and PsbW. This observation may explain the increased thermal tolerance of the *Δhik34* strain (unpublished data Iwane Suzuki, NIBB, Okasaki, Japan - personal communication) and indicates that the *Δhik34* mutation causes derepression of the *hsp* genes. Therefore, Hik34 functions to repress the expression of the *hsp* genes under normal growth similar to the function of HrcA in *B. subtilis* (Mogk *et al.*, 1997) and *Streptomyces* sp. (Servant and Mazodier, 2001). However, Hik34 may also function to activate the expression of certain genes under heat shock conditions as a reduced level of heat shock induced abundance was seen for several of the chaperones.

Comparison of the proteins which respond to heat shock with those under other environmental stresses demonstrates that similar genes are expressed under different environmental conditions. For example, DNA microarry analysis of cyanobacterial acclimation to high light (Hihara *et al.*, 2001) and the response to salt shock (Kanesaki *et al.*, 2002) demonstrated that these stresses, like heat shock, induced the expression of the molecular chaperones in *Synechocystis*. Furthermore, the *Δhik34* mutant *Synechocystis* strain was shown to display a reduced level of heat shock gene expression under salt shock conditions (Marin *et al.*, 2003). This result supports the observations for chaperonin expression under heat shock and suggests that Hik34 is a generic sensory histidine kinase involved in the regulation of *hsp* gene expression.

The *hsp* genes are some of the most conserved genes in nature yet the mechanism of their induction between organisms is very different even across prokaryotes. In *E. coli* σ-factors positively control the expression of *hsp* genes, where as in *B. subtilis* and *Streptomyces* sp. *hsp* expression is controlled through suppressors of gene transcription such HrcA (Mogk *et al.*, 1997; Servant and Mazodier, 2001). In *Synechocystis* the histidine kinase Hik34 appears to play a role in expression of *hsp* expression. A HrcA homology has also been identified and *Synechocystis* and its deletion demonstrated elevated expression of *hsp* genes (Nakamoto *et al.*, 2002). The difference in regulatory mechanisms but high conservation of *hsp* genes between prokaryotes suggests the *hsp* genes were establishment in the bacterial progenitor but the development of gene expression systems was post phylogentic divergence.

Finally, Hik34 appears to be involved in the positive expression of the hemolysin-like protein (HLP) in *Synechocystis*, as observed by the loss of this protein from the soluble protein fraction. However, HLP has not been identified as a protein involved in the heat shock response and therefore, Hik34 may be involved in the regulation of other genes. This is supported by the observations for the ribosomal L6 protein which is only slightly elevated under heat shock conditions yet is greatly elevated in abundance in *Δhik34* cells grown under normal conditions. This also supports the prediction that Hik34 functions as both a positive and negative regulator of gene expression.

4.3.5   Concluding Remarks

The data generated in this chapter has provided a comprehensive view of the heat shock response in cyanobacteria and offered evidence for a possible mechanism for the regulation of this response in these organisms. These results are also a platform for future research on the heat shock response in cyanobacteria, where the analysis of enzyme activity and concentration of metabolites could be investigated to test the hypotheses with regard to the elevation of some of the Calvin cycle enzymes and decline of Rubisco under heat shock. Furthermore, mutants can be constructed to identify the roles of the heat shock induced proteins not currently understood and further divulge the mechanism of heat perception and signal transduction, of which Rre13, shown to increase in abundance under heat shock, presents an ideal target.

In collaboration with Prof. Murata's Lab we intend to compare the proteomic data generated in this chapter with the data from DNA microarry analysis of the heat shock response, performed by Iwane Suzuki. It is predicted that although similarities will exist between the two data sets several differences in protein synthesis and gene expression will be detected. This is due to the different regulatory mechanisms at the level of transcription and translation and also the extent of post-translational processing. It is already evident from the 2D gels that there may be extensive PTM of proteins involved in the heat shock response, due to the number of different protein spots with varying pI's and MW's which represent single genes and the difference in their heat inducibility (Figure 4.19 and Table 4.3). The sequence of these individual spots needs to be analysed further via tandem mass spectrometry, to determine the

difference in these various protein forms and thus help deduce their function in the biological system.

CHAPTER 5

Investigating the mechanisms involved in acclimation of the

photosynthetic apparatus to high temperatures in

Synechocystis

5.1 Introduction

Photosynthetic organisms have the ability to acclimatise to high temperatures where their photosynthetic machinery displays an enhanced thermal-stability (Berry and Bjorkman 1980). The enhancement of photosynthetic stability is related to the protection of the PSII oxygen evolving machinery as this protein complex has been shown to be highly susceptible to heat inactivation (Yamashita and Butler, 1968; Santarius, 1975; Thompson *et al.*, 1989; Mamedov *et al.*, 1993).

Several efforts have been made to characterise factors involved in thermal stabilisation of the oxygen evolving complex. The photosynthetic apparatus is situated within the thylakoid membranes and because of this physical association it was hypothesised that the glycerolipids of the thylakoid membrane may contribute to the thermal stability of photosynthesis (Webb and Green 1991). Experimentation has shown that cells exposed to elevated growth temperatures demonstrate an increased level of saturated membrane lipids (Pearcy, 1978; Raison *et al.*, 1982; Thomas *et al.*, 1986) suggesting the involvement of fatty acid saturation in thermal adaptation. However, studies using mutant and transformant *Synechocystis* cells defective in desaturases have demonstrated that thermal stability is not affected by changes in the saturation of membrane lipids (Gombos *et al.*, 1992, 1994; Mamedov *et al.*, 1993; Wada *et al.*, 1994). Such observations have indicated that other factors are involved in the thermal adaptation process of photosynthesis.

It has been suggested that heat shock proteins ClpB, GroEL, HtpG and HspA may be involved in the thermal protection of the PSII complex against high temperature stress

(Lehel *et al.*, 1993a; Eriksson and Clarke, 1996; Heckathorn *et al.*, 1998; Tanaka and Nakamoto, 1999; Török *et al.*, 2001). However, western blot analysis of Hsp abundance in *Clamydomonas reinhardtii* have shown that at moderately high temperatures, where cells display increased thermal stability of oxygen evolution, the levels of Hsp chloroplast homologues Hsp60 Hsp70 and Hsp22 did not increase (Tanaka *et al.*, 2000). To support this data no Hsps have been found in the lumen of the thylakoid membrane, the site of oxygen evolution (Waters, 1995). Therefore it has been postulated that Hsps are not involved in the enhancement of thermal stability of the oxygen evolving machinery. Other factors such as carotenoids (Kerfeld *et al.*, 2003) and isoprene (Sharkey and Singsass, 1995) have also been linked to the mechanism of PSII thermal protection; however, it is unclear whether they are involved in the enhancement of thermal stability of the oxygen evolving machinery.

To elucidate the factors involved in the thermal adaptation process, Nishiyama and co-workers have extracted proteins from purified cyanobacterial membranes using Triton X-100 and analysed the heat stability of the detergent treated membranes by measuring oxygen evolution. Results showed that Triton X-100 treatment markedly reduced the heat stability of the oxygen-evolving apparatus and furthermore heat stability was recovered upon reconstitution of the membranes with the Triton extracted components (Nishiyama *et al.*, 1994). This indicated the involvement of the extracted components in heat stability of oxygen evolving activity. Chromatographic purification of the membrane extracted proteins and biochemical analysis revealed two components involved in thermal stabilisation of the oxygen evolving machinery, these being a low redox potential *c-type* monoheme cytochrome, Cytochrome (Cyt) c_{550} with a Mr of 15 kDa (Nishiyama *et al.*, 1994) and PsbU a 13 kDa protein

(Nishiyama et al., 1997). Furthermore, Nishiyama demonstrated that purified Cyt c_{550} and PsbU were individually able to restore a proportion of the thermal stability of the oxygen evolving machinery, but together they had a greater restorative effect (Nishiyama et al., 1997). Although this evidence suggests the involvement of PsbU and C_{550} in the stabilisation of the oxygen evolving machinery against heat inactivation further analysis has shown that these proteins do not change in abundance or become modified during acclimation to high temperature and are therefore likely constitutively expressed (Nishiyama et al., 1997; 1999). This indicates that these proteins constitutively stabilise the oxygen evolving machinery but do not directly modify the heat stability of the oxygen evolving machinery during acclimation to high temperature. It was subsequently demonstrated using targeted mutagenesis that inactivation of the psbU, Cyt c_{550} (psbV) and another gene, psbO, encoding the manganese stabilising polypeptide in Synechocystis prevented cells increasing the stability of their oxygen evolving machinery during thermal adaptation (Kimura et al., 2002). This observation indicated that although these proteins may not be directly involved in the enhancement of thermal stability, they may be involved in the mechanism, perhaps as a binding site for other, as not yet identified proteins, which them selves function to enhance the thermal stability of the oxygen evolving machinery.

In an attempt to discover these 'other' factors involved in the thermal adaptation process Nishiyama demonstrated that a thylakoid Triton extract from already heat acclimatised cells would promote acquired thermotolerance in non-acclimatised thylakoid membranes (Figure 5.1). This investigation demonstrated that protein factors must be present in the thylakoid extracts from acclimated cells which increase
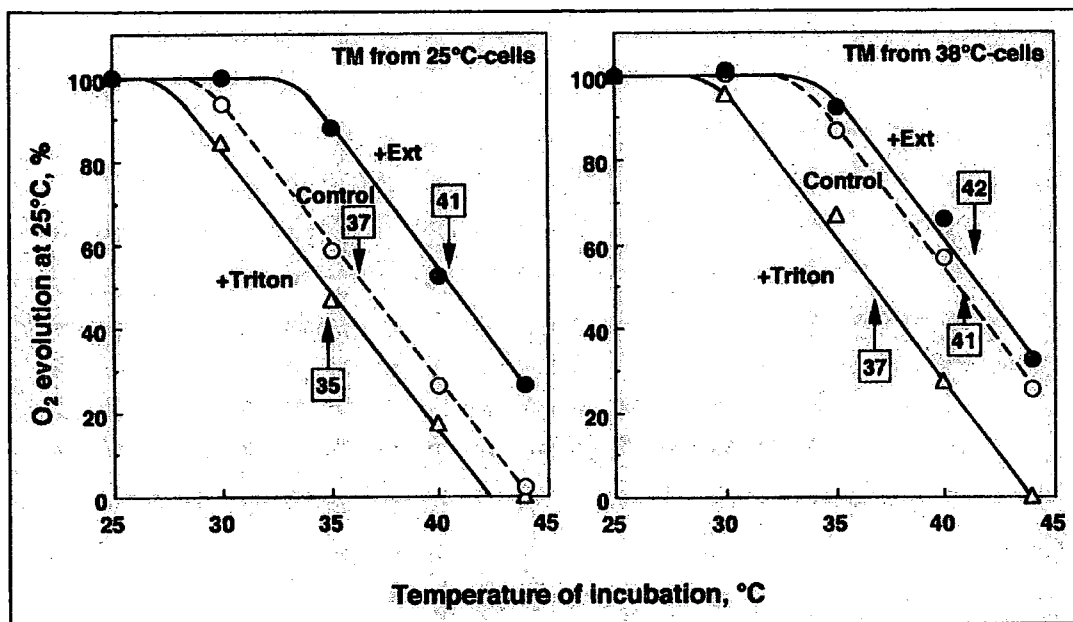
Figure 5.1. Heat inactivation profiles of the oxygen-evolving machinery in Triton X-100 treated thylakoid membranes from *Synechocystis* cells grown under normal conditions (25°C) and exposed to heat acclimation (38°C) for 1 hour.

Thylakoid membranes from cells grown under normal (25°C) and 1 hour heat acclimation (38°C) conditions were treated with 0.1 % Triton X-100 and subsequently both reconstituted with the concentrated Triton X-100 membrane extract from the heat acclimated membranes. ○, Thylakoid membranes with no treatment; Δ, thylakoid membranes after treatment with Triton X-100; ●, Thylakoid membranes reconstituted with the Triton X-100 extract from heat acclimated cells. The numbers within the squares signify temperatures for 50 % inactivation of oxygen evolution. TM = thylakoid membrane. Figure kindly provided by Yoshitaka Nishiyama (Satellite Venture Business Laboratory, Ehime University, Matsuyama, Japan)

the stability of the photosynthetic machinery against heat inactivation. In collaboration with Dr. Nishiyama, using 2-D DIGE technology and MS based protein identification techniques, thylakoid Triton extracts from heat acclimatised cells and non-acclimated cells will be compared in an attempt to discover and identify protein factors responsible for the acquisition of cellular thermotolerance.

5.2   Results

5.2.1   Pre-analysis of *Synechocystis* thylakoid Triton extracts.

Triton extracted membrane proteins from both control and heat acclimated *Synechocystis* cells, prepared by Nishiyama group (Ehime University, Matsuyama, Japan), were generated as previously described (Nishiyama *et al.*, 1994). In order to test the reproducibility of the thermal adaptation response, membrane proteins were extracted from 5 repeat experiments. The reduced thermal stability of the thylakoid membranes and the ability of the Triton extract to restore thermal stability was analysed for each sample by measuring oxygen evolution and through the implementation of a reconstitution assay, by Nishiyama group and as previously described (Nishiyama *et al.*, 1994). This was performed to confirm the successful isolation of components responsible for the thermal stabilisation of the oxygen evolving machinery. These Triton extracts were subsequently acetone precipitated (as described in the materials and method section) and transported to Durham University in absolute acetone and on solid CO_2.

Before proceeding into a comprehensive 2-D DIGE analysis to highlight proteins that may be involved in the thermal acclimation process, the precipitated thylakoid Triton extracts were visualised by SDS-PAGE (Figure 5.2) and mini pH 3-10 2-DE (Figure 5.3). The aim of this experimentation was to identify any obvious differences between normal and heat acclimated samples and to test sample reproducibility and also to determine the solubility of the samples and the IEF pH gradient which would provide the optimum resolution. This was accomplished by first removing any excess
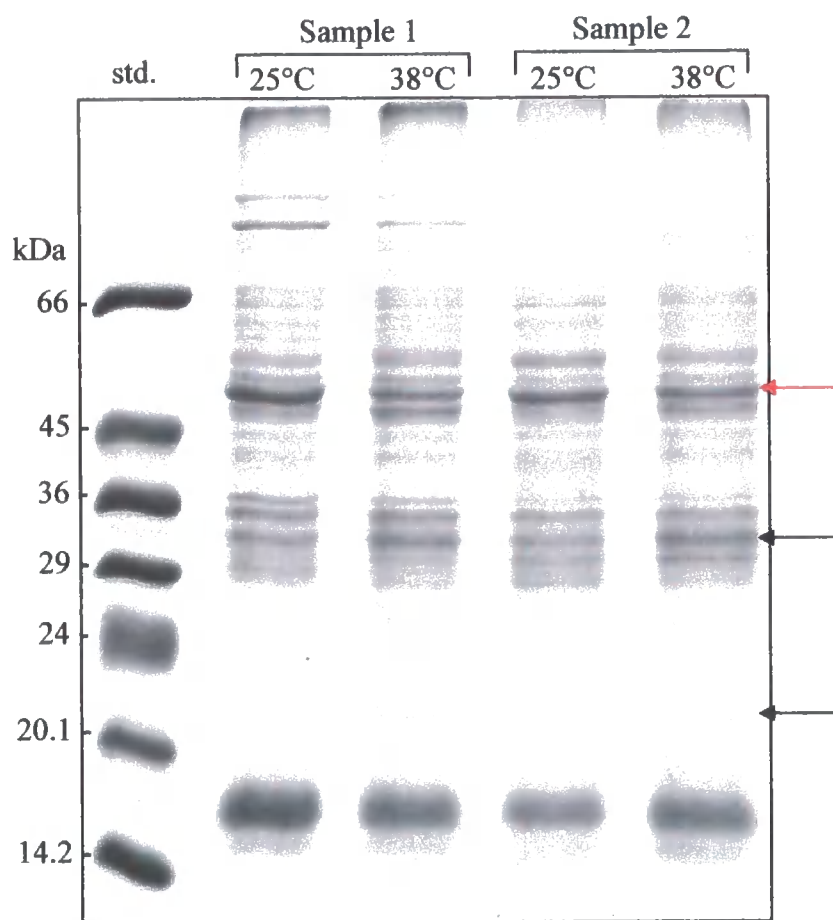
Figure 5.2. SDS-PAGE analysis of Triton X-100 membrane extracts from duplicate *Synechocystis* cell cultures grown under control (25°C) and 1 hour heat acclimation (38°C) conditions.

Aliquots of Triton X-100 membrane extracts containing 10 μg of protein were subjected to SDS-PAGE using 12 % acrylamide resolving gels and the resolved protein bands were stained with Coomassie blue. Black arrows indicate those bands increasing in abundance in response to the elevated temperature; red arrow indicates a protein band decreasing in abundance.
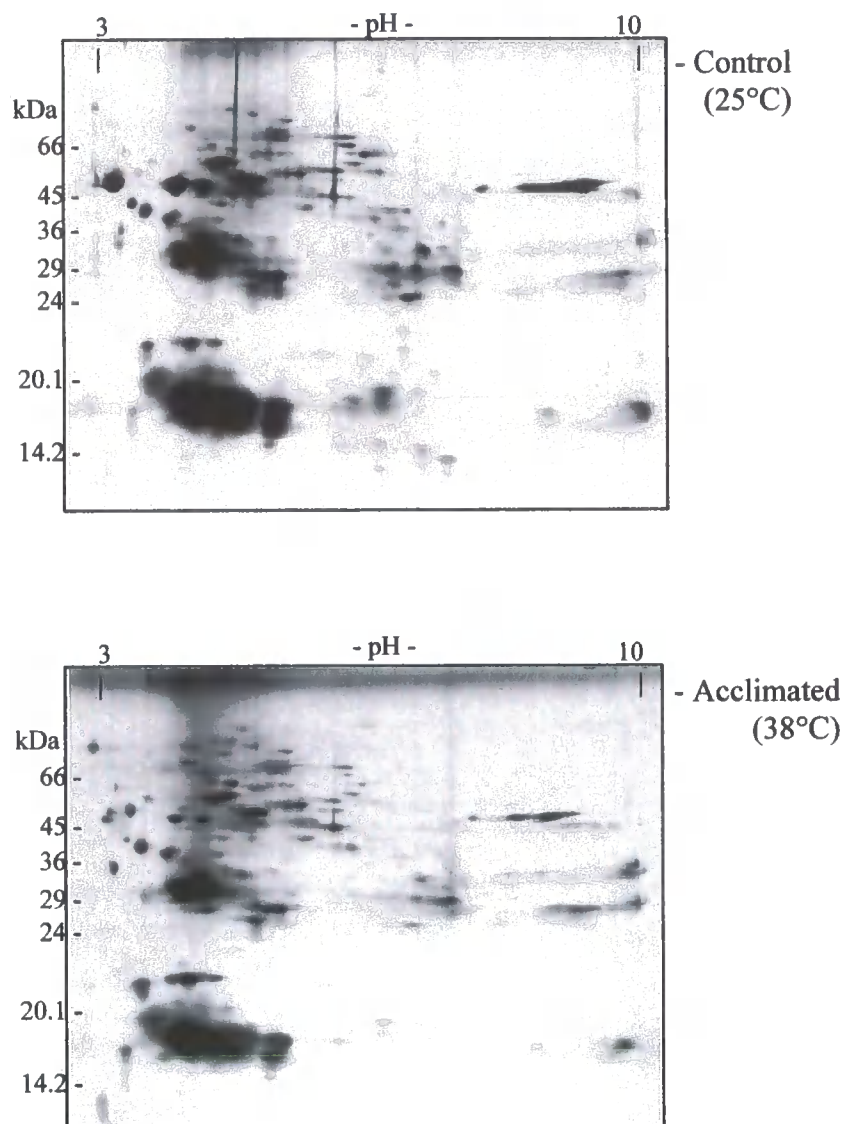
Figure 5.3. Mini pH 3-10 2-DE of Triton X-100 membrane extracts from *Synechocystis* **cells grown under normal (25°C) and 1 hour heat acclimation (38°C) conditions.**

An aliquot of each Triton X-100 membrane extract containing 20 μg of protein was loaded via IGR into separate 7 cm pH 3-10 IPG strips. Proteins were resolved via IEF followed by mini SDS PAGE using 12 % acrylamide resolving gels and the resolved spots were visualised via disruptive silver staining.

acetone from the protein precipitates and then allowing them to air dry before solubilising in lysis buffer and determining their protein concentration via modified Bradford assay. For SDS-PAGE an aliquot containing 10 µg of protein was then removed from each sample and precipitated with 80 % acetone (see materials and method section for procedure) to remove any urea that may interfere with the electrophoresis. Following this, protein precipitates were again allowed to air dry before being re-solubilised in 1 x SDS sample loading buffer, boiled for 2 minutes and loaded onto mini 12 % SDS polyacrylamide gels. Samples were electrophoresed and the resultant protein bands were visualised with Coomassie blue staining. This revealed that there were three membrane protein bands which displayed a distinct change in abundance following heat acclimation of cells (Figure 5.2). All samples were processed in this way and all displayed this same pattern (data not shown).

For mini 2-DE, 20 µg of each lysis buffer solubilised sample was in gel re-hydrated into separate 7 cm pH 3-10 IPG strips (Amersham Biosciences). IPG strips were focused and electrophoresed (as described in the materials and methods) and the resultant gels were stained with silver staining (Figure 5.3). This method of protein spot visualisation was used because sample quantity was minimal and it is the most sensitive technique for protein visualisation. Mini 2-DE revealed that samples were soluble and that several hundred individual membrane associated protein species were adequately resolved. This analysis also showed that like the *Synechocystis* soluble protein sample, although some basic proteins are present in the sample, the majority of proteins focused within the pH range 4-7. Using pH 3-10 IEF strips resulted in inadequate focusing of these acidic proteins and consequently all further analyses on this sample were conducted using pH 4-7 IPG strips.

5.2.2   Two Dimensional Differential In Gel Electrophoresis (2D DIGE) of Triton X_{100} thylakoid membrane extracts from exponential dividing Wt *Synechocystis* cultures grown under normal and 1 hour heat acclimation conditions.

Having established the reproducibility of all 5 control and 5 heat acclimated samples, the next phase of this investigation was to perform 2-D DIGE analysis. Protein samples were prepared for Cy labelling (see materials and methods) before 50 µg of each sample was labelled so that all 5 control samples were Cy3 labelled and all 5 heat shocked samples were Cy5 labelled. Also aliquots containing 12.5 µg of protein from each control and heat acclimated sample were pooled together and labelled with Cy2. All labeling reactions were performed at a protein concentration of 2.5 µg/µl and using 400 pmol of Cy dye per 50 µg of protein (see table 5.1 and material and methods section for details). The success of the Cy-Dye labelling reactions was confirmed by resolution of 2.5 µg of each sample on 12 % mini SDS polyacrylamide gels and visualisation of the labelled protein bands using a Typhoon 9200 variable mode scanner (Amersham Biosciences) (Figure 5.4). This analysis revealed that all samples had been successfully Cy labelled and that they were equally loaded.

Large format pH 4-7, 12 % polyacrylamide 2-D DIGE was performed using the same sample pairing system as was adopted for the heat shock investigation, i.e. the control and treated samples from each heat acclimation experiment were co-resolved in the same 2D gel. Therefore, 12.5 µg of control and heat acclimated samples from the same experiment were mixed together along with 12.5 µg of the pooled standard, generating 5 sample mixes. The remaining Cy labelled samples were stored at -20°C

Sample	[Sample] (μg/μl)	Protein (μg)	Sample Vol. (μl)	Buffer[a] Vol. (μl)	Cy3 (μl)	Cy5 (μl)	Cy2 (μl)	Labelling Vol. (μl)	10 mM Lysine (μl)	Final Vol. (μl)
1 control	6.66	50	7.5	10.5	1			19	1	20
2 control	5.26	50	9.5	8.5	1			19	1	20
3 control	5.05	50	9.9	8.1	1			19	1	20
4 control	5.38	50	9.3	8.7	1			19	1	20
5 control	5.55	50	9.0	9.0	1			19	1	20
1 acclimated	4.90	50	10.2	7.8		1		19	1	20
2 acclimated	6.25	50	8.0	10.0		1		19	1	20
3 acclimated	5.15	50	9.7	9.3		1		19	1	20
4 acclimated	5.88	50	8.5	9.5		1		19	1	20
5 acclimated	5.75	50	8.7	9.3		1		19	1	20
Pool standard*	-	250	45.15	44.85			5	90	5	100

Table 5.1. Standard procedure for Cy minimal Dye labelling of protein samples.
*Pooled standard contains 25 μg of each protein sample.
[a] Labelling buffer: 25 mM Tris-HCl (pH 9.5), 9 M urea, 2 M thiourea, 4 % (w/v) CHAPS.
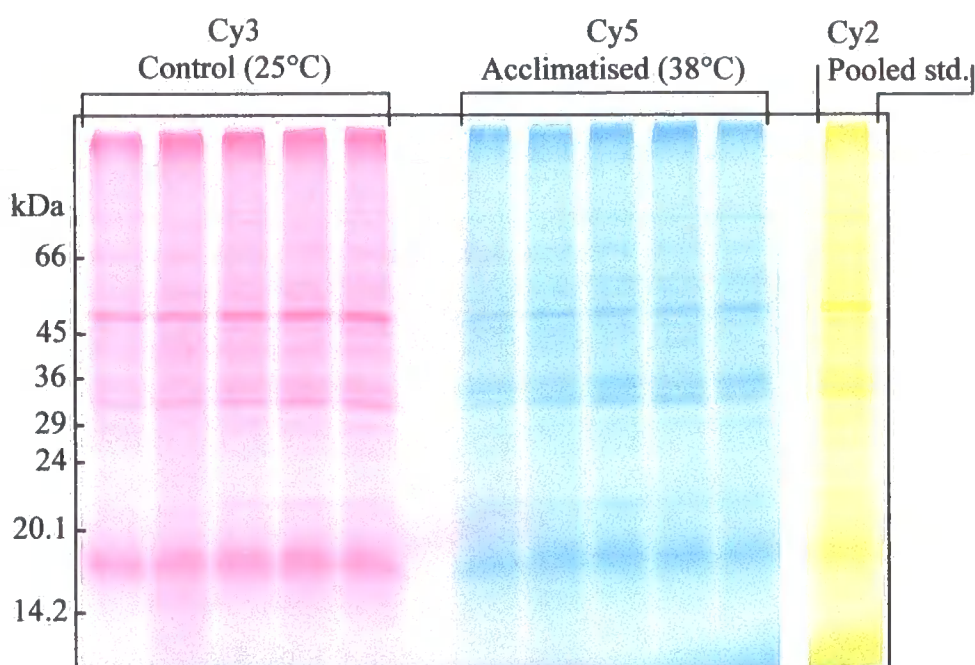
Figure 5.4. Cy labelled Triton X-100 membrane protein extracts from *Synechocystis* cells grown under both normal (25°C) and 1 heat acclimation (38°C) conditions.

A 1 µl aliquot from each Cy labeled sample containing 2.5 µg protein was subjected to SDS-PAGE using 12 % acrylamide resolving gels. Following electrophoresis, labelled bands were visualised using fluorescence imaging and the corresponding Cy-dye excitation and emission parameters.

until required. These 5 sample mixes were anodic cup loaded onto separate pre-hydrated 18 cm pH 4-7 IPG strips and focused using an Ettan™ IPGphor IEF system (Amersham Bioscience) for 70 kVh (see materials and methods section for details). Focused strips were equilibrated before loading onto individual large format SDS 12% polyacrylamide gels (260 x 200 x 1 mm) and cast within Ettan DALT low fluorescence glass cassettes (Amersham Biosciences). Gels were electrophoresed using the discontinuous buffer system of Laemmli (Laemmli, 1970) and an Ettan™ DALT*twelve* Large Format Vertical System (Amersham Biosciences) at 5 W/gel for 30 minutes followed by 17 W/gel until the dye front had reached the bottom. The resultant five replicate DIGE gels were visualised immediately using a Typhoon 9200 variable mode imager (Amersham Biosciences) and the designated excitation and emission parameters for each Cy-Dye (see materials and methods). The three Cy images within each DIGE gel were obtained simultaneously, and thus all three images can be viewed overlaid on top of each other (Figure 5.5). This way of viewing the gels presents some indication of protein spots which increase or decrease in abundance in response to the condition being studied. In Figure 5.4, an overlaid image of one of the five DIGE gels is shown, several green and red spots can be seen which represent proteins showing an increase and decrease in abundance, respectively. However, this must be in no way interpreted as being accurate as variations in protein loadings and scanning intensities have not yet been taken into consideration.

All five 2-D DIGE gels resolved well and displayed similar protein expression patterns as is seen in Figure 5.5. Therefore, the obtained images were cropped using Image Quant Tools (Amersham Biosciences), processed via DeCyder Batch Processor (Amersham Biosciences) and analysed using DeCyder BVA software (Amersham
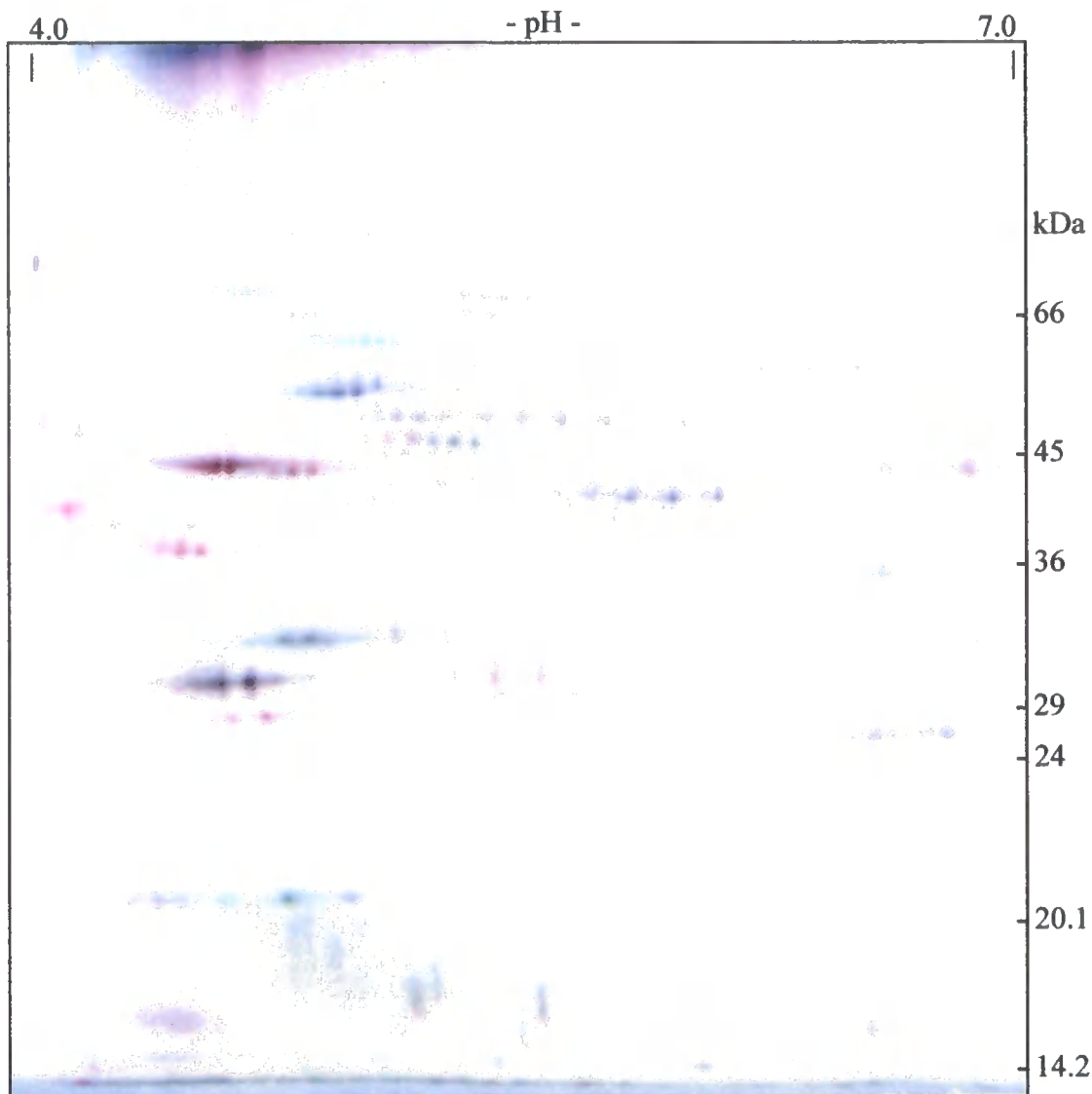
Figure 5.5. 2-D DIGE analysis of *Synechocystis* Triton X-100 membrane extract discovering changes in protein abundance following acclimatisation to high temperature (38°C) for 1 hour.

Equal 12.5 µg quantities of control (Cy3 labelled), heat acclimated (Cy5 labelled) and pooled internal standard (Cy2 labelled) samples were co-resolved through large format pH 4-7 12 % acrylamide 2-D gels. Labelled proteins were visualised immediately after electrophoresis detecting all three Cy-labelled samples. All 3 Cy images are viewed on top of one another as an overlay. Using this overlay image proteins having an increased or decreased abundance can be seen as green and red spots, respectively.

Biosciences). The BVA software automatically performed spot detection, matching and abundance quantification and also calculated the average change in abundance between the two conditions and executed a statistical t-test on this average data. All automatic spot detection and matching performed by the BVA software was manually confirmed and altered if necessary before selecting those spots having a > 1.2 fold average increase/decrease in abundance and a > 95 % statistical confidence. Protein spots with these criteria were believed to be biologically important and representative of the heat acclimation response. Using these criteria a total of 187 spots were selected for picking, 91 of which displayed an increase in abundance following heat acclimation and 96 a decrease in abundance. Also a further 19 spots that were seen to change in abundance > +/- 20 % and resolve in the same MW spot trains as other selected spots but were just below the statistical cut off, were also selected for identification. It was important to determine if these spot were the same as the statistically valid spots and consequently 206 spots were selected in total.

Having isolated the proteins of interest, the next stage of this investigation was to generate a preparative gel containing a higher quantity of protein from which spots could be picked for identification (Note: DIGE gels only contain a total of 37.5 μg of protein, this is an insufficient amount of protein per spot in order to obtain identification). To achieve this 200 μg and 800 μg of unlabelled Triton extracted membrane protein was loaded via Cup and IGR, respectively, into separate pH 4-7 18 cm IPG strips and focused as before for 70 kVh using an Ettan™ IPGphor IEF system (Amersham Biosciences). IGR method for sample loading was used because sample volume was high and large quantities could not be loaded via an anodic cup. A lower cup loaded 2D gel was generated in order to aid the comparison of the IGR loaded

picking gel to the cup loaded DIGE analytical gels. Precipitation and subsequent re-solubilisation could have been employed to concentrate the sample but the probability of selective loss of certain constituents was too high to risk. The focused strips were equilibrated before being loaded onto 1.5 mm thick large format 12 % polyacrylamide gels. The gels were electrophoresed in the same fashion as was undertaken for the DIGE gels and the resolved spots were visualised with MS compatible silver stain. Gels were imaged using a ProXPRESS imager (Genomic Solutions) and matched to the DIGE analytical gel images using Phoretix 2D evolution software (Nonlinear Dynamics). However, it was evident that some of the spots selected for identification were very low abundance on the preparative gel and therefore these spots were removed from the picking list due to the low probability of being able to attain identification. Consequently 192 (two full microtitre plates worth) were selected for identification.

Selected spots were manually picked (see materials and methods for details) into separate wells of a microtitre plate (Genomic Solutions) and digested overnight with trypsin using a Progest automated digestion robot (Genomic Solutions). The tryptic peptides were harvested and analysed via MALDI-ToF MS. The mass spectra given were used to search all entries in the NCBI non redundant database using the MASCOT search engine (http://www.matrixscience.com) (Perkins *et al.*, 1999). Of the 192 selected spots for identification 91 were positively identified having a MOWSE score greater than the probability threshold of 64. This is a hit rate of 47 %. As an example, the mass spectra and sequence coverage obtained for spot 23 (Table 5.2) identified as GroEL-1 60 kDa chaperonin is shown if Figure 5.6. A further 6 spots gave MALDI-PMF identification slightly lower than the probability threshold

A MALDI ToF mass spectra
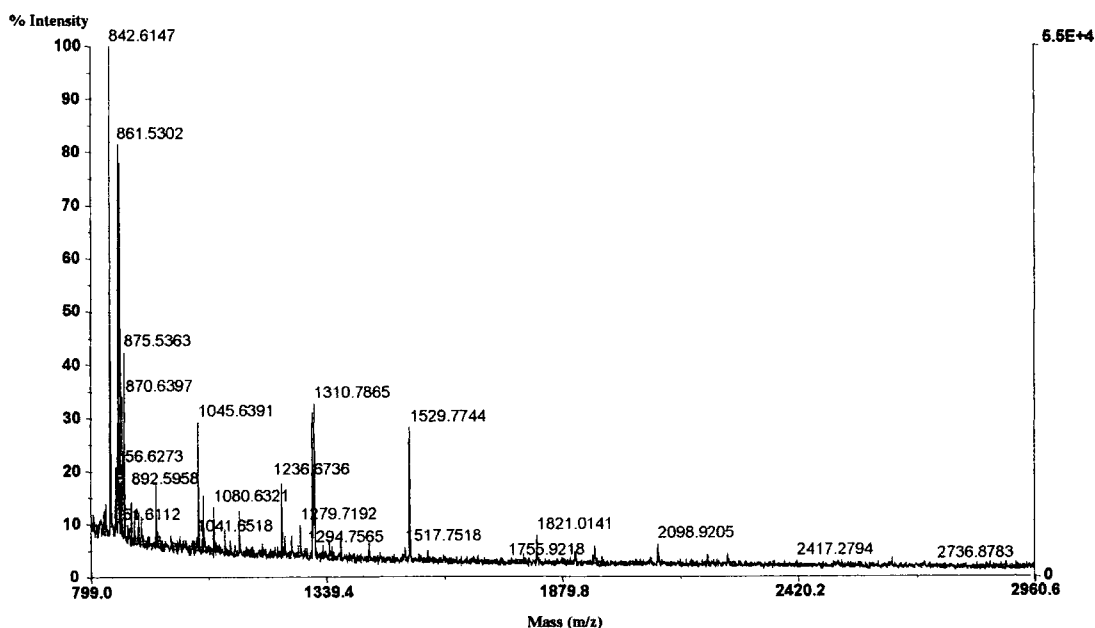
B GroEL-1 sequence coverage

```
  1 MAKSIIYNDE ARRALERGMD ILAEAVAVTL GPKGRNVVLE KKFGSPQIIN
 51 DGITIAKEIE LEDHVENTGV SLIRQAASKT NDVAGDGTTT ATVLAHAIVK
101 EGLRNVAAGA NPISLKRGID KATDFLVARI KEHAQPVGDS KAIAQVGAIS
151 AGNDEEVGQM IANAMDKVGQ EGVISLEEGK SMTTELEITE GMRFDKGYIS
201 PYFVTDAERM EAVLEDPRIL ITDKKINLVQ DLVPILEQVA RQGKPLLIIA
251 EDIEKEALAT LVVNRLRGVL NVAAVKAPGF GDRRKQMLED IATLTGGQVI
301 SEDAGLKLES ATVDSLGSAR RINITKDNTT IVAEGNEAAV KSRCEQIRRQ
351 IEETDSSYDK EKLQERLAKL AGGVAVIKVG AATETEMKDR KLRLEDAINA
401 TKAAVEEGIV PGGGTTLAHL APQLEDWATG NLKDEELTGA LIVARALPAP
451 LKRIAENAGQ NGAVISERVK EKEFNVGYNA ASLEYVDMLA AGIVDPAKVT
501 RSALQNAASI AGMVLTTECI VVDKPEKEKA PAGAPGGDFD Y
```

Figure 5.6. GroEL-1 60 kDa chaperonin identified via MALDI PMF.

A, MALDI ToF peptide ion spectrum of spot 23 (Table 5.2) identified as GroEL-1 60 kDa chaperonin with a MOWSE score of 174. **B**. MALDI ToF peptide coverage for the identified protein is highlighted (**bold**).

but were considered likely to be the particular identification attained. Also an additional 8 spots were identified via ESI MS-MS. In total 105 proteins were identified, this is a final percentage identification of 55 %. However, three spots not positively identified did show peptides within their MALDI-ToF mass spectra which matched peptides from mass spectra of identified proteins in neighbouring spots. This demonstrates that these proteins are probably the same identification as the neighbouring spot. All identified proteins are tabulated in Table 5.2 and their location on the silver stained preparative gels is shown in Figure 5.7a and 5.7b.
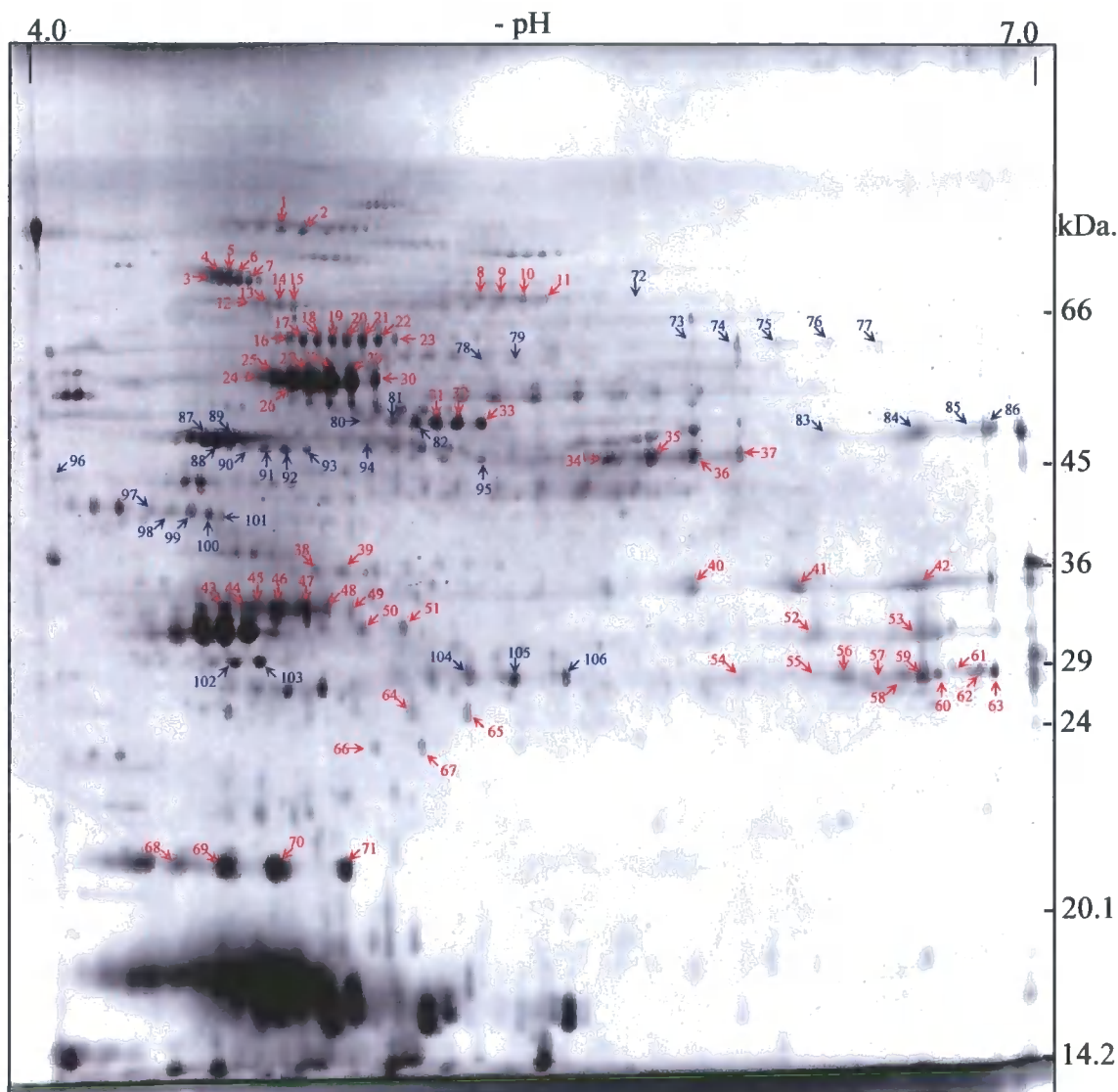
Figure 5.7a. Annotated silver stained preparative gel of identified *Synechocystis* Triton X-100 extracted membrane protein spots which show a change in steady state levels following acclimatisation of cells to heat conditions for 1 hour.

An aliquot of *Synechocystis* Triton X-100 extracted membrane protein containing 400 μg of protein was subjected to large format pH 4-7 2-DE using a 12 % acrylamide resolving gel and the resolved protein spots were visualised with MS compatible silver stain. Annotated spots are those shown to change in abundance following acclimation of cells to high temperature and which have been successfully identified via MALDI-ToF MS or ESI tandem MS. Spots labelled with red and blue arrows are those which display and increase or decrease in abundance, respectively.
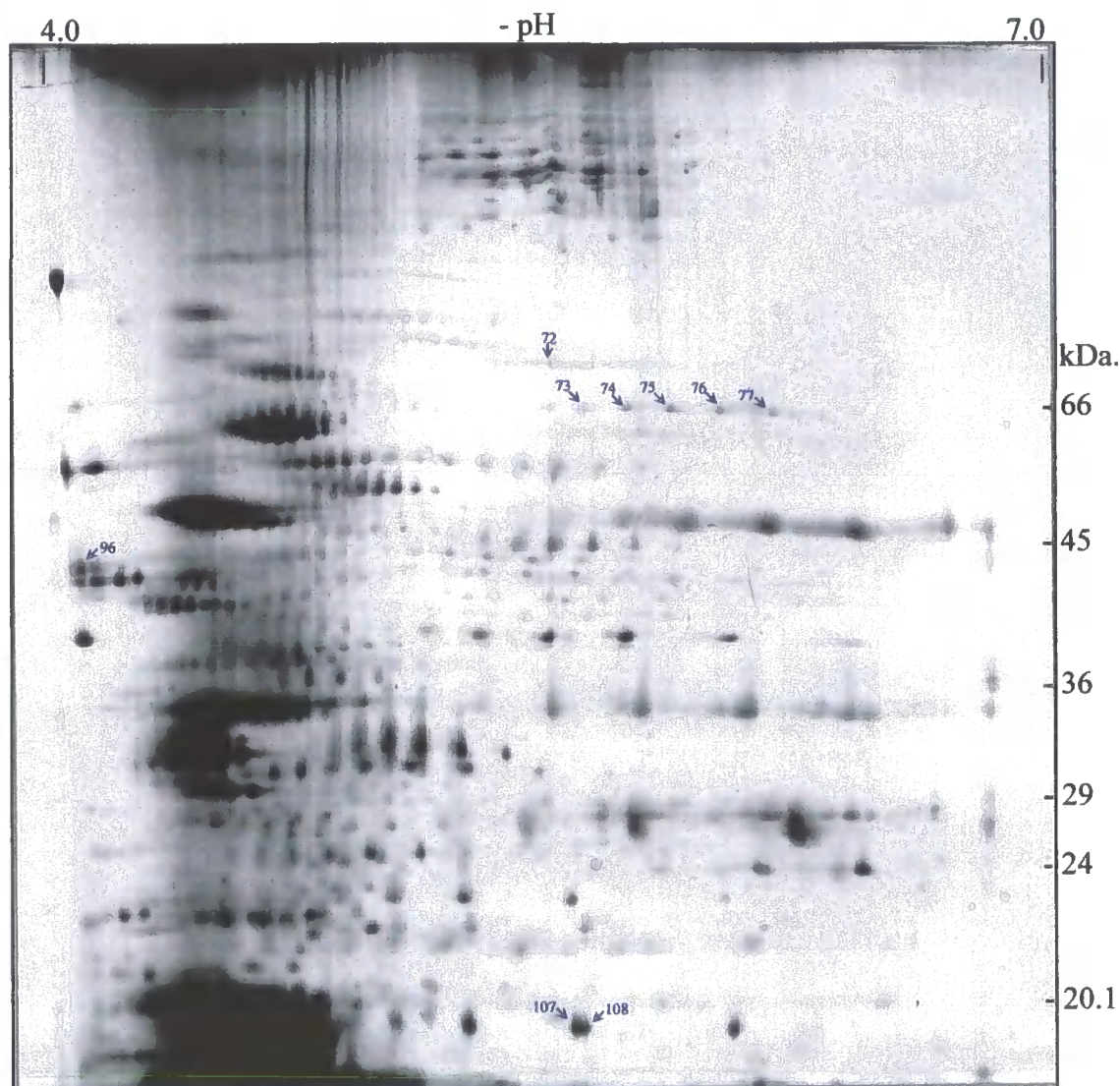
Figure 5.7b. Annotated silver stained preparative gel of identified *Synechocystis* Triton X-100 extracted membrane protein spots which show a change in steady state levels following acclimatisation of cells to heat conditions for 1 hour.

An aliquot of *Synechocystis* Triton X-100 extracted membrane protein containing 800 μg of protein was subjected to large format pH 4-7 2-DE using a 12 % acrylamide resolving gel and the resolved protein spots were visualised with MS compatible silver stain. Annotated spots are those successfully identified via PMF and show a change in abundance following acclimation of cells to heat and which were not detectable from the lower loaded gel. Spots labelled with red and blue arrows are those which display and increase or decrease in abundance, respectively.

Table 5.2. Identified Synechocystis membrane associated proteins which display a change in abundance following adaptation of cells to heat. A: increase in abundance (spots 1-71).

Spot No.	Paired Ratio	Paired T-test	Protein I.D. (gene)	ORF	MOWSE Score	Accession No.
1	2.74	0.00017	Phycobilisome LCM core-membrane linker (*apcE*)	slr0335	142	gi|16331244
2	2.45	9.30E-05	Phycobilisome LCM core-membrane linker (*apcE*)		111	
3	2.34	0.0014	70kDa heat shock protein (*dnaK-2*)		147	
4	2.50	0.00097	70kDa heat shock protein (*dnaK-2*)		147	
5	2.26	0.003	70kDa heat shock protein (*dnaK-2*)	sll0170	104	gi|16331261
6	2.27	2.40E-05	70kDa heat shock protein (*dnaK-2*)		116	
7	2.15	0.0016	70kDa heat shock protein (*dnaK-2*)		102	
8	1.47	0.0095	Succinate dehydrogenase flavoprotein subunit (*frdA*)		76	
9	1.42	0.017	Succinate dehydrogenase flavoprotein subunit (*frdA*)	slr1233	125	gi|16330111
10	1.42	0.057[a]	Succinate dehydrogenase flavoprotein subunit (*frdA*)		114	
11	1.22	0.066[a]	Succinate dehydrogenase flavoprotein subunit (*frdA*)		102	
12	1.47	0.0072	Squalene hopene cyclase (*shc*)	slr2089	89	gi|16330570

Table 5.2a continued.

Spot No.	Paired Ratio	Paired T-test	Protein I.D. (gene)	ORF	MOWSE Score	Accession No.
13	1.50	0.001	Squalene hopene cyclase (shc)		74	gi|16330570
14	1.44	0.0029	Squalene hopene cyclase (shc)	slr2089	66	
15	1.32	0.022	Squalene hopene cyclase (shc)		642*	
16	3.51	0.00063	60kDa chaperonin 2 (groEL-2)		100	gi|16331442
17	3.80	3.90E-06	60kDa chaperonin 2 (groEL-2)	sll0416	174	
18	4.10	2.10E-05	60kDa chaperonin 1 (groEL-1)		100	
19	3.76	5.00E-06	60kDa chaperonin 1 (groEL-1)		100	
20	4.38	6.90E-06	60kDa chaperonin 1 (groEL-1)	slr2076	101	gi|16330003
21	4.20	6.70E-06	60kDa chaperonin 1 (groEL-1)		166	
22	4.19	3.30E-05	60kDa chaperonin 1 (groEL-1)		186	
23	4.13	1.30E-05	60kDa chaperonin 1 (groEL-1)		174	
24	2.44	0.00048	ATP synthase beta subunit (atpB)	slr1329	189	gi|16330679

Table 5.2a continued.

Spot No.	Paired Ratio	Paired T-test	Protein I.D. (gene)	ORF	MOWSE Score	Accession No.
25	2.65	0.001	ATP synthase beta subunit (*atpB*)		237	
26	3.03	0.0041	ATP synthase beta subunit (*atpB*)	slr1329	257	gi|16330679
27	2.79	0.0067	ATP synthase beta subunit (*atpB*)		185	
28	2.29	0.0099	ATP synthase alpha subunit (*atpA*)	sll1326	146	gi|16329327
			ATP synthase beta subunit (*atpB*)	slr1329	272	gi|16330679
29	2.08	0.023	ATP synthase alpha subunit (*atpA*)	sll1326	172	gi|16329327
			ATP synthase beta subunit (*atpB*)	slr1329	171	gi|16330679
30	2.31	0.014	ATP synthase alpha subunit (*atpA*)	sll1326	243	gi|16329327
31	1.27	0.063 [a]	Protein synthesis elongation factor Tu (*tufA*)		593*	
32	1.37	0.057 [a]	Protein synthesis elongation factor Tu (*tufA*)	sll1099	208	gi|16330913
33	1.34	0.043	Protein synthesis elongation factor Tu (*tufA*)		167	
34	1.63	0.047	NADH dehydrogenase subunit 7 (*ndhH*)	slr0261	93	gi|16330531

Table 5.2a continued.

Spot No.	Paired Ratio	Paired T-test	Protein I.D. (gene)	ORF	MOWSE Score	Accession No.
35	1.68	0.073 [a]	NADH dehydrogenase subunit 7 (*ndhH*)		131	
36	1.72	0.081 [a]	NADH dehydrogenase subunit 7 (*ndhH*)	slr0261	119	gi|16330531
37	1.71	0.082 [a]	NADH dehydrogenase subunit 7 (*ndhH*)		125	
38	1.29	0.043	Water-soluble carotenoid protein		108*	
39	1.21	0.032	Water-soluble carotenoid protein	slr1963	102*	gi|16330780
40	1.67	0.0015	ABC transporter ATP-binding protein		75	
41	1.94	0.0026	1 common peptide with ABC transporter ATP-binding protein PMF	sll0759	-	gi|16331332
42	1.95	0.0058	1 common peptide with ABC transporter ATP-binding protein PMF		-	
43	1.96	0.0019	Phycobilisome rod linker polypeptide (*cpcC2*)	sll1579	119	
44	2.13	0.0034	Phycobilisome rod linker polypeptide (*cpcC2*)	sll1579	79	gi|16329822
45	1.76	0.066 [a]	Phycobilisome rod linker polypeptide (*cpcC2*)	sll1579	66	

Table 5.2a continued.

Spot No.	Paired Ratio	Paired T-test	Protein I.D. (gene)	ORF	MOWSE Score	Accession No.
46	2.06	0.0074	Hypothetical Protein	slr1590	511*	gi|16329578
			Apocytochrome f	sll1317	408*	gi|16330219
			Phycobilisome rod linker polypeptide (*cpcC2*)	sll1579	148*	gi|16329822
47	2.04	0.01	Phycobilisome rod linker polypeptide (*cpcC2*)	sll1579	83	gi|16329822
			Apocytochrome f	sll1317	78	gi|16330219
48	2.04	0.018	Phycobilisome rod linker polypeptide (*cpcC2*)	sll1579	82	gi|16329822
			Apocytochrome f	sll1317	103	gi|16330219
49	1.89	0.069 [a]	Phycobilisome rod linker polypeptide (*cpcC2*)	sll1579	107	gi|16329822
			Prohibitin (*phb*)	slr1106	59 [b]	gi|16329361
50	1.72	0.032	Prohibitin (*phb*)	slr1106	222	—
51	1.64	0.097 [a]	Prohibitin (*phb*)		240	gi|16329361

Table 5.2a continued.

Spot No.	Paired Ratio	Paired T-test	Protein I.D. (gene)	ORF	MOWSE Score	Accession No.
52	1.56	0.019	Phycobilisome rod linker polypeptide (*cpcC2*)	sll1579	119	gi|16329822
			Hypothetical protein	slr0606	83	gi|16332333
53	1.48	0.012	Phycobilisome rod linker polypeptide (*cpcC2*)	sll1579	106	gi|16329822
54	1.63	0.027	NADH dehydrogenase subunit, NdhI (*ndhI*)		72	
55	1.51	0.018	NADH dehydrogenase subunit, NdhI (*ndhI*)		84	
56	1.67	0.042	NADH dehydrogenase subunit, NdhI (*ndhI*)		69	
57	1.37	0.06 [a]	NADH dehydrogenase subunit, NdhI (*ndhI*)	sll0520	116	gi|16332085
58	1.69	0.043	NADH dehydrogenase subunit, NdhI (*ndhI*)		98	
59	1.77	0.028	NADH dehydrogenase subunit, NdhI (*ndhI*)		63 [b]	
60	1.57	0.06 [a]	4 common peptides with NADH dehydrogenase subunit, NdhI PMF		-	
61	1.31	0.056	Heme Oxygenase (*ho1*)	sll1184	86	gi|16329456
62	1.75	0.03	NADH dehydrogenase subunit, NdhI (*ndhI*)	sll0520	110	gi|16332085

Table 5.2a continued.

Spot No.	Paired Ratio	Paired T-test	Protein I.D. (gene)	ORF	MOWSE Score	Accession No.
63	1.82	0.046	NADH dehydrogenase subunit, NdhI (*ndhI*)	sll0520	76	gi|16332085
64	1.71	0.002	Hypothetical protein	sll0072	84	gi|16331470
65	1.95	0.0014	Hypothetical protein		108	
66	1.62	0.003	Hypothetical protein	slr1852	91	gi|16330239
67	1.84	0.0075	Hypothetical protein		83	
68	1.44	0.016	Phycocyanin beta chain (*cpcB*)		82	
69	1.70	0.0012	Phycocyanin beta chain (*cpcB*)	sll1577	92	gi|1652309
70	1.86	0.00019	Phycocyanin beta chain (*cpcB*)		121	
71	1.49	0.00086	Phycocyanin beta chain (*cpcB*)		92	

B: decrease in abundance (spots 72-108)

Spot No.	Paired Ratio	Paired T-test	Protein I.D. (gene)	ORF	MOWSE Score	Accession No.
72	-1.58	0.0049	Rubisco large subunit (*rbcL*)	slr0009	84	gi|16331392
73	-1.55	0.021	Beta carotene ketolase (*crtO*)	slr0088	100	gi|16331763

Table 5.2b continued.

Spot No.	Paired Ratio	Paired T-test	Protein I.D. (gene)	ORF	MOWSE Score	Accession No.
74	-1.73	0.0012	Beta carotene ketolase (*crtO*)		68	
75	-1.96	0.00033	Beta carotene ketolase (*crtO*)	slr0088	56 [b]	gi|16331763
76	-1.93	0.00032	Beta carotene ketolase (*crtO*)		68	
77	-1.77	0.0017	Beta carotene ketolase (*crtO*)		167	
78	-1.42	0.014	Hypothetical protein		76	
79	-1.4	0.0017	Hypothetical protein	sll0659	58 [b]	gi|16331966
80	-1.5	0.027	Hypothetical protein		63 [b]	
81	-2.12	0.0016	Hypothetical protein	slr1173	95	gi|16330940
82	-1.82	0.00026	Hypothetical protein		57 [b]	
83	-1.44	0.031	Geranylgeranyl hydrogenanase (*chlP*)		93	
84	-1.3	0.026	Geranylgeranyl hydrogenanase (*chlP*)	sll1091	90	gi|2493698
85	-1.33	0.0044	Geranylgeranyl hydrogenanase (*chlP*)		74	

Table 5.2b continued.

Spot No.	Paired Ratio	Paired T-test	Protein I.D. (gene)	ORF	MOWSE Score	Accession No.
86	-1.33	0.049	Geranylgeranyl hydrogenanase (chlP)	sll1091	77	gi|2493698
87	-1.75	0.016	ABC-type urea transport system substrate-binding protein, periplasmic protein (urtA)		153	
88	-2.4	0.0027	ABC-type urea transport system substrate-binding protein, periplasmic protein (urtA)	slr0447	190	gi|16331081
89	-2.4	0.0051	ABC-type urea transport system substrate-binding protein, periplasmic protein (urtA)		736*	
90	-1.31	0.02	Nitrate/nitite transport substrate-binding protein (ntrA)		102	
91	-1.39	0.04	Nitrate/nitite transport substrate-binding protein (ntrA)		111	
			Nitrate/nitite transport substrate-binding protein (ntrA)	sll1450		gi|16330084
92	-1.76	0.0099	Nitrate/nitite transport substrate-binding protein (ntrA)		116	
93	-2.11	0.0045	Nitrate/nitite transport substrate-binding protein (ntrA)		605*	
94	-1.42	0.044	Ferrochelatase (hemH, scpA)	slr0839	67	gi|16331725

Table 5.2b continued.

Spot No.	Paired Ratio	Paired T-test	Protein I.D. (gene)	ORF	MOWSE Score	Accession No.
95	-1.35	0.0039	Type II NADH dehydrogenase (*ndbB*)	slr1743	99	gi|16330375
96	-3.14	0.017	phosphate-binding periplasmic protein precursor	sll0680	77	gi|16331543
97	-2.01	0.019	Hypothetical Protein (Peptidyl-prolyl cis-trans isomerase)		115	
98	-1.93	0.03	Hypothetical Protein (Peptidyl-prolyl cis-trans isomerase)	sll0408	117	gi|16331452
99	-1.99	0.017	Hypothetical Protein (Peptidyl-prolyl cis-trans isomerase)		69	
100	-2.07	0.0059	Iron transport system substrate-binding protein (*futA1*, *sufA*)	slr1295	175*	gi|16329434
101	-1.91	0.0072	Iron transport system substrate-binding protein (*futA1*, *sufA*)		152	
102	-1.89	0.014	Periplasmic protein, function unknown	sll1784	82	gi|16330237
103	-1.93	0.015	Periplasmic protein, function unknown		68	
104	-1.13	0.025	Glutathione S-transferase	sll1545	89	gi|16332243

- 353 -

Table 5.2b continued.

Spot No.	Paired Ratio	Paired T-test	Protein I.D. (gene)	ORF	MOWSE Score	Accession No.
105	-1.24	0.043	Glutathione S-transferase	sll1545	75	gi|16332243
106	-1.49	0.0058	Glutathione S-transferase		72	
107	-1.62	0.04	Hypothetical protein	slr0362	78	gi|1001458
108	-1.68	0.0098	Hypothetical protein		91	

Changes in protein abundance (Paired Ratio) are represented as a fold change and negative values indicate a decreased abundance, for example a value of -1.33 indicates this protein decreases in abundance from steady stage levels by 1.33 fold or by 33%.

* Proteins identified via ESI MS-MS.

[a] DIGE data below statistically valid threshold.

[b] MOWSE scores below statistically valid cut off.

5.2.3   Classical heat shock proteins are the most highly induced proteins from steady state levels present in the thylakoid membrane following acclimation of cells to high temperature.

The thylakoid associated proteins which increase in abundance by the greatest amount following acclimation of *Synechocystis* to high temperature are the GroEL-1 and GroEL-2 Hsps. GroEL-1 increases as much as 4.38 fold (spot 20) and GroEL-2 as much as 3.80 fold (spot 17). The GroEL proteins of *Synechocystis* have been previously reported to attach to the thylakoid membrane upon exposure of cells heat shock (Kovács *et al.*, 1994). This investigation also showed that both weak and strong associations of GroEL proteins with the thylakoid membrane were identifiable. Strong associations were only removed by detergent and contained both GroEL-1 and GroEL-2 proteins in a ratio of approximately 1:1, where as only GroEL-1 was present in the NaCl extracted pool of weakly associated proteins. GroEL-1 and -2 proteins have been thought to be able to form homo- and hetero-oligiomers (Kovács *et al.*, 2001). Therefore the strongly thylakoid associated GroEL-1 and GroEL-2 proteins may form hetero-oligomers where as the weakly associated GroEL-1 may be present as a homo-oligomer. The greater quantity of GroEL-1 than GroEL-2 seen to associate with the thylakoid in this proteomic investigation supports this hypothesis.

Another classical Hsp also observed to increase in the amount of association to the thylakoid membrane following acclimation of cells to high temperature was the DnaK-2 protein. This was seen to increase in abundance as much as 2.5 fold (spot 4). Investigation into the cyanobacterium *Synechococcus* pc PCC 7942 revealed that the DnaK-3 protein was associated on the cytosolic side of the thylakoid membrane

surface (Nimura *et al.*, 1996). This observation that chaperonins associate with the membrane has been observed in many other organisms both eukaryotic and prokaryotic (Bochkareva *et al.*, 1998).

5.2.4 Increased abundance of the thylakoid associated squalene-hopene cyclase protein may promote the stabilisation of heat-fluidised membranes.

The squalene-hopene cyclase protein increases as high as 1.50 fold (spot 13) in abundance following heat acclimation. This protein is involved in the synthesis of pentacyclic hopanoids from squalene, a class of eubacterial lipids which are very similar in structure to sterols. Because of this they share similar properties. Just as sterols, such as cholesterol, are involved in the condensation and thus stabilisation of membranes in higher organisms, so are hopanoids in bacterial membranes. Two recent investigations have expanded the biological function of hopanoids. In *Streptomyces* sp. hopanoids abundant in the membranes of aerial mycelium possibly alleviate stress by diminishing water permeability across the membrane (Poralla *et al.*, 2000). In addition, the symbiotic nitrogen fixing *Frankia* bacteria contain special vesicles made primarily of hopanoids which enclose the highly oxygen-sensitive nitrogenase enzyme. These hopanoid membranes prevent oxygen diffusion and take part in an oxygen protection mechanism of the nitrogenase enzyme (Dobritsa *et al.*, 2001). These observations indicate that hopanoids increase the rigidity and decrease the permeability of membranes and due to the proposed theory that elevated temperatures increase membrane fluidity and permeability (Vigh *et al.*, 1998) explains why their abundance may be elevated in the membranes of cells acclimated to high temperatures. Although there is no direct data that supports this statement, the

discovery that the primary enzyme involved in the biosynthesis of hopanoids from squalene is elevated in abundance in the membranes of cells acclimated to high temperature is concrete evidence that this occurring.

5.2.5 Thylakoid membranes from heat acclimated cells display an increased level of certain protein constituents involved in photosynthesis and respiration.

The most frequently represented cellular process seen to be up regulated in *Synechocystis* thylakoid membranes following acclimation to high temperature is photosynthesis and respiration. Here, three constituents of the phycobilisome, namely the core membrane linker (ApcE), rod linker (CpcC2) and phycocyanin β-subunit (CpcB), increase as much as 2.74 fold (spot 1), 2.13 fold (spot 44) and 1.86 fold (spot 70), respectively. Both the core membrane linker and phycocyanin are known to contain covalently linked phycobilin chromophores (Ajlani and Vernotte, 1998) and because of this their intrinsic fluorescence has been shown to be detectable when using the Cy-Dye excitation and emission detection parameters of the Typhoon (Amersham Biosciences) fluorescence imager (see Chapter 4). Consequently, these proteins were removed from DIGE analysis in Chapter 4 because of the interference of their intrinsic fluorescence in correct quantification of protein abundance. Unfortunately, no analysis of intrinsic fluorescence in the membrane protein fraction was performed due to limited sample quantity and therefore the presence of intrinsic fluorescence in these protein spots cannot be confirmed. However, looking back at the initial SDS-PAGE analysis (Figure 5.2), a low molecular weight protein band of approximately 21 kDa is immediately identifiable as increasing in abundance following acclimation of cells to high temperature. The protein spots identified as

phycocyanin β-subunit (spots 68-71) also resolved at this MW, with no other proteins resolving in the same location and therefore it is probable that although quantification may be inaccurate this protein is elevated in abundance in the membranes of heat acclimated *Synechocystis* cells. Rod linkers in *Synechocystis* do not have any intrinsic fluorescence, although in red algae they do. This suggests the detected elevated abundance for the phycocyanin rod linker protein (CpcC2) is a real biological response and therefore this may indicate that the same response may occur for other phycobilisome linkers. Perhaps then the elevation of core membrane linker abundance in the thylakoid membrane is a real biological response despite the interference from its intrinsic fluorescence.

Another protein shown to increase in abundance following acclimation to high temperature and yet known to have intrinsic fluorescence (previously demonstrated in Chapter 4 to be detectable using a Typhoon fluorescence imager) is the succinate dehydrogenase flavoprotein (spots 8-11). Because there is no additional evidence which indicates that this protein may be elevated following exposure of cells to elevated temperature, this result can not be considered definitive and requires further investigation.

Other elevated components of the photosynthetic and respiratory machinery in heat acclimated *Synechocystis* thylakoid membranes include the apocytochrome f, a constituent of the photosynthetic cytochrome b_6f complex seen to increase as much as 2.06 fold (spot 46), two subunits of the NAD(P)H dehydrogenase complex (type I) (NDH-1), namely NdhI and NdhH which increase as much as 1.72 fold (spot 36) and 1.82 fold (spot 63), respectively, and the α and β ATP synthase subunits which

increase by 3.03 fold (spot 26) 2.31 fold (spot 30), respectively. Just to clarify, although the localisation of the photosynthetic machinery is well known to exist in the thylakoid membrane, the localisation of the respiratory machinery has been reported to be situated on both the plasma and thylakoid membrane (Berger *et al.*, 1991; Dzelzkalns *et al.*, 1994). However in *Synechocystis* recent evidence has demonstrated the NAD(P)H dehydrogenase complex of the respiratory machinery to be largely, if not exclusively, confined to the thylakoid membrane (Ohkawa *et al.*, 2001). The cytochrome $b_6 f$ complex and NAD(P)H dehydrogenase complex both function to generate a proton gradient across the membrane via the transfer electrons. Apocytochrome f transfers electrons from PSII to PSI where it receives electrons from the Rieske iron-sulphur protein and passes them to plastocyanin. The NAD(P)H dehydrogenase complex shuttles electrons from NAD(P)H, via flavin mononucleotide (FMN) and iron-sulphur (Fe-S) centres, to quinones in the respiratory chain. The generated proton gradient across the membrane subsequently drives ATP synthesis at the ATP synthase complex where the regulatory and catalytic subunits of this reaction are the α and β subunits, respectively. This evidence indicates that the maintenance of a protein gradient via shuttling of electrons in both respiration and photosynthesis and the subsequent synthesis of ATP is integral to the cells acclimation to high temperature. Perhaps this increases the amount of freely available ATP for the action of ATP dependent proteases and chaperones which function to stabilise the membrane against the effects of thermal stress.

There is little evidence in current the literature base to support this hypothesis, however, recent studied investigating the effect of CO_2 concentration on NAD(P)H activity also in *Synechocystis* have demonstrated that the NdhI and NdhH subunits are

elevated in cells grown under low CO_2 concentration, thus increasing the activity of the NAD(P)H complex (Deng *et al.*, 2003). This indicates that this system functions to acclimatise cyanobacterial cells to low CO_2 levels. It is therefore possible the same system operates for acclimation to high temperature. This is further evidence which supports the observations made in Chapter 4 that cells exposed to high temperatures display a phenotype similar to that observed in cells starved of carbon. To recap under heat shock the Rubisco protein, known to be regulated by the availability of CO_2, was seen to decrease in abundance. Rubisco is also seen to decrease in abundance in heat acclimated thylakoid membranes (spot 72). Furthermore, the CcmM protein involved in carbon concentration was seen to decrease in abundance following exposure of cells to heat shock and the LexA protein known to increase in abundance under carbon limiting conditions also increases in abundance in heat shocked cells.

5.2.6 Other thylakoid associated proteins which increase in abundance following acclimation of cells to high temperature.

An overview of the various cellular functions which are represented by thylakoid proteins displaying an induced level of expression following acclimation of cells to high temperature is shown in Figure 5.8a. As already discussed, chaperonins and photosynthesis/respiration are the most represented cellular functions and show the largest increases in abundance from steady state levels. Other proteins which do increase in abundance, but not as high, include the water soluble carotenoid protein which increases as much as 1.29 fold (spot 38) and the protein synthesis elongation factor Tu which increases by 1.37 fold (spot 32). Both of these proteins have been previously shown to increase in abundance in the soluble protein fraction following
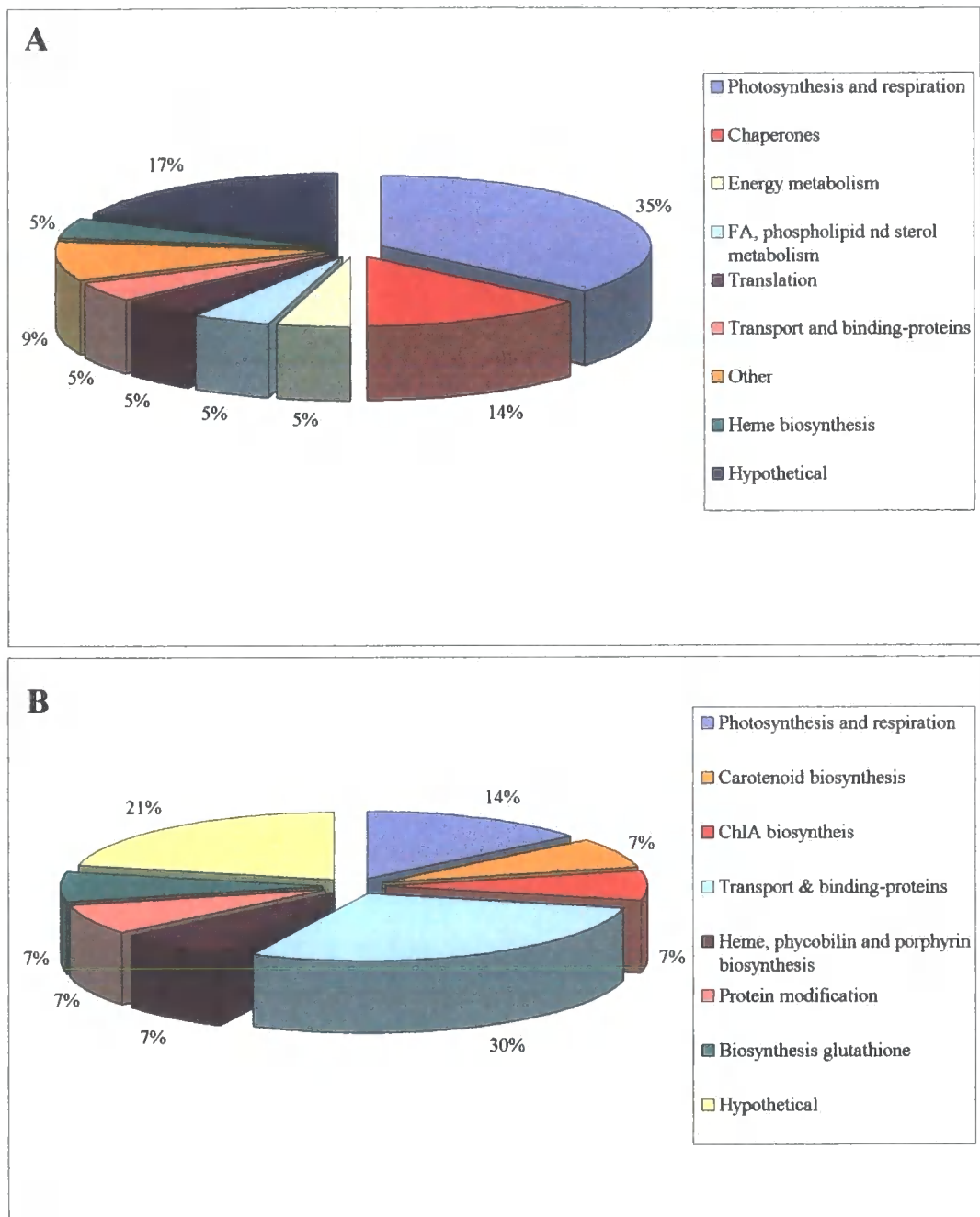
Figure 5.8. Thylakoid membrane proteins displaying increased (A) or decreased (B) abundance following acclimation of cells to high temperature organised by cellular function.

The number of proteins in each functional category is displayed as a percentage.

exposure of cells to heat shock (see Chapter 4), however, because these proteins are soluble, their presence at the thylakoid membrane is unexpected. Explanation for this can be described through one of two possibilities; (i) the prepared thylakoid membrane extracts are not pure and contain soluble contaminants, or (ii) these proteins like chaperones attach to the membrane.

As previously discussed in Chapter 4, the water soluble carotenoid protein contains the 3-hydroxyechinenone carotenoid pigment and has several photoprotection functions including protection against light-induced damage by quenching singlet oxygen, superoxide anion radicals, or triplet-state chlorophyll (Kerfeld *et al.*, 2003). However, a transport function of the carotenoid protein has been proposed in cyanobacteria where by it translocates carotenoids from their site of synthesis in the thylakoid membrane to the plasma or outer membrane where they form a photoprotective barrier (Jurgens and Weckesser, 1985). Perhaps this barrier is also heat protective and may explain the location of this protein at the thylakoid membrane. Furthermore if this protein is inserted into the membrane, perhaps the parallel packing increases the rigidity of the membrane in response to heat induced fluidisation (Vigh *et al.*, 1998).

The presence of the translational elongation factor Tu (EF-Tu) at the thylakoid membrane is less easily explained. This protein promotes the GTP-dependent binding of aminoacyl-tRNA to the A-site of ribosomes during protein biosynthesis. As previously mentioned EF-Tu has been seen to increase in abundance following exposure of cells to heat shock along with several other translational elongation

factors (see Chapter 4). However, perhaps this protein has a secondary function which is performed at the thylakoid membrane.

Another protein seen to increase in abundance at the thylakoid membrane following acclimation to high temperature is the ABC transporter ATP-binding protein which accumulates as much as 1.95 fold (spot 42) from basal levels. Little is known about the function of this protein; however, upon analysis of the repressed proteins in acclimated thylakoid membranes (Table 5.2) four transporter binding proteins demonstrate a decrease in abundance. The elevation of the ATP-binding protein is therefore inconsistent with this trend. However, remembering that ATP synthesis is probably elevated in heat acclimatised cells, as shown by the increase in ATP synthase subunits and proteins involved the generation of a proton gradient, perhaps the translocation of ATP is required into the thylakoid lumen for the action of ATP dependant proteins such as the ATPase chaperones, although no thylakoid lumenal chaperone has been reported (Waters, 1995).

5.2.7 Thylakoid associated proteins which decrease in abundance following acclimation of cells to high temperature.

A global view of the various cellular functions which are represented by thylakoid proteins displaying a decreased level of expression following acclimation of cells to high temperature is shown in Figure 5.8b. Of these cellular functions, transporter substrate-binding proteins (Sbp's) are the most frequent of proteins to be repressed following heat acclimation. These proteins are involved in the acquisition of compounds for subsequent transport through integral membrane channels which

- 363 -

operate through systems known as ABC-type transporters and those demonstrated to be suppressed include the urea, nitrate/nitrite, phosphate and iron binding proteins. The urea Sbp is suppressed as much as -2.4 fold (spot 88, 89), the phosphate Sbp by -3.14 fold (spot 96), the nitrate/nitrite Sbp as high as -2.11 fold (spot 93) and the iron Sbp as much as -2.07 fold (spot 100). The significance of their suppression is difficult to predict as the only currently reported data concerning the regulation of their expression is related to the deprivation of the compound they are involved in transporting. Such data has been reported in cyanobacteria for phosphate (Scanlan *et al.*, 1993) iron (Katoh *et al.*, 2001) and urea (Valladares *et al.*, 2002) ABC transporters where starvation of the related compound resulted in induced expression of the transporter components. However, in keeping with the knowledge that elevated temperature results in increased membrane permeability and loss of protein constituents, perhaps the binding proteins of ABC transporters are dissociated following exposure to elevated temperature. Furthermore, because these proteins play no role in acclimation to heat they are not replaced until the cell is returned to normal physiological conditions.

A number of proteins which are involved in the biosynthesis of chromophores in light harvesting proteins are suppressed in the thylakoid membranes of *Synechocystis* following acclimation to high temperature. These include the geranylgeranyl hydrogenase, involved in ChlA biosynthesis (Addlesee *et al.*, 1996), ferrochelatase (HemH) which is involved in the biosynthesis of photoheme from photoporphyrin and which is subsequently used to synthesise phycobilin chromophores in phycobiliproteins, and β-carotene ketolase involved in the biosynthesis of echinenone from β-carotene, suggested to be closely associated to the reaction centres in

thylakoid membranes (Fernandez-Gonzalez *et al.*, 1997). It seems contradictory to previous observations that although the phycobillin and echinenone containing light harvesting phycocyanin and water soluble carotenoid proteins increase in abundance in the thylakoid membranes of heat acclimated cells, the enzymes involved in the synthesis of their corresponding pigment containing prosthetic groups are suppressed. Explanation of this observation will require further analysis. However, the *Synechocystis* ferrochelatase protein has been shown to contain a chlorophyll a binding (Cab) domain and disruption of the gene resulted in increased tolerance to high light intensity in *Synechocystis* with a reduced PSI content (Funk and Vermaas, 1999) Perhaps, loss of this protein from the thylakoid membrane increases the tolerance of photosynthesis to high temperature.

Also observed to decrease in abundance is the Type II NADH dehydrogenase (NDH-2) NdbB, which does so by -1.35 fold (spot 95). Unlike NDH-1, which is a multi-subunit complex, NDH-2 consists of a single subunit and does not contain iron-sulfur clusters or appear to translocate protons across the membrane even though the complex is membrane associated and has FAD as the prosthetic group. Consequently it has been proposed that NDH-2s do not have a catalytic role in respiration and instead, perform a regulatory function. This was predicted from the observation that disruption of the NDH-2 genes in cyanobacterial strains with reduced PSI content displayed increased light tolerance (Howitt *et al.*, 1999). Perhaps, this is also true for elevated temperature.

The observations that disruption of the ferrochelatase and NDH-2 genes in cyanobacteria increases the tolerance to high light is consistent with data obtained

from analysis of the heat shock response reported in chapter 4 of this thesis. These results demonstrated that the same proteins change in abundance, both up and down, in the response to both heat shock and high light and consequently it was predicted that the cell may perceive the high light and heat signals through a similar mechanism.

The glutathione S-transferase (GST) protein was also shown to decrease in abundance in the thylakoid membranes of cells acclimated to elevated temperature. GSTs are involved in a variety of cellular processes including detoxification of herbicides, cell signalling pathways and regulation of apoptosis, and have been characterised in many organisms, both prokaryotic and eukaryotic (Dixon *et al.*, 2002). Although the roles of GSTs have not been demonstrated in cyanobacteria, there is the possibility of the involvement in cell signalling pathways where both positive and negative regulation of signalling pathways via GSTs have been demonstrated in other organisms (Loyall *et al.*, 2000; Ryoo *et al.*, 2004).

Finally, the peptidyl prolyl cis-trans isomerse (PPIase) previously shown to be elevated in the soluble fraction of cells exposed to heat shock (chapter 4), was also identified as changing in abundance at the thylakoid membrane following acclimation of cells to high temperature. However, this protein decreased in abundance in the membranes of cells acclimatised to heat. PPIases have been shown to be involved in regulatory mechanisms by modifying serine/threonine phosphorylation sites (Smet *et al.*, 2004) and therefore it is possible that in response to elevated temperature this protein translocates from the membrane due to increased membrane fluidity to the cytosol where it functions to regulate the phosphorylation of a two component signal

transduction pathway, activating the expression of genes involved in the response to high temperature. Perhaps this enzyme is the upstream regulator of Hik34 activity.

5.3   Discussion

The PSII oxygen-evolving machinery is the most susceptible component of the photosynthetic apparatus to high temperature inactivation (Berry and Björkman, 1980; Mamedov *et al.*, 1993). However, photosynthetic organisms can enhance the thermal stability of their oxygen-evolving machinery in response to elevated environmental temperature (Berry and Björkman, 1980; Nishiyama *et al.*, 1993; Tanaka *et al.*, 2000). Components in *Synechocystis* previously reported to be involved in the thermal stabilisation of the photosynthetic machinery include the PsbU, MSP (PsbO) and Cyt c_{550} protiens. These proteins are attached to the PSII manganese cluster, the catalytic site for oxygen evolution, and deletion of the genes encoding these proteins results in absolute loss of ability to enhance the thermal stability of oxygen evolution (Kimura *et al.*, 2002). However, PsbU, Cyt_{550} and PsbO proteins were reported to be constitutively expressed regardless of growth temperature (Nishiyama *et al.*, 1999) and therefore it has been proposed that other protein factors are involved in the enhancement of PSII thermal stability. Although, in the previous chapter PsbO, localised in the soluble cell fraction, was shown to increase in abundance following exposure of *Synechocystis* cells to heat shock, suggesting this prediction is incorrect and that PsbO is elevated to enhance the thermal stability of the oxygen evolving machinery. This protein was localised in the soluble fraction because it is weakly associated to the thylakoid membrane and is dissociated following cell breakage and fractionation procedures.

In this proteomic investigation comparing thylakoid membrane extracts from normal and heat acclimatised cells, no PSII specific proteins have been identified as

- 368 -

candidates for direct thermal stabilisation of the oxygen evolving machinery. Instead a variety of other proteins have been identified which may function to stabilise the photosynthetic machinery through other pathways.

5.3.1 Stabilisation of heat fluidised membranes by chaperone association and insertion of sterol-like hopenes.

GroEL-1, GroEL-2 and DnaK-2 chaperonins have been demonstrated to be specifically translocated to, and associate with the thylakoid membrane in heat acclimated cells. It has been proposed that membrane bound Hsps might act like their soluble counterparts and function to prevent denaturisation of membrane bound enzymes (Patriarca and Maresca 1990; Török et al., 1997). Furthermore, in keeping with the theory that heat shock decreases membrane stability and increases membrane fluidity/permeability, resulting in a loss of associated proteins (Revathi et al., 1994; Mejia et al., 1995), the accumulation of specific Hsps in or at the membrane may promote rigidification of the heat-fluidised membrane. This returns the membrane to its original state prior to heat shock and thus preserving structural and functional integrity, such as oxygen evolution (Török et al., 1997). This ability of chaperones to directly amend membrane structure presents a temporary and rapid response mechanism for thermal adaptation. This function has been demonstrated for the sHspA chaperonin which was shown to be involved in stabilisation of oxygen evolution, as inactivation of the gene encoding this protein greatly reduced the rate of oxygen evolution in heat stressed cells (Lee et al., 2000). Subsequent analysis revealed that this protein functions as a membrane stabilising factor and re-establishes membrane order (Török et al., 2001). Therefore chaperones have dual roles in the

recovery and protection of thermally injured cells, as members of the multi chaperone network and also in the stabilisation of heat-fluidised membranes.

A second mechanism by which heat-fluidised membranes may be stabilised is by the insertion of hopenoids into the membrane bilayer. The squalene hopene cyclase protein, responsible for the biosynthesis of these sterol-like compounds, is situated at the membrane and the increased quantity of this enzyme indicates increased biosynthesis and thus insertion of hopenoids in to the thylakoid membrane. A direct analysis of hopene content in heat acclimated membranes will clarify this theory.

5.3.2 Elevated phycobilisome constituents are involved in acclimation to high temperature

The phycocyanin β subunit and the corresponding linker polypeptide were shown to be elevated in abundance in heat acclimated thylakoid membranes. This was an unexpected result as heat shock has previously shown to disassemble phycobilisomes (Mao *et al.*, 2003), which was also demonstrated in chapter 4 of this thesis. It is possible that the explanation of this response comes from the observations that cyanobacteria are known to respond to a variety of stresses by varying their phycobilisome rod content (reviewed by Cohen-Bazire and Bryant, 1982; MacColl, 1998). For example the content of phycoerythrin and phycocyanin biliproteins vary depending on the wavelength of light available for growth. In predominantly green light conditions (in deep waters) the content of phycoerythrin increases which better absorbs light at this wavelength, whereas when grown in predominantly red light environments the content of phycocyanin increases. This is also true for the rod linker

polypeptides in which specific proteins are required for the different biliprotein links (i.e PE-PC and PC-PC and PE-PE) (reviewed by MacColl, 1998). *Synechocystis* sp. PCC 6803 does not contain any phycoerythrin, but perhaps under elevated temperature it increases the size its phycobiliosme rod antennae and therefore requiring a greater quantity of phycocyanin and the corresponding linker polypeptides. This theory is supported by the observations that thermophilic species of cyanobacteria have exceptionally large temperature-resistant rods which are stable at a variety of temperatures form 10-80°C (Edwards *et al.*, 1997). Perhaps by increasing the size of the rod, the stability under high temperature is greater.

5.3.3   Other   membrane   proteins   involved   in   the   acclimation   of photosynthesis to high temperature

Subunits of the cytochrome b_6f complex, the Type I NADH dehydrogenase and the ATP synthase complex have been shown to display increased abundance in heat acclimated *Synechocystis* membranes. It has been predicted that these proteins contribute to the thermal stabilisation of the functional complexes they make up and therefore allowing photosynthesis and respiration to continue to operate. However, to my knowledge there is no report of increased thermal stability of these complexes via their integral components following exposure to mild elevated temperatures. It is also possible that these elevated processes function to increase the output of ATP in the cell, for which the demand is likely to be higher under elevated temperatures due to the increased action of the ATP dependant proteases and chaperones.

5.3.4　Loss of thylakoid protein constituents displays selective replacement

Fifteen unique membrane proteins were observed to display a decreased abundance following acclimation of cells to high temperature. It is possible that these proteins are displaced from the membrane as a result of heat induced fluidisation and they are not replaced by newly synthesised and translocated proteins. This suggests that these proteins are probably not essential for the acclimation of photosynthesis to high temperature.

5.3.5　Concluding Remarks

A variety of mechanisms appear to be employed by cyanobacteria in order to acclimatise their photosynthetic machinery to high temperature. These include, i) the association of specific protein constituents which function to protect their target binding sites against heat inactivation, ii) the insertion of hopenes to increase the rigidity of the heat-fluidised membranes, iii) the association of cytosolic chaperones to help refold denatured membrane localised enzymes and restore membrane rigidity and physical order, and iv) the association of photprotective carotenoid proteins. This diverse range of adaptive mechanisms reflects the ability of cyanobacteria to survive in many different extreme environments. Elucidation of the exact function of the elevated proteins in the acclimation mechanism will require further analysis using gene knockout mutants, however an ideal biological system and assay have been established which will aid the further characterisation of these proteins.

Further analysis of the heat acclimation response is required at the low molecular weight protein level as several low molecular weight photosynthetic components have been predicted to be involved in acclimation of photosynthesis to high temperature. These include the Cyt_{550} and PsbU proteins associated to the PSII manganese cluster and the PsbW and PsaC proteins shown to increase in abundance in cells exposed to heat shock (see chapter 4). Also, as seen in the soluble protein fraction, several proteins involved in heat acclimation of the thylakoid membrane are represented by multiple spots with different pI's and which vary in the extend of the change in abundance. Therefore there is a requirement to analyse the difference in the structures of these protein forms and determine if they have any role in the biological response to heat acclimation.

CHAPTER 6

General Discussion

Synechocystis sp. PCC 6803 is a model experimental organism and has been exploited in this thesis for an in-depth investigation of the heat shock and acclimation responses of cyanobacteria. Its ease of large scale growth and rapid division, in an environment continually aerated with 1 % CO_2, together with the application of optimised cell breakage methods for the liberation of protein has provided ample biological material for analysis. Furthermore, the availability of the entire genome sequence has enabled the application of proteomic techniques. Cyanobacteria are ideal organisms for investigating stress responses and survival mechanisms employed by photosynthetic organisms due to their remarkable ability to survive in a variety of hostile environments.

The initial objective of this thesis was to establish 2D electrophoresis and peptide mass fingerprint (PMF) technology for the analysis of *Synechocystis* proteins and to use this technology to determine the complexity of the *Synechocystis* proteome and identify proteins spots resolved on 2D gels. The *Synechocystis* proteins were best resolved via cup loaded 2-DE using acidic pH gradients where high resolution of proteins spots was achieved with the application of a narrow range 'zoom' IPG gradient spanning a single pH unit. MALDI PMF analysis of 192 protein spots excised from a large format Coomassie stained zoom 2D gel generated 105 positive identifications which represented 74 unique proteins. Identified proteins included representatives of photosynthesis, molecular chaperones, transcription, translation, amino acid biosynthesis, energy metabolism, and others. In total, members of 14 different functional classes were identified along with 10 hypothetical proteins not previously mapped on 2D gels, demonstrating their existence in the soluble protein fraction and location on the 2D gel. The presence of multiple protein spots for

individual gene transcripts was immediately apparent, previously supported by other proteomic mapping exercises (Sazuka *et al.*, 1999; Wang *et al.*, 2000).

2-DE and PMF technology was successfully applied for the analysis of *Synechocystis* proteome and was established as a high throughput method. Therefore, this technology was applied to analyse the response to heat shock and its regulation in cyanobacteria. The initial analysis of *de novo* protein synthesis under heat shock via radiolabelling allowed the detection of a suitable time frame over which to study the heat shock response. One hour of heat shock demonstrated the highest level of synthesis for most soluble proteins synthesised under heat shock conditions, an observation supported by Borbely *et al* (1985). Multiple repeat control and 1 hour heat shocked samples were resolved on separate SYPRO™ Ruby stained 2D gels and their subsequent comparison generated 18 heat shock responsive proteins increasing in abundance. 14 of these were statistically valid changes and were characterised as being the 60, 70, 90 and 100 kDa Hsps. This quantity of data is a marked difference in the large number of genes transcripts known to change in abundance in response to heat shock (Iwane Suzuki, NIBB – personal communication) and also those known to change in response to other stresses such as, salt (Kanesaki *et al.*, 2002), high light (Hihara *et al.*, 2001) and chilling (Suzuki *et al.*, 2001). This was believed to be due to the inherent system variation between 2D gels and the specking arefact of SYPRO™ staining. Consequently, 2D DIGE technology was subsequently employed in the comparison of soluble proteomes from cells grown under normal and 1 hour heat shock conditions due to its ability to accurately identify changes as small as 10 % at the 95 % confidence limit (Tonge *et al.*, 2001). This analysis detected proteins with elevated or suppressed changes in abundance and generated 210 and 321 heat shock

responsive protein spots in the 34-44 °C and 30-42°C heat shock regimes investigated, respectively. Changes in abundance as high as over 19 fold and as low as 10 % were detected. This quantity and quality of data was a marked improvement from that identified via SYPRO analysis and illustrating the dynamic range and improved accuracy and sensitivity of the 2D DIGE technique. Of these heat shock responsive proteins spots detected via 2D DIGE, 288 were processed via PMF MS and 175 were characterised. The majority of identified proteins were those increasing in abundance following exposure to heat shock and were shown to represent over 18 different function classes. Several hypothetical proteins were also characterised in the response to heat shock, thus adding to assignment of their function. Of the identified proteins, the classical Hsps were seen to change by the greatest amounts, all of which have been previously characterised in the response to elevated temperature and other environmental stresses. However, perhaps the most interesting proteins seen to increase in abundance in response to heat were constituents of the photosynthetic machinery, proteins involved in the carbon fixation Calvin cycle and proteins with probable regulatory functions such as the PPIase and response regulators. Furthermore, there are several proteins changing in abundance, both increased and decreased, which have been previously characterised in response to other stresses, such as the Rubisco, LexA and CcmM proteins seen respond to carbon availability, and the phycobilisome constituents and response regulator 26 in response to high light. This evidence suggests that similar mechanisms are involved in the response to these stresses. Whether in heat shock they are all involved in the primary response or in secondary knock-on effects has yet to be determined.

This analysis has provided a global view of the responses to heat shock in the soluble proteins of *Synechocystis*, to my knowledge the first report in a cyanobacterium. It has demonstrated that the response to heat is not just to elevate the expression of the molecular chaperones and proteases, but also many other cellular processes respond such as photosynthesis, energy metabolism, transcription and translation and are possibly involved in the survival under heat shock. Changes in the photosynthetic PSII complex in response to heat have been characterised, where changes in phycobilisome structure have been mentioned (Cohen-Bazire and Bryant, 1982; MacColl, 1998; Mao *et al.*, 2003) and protection of the oxygen evolution machinery against heat inactivation has been well documented (Berry and Björkman, 1980; Mamedov *et al.*, 1993; Nishiyama *et al.*, 1993; Shen *et al.*, 1997; Tanaka *et al.*, 2000). This analysis has added to the knowledge concerning changes in the photosynthetic machinery under heat shock, presenting other proteins possibly involved in the thermal stabilisation and adaptation of the phycobilisome, PSII, PSI, and ATP synthase complexes. However, changes in energy metabolism, transcription/translation, amino acid biosynthesis, response mechanisms and other cellular processes are less well researched. This analysis has demonstrated that the molecular organisation of these cellular process are altered in response to heat and provides an ideal platform for further research into their function under heat shock.

In this thesis the role of the histidine kinase Hik34 in the heat shock response has been investigated through the utilisation of the *Δhik34* gene knockout strain of *Synechocystis*. It has been theorised that this protein is involved in the suppression of *hsp* gene expression under normal growth due to the elevated heat tolerant phenotype of the *Δhik34* strain and indication that *hsp* gene transcripts are elevated under normal

growth (Iwane Suzuki, NIBB - personal communication). A comparison of the soluble proteome in wild type and *Δhik34* cells under normal growth, reported in this thesis, has confirmed the observation that Hik34 is involved in the expression of *hsp* genes, as the *Δhik34* knockout mutant demonstrated derepression of *hsp* genes. However, a positive expression role of Hik34 was also demonstrated in this thesis, through the observed inability of the *Δhik34* strain to express the hemolysin protein in the soluble fraction and also through the reduced heat shock induced Hsp level in this strain. This is supported by a previously reported positive regulation role of Hik34 in *hsp* expression in response of *Synechocystis* to salt shock (Marin *et al.*, 2003). Furthermore Hik34 appears to be involved in the regulation of genes not involved in the heat shock response. These results describe a novel heat shock response regulator in cyanobacteria, where the only other previously reported regulator of *hsp* gene expression in cyanobacteria in the *B. subtilis*-like HrcA repressor (Nakamoto *et al.*, 2002). Furthermore, no positive regulation of gene expression under heat shock has been previously reported in cyanobacteria.

The final objective of this thesis was to apply the established 2D DIGE proteomic technology to an investigation into the heat acclimation of the photosynthetic apparatus and more specifically the oxygen evolving machinery. Previous research demonstrated the role of the manganese stabilising polypeptide (MSP), PsbU and Cyt c_{550} proteins in this stabilisation of the oxygen evolving machinery (Kimura *et al.*, 2002), but not a direct role in increased thermotolerance. Thylakoid associated proteins from 1 hour heat acclimated cells and non-acclimated cells were compared via 2D DIGE which revealed 206 spots to change in abundance, 105 of which were positively identified. Of these characterised proteins the GroEL-1, GroEL-2 and

DnaK chaperones increased in abundance by the greatest amount following heat acclimation. These proteins have been previously shown to associate with the membrane (Kovács *et al.*, 2001, Nimura *et al.*, 1996) and potential roles in membrane stabilisation and membrane protein refolding have been reported for chaperones in cells under heat shock (Vigh *et al.*, 1998, Török *et al.*, 1997). Another protein seen to increase in abundance which has had a previously reported role in membrane stabilisation is squalene holpene cyclase (Poralla *et al.*, 2000). These results have suggested that the membrane is destabilised under heat shock and that chaperonins and hopenes function to restore membrane order. This has been supported by the observations of increase membrane fluidity following heat shock (Revathi *et al.*, 1994; Mejia *et al.*, 1995). Components of the photosynthetic and respiratory machinery may also be involved in acclimatisation to high temperature, including phycocyanin and the associated rod linker polypeptides and subunits of the ATP synthase, cytochrome b_6f complex and the type I NAD(P)H dehydrogenase complexes. These results suggest that these proteins are involved in the heat stabilisation of the complexes they are associated with and also they may be involved in the increased production of ATP for subsequent use by ATP dependent molecular chaperone and proteases. Additional to these proteins, which are elevated under heat acclimation conditions, several others were seen to decrease in abundance from the membrane, such as substrate binding proteins. It appears that these proteins are lost from the membrane due to the reported heat induced membrane fluidisation (Revathi *et al.*, 1994; Mejia *et al.*, 1995) and are not replaced by newly synthesised proteins. Finally, there is further evidence in this analysis of the heat acclimation response which supports an observation made from analysis of the heat shock response in chapter 4, that similar responses to carbon starvation and high light are detected in the

response to high temperature. These proteins include NAD(P)H dehydrogenase subunits which have been seen to respond to carbon starvation (Deng *et al.*, 2003) and also the NADH type II and ferrochelatase seen to respond under high light (Howitt *et al.*, 1999; Funk and Vermass, 1999).

This analysis has characterised several proteins that possibly promote stabilisation of the thylakoid membrane and its associated complexes under high temperature, which together function to acclimate the cell and develop thermotolerance. No evidence has been generated which indicates specific protein factors that promote the direct stabilisation of the PSII oxygen evolving machinery, as observed under the acquired thermotolerance. However, it is predicted that future analysis of the low molecular weight proteins, not visualised in the 12 % polyacrylamide gels, may provide candidate proteins for this, as already shown in the 15 % acrylamide analysis of the heat shock response.

The work described in this thesis can not be said to have provided a complete answer to the mechanisms employed by cyanobacteria to survive under heat shock conditions, sense heat and regulate gene expression and also acclimatise to high temperature. However, it does provide an excellent basis for future work. The analysis of enzyme activity and concentration of metabolites will establish whether the Calvin cycle is elevated under heat shock and whether the electron transport and proton translocation across the thylakoid membrane is elevated to increase ATP synthesis. Furthermore, numerous genes have been highlighted for mutagenesis to decipher their role in cellular survival under heat shock, heat induced gene expression and acclimatisation to high temperature. Several hypothetical proteins have also been shown to be

involved in the heat acclimation and shock responses. Mutagenesis of the genes encoding these proteins will help elucidate their function in cyanobacteria. Other future work will involve the application of interactomic technology, such as TAP tagging for the analysis protein-protein interactions under heat acclimation conditions to help elucidate the roles of membrane associated chaperonins. Also, the analysis of *Synechocystis* response regulator (rre) gene knockout strains will allow the identification of a DNA-binding *hsp* gene transcriptional regulator, of which Hik34 controls the activity through a two-component signal transduction mechanism.

The potential of proteomics to decipher the cellular state has been demonstrated in this thesis where the successful application of 2D DIGE technology has been the most striking. However, due to the limitations of 2D-E with respect to low abundant proteins, several proteins involved in the heat shock and acclimation responses have been unidentified. The application of ICAT for the characterisation of these proteins is a possible approach due to the ability, if sample quaintly is not limiting, to analyse low abundant protein species. It is also the intention to compare the proteomic data from both the heat shock and acclimation investigations with the global analysis of mRNA expression under the same experimental conditions via DNA microarray. As little correlation between transcript and protein levels has been previously shown (Gygi *et al.*, 1999), it is predicted that this comparison will demonstrate that not all proteins seen to change in abundance will correlate with a change in the mRNA level. This is due to differences in regulation at the level of transcription and translation and also post translational processing.

Cyanobacteria are amongst the most resistant organisms to environmental stress. Analysis of the genes expressed, the proteins synthesised/modified and the protein-protein interactions under conditions such as high temperature, high light, drought and cold will allow scientists to better understand the mechanisms employed by these organisms to survive and inhabit such environments.

CHAPTER 7

References

Addlesee, H. A., Gibson, L. C., Jensen, P. E. and Hunter, C. N. (1996). Cloning, sequencing and functional assignment of the chlorophyll biosynthesis gene, chlP, of Synechocystis sp. PCC 6803. *FEBS Lett.* **389**, (2), 126-130.

Aebersold, R. H., Teplow, D. B., Hood, L. E. and Kent, S. B. (1986). Electroblotting onto activated glass. High efficiency preparation of proteins from analytical sodium dodecyl sulfate-polyacrylamide gels for direct sequence analysis. *J Biol Chem.* **261**, (9), 4229-4238.

Aebersold, R. H., Leavitt, J., Saavedra, R. A., Hood, L. E. and Kent, S. B. (1987). Internal amino acid sequence analysis of proteins separated by one- or two-dimensional gel electrophoresis after in situ protease digestion on nitrocellulose. *Proc Natl Acad Sci U S A.* **84**, (20), 6970-6974.

Aebersold, R. and Goodlett, D. R. (2001). Mass spectrometry in proteomics. *Chem Rev.* **101**, (2), 269-295.

Agashe, V. R., Guha, S., Chang, H. C., Genevaux, P., Hayer-Hartl, M., Stemp, M., Georgopoulos, C., Hartl, F. U. and Barral, J. M. (2004). Function of trigger factor and DnaK in multidomain protein folding: increase in yield at the expense of folding speed. *Cell.* **117**, (2), 199-209.

Ajlani, G. and Vernotte, C. (1998). Deletion of the PB-loop in the L(CM) subunit does not affect phycobilisome assembly or energy transfer functions in the cyanobacterium Synechocystis sp. PCC6714. *Eur J Biochem.* **257**, (1), 154-159.

Alban, A., David, S. O., Bjorkesten, L., Andersson, C., Sloge, E., Lewis, S. and Currie, I. (2003). A novel experimental design for comparative two-dimensional gel analysis: two-dimensional difference gel electrophoresis incorporating a pooled internal standard. *Proteomics.* **3**, (1), 36-44.

Al-Khaldi, S. F., Coker, J., Shen, J. R. and Burnap, R. L. (2000). Characterization of site-directed mutants in manganese-stabilizing protein (MSP) of Synechocystis sp. PCC6803 unable to grow photoautotrophically in the absence of cytochrome c-550. *Plant Mol Biol.* **43**, (1), 33-41.

Allakhverdiev, S. I., Nishiyama, Y., Suzuki, I., Tasaka, Y. and Murata, N. (1999). Genetic engineering of the unsaturation of fatty acids in membrane lipids alters the tolerance of Synechocystis to salt stress. *Proc Natl Acad Sci U S A.* **96**, (10), 5862-5867.

Allakhverdiev, S. I., Sakamoto, A., Nishiyama, Y., Inaba, M. and Murata, N. (2000a). Ionic and osmotic effects of NaCl-induced inactivation of photosystems I and II in Synechococcus sp. *Plant Physiol.* **123**, (3), 1047-1056.

Allakhverdiev, S. I., Sakamoto, A., Nishiyama, Y. and Murata, N. (2000b). Inactivation of photosystems I and II in response to osmotic stress in Synechococcus. Contribution of water channels. *Plant Physiol.* **122**, (4), 1201-1208.

Allakhverdiev, S. I., Kinoshita, M., Inaba, M., Suzuki, I. and Murata, N. (2001). Unsaturated fatty acids in membrane lipids protect the photosynthetic machinery against salt-induced damage in Synechococcus. *Plant Physiol.* **125**, (4), 1842-1853.

Allakhverdiev, S. I., Nishiyama, Y., Miyairi, S., Yamamoto, H., Inagaki, N., Kanesaki, Y. and Murata, N. (2002). Salt stress inhibits the repair of photodamaged photosystem II by suppressing the transcription and translation of psbA genes in synechocystis. *Plant Physiol.* **130**, (3), 1443-1453.

Allakhverdiev, S. I., Hayashi, H., Nishiyama, Y., Ivanov, A. G., Aliev, J. A., Klimov, V. V., Murata, N. and Carpentier, R. (2003a). Glycinebetaine protects the D1/D2/Cytb559 complex of photosystem II against photo-induced and heat-induced inactivation. *J Plant Physiol.* **160**, (1), 41-49.

Allakhverdiev, S. I., Mohanty, P. and Murata, N. (2003b). Dissection of photodamage at low temperature and repair in darkness suggests the existence of an intermediate form of photodamaged photosystem II. *Biochemistry.* **42**, (48), 14277-14283.

Allakhverdiev, S. I. and Murata, N. (2004). Environmental stress inhibits the synthesis de novo of proteins involved in the photodamage-repair cycle of Photosystem II in Synechocystis sp. PCC 6803. *Biochim Biophys Acta.* **1657**, (1), 23-32.

Allen, M. B. (1952). The cultivation of Myxophyceae. *Arch Mikrobiol.* **17**, 34-53.

Allen, M. M. (1968). Simple conditions for growth of unicellular blue-green algae on plates. *Journal of Phycology.* **4**, 1-3.

Altschul, S. F., Madden, T. L., Schaffer, A. A., Zhang, J., Zhang, Z., Miller, W. and Lipman, D. J. (1997). Gapped BLAST and PSI-BLAST: a new generation of protein database search programs. *Nucleic Acids Res.* **25**, (17), 3389-3402.

Annan, R. S. and Carr, S. A. (1997). The essential role of mass spectrometry in characterizing protein structure: mapping posttranslational modifications. *J Protein Chem.* **16**, (5), 391-402.

Appleby, J. L., Parkinson, J. S. and Bourret, R. B. (1996). Signal transduction via the multi-step phosphorelay: not necessarily a road less traveled. *Cell.* **86**, (6), 845-848.

Armond, P. A., Schreiber, U. and Björkmann, O. (1978). Photosynthetic acclimation to temperature in the desert shrub, *Larreaa divaricata.* II. Light-harvesting efficiency and electro transport. *Plant Physiol.* **61**, 411-415.

Ashby, M. K. and Mullineaux, C. W. (1999). Cyanobacterial ycf27 gene products regulate energy transfer from phycobilisomes to photosystems I and II. *FEMS Microbiol Lett.* **181**, (2), 253-260.

Baier, K., Lehmann, H., Stephan, D. P. and Lockau, W. (2004). NblA is essential for phycobilisome degradation in Anabaena sp. strain PCC 7120 but not for development of functional heterocysts. *Microbiology.* **150**, (Pt 8), 2739-2749.

Bardwell, J. C. and Craig, E. A. (1988). Ancient heat shock gene is dispensable. *J Bacteriol.* **170**, (7), 2977-2983.

Beavis, R. C. and Chait, B. T. (1989). Cinnamic acid derivatives as matrices for ultraviolet laser desorption mass spectrometry of proteins. *Rapid Commun Mass Spectrom.* **3**, (12), 432-435.

Berger, S., Ellersiek, U. and Steinmuller, K. (1991). Cyanobacteria contain a mitochondrial complex I-homologous NADH-dehydrogenase. *FEBS Lett.* **286**, (1-2), 129-132.

Berkelman, T. and Stenstedt, T. (2001). 2-D Electrophoresis uisng immobilized pH gradients: Principles and Methods. *Amersham Biosciences Handbook.*

Berry, J. and Björkman, O. (1980). Photosynthetic response and adaptation to temperature in higher plants. *Ann Rev. Plant. Physiol.* **21**, 491-543.

Bhagwat, A. A. and Apte, S. K. (1989). Comparative analysis of proteins induced by heat shock, salinity, and osmotic stress in the nitrogen-fixing cyanobacterium Anabaena sp. strain L-31. *J Bacteriol.* **171**, (9), 5187-5189.

Bhaya, D., Watanabe, N., Ogawa, T. and Grossman, A. R. (1999). The role of an alternative sigma factor in motility and pilus formation in the cyanobacterium Synechocystis sp. strain PCC6803. *Proc Natl Acad Sci U S A.* **96**, (6), 3188-3193.

Biemann, K. (1990). Namenclature for peptide fragment ions (positive ions). [Apendix 5]. *Methods in Enzymol.* **193**, 110-149.

Bjellqvist, B., Ek, K., Righetti, P. G., Gianazza, E., Görg, A., Westermeier, R. and Postel, W. (1982). Isoelectric focusing in immobilized pH gradients: principle, methodology and some applications. *J Biochem Biophys Methods*. **6**, (4), 317-339.

Bjellqvist, B., Pasquali, C., Ravier, F., Sanchez, J. C. and Hochstrasser, D. (1993). A nonlinear wide-range immobilized pH gradient for two-dimensional electrophoresis and its definition in a relevant pH scale. *Electrophoresis*. **14**, (12), 1357-1365.

Blackstock, W. P. and Weir, M. P. (1999). Proteomics: quantitative and physical mapping of cellular proteins. *Trends Biotechnol*. **17**, 121-127.

Blankenship, R. E. and Prince, R. C. (1985). Excited-state redox potentials and the Z scheme of photosynthesis. *Trends Biochem Sci*. **10**, 382-383.

Bochkareva, E. S., Solovieva, M. E. and Girshovich, A. S. (1998). Targeting of GroEL to SecA on the cytoplasmic membrane of Escherichia coli. *Proc Natl Acad Sci U S A*. **95**, (2), 478-483.

Borbely, G., Suranyi, G., Korcz, A. and Palfi, Z. (1985). Effect of heat shock on protein synthesis in the cyanobacterium Synechococcus sp. strain PCC 6301. *J Bacteriol*. **161**, (3), 1125-1130.

Borchers, C., Peter, J. F., Hall, M. C., Kunkel, T. A. and Tomer, K. B. (2000). Identification of in-gel digested proteins by complementary peptide mass fingerprinting and tandem mass spectrometry data obtained on an electrospray ionization quadrupole time-of-flight mass spectrometer. *Anal Chem*. **72**, (6), 1163-1168.

Borkovich, K. A., Farrelly, F. W., Finkelstein, D. B., Taulien, J. and Lindquist, S. (1989). hsp82 is an essential protein that is required in higher concentrations for growth of cells at higher temperatures. *Mol Cell Biol*. **9**, (9), 3919-3930.

Bradford, M. M. (1976). A rapid and sensitive method for the quantitation of microgram quantities of protein utilizing the principle of protein-dye binding. *Anal Biochem.* **72**, 248-254.

Brown, J. L. and Roberts, W. K. (1976). Evidence that approximately eighty per cent of the soluble proteins from Ehrlich ascites cells are Nalpha-acetylated. *J Biol Chem.* **251**, (4), 1009-1014.

Brown, J. L. (1979). A comparison of the turnover of alpha-N-acetylated and nonacetylated mouse L-cell proteins. *J Biol Chem.* **254**, (5), 1447-1449.

Bryant, D. A. and Cohen-Bazire, G. (1981). Effects of chromatic illumination on cyanobacterial phycobilisomes. Evidence for the specific induction of a second pair of phycocyanin subunits in Pseudanabaena 7409 grown in red light. *Eur J Biochem.* **119**, (2), 415-424.

Buchner, J. (1999). Hsp90 & Co. - a holding for folding. *Trends Biochem Sci.* **24**, (4), 136-141.

Bukau, B. and Horwich, A. L. (1998). The Hsp70 and Hsp60 chaperone machines. *Cell.* **92**, (3), 351-366.

Cannon, S., Wang, P. and Roy, H. (1986). Inhibition of ribulose bisphosphate carboxylase assembly by antibody to a binding protein. *J Cell Biol.* **103**, (4), 1327-1335.

Cheng, M. Y., Hartl, F. U., Martin, J., Pollock, R. A., Kalousek, F., Neupert, W., Hallberg, E. M., Hallberg, R. L. and Horwich, A. L. (1989). Mitochondrial heat-shock protein hsp60 is essential for assembly of proteins imported into yeast mitochondria. *Nature.* **337**, (6208), 620-625.

Chang, C. and Meyerowitz, E. M. (1994). Eukaryotes have "two-component" signal transducers. *Res Microbiol.* **145**, (5-6), 481-486.

Chitnis, P. R. and Nelson, N. (1991). Molecular cloning of the genes encoding two chaperone proteins of the cyanobacterium Synechocystis sp. PCC 6803. *J Biol Chem.* **266**, (1), 58-65.

Choi, J. S., Kim, D. S., Lee, J., Kim, S. J., Kim, S. I., Kim, Y. H., Hong, J., Yoo, J. S., Suh, K. H. and Park, Y. M. (2000). Proteome analysis of light-induced proteins in Synechocystis sp. PCC 6803: identification of proteins separated by 2D-PAGE using N-terminal sequencing and MALDI-TOF MS. *Mol Cells.* **10**, (6), 705-711.

Clarke, S. (1992). Protein isoprenylation and methylation at carboxyl-terminal cysteine residues. *Annu Rev Biochem.* **61**, 355-386.

Clauser, K. R., Baker, P. and Burlingame, A. L. (1999). Role of accurate mass measurement (+/- 10 ppm) in protein identification strategies employing MS or MS/MS and database searching. *Anal Chem.* **71**, (14), 2871-2882.

Cohen-Bazire, G. and Bryant, D. A. (1982). Phycobilisomes: Composition and Structure. In: The Biology of Cyanobacteria. (N. G. Carr and B. A. Whitton, eds.) pp. Blackwell Scientific Publications. (Oxford, UK).

Craig, E. A. and Gross, C. A. (1991). Is hsp70 the cellular thermometer? *Trends Biochem Sci.* **16**, (4), 135-140.

Davis, M. T. and Lee, T. D. (1997). Variable flow liquid chromatography-tendem mass spectrometry and the comprehensive analysis of complex protiein digest mixtures. *J. Am. Soc. Mass. Spectrom.* **8**, 110-121.

De Leenheer, A. P. and Thienpont, L. M. (1992). Application of isotope dillution-mass spectrometry in clinical chemistry, pharmacokinetics, and toxicology. *Mass Spectrom Rev.* **11**, 249-307.

de Marsac, N. T. and Cohen-bazire, G. (1977). Molecular composition of cyanobacterial phycobilisomes. *Proc Natl Acad Sci U S A.* **74**, (4), 1635-1639.

Deng, Y., Ye, J. and Mi, H. (2003). Effects of low CO2 on NAD(P)H dehydrogenase, a mediator of cyclic electron transport around photosystem I in the cyanobacterium synechocystis PCC6803. *Plant Cell Physiol.* **44**, (5), 534-540.

Derre, I., Rapoport, G. and Msadek, T. (1999). CtsR, a novel regulator of stress and heat shock response, controls clp and molecular chaperone gene expression in gram-positive bacteria. *Mol Microbiol.* **31**, (1), 117-131.

Deshnium, P., Gombos, Z., Nishiyama, Y. and Murata, N. (1997). The action in vivo of glycine betaine in enhancement of tolerance of Synechococcus sp. strain PCC 7942 to low temperature. *J Bacteriol.* **179**, (2), 339-344.

Deuerling, E., Schulze-Specking, A., Tomoyasu, T., Mogk, A. and Bukau, B. (1999). Trigger factor and DnaK cooperate in folding of newly synthesized proteins. *Nature.* **400**, (6745), 693-696.

Dilley, R. A., Nishiyama, Y., Gombos, Z. and Murata, N. (2001). Bioenergetic responses of Synechocystis 6803 fatty acid desaturase mutants at low temperatures. *J Bioenerg Biomembr.* **33**, (2), 135-141.

Dixon, D. P., Lapthorn, A. and Edwards, R. (2002). Plant glutathione transferases. *Genome Biol.* **3**, (3), REVIEWS3004.

Dobritsa, S. V., Potter, D., Gookin, T. E. and Berry, A. M. (2001). Hopanoid lipids in Frankia: identification of squalene-hopene cyclase gene sequences. *Can J Microbiol.* **47**, (6), 535-540.

Doering, T. L., Masterson, W. J., Hart, G. W. and Englund, P. T. (1990). Biosynthesis of glycosyl phosphatidylinositol membrane anchors. *J Biol Chem.* **265**, (2), 611-614.

Domain, F., Houot, L., Chauvat, F. and Cassier-Chauvat, C. (2004). Function and regulation of the cyanobacterial genes lexA, recA and ruvB: LexA is critical to the survival of cells facing inorganic carbon starvation. *Mol Microbiol.* **53**, (1), 65-80.

Dove, A. (1999). Proteomics: translating genomics into products? *Nat Biotechnol.* **17**, (3), 233-236.

Duke, C. S., Cezeaux, A. and Allen, M. M. (1989). Changes in polypeptide composition of Synechocystis sp. strain 6308 phycobilisomes induced by nitrogen starvation. *J Bacteriol.* **171**, (4), 1960-1966.

Dunn, M. J. (1987). Two-dimensional gel electrophoresis of proteins. *J Chromatogr.* **418**, 145-185.

Dunn, M. J. and Görg, A. (2001). Two-dimesional polyacrylamide gel electrophoresis for proteome analysis. In: Proteomics: from protein sequence to function. (S. R. Pennington and M. J. Dunn, eds.) pp. 43-63, BIOS Scientific Publishers. (Oxford, UK).

Dvornyk, V. and Nevo, E. (2003). Genetic polymorphism of cyanobacteria under permanent natural stress: a lesson from the "Evolution Canyons". *Res Microbiol.* **154**, (2), 79-84.

Dzelzkalns, V. A. and Bogorad, L. (1986). Stable transformation of the cyanobacterium Synechocystis sp. PCC 6803 induced by UV irradiation. *J Bacteriol.* **165**, (3), 964-971.

Dzelzkalns, V. A., Obinger, C., Regelsberger, G., Niederhauser, H., Kamensek, M., Peschek, G. A. and Bogorad, L. (1994). Deletion of the structural gene for the NADH-dehydrogenase subunit 4 of Synechocystis 6803 alters respiratory properties. *Plant Physiol.* **106**, (4), 1435-1442.

Echlin, P. and Morris, I. (1965). The Relationship between Blue-Green Algae and Bacteria. *Biol Rev Camb Philos Soc.* **40**, 143-187.

Eckardt, N. A. and Portis Jr, A. R. (1997). Heat Denaturation Profiles of Ribulose-1,5-Bisphosphate Carboxylase/Oxygenase (Rubisco) and Rubisco Activase and the Inability of Rubisco Activase to Restore Activity of Heat-Denatured Rubisco. *Plant Physiol.* **113**, (1), 243-248.

Edwards, M. R., Hauer, C., Stack, R. F., Eisele, L. E. and MacColl, R. (1997). Thermophilic C-phycocyanin: Effect of temperature, monomer stability, and structure. *Biochim. Biophys. Acta.* **1321**, 157–164.

Ellis, R. J. (1996). Revisiting the Anfinsen cage. *Fold Des.* **1**, (1), R9-15.

Ellis, R. J. (2000). Chaperone substrates inside the cell. *Trends Biochem Sci.* **25**, (5), 210-212.

Ellis, R. J. (2001). Molecular chaperones: Inside and outside the Anfinsen cage. *Current Biology.* **11**, R1038-R1040.

Ellis, R. J. and van der Vies, S. M. (1991). Molecular chaperones. *Annu. Rev. Biochem.* **60**, 321-347.

Enami, I., Kikuchi, S., Fukuda, T., Ohta, H. and Shen, J. R. (1998). Binding and functional properties of four extrinsic proteins of photosystem II from a red alga, Cyanidium caldarium, as studied by release-reconstitution experiments. *Biochemistry.* **37**, (9), 2787-2793.

Engelman, D. M., Steitz, T. A. and Goldman, A. (1986). Identifying nonpolar transbilayer helices in amino acid sequences of membrane proteins. *Annu Rev Biophys Biophys Chem.* **15**, 321-353.

Eriksson, M. J. and Clarke, A. K. (1996). The heat shock protein ClpB mediates the development of thermotolerance in the cyanobacterium Synechococcus sp. strain PCC 7942. *J Bacteriol.* **178**, (16), 4839-4846.

Eriksson, J., Chait, B. T. and Fenyo, D. (2000). A statistical basis for testing the significance of mass spectrometric protein identification results. *Anal Chem.* **72**, (5), 999-1005.

Ewalt, K. L., Hendrick, J. P., Houry, W. A. and Hartl, F. U. (1997). In vivo observation of polypeptide flux through the bacterial chaperonin system. *Cell.* **90**, (3), 491-500.

Fayet, O., Ziegelhoffer, T. and Georgopoulos, C. (1989). The groES and groEL heat shock gene products of Escherichia coli are essential for bacterial growth at all temperatures. *J Bacteriol.* **171**, (3), 1379-1385.

Feder, M. E. and Hofmann, G. E. (1999). Heat-shock proteins, molecular chaperones, and the stress response: evolutionary and ecological physiology. *Annu Rev Physiol.* **61**, 243-282.

Fenn, J. B., Mann, M., Meng, C. K., Wong, S. F. and Whitehouse, C. M. (1989). Electrospray ionization for mass spectrometry of large biomolecules. *Science*. **246**, (4926), 64-71.

Ferjani, A., Mustardy, L., Sulpice, R., Marin, K., Suzuki, I., Hagemann, M. and Murata, N. (2003). Glucosylglycerol, a compatible solute, sustains cell division under salt stress. *Plant Physiol*. **131**, (4), 1628-1637.

Fernandez-Gonzalez, B., Sandmann, G. and Vioque, A. (1997). A new type of asymmetrically acting beta-carotene ketolase is required for the synthesis of echinenone in the cyanobacterium Synechocystis sp. PCC 6803. *J Biol Chem*. **272**, (15), 9728-9733.

Fernandez-Patron, C., Castellanos-Serra, L., Hardy, E., Guerra, M., Estevez, E., Mehl, E. and Frank, R. W. (1998). Understanding the mechanism of the zinc-ion stains of biomacromolecules in electrophoresis gels: generalization of the reverse-staining technique. *Electrophoresis*. **19**, (14), 2398-2406.

Ferro, M., Seigneurin-Berny, D., Rolland, N., Chapel, A., Salvi, D., Garin, J. and Joyard, J. (2000). Organic solvent extraction as a versatile procedure to identify hydrophobic chloroplast membrane proteins. *Electrophoresis*. **21**, (16), 3517-3526.

Fleischmann, R. D., Adams, M. D., White, O., Clayton, R. A., Kirkness, E. F., Kerlavage, A. R., Bult, C. J., Tomb, J. F., Dougherty, B. A., Merrick, J. M. and et al. (1995). Whole-genome random sequencing and assembly of Haemophilus influenzae Rd. *Science*. **269**, (5223), 496-512.

Fork, D. C., Sen, A. and Williams, W. P. (1987). The relationship between heat-stress and photobleaching in green and blue-algae. *Photosynth. Res*. **11**, 71-87.

Frederick, J. F. (1981). Origins and Evolution of Eukaryotic Intracellular Organells. *Ann. N.Y. Acad. Sci*. **361**, 512.

Friedman, D. I. (1984). Interaction of bacteriophage and host macromolecules in the growth of bacteripphage λ. *Microbiol Rev.* **48**, 299-235.

Friedman, D. B., Hill, S., Keller, J. W., Merchant, N. B., Levy, S. E., Coffey, R. J. and Caprioli, R. M. (2004). Proteome analysis of human colon cancer by two-dimensional difference gel electrophoresis and mass spectrometry. *Proteomics.* **4**, (3), 793-811.

Frishman, D., Albermann, K., Hani, J., Heumann, K., Metanomski, A., Zollner, A. and Mewes, H. W. (2001). Functional and structural genomics using PEDANT. *Bioinformatics.* **17**, (1), 44-57.

Frishman, D., Mokrejs, M., Kosykh, D., Kastenmuller, G., Kolesov, G., Zubrzycki, I., Gruber, C., Geier, B., Kaps, A., Albermann, K., Volz, A., Wagner, C., Fellenberg, M., Heumann, K. and Mewes, H. W. (2003). The PEDANT genome database. *Nucleic Acids Res.* **31**, (1), 207-211.

Frydman, J. (2001). Folding of newly translated proteins in vivo: the role of molecular chaperones. *Annu Rev Biochem.* **70**, 603-647.

Fujiki, Y., Hubbard, A. L., Fowler, S. and Lazarow, P. B. (1982). Isolation of intracellular membranes by means of sodium carbonate treatment: application to endoplasmic reticulum. *J Cell Biol.* **93**, (1), 97-102.

Fulda, S., Huang, F., Nilsson, F., Hagemann, M. and Norling, B. (2000). Proteomics of Synechocystis sp. strain PCC 6803. Identification of periplasmic proteins in cells grown at low and high salt concentrations. *Eur J Biochem.* **267**, (19), 5900-5907.

Funk, C. and Vermaas, W. (1999). A cyanobacterial gene family coding for single-helix proteins resembling part of the light-harvesting proteins from higher plants. *Biochemistry.* **38**, (29), 9397-9404.

Gantt (1994). Supramolecular Membrane Organization. In: The Molecular Biology of Cyanobacteria. (D. A. Bryant, eds.) pp. Kluwer Academic Publishers. (Dordrecht, The Netherlands).

Garcia-Dominguez, M., Muro-Pastor, M. I., Reyes, J. C. and Florencio, F. J. (2000). Light-dependent regulation of cyanobacterial phytochrome expression. *J Bacteriol.* **182**, (1), 38-44.

Gatenby, A. A., van der Vies, S. M. and Bradley, D. (1985). Assembly in E. coli of a functional muli-subunit ribulose bisphosphate carboxylase from a blue green alga. *Nature.* **314**, 617-620.

Georgopoulos, C. P., Hendrix, R. W., Casjens, S. R. and Kaiser, A. D. (1973). Host participation in bacteriophage lambda head assembly. *J Mol Biol.* **76**, (1), 45-60.

Georgopoulos, C. and Welch, W. J. (1993). Role of the major heat shock proteins as molecular chaperones. *Annu Rev Cell Biol.* **9**, 601-634.

Gibbs, R. A., Weinstock, G. M., Metzker *et al.*, and Collins, F. (2004). Genome sequence of the Brown Norway rat yields insights into mammalian evolution. *Nature.* **428**, (6982), 493-521.

Glatz, A., Horváth, I., Varvasovszki, V., Kovács, E., Török, Z. and Vigh, L. (1997). Chaperonin genes of the Synechocystis PCC 6803 are differentially regulated under light-dark transition during heat stress. *Biochem Biophys Res Commun.* **239**, (1), 291-297.

Glazer, A. N. and Fang, S. (1973). Chromophore content of blue-green algal phycobiliproteins. *J Biol Chem.* **248**, (2), 659-662.

Glazer, A. N. and Hixson, C. S. (1975). Characterization of R-phycocyanin. Chromophore content of R-phycocyanin and C-phycoerythrin. *J Biol Chem*. **250**, (14), 5487-5495.

Golecki, J. R. and Drews, G. (1982). Supramolecular organisation and composition of membranes. In: The Biology of Cyanobacteria. (N. G. Carr and B. A. Whitton, eds.) pp. Blackwell Scientific Publications. (Oxford, UK).

Gombos, Z., Wada, H. and Murata, N. (1992). Unsaturation of fatty acids in membrane lipids enhances tolerance of the cyanobacterium Synechocystis PCC6803 to low-temperature photoinhibition. *Proc Natl Acad Sci U S A*. **89**, (20), 9959-9963.

Gombos, Z., Wada, H., Hideg, E. and Murata, N. (1994). The unsaturation of membrane lipids stabilizes photosynthesis against heat stress. *Plant Physiol*. **104**, 563-567.

Görg, A., Postel, W. and Gunther, S. (1988). The current state of two-dimensional electrophoresis with immobilized pH gradients. *Electrophoresis*. **9**, (9), 531-546.

Görg, A., Obermaier, C., Boguth, G. and Weiss, W. (1999). Recent developments in two-dimensional gel electrophoresis with immobilized pH gradients: wide pH gradients up to pH 12, longer separation distances and simplified procedures. *Electrophoresis*. **20**, (4-5), 712-717.

Görg, A., Obermaier, C., Boguth, G., Harder, A., Scheibe, B., Wildgruber, R. and Weiss, W. (2000). The current state of two-dimensional electrophoresis with immobilized pH gradients. *Electrophoresis*. **21**, (6), 1037-1053.

Gotz, T., Windhovel, U., Boger, P. and Sandmann, G. (1999). Protection of photosynthesis against ultraviolet-B radiation by carotenoids in transformants of the cyanobacterium synechococcus PCC7942. *Plant Physiol*. **120**, (2), 599-604.

Granier, F. (1988). Extraction of plant proteins for two-dimensional electrophoresis. *Electrophoresis.* **9**, (11), 712-718.

Grigorieva, G. and Shestakov, S. V. (1982). Transformation in the cyanobacterium Synechocystis sp. PCC 6803. *FEMS Microbiology Letters.* **13**, 367-370.

Grossman, A. R., Schaefer, M. R., Chiang, G. G. and Collier, J. L. (1993). The phycobilisome, a light-harvesting complex responsive to environmental conditions. *Microbiol Rev.* **57**, (3), 725-749.

Grossman, A. R., Bhaya, D. and He, Q. (2001). Tracking the light environment by cyanobacteria and the dynamic nature of light harvesting. *J Biol Chem.* **276**, (15), 11449-11452.

Gupta, R. S. (1990). Sequence and structural homology between a mouse T-complex protein TCP-1 and the 'chaperonin' family of bacterial (GroEL, 60-65 kDa heat shock antigen) and eukaryotic proteins. *Biochem Int.* **20**, (4), 833-841.

Gygi, S. P., Rist, B., Gerber, S. A., Turecek, F., Gelb, M. H. and Aebersold, R. (1999a). Quantitative analysis of complex protein mixtures using isotope-coded affinity tags. *Nat Biotechnol.* **17**, (10), 994-999.

Gygi, S. P., Rochon, Y., Franza, B. R. and Aebersold, R. (1999b). Correlation between protein and mRNA abundance in yeast. *Mol Cell Biol.* **19**, (3), 1720-1730.

Haebel, S., Albrecht, T., Sparbier, K., Walden, P., Korner, R. and Steup, M. (1998). Electrophoresis-related protein modification: alkylation of carboxy residues revealed by mass spectrometry. *Electrophoresis.* **19**, (5), 679-686.

Hagemann, M., Tchel, D. and Rensing, L. (1991). Comparison of salt-induced and hest-induced alterations of protein synthesis in the cyanobacterium Synechocystis sp. PCC 6803. *Archives of Microbiology.* **155**, (6), 587-592.

Hagemann, M., Golldack, D., Biggins, J. and Erdmann, N. (1993). SAlt-dependent protein-phosporylation in the cyanobacterium Synechocystis PCC-6803. *FEMS Microbiology Letters.* **113**, (2), 205-210.

Haley, D. A., Bova, M. P., Huang, Q. L., McHaourab, H. S. and Stewart, P. L. (2000). Small heat-shock protein structures reveal a continuum from symmetric to variable assemblies. *J Mol Biol.* **298**, (2), 261-272.

Harmon, F. G., Rehrauer, W. M. and Kowalczykowski, S. C. (1996). Interaction of Escherichia coli RecA protein with LexA repressor. II. Inhibition of DNA strand exchange by the uncleavable LexA S119A repressor argues that recombination and SOS induction are competitive processes. *J Biol Chem.* **271**, (39), 23874-23883.

Hartinger, J., Stenius, K., Hogemann, D. and Jahn, R. (1996). 16-BAC/SDS-PAGE: a two-dimensional gel electrophoresis system suitable for the separation of integral membrane proteins. *Anal Biochem.* **240**, (1), 126-133.

Hartl, F. U. and Neupert, W. (1990). Protein sorting to mitochondria: evolutionary conservations of folding and assembly. *Science.* **247**, (4945), 930-938.

Hartl, F. U., Martin, J. and Neupert, W. (1992). Protein folding in the cell: the role of molecular chaperones Hsp70 and Hsp60. *Annu Rev Biophys Biomol Struct.* **21**, 293-322.

Hartl, F. U. (1996). Molecular chaperones in cellular protein folding. *Nature.* **381**, (6583), 571-579.

Haynes, P. A., Gygi, S. P., Figeys, D. and Aebersold, R. (1998). Proteome analysis: biological assay or data archive? *Electrophoresis.* **19**, (11), 1862-1871.

Heckathorn, S. A., Downs, C. A., Sharkey, T. D. and Coleman, J. S. (1998). The small, methionine-rich chloroplast heat-shock protein protects photosystem II electron transport during heat stress. *Plant Physiol.* **116**, 439-444.

Hecker, M. and Volker, U. (1998). Non-specific, general and multiple stress resistance of growth-restricted Bacillus subtilis cells by the expression of the sigmaB regulon. *Mol Microbiol.* **29**, (5), 1129-1136.

Hemmingsen, S. M., Woolford, C., van der Vies, S. M., Tilly, K., Dennis, D. T., Georgopoulos, C. P., Hendrix, R. W. and Ellis, R. J. (1988). Homologous plant and bacterial proteins chaperone oligomeric protein assembly. *Nature.* **333**, (6171), 330-334.

Hendrick, J. P. and Hartl, F. U. (1993). Molecular chaperone functions of heat-shock proteins. *Annu Rev Biochem.* **62**, 349-384.

Hendrix, R. W. (1979). Purification and properties of groE, a host protein involved in bacteriophage assembly. *J Mol Biol.* **129**, (3), 375-392.

Herbert, B. R., Molloy, M. P., Gooley, A. A., Walsh, B. J., Bryson, W. G. and Williams, K. L. (1998). Improved protein solubility in two-dimensional electrophoresis using tributyl phosphine as reducing agent. *Electrophoresis.* **19**, (5), 845-851.

Herdman, M., Janvier, M., Waterbury, J. B., Rippka, R. and Stanier, R. Y. (1979). Deoxyribonucleic acid base composition of cyanobacteria. *J. Gen. Microbiol.* **111**, 63-71.

Herman, C., Thevenet, D., D'Ari, R. and Bouloc, P. (1995). Degradation of sigma 32, the heat shock regulator in Escherichia coli, is governed by HflB. *Proc Natl Acad Sci U S A.* **92**, (8), 3516-3520.

Herranen, M., Battchikova, N., Zhang, P., Graf, A., Sirpio, S., Paakkarinen, V. and Aro, E. M. (2004). Towards functional proteomics of membrane protein complexes in Synechocystis sp. PCC 6803. *Plant Physiol.* **134**, (1), 470-481.

Heukeshoven, J. and Dernick, R. (1988). Improved silver staining procedure for fast staining in PhastSystem Development Unit. I. Staining of sodium dodecyl sulfate gels. *Electrophoresis.* **9**, (1), 28-32.

Hewick, R. M., Hunkapiller, M. W., Hood, L. E. and Dreyer, W. J. (1981). A gas-liquid solid phase peptide and protein sequenator. *J Biol Chem.* **256**, (15), 7990-7997.

Hihara, Y., Sonoike, K. and Ikeuchi, M. (1998). A novel gene, pmgA, specifically regulates photosystem stoichiometry in the cyanobacterium Synechocystis species PCC 6803 in response to high light. *Plant Physiol.* **117**, (4), 1205-1216.

Hihara, Y., Kamei, A., Kanehisa, M., Kaplan, A. and Ikeuchi, M. (2001). DNA microarray analysis of cyanobacterial gene expression during acclimation to high light. *Plant Cell.* **13**, (4), 793-806.

Hihara, Y., Sonoike, K., Kanehisa, M. and Ikeuchi, M. (2003). DNA microarray analysis of redox-responsive genes in the genome of the cyanobacterium Synechocystis sp. strain PCC 6803. *J Bacteriol.* **185**, (5), 1719-1725.

Hirani, T. A., Suzuki, I., Murata, N., Hayashi, H. and Eaton-Rye, J. J. (2001). Characterization of a two-component signal transduction system involved in the induction of alkaline phosphatase under phosphate-limiting conditions in Synechocystis sp. PCC 6803. *Plant Mol Biol.* **45**, (2), 133-144.

Hodges, P. E., Payne, W. E. and Garrels, J. I. (1998). The Yeast Protein Database (YPD): a curated proteome database for Saccharomyces cerevisiae. *Nucleic Acids Res.* **26**, (1), 68-72.

Horváth, I., Glatz, A., Varvasovszki, V., Török, Z., Pali, T., Balogh, G., Kovács, E., Nadasdi, L., Benko, S., Joo, F. and Vigh, L. (1998). Membrane physical state controls the signaling mechanism of the heat shock response in Synechocystis PCC 6803: identification of hsp17 as a "fluidity gene". *Proc Natl Acad Sci U S A*. **95**, (7), 3513-3518.

Howitt, C. A., Udall, P. K. and Vermaas, W. F. (1999). Type 2 NADH dehydrogenases in the cyanobacterium Synechocystis sp. strain PCC 6803 are involved in regulation rather than respiration. *J Bacteriol*. **181**, (13), 3994-4003.

Hsiao, H. Y., He, Q., Van Waasbergen, L. G. and Grossman, A. R. (2004). Control of photosynthetic and high-light-responsive genes by the histidine kinase DspA: negative and positive regulation and interactions between signal transduction pathways. *J Bacteriol*. **186**, (12), 3882-3888.

Huang, F., Parmryd, I., Nilsson, F., Persson, A. L., Pakrasi, H. B., Andersson, B. and Norling, B. (2002). Proteomics of Synechocystis sp. strain PCC 6803: identification of plasma membrane proteins. *Mol Cell Proteomics*. **1**, (12), 956-966.

Huckauf, J., Nomura, C., Forchhammer, K. and Hagemann, M. (2000). Stress responses of Synechocystis sp. strain PCC 6803 mutants impaired in genes encoding putative alternative sigma factors. *Microbiology*. **146 (Pt 11)**, 2877-2889.

Hughes, T. R., Marton, M. J., Jones, A. R., Roberts, C. J., Stoughton, R., Armour, C. D., Bennett, H. A., Coffey, E., Dai, H., He, Y. D., Kidd, M. J., King, A. M., Meyer, M. R., Slade, D., Lum, P. Y., Stepaniants, S. B., Shoemaker, D. D., Gachotte, D., Chakraburtty, K., Simon, J., Bard, M. and Friend, S. H. (2000). Functional discovery via a compendium of expression profiles. *Cell*. **102**, (1), 109-126.

Hunter, T. (1995). Protein kinases and phosphatases: the yin and yang of protein phosphorylation and signaling. *Cell*. **80**, (2), 225-236.

Iliopoulos, I., Tsoka, S., Andrade, M. A., Janssen, P., Audit, B., Tramontano, A., Valencia, A., Leroy, C., Sander, C. and Ouzounis, C. A. (2001). Genome sequences and great expectations. *Genome Biol.* **2**, (1), INTERACTIONS0001.

Inaba, M., Suzuki, I., Szalontai, B., Kanesaki, Y., Los, D. A., Hayashi, H. and Murata, N. (2003). Gene-engineered rigidification of membrane lipids enhances the cold inducibility of gene expression in synechocystis. *J Biol Chem.* **278**, (14), 12191-12198.

Initiative, T. A. (2000). Analysis of the genome sequence of the flowering plant Arabidopsis thaliana. *Nature.* **408**, (6814), 796-815.

Iyer, V., Fernandes, T. and Apte, S. K. (1994). A role for osmotic stress-induced proteins in the osmotolerance of a nitrogen-fixing cyanobacterium, Anabaena sp. strain L-31. *J Bacteriol.* **176**, (18), 5868-5870.

Jaenicke, R. (1991). Protein folding: local structures, domains, subunits, and assemblies. *Biochemistry.* **30**, (13), 3147-3161.

Jakob, U., Lilie, H., Meyer, I. and Buchner, J. (1995). Transient interaction of Hsp90 with early unfolding intermediates of citrate synthase. Implications for heat shock in vivo. *J Biol Chem.* **270**, (13), 7288-7294.

Jardine, I. (1990). Molecular weight analysis of proteins. *Methods in Enzymol.* **193**, 441-445.

Jay, G. D., Culp, D. J. and Jahnke, M. R. (1990). Silver staining of extensively glycosylated proteins on sodium dodecyl sulfate-polyacrylamide gels: enhancement by carbohydrate-binding dyes. *Anal Biochem.* **185**, (2), 324-330.

Jensen, O. N., Podtelejnikov, A. V. and Mann, M. (1997). Identification of the components of simple protein mixtures by high-accuracy peptide mass mapping and database searching. *Anal Chem.* **69**, (23), 4741-4750.

Jensen, O. N. (2004). Modification-specific proteomics: characterization of post-translational modifications by mass spectrometry. *Curr Opin Chem Biol.* **8**, (1), 33-41.

Johnson, D. R., Bhatnagar, R. S., Knoll, L. J. and Gordon, J. I. (1994). Genetic and biochemical studies of protein N-myristoylation. *Annu Rev Biochem.* **63**, 869-914.

Jurgens, U. J. and Weckesser, J. (1985). Carotenoid-containing outer membrane of Synechocystis sp. strain PCC6714. *J Bacteriol.* **164**, (1), 384-389.

Kakimoto, T. (1996). CKI1, a histidine kinase homolog implicated in cytokinin signal transduction. *Science.* **274**, (5289), 982-985.

Kaneko, T., Tanaka, A., Sato, S., Kotani, H., Sazuka, T., Miyajima, N., Sugiura, M. and Tabata, S. (1995). Sequence analysis of the genome of the unicellular cyanobacterium Synechocystis sp. strain PCC6803. I. Sequence features in the 1 Mb region from map positions 64% to 92% of the genome. *DNA Res.* **2**, (4), 153-166, 191-158.

Kaneko, T., Sato, S., Kotani, H., Tanaka, A., Asamizu, E., Nakamura, Y., Miyajima, N., Hirosawa, M., Sugiura, M., Sasamoto, S., Kimura, T., Hosouchi, T., Matsuno, A., Muraki, A., Nakazaki, N., Naruo, K., Okumura, S., Shimpo, S., Takeuchi, C., Wada, T., Watanabe, A., Yamada, M., Yasuda, M. and Tabata, S. (1996). Sequence analysis of the genome of the unicellular cyanobacterium Synechocystis sp. strain PCC6803. II. Sequence determination of the entire genome and assignment of potential protein-coding regions. *DNA Res.* **3**, (3), 109-136.

Kanesaki, Y., Suzuki, I., Allakhverdiev, S. I., Mikami, K. and Murata, N. (2002). Salt stress and hyperosmotic stress regulate the expression of different sets of genes in Synechocystis sp. PCC 6803. *Biochem Biophys Res Commun*. **290**, (1), 339-348.

Kang, P. J., Ostermann, J., Shilling, J., Neupert, W., Craig, E. A. and Pfanner, N. (1990). Requirement for hsp70 in the mitochondrial matrix for translocation and folding of precursor proteins. *Nature*. **348**, (6297), 137-143.

Karras, M. and Hillenkamp, F. (1988). Laser desorption ionisation of proteins with molecular masses exceeding 10 000 daltons. *Anal Chem*. **63**, 174-178.

Katoh, H., Hagino, N., Grossman, A. R. and Ogawa, T. (2001). Genes essential to iron transport in the cyanobacterium Synechocystis sp. strain PCC 6803. *J Bacteriol*. **183**, (9), 2779-2784.

Kerfeld, C. A., Sawaya, M. R., Brahmandam, V., Cascio, D., Ho, K. K., Trevithick-Sutton, C. C., Krogmann, D. W. and Yeates, T. O. (2003). The crystal structure of a cyanobacterial water-soluble carotenoid binding protein. *Structure (Camb)*. **11**, (1), 55-65.

Kim, K. K., Kim, R. and Kim, S. H. (1998). Crystal structure of a small heat-shock protein. *Nature*. **394**, (6693), 595-599.

Kimura, A., Eaton-Rye, J. J., Morita, E. H., Nishiyama, Y. and Hayashi, H. (2002). Protection of the oxygen-evolving machinery by the extrinsic proteins of photosystem II is essential for development of cellular thermotolerance in Synechocystis sp. PCC 6803. *Plant Cell Physiol*. **43**, (8), 932-938.

Klose, J. (1999). Genotypes and phenotypes. *Electrophoresis*. **20**, (4-5), 643-652.

Kobayashi, M., Ishizuka, T., Katayama, M., Kanehisa, M., Bhattacharyya-Pakrasi, M., Pakrasi, H. B. and Ikeuchi, M. (2004). Response to oxidative stress involves a novel peroxiredoxin gene in the unicellular cyanobacterium Synechocystis sp. PCC 6803. *Plant Cell Physiol.* **45**, (3), 290-299.

Kormanec, J., Homerova, D., Barak, I. and Sevcikova, B. (1999). A new gene, sigG, encoding a putative alternative sigma factor of Streptomyces coelicolor A3(2). *FEMS Microbiol Lett.* **172**, (2), 153-158.

Kovács, E., Török, Z., Horváth, I. and Vigh, L. (1994). Heat-stress induces association of the GroEL-analog chaperonin with the thylakoid membranes incyanobacterium *Synechocystis* PCC 6803. *Plant Physiol. Biochem.* **32**, 285-293.

Kovács, E., van der Vies, S. M., Glatz, A., Török, Z., Varvasovszki, V., Horváth, I. and Vigh, L. (2001). The chaperonins of Synechocystis PCC 6803 differ in heat inducibility and chaperone activity. *Biochem Biophys Res Commun.* **289**, (4), 908-915.

Kunst, F., Ogasawara, N., Moszer, I., Albertini, A. M., Alloni, G., Azevedo, V., Bertero, M. G., Bessieres, P., Bolotin, A., Borchert, S., Borriss, R., Boursier, L., Brans, A., Braun, M., Brignell, S. C., Bron, S., Brouillet, S., Bruschi, C. V., Caldwell, B., Capuano, V., Carter, N. M., Choi, S. K., Codani, J. J., Connerton, I. F., Danchin, A. and et al. (1997). The complete genome sequence of the gram-positive bacterium Bacillus subtilis. *Nature.* **390**, (6657), 249-256.

Kyrpides, N. C. (1999). Genomes OnLine Database (GOLD 1.0): a monitor of complete and ongoing genome projects world-wide. *Bioinformatics.* **15**, (9), 773-774.

Laemmli, U. K. (1970). Cleavage of structural proteins during the assembly of the head of bacteriophage T4. *Nature.* **227**, (259), 680-685.

Lander, E. S., Linton, L. M., Birren, B., *et al.*, and Chen, Y. J. (2001). Initial sequencing and analysis of the human genome. *Nature*. **409**, (6822), 860-921.

Langer, T., Lu, C., Echols, H., Flanagan, J., Hayer, M. K. and Hartl, F. U. (1992a). Successive action of DnaK, DnaJ and GroEL along the pathway of chaperone-mediated protein folding. *Nature*. **356**, (6371), 683-689.

Langer, T., Pfeifer, G., Martin, J., Baumeister, W. and Hartl, F. U. (1992b). Chaperonin-mediated protein folding: GroES binds to one end of the GroEL cylinder, which accommodates the protein substrate within its central cavity. *Embo J.* **11**, (13), 4757-4765.

Lashkari, D. A., DeRisi, J. L., McCusker, J. H., Namath, A. F., Gentile, C., Hwang, S. Y., Brown, P. O. and Davis, R. W. (1997). Yeast microarrays for genome wide parallel genetic and gene expression analysis. *Proc Natl Acad Sci U S A*. **94**, (24), 13057-13062.

Lee, N., Goodlett, D. R., Ishitani, A., Marquardt, H. and Geraghty, D. E. (1998a). HLA-E surface expression depends on binding of TAP-dependent peptides derived from certain HLA class I signal sequences. *J Immunol*. **160**, (10), 4951-4960.

Lee, S., Prochaska, D. J., Fang, F. and Barnum, S. R. (1998b). A 16.6-kilodalton protein in the Cyanobacterium synechocystis sp. PCC 6803 plays a role in the heat shock response. *Curr Microbiol*. **37**, (6), 403-407.

Lee, G. J. and Vierling, E. (2000). A small heat shock protein cooperates with heat shock protein 70 systems to reactivate a heat-denatured protein. *Plant Physiol*. **122**, (1), 189-198.

Lehel, C., Wada, H., Kovács, E., Török, Z., Gombos, Z., Horváth, I., Murata, N. and Vigh, L. (1992). Heat shock protein synthesis of the cyanobacterium Synechocystis PCC 6803: purification of the GroEL-related chaperonin. *Plant Mol Biol*. **18**, (2), 327-336.

Lehel, C., Gombos, Z., Török, Z. and Vigh, L. (1993a). Growth temperature modulates thermotolerance and heat shock response in cyanobacterium *Synechocystis* PCC 6803. *Plant Physiol Biochem*. **31**, 81-88.

Lehel, C., Los, D., Wada, H., Gyorgyei, J., Horvath, I., Kovacs, E., Murata, N. and Vigh, L. (1993b). A second groEL-like gene, organized in a groESL operon is present in the genome of Synechocystis sp. PCC 6803. *J Biol Chem*. **268**, (3), 1799-1804.

Leonhardt, S. A., Fearson, K., Danese, P. N. and Mason, T. L. (1993). HSP78 encodes a yeast mitochondrial heat shock protein in the Clp family of ATP-dependent proteases. *Mol Cell Biol*. **13**, (10), 6304-6313.

Liang, P. and Pardee, A. B. (1992). Differential display of eukaryotic messenger RNA by means of the polymerase chain reaction. *Science*. **257**, (5072), 967-971.

Liberek, K., Marszalek, J., Ang, D., Georgopoulos, C. and Zylicz, M. (1991a). Escherichia coli DnaJ and GrpE heat shock proteins jointly stimulate ATPase activity of DnaK. *Proc Natl Acad Sci U S A*. **88**, (7), 2874-2878.

Liberek, K., Skowyra, D., Zylicz, M., Johnson, C. and Georgopoulos, C. (1991b). The Escherichia coli DnaK chaperone, the 70-kDa heat shock protein eukaryotic equivalent, changes conformation upon ATP hydrolysis, thus triggering its dissociation from a bound target protein. *J Biol Chem*. **266**, (22), 14491-14496.

Link, A. J., Eng, J., Schieltz, D. M., Carmack, E., Mize, G. J., Morris, D. R., Garvik, B. M. and Yates, J. R., 3rd (1999). Direct analysis of protein complexes using mass spectrometry. *Nat Biotechnol*. **17**, (7), 676-682.

Link, A. J., Eng, J., Schieltz, D. M., Carmack, E., Mize, G. J., Morris, D. R., Garvik, B. M. and Yates, J. R., 3rd (1999). Direct analysis of protein complexes using mass spectrometry. *Nat Biotechnol.* **17**, (7), 676-682.

Loo, J. A., Edmonds, C. G. and Smith, R. D. (1993). Tandem mass spectrometry of very large molecules. 2. Dissociation of multiply charged proline-containing proteins from electrospray ionization. *Anal Chem.* **65**, (4), 425-438.

Lorkovic, Z. J., Schroder, W. P., Pakrasi, H. B., Irrgang, K. D., Herrmann, R. G. and Oelmuller, R. (1995). Molecular characterization of PsbW, a nuclear-encoded component of the photosystem II reaction center complex in spinach. *Proc Natl Acad Sci U S A.* **92**, (19), 8930-8934.

Los, D. A. and Murata, N. (1999). Responses to cold shock in cyanobacteria. *J Mol Microbiol Biotechnol.* **1**, (2), 221-230.

Lowry, O. H., Rosebrough, N. J., Farr, A. L. and Randall, R. J. (1951). Protein measurement with the Folin phenol reagent. *J Biol Chem.* **193**, (1), 265-275.

Loyall, L., Uchida, K., Braun, S., Furuya, M. and Frohnmeyer, H. (2000). Glutathione and a UV light-induced glutathione S-transferase are involved in signaling to chalcone synthase in cell cultures. *Plant Cell.* **12**, (10), 1939-1950.

Luque, I., Zabulon, G., Contreras, A. and Houmard, J. (2001). Convergence of two global transcriptional regulators on nitrogen induction of the stress-acclimation gene nblA in the cyanobacterium Synechococcus sp. PCC 7942. *Mol Microbiol.* **41**, (4), 937-947.

MacColl, R. (1998). Cyanobacterial phycobilisomes. *J Struct Biol.* **124**, (2-3), 311-334.

Maeda, T., Wurgler-Murphy, S. M. and Saito, H. (1994). A two-component system that regulates an osmosensing MAP kinase cascade in yeast. *Nature.* **369**, (6477), 242-245.

Mamedov, M. D., Hayashi, H. and Murata, N. (1993). Effects of glycinebetaine and unsaturation of membrane lipids on heat stability of photosynthetic electron-transport and phosphorylation reactions in *Synechocystis* sp. PCC 6803. *Biochem Biophys Acta.* **1142**, 1-5.

Mann, M. and Wilm, M. (1994). Error-tolerant identification of peptides in sequence databases by peptide sequence tags. *Anal Chem.* **66**, (24), 4390-4399.

Mao, H. B., Li, G. F., Li, D. H., Wu, Q. Y., Gong, Y. D., Zhang, X. F. and Zhao, N. M. (2003). Effects of glycerol and high temperatures on structure and function of phycobilisomes in Synechocystis sp. PCC 6803. *FEBS Lett.* **553**, (1-2), 68-72.

Marin, K., Suzuki, I., Yamaguchi, K., Ribbeck, K., Yamamoto, H., Kanesaki, Y., Hagemann, M. and Murata, N. (2003). Identification of histidine kinases that act as sensors in the perception of salt stress in Synechocystis sp. PCC 6803. *Proc Natl Acad Sci U S A.* **100**, (15), 9061-9066.

McMullin, T. W. and Hallberg, R. L. (1987). A normal mitochondrial protein is selectively synthesized and accumulated during heat shock in Tetrahymena thermophila. *Mol Cell Biol.* **7**, (12), 4414-4423.

Mejia, R., Gomez-Eichelmann, M. C. and Fernandez, M. S. (1995). Membrane fluidity of Escherichia coli during heat-shock. *Biochim Biophys Acta.* **1239**, (2), 195-200.

Mereschkowsky, C. (1905). Über Natur and Ursprung der Chromatophoren in Pflanzenreiche. *Biol Centr.* **25**, 593-604.

Meyer, T. S. and Lamberts, B. L. (1965). Use of coomassie brilliant blue R250 for the electrophoresis of microgram quantities of parotid saliva proteins on acrylamide-gel strips. *Biochim Biophys Acta.* **107,** (1), 144-145.

Mikami, K., Dulai, S., Suplice, R., Takahashi, S., Ferjani, A., Suzuki, I. and Murata, N. (2003). Histidine kinases, Hik2, Hik6 and Hik33, in Synechocystis sp. PCC 6803 are involved in the Tolerance of photosystem II to environmental stress. *Plant Cell Physiol.* **43 Suppl,** S82-S82.

Missiakas, D. and Raina, S. (1998). The extracytoplasmic function sigma factors: role and regulation. *Mol Microbiol.* **28,** (6), 1059-1066.

Mizuno, T., Kaneko, T. and Tabata, S. (1996). Compilation of all genes encoding bacterial two-component signal transducers in the genome of the cyanobacterium, Synechocystis sp. strain PCC 6803. *DNA Res.* **3,** (6), 407-414.

Model, P., Jovanovic, G. and Dworkin, J. (1997). The Escherichia coli phage-shock-protein (psp) operon. *Mol Microbiol.* **24,** (2), 255-261.

Mogk, A., Homuth, G., Scholz, C., Kim, L., Schmid, F. X. and Schumann, W. (1997). The GroE chaperonin machine is a major modulator of the CIRCE heat shock regulon of Bacillus subtilis. *Embo J.* **16,** (15), 4579-4590.

Mogk, A., Tomoyasu, T., Goloubinoff, P., Rudiger, S., Roder, D., Langen, H. and Bukau, B. (1999). Identification of thermolabile Escherichia coli proteins: prevention and reversion of aggregation by DnaK and ClpB. *Embo J.* **18,** (24), 6934-6949.

Molloy, M. P., Herbert, B. R., Walsh, B. J., Tyler, M. I., Traini, M., Sanchez, J. C., Hochstrasser, D. F., Williams, K. L. and Gooley, A. A. (1998). Extraction of membrane proteins by differential solubilization for separation using two-dimensional gel electrophoresis. *Electrophoresis.* **19,** (5), 837-844.

Morgan, T. R., Shand, J. A., Clarke, S. M. and Eaton-Rye, J. J. (1998). Specific requirements for cytochrome c-550 and the manganese-stabilizing protein in photoautotrophic strains of Synechocystis sp. PCC 6803 with mutations in the domain Gly-351 to Thr-436 of the chlorophyll-binding protein CP47. *Biochemistry.* **37**, (41), 14437-14449.

Morimoto, R. I. (1998). Regulation of the heat shock transcriptional response: cross talk between a family of heat shock factors, molecular chaperones, and negative regulators. *Genes Dev.* **12**, (24), 3788-3796.

Muramatsu, M. and Hihara, Y. (2003). Transcriptional regulation of genes encoding subunits of photosystem I during acclimation to high-light conditions in Synechocystis sp. PCC 6803. *Planta.* **216**, (3), 446-453.

Muro-Pastor, A. M., Herrero, A. and Flores, E. (2001). Nitrogen-regulated group 2 sigma factor from Synechocystis sp. strain PCC 6803 involved in survival under nitrogen stress. *J Bacteriol.* **183**, (3), 1090-1095.

Nagai, T., Ru, S., Katoh, A., Dong, S. and Kuwabara, T. (2001). An extracellular hemolysin homolog from cyanobacterium Synechocystis sp. PCC6803. *In Proceedings of the 12th International Congress on Photosynthesis.* S36-010.

Nagarka, S. (2002). Cyanobacteria culture collection: a unique resource for ecology and biotechnology research. *Porcupine: Newsletter of the Department of Ecology and Biodiversity, The University of Hong Kong.* **25**, 22-23.

Nakai, M., Nohara, T., Sugita, D. and Endo, T. (1994). Identification and characterization of the sec-A protein homologue in the cyanobacterium Synechococcus PCC7942. *Biochem Biophys Res Commun.* **200**, (2), 844-851.

Nakamoto, H., Suzuki, N. and Roy, S. K. (2000). Constitutive expression of a small heat-shock protein confers cellular thermotolerance and thermal protection to the photosynthetic apparatus in cyanobacteria. *FEBS Lett.* **483**, (2-3), 169-174.

Nakamoto, H., Tanaka, N. and Ishikawa, N. (2001). A novel heat shock protein plays an important role in thermal stress management in cyanobacteria. *J Biol Chem.* **276**, (27), 25088-25095.

Nakamoto, H., Suzuki, M. and Kojima, K. (2002). Regulation of heat shock gene transcription in cyanobacteria. *Plant Cell Pysiol.* **43 Suppl**, s115-s115.

Nakamura, Y., Kaneko, T., Hirosawa, M., Miyajima, N. and Tabata, S. (1998). CyanoBase, a www database containing the complete nucleotide sequence of the genome of Synechocystis sp. strain PCC6803. *Nucleic Acids Res.* **26**, (1), 63-67.

Narberhaus, F. (1999). Negative regulation of bacterial heat shock genes. *Mol Microbiol.* **31**, (1), 1-8.

Nash, D., Miyao, M. and Murata, N. (1985). Heat inactivation of oxygen evolution in photosystem II particles and its acceleration by chloride depletion adn manganese. *Biochem Biophys Acta.* **807**, 127-133.

Neidhardt, F. C., VanBogelen, R. A. and Vaughn, V. (1984). The genetics and regulation of heat-shock proteins. *Annu Rev Genet.* **18**, 295-329.

Nelson, R. J., Ziegelhoffer, T., Nicolet, C., Werner-Washburne, M. and Craig, E. A. (1992). The translation machinery and 70 kd heat shock protein cooperate in protein synthesis. *Cell.* **71**, (1), 97-105.

Nelson, R. W., Nedelkov, D. and Tubbs, K. A. (2000). Biosensor chip mass spectrometry: a chip-based proteomics approach. *Electrophoresis.* **21**, (6), 1155-1163.

Neuhoff, V., Arold, N., Taube, D. and Ehrhardt, W. (1988). Improved staining of proteins in polyacrylamide gels including isoelectric focusing gels with clear background at nanogram sensitivity using Coomassie Brilliant Blue G-250 and R-250. *Electrophoresis.* **9**, (6), 255-262.

Nimura, K., Yoshikawa, H. and Takahashi, H. (1996). DnaK3, one of the three DnaK proteins of cyanobacterium Synechococcus sp. PCC7942, is quantitatively detected in the thylakoid membrane. *Biochem Biophys Res Commun.* **229**, (1), 334-340.

Nimura, K., Takahashi, H. and Yoshikawa, H. (2001). Characterization of the dnaK multigene family in the Cyanobacterium Synechococcus sp. strain PCC7942. *J Bacteriol.* **183**, (4), 1320-1328.

Nishiyama, Y., Kovacs, E., Lee, C. B., Hayashi, H., Watanabe, T. and Murata, N. (1993). Photosynthetic adaptation to high temperatures associated with thylakoid membranes of Synechococcus PCC7002. *Plant Cell Physiol.* **34**, (2), 337-343.

Nishiyama, Y., Hayashi, H., Watanabe, T. and Murata, N. (1994). Photosynthetic oxygen evolution is stabilized by cytochrome c550 against heat inactivation in Synechococcus sp. PCC 7002. *Plant Physiol.* **105**, (4), 1313-1319.

Nishiyama, Y., Los, D. A., Hayashi, H. and Murata, N. (1997). Thermal protection of the oxygen-evolving machinery by PsbU, an extrinsic protein of photosystem II, in Synechococcus species PCC 7002. *Plant Physiol.* **115**, (4), 1473-1480.

Nishiyama, Y., Los, D. A. and Murata, N. (1999). PsbU, a protein associated with photosystem II, is required for the acquisition of cellular thermotolerance in synechococcus species PCC 7002. *Plant Physiol.* **120**, (1), 301-308.

Nishiyama, Y., Yamamoto, H., Allakhverdiev, S. I., Inaba, M., Yokota, A. and Murata, N. (2001). Oxidative stress inhibits the repair of photodamage to the photosynthetic machinery. *Embo J.* **20**, (20), 5587-5594.

Norling, B., Zak, E., Andersson, B. and Pakrasi, H. (1998). 2D-isolation of pure plasma and thylakoid membranes from the cyanobacterium Synechocystis sp. PCC 6803. *FEBS Lett.* **436**, (2), 189-192.

O'Farrell, P. H. (1975). High resolution two-dimensional electrophoresis of proteins. *J Biol Chem.* **250**, (10), 4007-4021.

O'Farrell, P. Z., Goodman, H. M. and O'Farrell, P. H. (1977). High resolution two-dimensional electrophoresis of basic as well as acidic proteins. *Cell.* **12**, (4), 1133-1141.

Ogawa, T., Bao, D. H., Katoh, H., Shibata, M., Pakrasi, H. B. and Bhattacharyya-Pakrasi, M. (2002). A two-component signal transduction pathway regulates manganese homeostasis in Synechocystis 6803, a photosynthetic organism. *J Biol Chem.* **277**, (32), 28981-28986.

Ohkawa, H., Sonoda, M., Shibata, M. and Ogawa, T. (2001). Localization of NAD(P)H dehydrogenase in the cyanobacterium Synechocystis sp. strain PCC 6803. *J Bacteriol.* **183**, (16), 4938-4939.

Ort (2001). When there is too much light. *Plant Physiol.* **125**, 29–32.

Ostermann, J., Horwich, A. L., Neupert, W. and Hartl, F. U. (1989). Protein folding in mitochondria requires complex formation with hsp60 and ATP hydrolysis. *Nature.* **341**, (6238), 125-130.

Padan, E. and Cohen, Y. (1982). Anoxygenic Photosynthesis. In: The Biology of Cyanobacteria. (N. G. Carr and B. A. Whitton, eds.) pp. 215-235, Blackwell Scientific Publications. (Oxford, UK).

Pappin, D. J., Hojrup, P. and Bleasby, A. J. (1993). Rapid identification of proteins by peptide-mass fingerprinting. *Curr Biol.* **3**, (6), 327-332.

Pardo, M., Ward, M., Pitarch, A., Sanchez, M., Nombela, C., Blackstock, W. and Gil, C. (2000). Cross-species identification of novel Candida albicans immunogenic proteins by combination of two-dimensional polyacrylamide gel electrophoresis and mass spectrometry. *Electrophoresis.* **21**, (13), 2651-2659.

Park, C. M., Kim, J. I., Yang, S. S., Kang, J. G., Kang, J. H., Shim, J. Y., Chung, Y. H., Park, Y. M. and Song, P. S. (2000). A second photochromic bacteriophytochrome from Synechocystis sp. PCC 6803: spectral analysis and down-regulation by light. *Biochemistry.* **39**, (35), 10840-10847.

Parsell, D. A., Kowal, A. S., Singer, M. A. and Lindquist, S. (1994). Protein disaggregation mediated by heat-shock protein Hsp104. *Nature.* **372**, (6505), 475-478.

Patriarca, E. J. and Maresca, B. (1990). Acquired thermotolerance following heat shock protein synthesis prevents impairment of mitochondrial ATPase activity at elevated temperatures in Saccharomyces cerevisiae. *Exp Cell Res.* **190**, (1), 57-64.

Patterson, S. D. (1995a). Matrix-assisted laser-desorption/ionization mass spectrometric approaches for the identification of gel-separated proteins in the 5-50 pmol range. *Electrophoresis.* **16**, (7), 1104-1114.

Patterson, S. D. and Aebersold, R. (1995b). Mass spectrometric approaches for the identification of gel-separated proteins. *Electrophoresis.* **16**, (10), 1791-1814.

Patterson, S. D., Aebersold, R. and Goodlett, D. R. (2001). Mass spectrometry-based mathods for protein identification and phosphorylation site analysis. In: Proteomics: from protein sequence to function. (S. R. Pennington and M. J. Dunn, eds.) pp. BIOS Scientific Publishers. (Oxford, UK).

Patton, W. F., Lopez, M. F., Barry, P. and Skea, W. M. (1991). A mechanically strong matrix for protein electrophoresiswith enhanced silver staining properties. *Biotechniques.* **12**, 580-585.

Patton, W. (2001). Detecting proteins in polyacrylamide gels and on electroblot membranes. In: Proteomics: from protein sequence to function. (M. S. Pennington and M. J. Dunn, eds.) pp. 65-86, BIOS Scientific Publishers Ltd. (Oxford, UK).

Patton, W. F., Schulenberg, B. and Steinberg, T. H. (2002). Two-dimensional gel electrophoresis; better than a poke in the ICAT? *Curr Opin Biotechnol.* **13**, (4), 321-328.

Pearce, M. L. and Slabas, A. R. (1998). Phosphatidate phosphatases from avocado (Persea americana) - purification, substrate specificity and possible metabolic implications for the Kennedy pathway and cell signalling in plants. *The Plant Journal.* **14**, (5), 555-564.

Pearcy, R. W. (1978). Effect of growth temperature on the fatty acid composition of the leaf in *Atriplex lentiformis* (torr.) wats. *Plant Physiol.* **61**, 484-486.

Peary, J. A. and Castenholz, R. W. (1964). Temperature strains of a thermophilic blue-green alga. *Nature.* **202**, 720-721.

Pennington, S. R. and Dunn, M. J. (2001). The role of proteomics in meeting the post-genome challenge. In: Proteomics: from protein sequence to function. (S. R. Pennington and M. J. Dunn, eds.) pp. xvii-xxii, BIOS Scientific Publishers. (Oxford, UK).

Pennington, K., McGregor, E., Beasley, C. L., Everall, I., Cotter, D. and Dunn, M. J. (2004). Optimization of the first dimension for separation by two-dimensional gel electrophoresis of basic proteins from human brain tissue (Proteomics 2004, vol. 4, issue 1, pp. 27-30). *Proteomics.* **4**, (5), 1519.

Perkins, D. N., Pappin, D. J., Creasy, D. M. and Cottrell, J. S. (1999). Probability-based protein identification by searching sequence databases using mass spectrometry data. *Electrophoresis.* **20**, (18), 3551-3567.

Peterson, G. L. (1979). Review of the Folin phenol protein quantitation method of Lowry, Rosebrough, Farr and Randall. *Anal Biochem.* **100**, (2), 201-220.

Pirkkala, L., Nykanen, P. and Sistonen, L. (2001). Roles of the heat shock transcription factors in regulation of the heat shock response and beyond. *Faseb J.* **15**, (7), 1118-1131.

Pirkl, F. and Buchner, J. (2001). Functional analysis of the Hsp90-associated human peptidyl prolyl cis/trans isomerases FKBP51, FKBP52 and Cyp40. *J Mol Biol.* **308**, (4), 795-806.

Pleissner, K. P., Oswald, H. and Wegner, S. (2001). Image analysis of two-dimensional gels. In: Proteomics: from protein sequence to function. (M. S. Pennington and M. J. Dunn, eds.) pp. BIOS Scientific Publishers Ltd. (Oxford, UK).

Popot, J. L. (1993). Integral membrane protein structure: transmembrane protein α helices as autonomous folding domains. *Curr Opin Struct Biol.* **3**, 512-540.

Poralla, K., Muth, G. and Hartner, T. (2000). Hopanoids are formed during transition from substrate to aerial hyphae in Streptomyces coelicolor A3(2). *FEMS Microbiol Lett.* **189**, (1), 93-95.

Prentki, P., Binda, A. and Epstein, A. (1991). Plasmid vectors for selecting IS1-promoted deletions in cloned DNA: sequence analysis of the omega interposon. *Gene.* **103**, (1), 17-23.

Rabilloud, T., Valette, C. and Lawrence, J. J. (1994). Sample application by in-gel rehydration improves the resolution of two-dimensional electrophoresis with immobilized pH gradients in the first dimension. *Electrophoresis.* **15**, (12), 1552-1558.

Raison, J. K., Roberts, J. K. M. and Berry, J. A. (1982). Correlation between the thermal stability of chloroplast (thylakoid) membranes and the composition and fluidity of their polar lipids upon acclimation of the higher plant *Nerium oleander* to growth temperature. *Biochem Biophys Acta.* **688**, 218-228.

Rajaram, H. and Kumar Apte, S. (2003). Heat-shock response and its contribution to thermotolerance of the nitrogen-fixing cyanobacterium Anabaena sp. strain L-31. *Arch Microbiol.* **179**, (6), 423-429.

Ramagli, L. and Rodriguez, L. (1985). Quantitation of microgram amounts of protein in two dimensional polyacrylamide gel electrophoresis sample buffer. *Electrophoresis.* **6**, 559-563.

Reading, D. S., Hallberg, R. L. and Myers, A. M. (1989). Characterisation of the yeast HSP60 gene encoding for a mitochondrial essambly factor. *Nature.* **337**, 655-659.

Revathi, C. J., Chattopadhyay, A. and Srinivas, U. K. (1994). Change in membrane organization induced by heat shock. *Biochem Mol Biol Int.* **32**, (5), 941-950.

Richaud, C., Zabulon, G., Joder, A. and Thomas, J. C. (2001). Nitrogen or sulfur starvation differentially affects phycobilisome degradation and expression of the nblA gene in Synechocystis strain PCC 6803. *J Bacteriol.* **183**, (10), 2989-2994.

Rigaut, G., Shevchenko, A., Rutz, B., Wilm, M., Mann, M. and Seraphin, B. (1999). A generic protein purification method for protein complex characterization and proteome exploration. *Nat Biotechnol.* **17,** (10), 1030-1032.

Rippka, R., Deruelles, J., Waterbury, J. B., Herdman, M. and Stanier, R. Y. (1979). Generic assignments, strain histories and properties of pure strains of cyanobacteria. *J. Gen. Microbiol.* **111,** 1-61.

Ritossa, F. M. (1962). A new puffing pattern induced by temperature shock and DNP in Drosophila. *Experientia.* **18,** 571-573.

Roepstorff, P. and Fohlman, J. (1984). Proposal for a common nomenclature for sequence ions in mass spectra of peptides. *Biomed Mass Spectrom.* **11,** (11), 601.

Rosenfeld, J., Capdevielle, J., Guillemot, J. C. and Ferrara, P. (1992). In-gel digestion of proteins for internal sequence analysis after one- or two-dimensional gel electrophoresis. *Anal Biochem.* **203,** (1), 173-179.

Roy, S. K., Hiyama, T. and Nakamoto, H. (1999). Purification and characterization of the 16-kDa heat-shock-responsive protein from the thermophilic cyanobacterium Synechococcus vulcanus, which is an alpha-crystallin-related, small heat shock protein. *Eur J Biochem.* **262,** (2), 406-416.

Ryoo, K., Huh, S. H., Lee, Y. H., Yoon, K. W., Cho, S. G. and Choi, E. J. (2004). Negative regulation of MEKK1-induced signaling by glutathione S-transferase Mu. *J Biol Chem.*

Sabounchi-Schutt, F., Astrom, J., Olsson, I., Eklund, A., Grunewald, J. and Bjellqvist, B. (2000). An immobiline DryStrip application method enabling high-capacity two-dimensional gel electrophoresis. *Electrophoresis.* **21,** (17), 3649-3656.

Saito, H. (2001). Histidine phosphorylation and two-component signaling in eukaryotic cells. *Chem Rev.* **101**, (8), 2497-2509.

Salvucci, M. E. and Crafts-Brandner, S. J. (2004). Relationship between the heat tolerance of photosynthesis and the thermal stability of rubisco activase in plants from contrasting thermal environments. *Plant Physiol.* **134**, (4), 1460-1470.

Sanchez, J. C., Rouge, V., Pisteur, M., Ravier, F., Tonella, L., Moosmayer, M., Wilkins, M. R. and Hochstrasser, D. F. (1997). Improved and simplified in-gel sample application using reswelling of dry immobilized pH gradients. *Electrophoresis.* **18**, (3-4), 324-327.

Sanders, S. L., Whitfield, K. M., Vogel, J. P., Rose, M. D. and Schekman, R. W. (1992). Sec61p and BiP directly facilitate polypeptide translocation into the ER. *Cell.* **69**, (2), 353-365.

Santarius, K. A. (1975). Sites of heat sensitivity in chloroplasts and differential inactivation of cyclic and noncyclic photophosphorylation by heating. *J. Therm Biol.* **1**, 101-107.

Santoni, V., Rabilloud, T., Doumas, P., Rouquie, D., Mansion, M., Kieffer, S., Garin, J. and Rossignol, M. (1999). Towards the recovery of hydrophobic proteins on two-dimensional electrophoresis gels. *Electrophoresis.* **20**, (4-5), 705-711.

Santoni, V., Molloy, M. and Rabilloud, T. (2000). Membrane proteins and proteomics: un amour impossible? *Electrophoresis.* **21**, (6), 1054-1070.

Sazuka, T. and Ohara, O. (1997). Towards a proteome project of cyanobacterium Synechocystis sp. strain PCC6803: linking 130 protein spots with their respective genes. *Electrophoresis.* **18**, (8), 1252-1258.

Sazuka, T., Yamaguchi, M. and Ohara, O. (1999). Cyano2Dbase updated: linkage of 234 protein spots to corresponding genes through N-terminal microsequencing. *Electrophoresis.* **20**, (11), 2160-2171.

Scanlan, D. J., Mann, N. H. and Carr, N. G. (1993). The response of the picoplanktonic marine cyanobacterium Synechococcus species WH7803 to phosphate starvation involves a protein homologous to the periplasmic phosphate-binding protein of Escherichia coli. *Mol Microbiol.* **10**, (1), 181-191.

Scheler, C., Lamer, S., Pan, Z., Li, X. P., Salnikow, J. and Jungblut, P. (1998). Peptide mass fingerprint sequence coverage from differently stained proteins on two-dimensional electrophoresis patterns by matrix assisted laser desorption/ionization-mass spectrometry (MALDI-MS). *Electrophoresis.* **19**, (6), 918-927.

Schirmer, E. C., Glover, J. R., Singer, M. A. and Lindquist, S. (1996). HSP100/Clp proteins: a common mechanism explains diverse functions. *Trends Biochem Sci.* **21**, (8), 289-296.

Schmitt, M., Neupert, W. and Langer, T. (1996). The molecular chaperone Hsp78 confers compartment-specific thermotolerance to mitochondria. *J Cell Biol.* **134**, (6), 1375-1386.

Schopf, J. W. (1993). Microfossils of the Early Archean Apex chert: new evidence of the antiquity of life. *Science.* **260**, 640-646.

Schulenberg, B., Arnold, B. and Patton, W. F. (2003). An improved mechanically durable electrophoresis gel matrix that is fully compatible with fluorescence-based protein detection technologies. *Proteomics.* **3**, (7), 1196-1205.

Schulz, G. E. (1993). Bacterial porins: structure and function. *Curr Opin Cell Biol.* **5**, (4), 701-707.

Seidler, A. (1996). The extrinsic polypeptides of photosystem II. *Biochem Biophys Acta.* **1277**, 35-60.

Seigneurin-Berny, D., Rolland, N., Garin, J. and Joyard, J. (1999). Technical Advance: Differential extraction of hydrophobic proteins from chloroplast envelope membranes: a subcellular-specific proteomic approach to identify rare intrinsic membrane proteins. *Plant J.* **19**, (2), 217-228.

Servant, P. and Mazodier, P. (2001). Negative regulation of the heat shock response in Streptomyces. *Arch Microbiol.* **176**, (4), 237-242.

Shalon, D., Smith, S. J. and Brown, P. O. (1996). A DNA microarray system for analyzing complex DNA samples using two-color fluorescent probe hybridization. *Genome Res.* **6**, (7), 639-645.

Sharkey, T. D. and L., S. E. (1995). Why plants emit isoprene. *Nature.* **374**, 769.

Shaw, J., Rowlinson, R., Nickson, J., Stone, T., Sweet, A., Williams, K. and Tonge, R. (2003). Evaluation of saturation labelling two-dimensional difference gel electrophoresis fluorescent dyes. *Proteomics.* **3**, (7), 1181-1195.

Shen, J. R., Burnap, R. L. and Inoue, Y. (1995a). An independent role of cytochrome c-550 in cyanobacterial photosystem II as revealed by double-deletion mutagenesis of the psbO and psbV genes in Synechocystis sp. PCC 6803. *Biochemistry.* **34**, (39), 12661-12668.

Shen, J. R., Vermaas, W. and Inoue, Y. (1995b). The role of cytochrome c-550 as studied through reverse genetics and mutant characterization in Synechocystis sp. PCC 6803. *J Biol Chem.* **270**, (12), 6901-6907.

Shen, J. R., Ikeuchi, M. and Inoue, Y. (1997). Analysis of the psbU gene encoding the 12-kDa extrinsic protein of photosystem II and studies on its role by deletion mutagenesis in Synechocystis sp. PCC 6803. *J Biol Chem.* **272**, (28), 17821-17826.

Shen, J. R., Qian, M., Inoue, Y. and Burnap, R. L. (1998). Functional characterization of Synechocystis sp. PCC 6803 delta psbU and delta psbV mutants reveals important roles of cytochrome c-550 in cyanobacterial oxygen evolution. *Biochemistry.* **37**, (6), 1551-1558.

Shevchenko, A., Jensen, O. N., Podtelejnikov, A. V., Sagliocco, F., Wilm, M., Vorm, O., Mortensen, P., Boucherie, H. and Mann, M. (1996a). Linking genome and proteome by mass spectrometry: large-scale identification of yeast proteins from two dimensional gels. *Proc Natl Acad Sci U S A.* **93**, (25), 14440-14445.

Shevchenko, A., Wilm, M., Vorm, O. and Mann, M. (1996b). Mass spectrometric sequencing of proteins silver-stained polyacrylamide gels. *Anal Chem.* **68**, (5), 850-858.

Shi, L. X., Lorkovic, Z. J., Oelmuller, R. and Schroder, W. P. (2000). The low molecular mass PsbW protein is involved in the stabilization of the dimeric photosystem II complex in Arabidopsis thaliana. *J Biol Chem.* **275**, (48), 37945-37950.

Sidler, W. A. (1994). Phycobilisome and Phycobiliprotein Structures. In: The Molecular Biology of Cyanobacteria. (D. A. Bryant, eds.) pp. 139, Kluwer Academic Publishers. (Dordrecht, The Netherlands).

Simon, W. J., Hall, J. J., Suzuki, I., Murata, N. and Slabas, A. R. (2002). Proteomic study of the soluble proteins from the unicellular cyanobacterium Synechocystis sp. PCC6803 using automated matrix-assisted laser desorption/ionization-time of flight peptide mass fingerprinting. *Proteomics.* **2**, (12), 1735-1742.

Smet, C., Sambo, A. V., Wieruszeski, J. M., Leroy, A., Landrieu, I., Buee, L. and Lippens, G. (2004). The peptidyl prolyl cis/trans-isomerase Pin1 recognizes the phospho-Thr212-Pro213 site on Tau. *Biochemistry*. **43**, (7), 2032-2040.

Smith, A. J. (1982). Modes of Cyanobacterial Carbon Metabolism. In: The Biology of Cyanobacteria. (B. A. Whitton and N. G. Carr, eds.) pp. 47-85, Blackwell Scientific Publications. (Oxford, UK).

Somero, G. N. (1995). Proteins and temperature. *Annu Rev Physiol*. **57**, 43-68.

Song, L., Hobaugh, M. R., Shustak, C., Cheley, S., Bayley, H. and Gouaux, J. E. (1996). Structure of staphylococcal alpha-hemolysin, a heptameric transmembrane pore. *Science*. **274**, (5294), 1859-1866.

Sonoike, K., Hihara, Y. and Ikeuchi, M. (2001). Physiological significance of the regulation of photosystem stoichiometry upon high light acclimation of Synechocystis sp. PCC 6803. *Plant Cell Physiol*. **42**, (4), 379-384.

Squires, C. L., Pedersen, S., Ross, B. M. and Squires, C. (1991). ClpB is the Escherichia coli heat shock protein F84.1. *J Bacteriol*. **173**, (14), 4254-4262.

Stanier, R. Y. and Cohen-Bazire, G. (1977). Phototrophic prokaryotes: the cyanobacteria. *Annu Rev Microbiol*. **31**, 225-274.

Stanier, R. Y. and Van Niel, C. B. (1962). The concept of a bacterium. *Arch Mikrobiol*. **42**, 17-35.

Stanier, R. Y., Kunisawa, R., Mandel, M. and Cohen-Bazire, G. (1971). Purification and properties of unicellular blue-green algae (order Chroococcales). *Bacteriol Rev*. **35**, (2), 171-205.

Steinberg, T. H., Jones, L. J., Haugland, R. P. and Singer, V. L. (1996a). SYPRO orange and SYPRO red protein gel stains: one-step fluorescent staining of denaturing gels for detection of nanogram levels of protein. *Anal Biochem.* **239**, (2), 223-237.

Steinberg, T. H., Haugland, R. P. and Singer, V. L. (1996b). Applications of SYPRO orange and SYPRO red protein gel stains. *Anal Biochem.* **239**, (2), 238-245.

Strain, H. H., Thomas, M. R. and Katz, J. J. (1963). Spectral absorption properties of ordinary and fully deuteriated chlorophylls a and b. *Biochim. Biophys. Acta.* **75**, 306-311.

Suttorp, N., Floer, B., Schnittler, H., Seeger, W. and Bhakdi, S. (1990). Effects of Escherichia coli hemolysin on endothelial cell function. *Infect Immun.* **58**, (11), 3796-3801.

Suzuki, I., Kanesaki, Y., Mikami, K., Kanehisa, M. and Murata, N. (2001). Cold-regulated genes under control of the cold sensor Hik33 in Synechocystis. *Mol Microbiol.* **40**, (1), 235-244.

Suzuki, I., Los, D. A., Kanesaki, Y., Mikami, K. and Murata, N. (2000a). The pathway for perception and transduction of low-temperature signals in Synechocystis. *Embo J.* **19**, (6), 1327-1334.

Suzuki, I., Los, D. A. and Murata, N. (2000b). Perception and transduction of low-temperature signals to induce desaturation of fatty acids. *Biochem Soc Trans.* **28**, (6), 628-630.

Suzuki, I. and Murata, N. (2003). Analysis of gene expression under heat shock conditions in the Cyanobacterium *Synechocystis* sp. PCC 6803. *Plant Cell Physiol.* **43** Suppl., S82-S82.

Suzuki, S., Ferjani, A., Suzuki, I. and Murata, N. (2004). The SphS-SphR two component system is the exclusive sensor for the induction of gene expression in response to phosphate limitation in synechocystis. *J Biol Chem.* **279**, (13), 13234-13240.

Switzer, R. C., 3rd, Merril, C. R. and Shifrin, S. (1979). A highly sensitive silver stain for detecting proteins and peptides in polyacrylamide gels. *Anal Biochem.* **98**, (1), 231-237.

Tanaka, N., Hiyama, T. and Nakamoto, H. (1997). Cloning, characterization and functional analysis of groESL operon from thermophilic cyanobacterium Synechococcus vulcanus. *Biochim Biophys Acta.* **1343**, (2), 335-348.

Tanaka, N. and Nakamoto, H. (1999). HtpG is essential for the thermal stress management in cyanobacteria. *FEBS Lett.* **458**, (2), 117-123.

Tanaka, Y., Nishiyama, Y. and Murata, N. (2000). Acclimation of the photosynthetic machinery to high temperature in Chlamydomonas reinhardtii requires synthesis de novo of proteins encoded by the nuclear and chloroplast genomes. *Plant Physiol.* **124**, (1), 441-449.

Tatsuta, T., Tomoyasu, T., Bukau, B., Kitagawa, M., Mori, H., Karata, K. and Ogura, T. (1998). Heat shock regulation in the ftsH null mutant of Escherichia coli: dissection of stability and activity control mechanisms of sigma32 in vivo. *Mol Microbiol.* **30**, (3), 583-593.

Thomas, P. G., Dominy, P. J., Vigh, L., Mansourian, A. R., Quinn, P. J. and Williams, W. P. (1986). Increased thermal stability of pigment protein complexes of pea thylakoids following atalytic hydrogenation of membrane lipids. *Biochem Biophys Acta.* **849**, 131-140.

Thompson, L. K., Blaylock, R., Sturtevant, J. M. and Brudvig, G. W. (1989).
Molecular basis of the heat denaturation of photosystem II. *Biochemistry*. **28**, (16), 6686-6695.

Tissieres, A., Mitchell, H. K. and Tracy, U. M. (1974). Protein synthesis in salivary
glands of Drosophila melanogaster: relation to chromosome puffs. *J Mol Biol*. **84**, (3),
389-398.

Tomoyasu, T., Gamer, J., Bukau, B., Kanemori, M., Mori, H., Rutman, A. J.,
Oppenheim, A. B., Yura, T., Yamanaka, K., Niki, H. and et al. (1995). Escherichia
coli FtsH is a membrane-bound, ATP-dependent protease which degrades the heat-shock
transcription factor sigma 32. *Embo J*. **14**, (11), 2551-2560.

Tomoyasu, T., Ogura, T., Tatsuta, T. and Bukau, B. (1998). Levels of DnaK and DnaJ
provide tight control of heat shock gene expression and protein repair in Escherichia coli.
Mol Microbiol. **30**, (3), 567-581.

Tonge, R., Shaw, J., Middleton, B., Rowlinson, R., Rayner, S., Young, J., Pognan, F.,
Hawkins, E., Currie, I. and Davison, M. (2001). Validation and development of
fluorescence two-dimensional differential gel electrophoresis proteomics technology.
Proteomics. **1**, (3), 377-396.

Török, Z., Horváth, I., Goloubinoff, P., Kovács, E., Glatz, A., Balogh, G. and Vigh,
L. (1997). Evidence for a lipochaperonin: association of active protein-folding GroESL
oligomers with lipids can stabilize membranes under heat shock conditions. *Proc Natl
Acad Sci U S A*. **94**, (6), 2192-2197.

Török, Z., Goloubinoff, P., Horváth, I., Tsvetkova, N. M., Glatz, A., Balogh, G., Varvasovszki, V., Los, D. A., Vierling, E., Crowe, J. H. and Vigh, L. (2001). Synechocystis HSP17 is an amphitropic protein that stabilizes heat-stressed membranes and binds denatured proteins for subsequent chaperone-mediated refolding. *Proc Natl Acad Sci U S A.* **98**, (6), 3098-3103.

Tyres, M. and Mann, M. (2003). From geniomics to proteomics. *Nature.* **422**, 193-197.

Unlu, M., Morgan, M. E. and Minden, J. S. (1997). Difference gel electrophoresis: a single gel method for detecting changes in protein extracts. *Electrophoresis.* **18**, (11), 2071-2077.

Valladares, A., Montesinos, M. L., Herrero, A. and Flores, E. (2002). An ABC-type, high-affinity urea permease identified in cyanobacteria. *Mol Microbiol.* **43**, (3), 703-715. Van Baalen, C. (1962). Studies on marine blue-green algae. *Bot Mar.* **4**, 129-139.

van den Ussel, P., Norman, D. G. and Quinlan, R. A. (1999). Molecular chaperones: Small heat shock proteins in the lime light. *Current Biology.* **9**, R103-R105.

VanBogelen, R. A., Abshire, K. Z., Moldover, B., Olson, E. R. and Neidhardt, F. C. (1997). Escherichia coli proteome analysis using the gene-protein database. *Electrophoresis.* **18**, (8), 1243-1251.

Varvasovszki, V., Glatz, A., Shigapova, N., Josvay, K., Vigh, L. and Horváth, I. (2003). Only one dnaK homolog, dnaK2, is active transcriptionally and is essential in Synechocystis. *Biochem Biophys Res Commun.* **305**, (3), 641-648.

Veinger, L., Diamant, S., Buchner, J. and Goloubinoff, P. (1998). The small heat-shock protein IbpB from Escherichia coli stabilizes stress-denatured proteins for subsequent refolding by a multichaperone network. *J Biol Chem.* **273**, (18), 11032-11037.

Velculescu, V. E., Zhang, L., Vogelstein, B. and Kinzler, K. W. (1995). Serial analysis of gene expression. *Science*. **270**, (5235), 484-487.

Velculescu, V. E., Zhang, L., Zhou, W., Vogelstein, J., Basrai, M. A., Bassett, D. E., Jr., Hieter, P., Vogelstein, B. and Kinzler, K. W. (1997). Characterization of the yeast transcriptome. *Cell*. **88**, (2), 243-251.

Versteeg, S., Mogk, A. and Schumann, W. (1999). The Bacillus subtilis htpG gene is not involved in thermal stress management. *Mol Gen Genet*. **261**, (3), 582-588.

Vigh, L., Maresca, B. and Harwood, J. L. (1998). Does the membrane's physical state control the expression of heat shock and other genes? *Trends Biochem Sci*. **10**, 369-374

Viitanen, P. V., Gatenby, A. A. and Lorimer, G. H. (1992). Purified chaperonin 60 (groEL) interacts with the nonnative states of a multitude of Escherichia coli proteins. *Protein Sci*. **1**, (3), 363-369.

Vorm, O., Roepstorff, P. and Mann, M. (1994). Improved resolution and very high sensitivity in MALDI TOF of matrix surfaces made by fast evaporation. *Analytical Chemistry*. **66**, (19), 3281-3287.

Wada, H., Gombos, Z. and Murata, N. (1990). Enhancement of chilling tolerance of a cyanobacterium by genetic manipulation of fatty acid desaturation. *Nature*. **347**, (6289), 200-203.

Wada, H., Gombos, Z. and Murata, N. (1994). Contribution of membrane lipids to the ability of the photosynthetic machinery to tolerate temperature stress. *Proc Natl Acad Sci U S A*. **91**, 4273-4277.

Wang, Y., Sun, J. and Chitnis, P. R. (2000). Proteomic study of the peripheral proteins from thylakoid membranes of the cyanobacterium Synechocystis sp. PCC 6803. *Electrophoresis.* **21**, (9), 1746-1754.

Waters, E. R. (1995). The molecular evolution of the small heat shock proteins in plants. *Genetics.* **141**, 785-795.

Webb, R., Reddy, K. J. and Sherman, L. A. (1990). Regulation and sequence of the Synechococcus sp. strain PCC 7942 groESL operon, encoding a cyanobacterial chaperonin. *J Bacteriol.* **172**, (9), 5079-5088.

Webb, M. S. and R., G. B. (1991). Biochemical and biophysical properties of thylakoid acyl lipids. *Biochem Biophys Acta.* **1060**, 133-158.

Welch, W. J. (1992). Mammalian stress response: cell physiology, structure/function of stress proteins, and implications for medicine and disease. *Physiol Rev.* **72**, (4), 1063-1081.

White, A. W. (1974). Growth of two facultatively heterotrophic marine centric diatoms. *J Phycol.* **10**, 292-300.

Whitton, B. A. and Carr, N. G. (1982). Cyanobacteria: Current Perspectives. In: The Biology of Cyanobacteria. (N. G. Carr and B. A. Whitton, eds.) pp. 1-8, Blackwell Scientific Publications. (Oxford, UK).

Wickner, S., Gottesman, S., Skowyra, D., Hoskins, J., McKenney, K. and Maurizi, M. R. (1994). A molecular chaperone, ClpA, functions like DnaK and DnaJ. *Proc Natl Acad Sci U S A.* **91**, (25), 12218-12222.

Wiech, H., Buchner, J., Zimmermann, R. and Jakob, U. (1992). Hsp90 chaperones protein folding in vitro. *Nature.* **358**, (6382), 169-170.

Wildgruber, R., Harder, A., Obermaier, C., Boguth, G., Weiss, W., Fey, S. J., Larsen, P. M. and Görg, A. (2000). Towards higher resolution: two-dimensional electrophoresis of Saccharomyces cerevisiae proteins using overlapping narrow immobilized pH gradients. *Electrophoresis*. **21**, (13), 2610-2616.

Wilkins, M. R., Gasteiger, E., Sanchez, J. C., Bairoch, A. and Hochstrasser, D. F. (1998). Two-dimensional gel electrophoresis for proteome projects: the effects of protein hydrophobicity and copy number. *Electrophoresis*. **19**, (8-9), 1501-1505.

Wilkins, M. R., Pasquali, C., Appel, R. D., Ou, K., Golaz, O., Sanchez, J. C., Yan, J. X., Gooley, A. A., Hughes, G., Humphery-Smith, I., Williams, K. L. and Hochstrasser, D. F. (1996). From proteins to proteomes: large scale protein identification by two-dimensional electrophoresis and amino acid analysis. *Biotechnology (N Y)*. **14**, (1), 61-65.

Yalovsky, S., Paulsen, H., Michaeli, D., Chitnis, P. R. and Nechushtai, R. (1992). Involvement of a chloroplast HSP70 heat shock protein in the integration of a protein (light-harvesting complex protein precursor) into the thylakoid membrane. *Proc Natl Acad Sci U S A*. **89**, (12), 5616-5619.

Yamaguchi, K., Suzuki, I., Yamamoto, H., Lyukevich, A., Bodrova, I., Los, D. A., Piven, I., Zinchenko, V., Kanehisa, M. and Murata, N. (2002). A two-component Mn2+-sensing system negatively regulates expression of the mntCAB operon in Synechocystis. *Plant Cell*. **14**, (11), 2901-2913.

Yamashita, T. and Butler, W. L. (1968). Inhibition of chloroplasts by UV-irradiation and heat-treatment. *Plant Physiol*. **43**, 2037-2040.

Yan, J. X., Devenish, A. T., Wait, R., Stone, T., Lewis, S. and Fowler, S. (2002). Fluorescence two-dimensional difference gel electrophoresis and mass spectrometry based proteomic analysis of Escherichia coli. *Proteomics.* **2**, (12), 1682-1698.

Yan, W., Lee, H., Deutsch, E. W., Lazaro, C. A., Tang, W., Chen, E., Fausto, N., Katze, M. G. and Aebersold, R. (2004). A dataset of human liver proteins identified by protein profiling via isotope coded affinity tag (ICAT) and tandem mass spectrometry. *Mol Cell Proteomics.*

Yates, J. R., 3rd, Eng, J. K., McCormack, A. L. and Schieltz, D. (1995). Method to correlate tandem mass spectra of modified peptides to amino acid sequences in the protein database. *Anal Chem.* **67**, (8), 1426-1436.

Yonehara, M., Minami, Y., Kawata, Y., Nagai, J. and Yahara, I. (1996). Heat-induced chaperone activity of HSP90. *J Biol Chem.* **271**, (5), 2641-2645.

Yordanov, I., Dilova, S., Petkova, R., Pangelova, T., Goltsev, V. and Suss, K.-H. (1986). Mechanisms of the temperature damage and acclimation of the photosynthetic apparatus. *Photobiochem Photobiophys.* **12**, 147-155.

Young, R. A. (2000). Biomedical discovery with DNA arrays. *Cell.* **102**, (1), 9-15.

Yu, J., Smart, L. B., Jung, Y. S., Golbeck, J. and McIntosh, L. (1995). Absence of PsaC subunit allows assembly of photosystem I core but prevents the binding of PsaD and PsaE in Synechocystis sp. PCC6803. *Plant Mol Biol.* **29**, (2), 331-342.

Yu, J., Vassiliev, I. R., Jung, Y. S., Golbeck, J. H. and McIntosh, L. (1997). Strains of synechocystis sp. PCC 6803 with altered PsaC. I. Mutations incorporated in the cysteine ligands of the two [4Fe-4S] clusters FA and FB of photosystem I. *J Biol Chem.* **272**, (12), 8032-8039.

Yura, T. and Nakahigashi, K. (1999). Regulation of the heat-shock response. *Curr Opin Microbiol.* **2**, (2), 153-158.

Zeilstra-Ryalls, J., Fayet, O. and Georgopoulos, C. (1991). The universally conserved GroE (Hsp60) chaperonins. *Annu Rev Microbiol.* **45**, 301-325.

Zsiros, O., Varkonyi, Z., Kovács, A., Farkas, T., Gombos, Z. and Garab, G. (2000). Induction of polyunsaturated fatty-acid synthesis enhances tolerance of a cyanobacterium, Cylindrospermopsis raciborskii, to low-temperature photoinhibition. *Indian J Biochem Biophys.* **37**, (6), 470-476.

Zubarev, R. A., Håkansson, P. and Sundqvist, B. (1996). Accuracy Requirements for Peptide Characterization by Monoisotopic Molecular Mass Measurements. *Anal Chem.* **68**, 4060-4063.

Zuber, U. and Schumann, W. (1994). CIRCE, a novel heat shock element involved in regulation of heat shock operon dnaK of Bacillus subtilis. *J Bacteriol.* **176**, (5), 1359-1363.

Appendix 1

List of MALDI PMF identified *Synechocystis* sp. PCC 6803 soluble proteins.

Appendix 1. List of identified *Synechocystis* sp. PCC 6803 soluble proteins.

Spot No.	Protein Identification	MOWSE Score	ORF	Accession No. NCBI	Gel MW (kDa)/pI	Predicted MW (Da)/pI [c]
1	Cytochrome c$_{550}$	2.29×10^3	sll0258	2493975	18.0 / 4.51	17884 / 4.8
2	**Trigger factor**	1.28×10^8	sll0533	2499015	61.8 / 4.50	52610 / 4.3
3	**Hypothetical protein**	1.36×10^4	sll0408	7469882	37.9 / 4.55	43910 / 4.7
4	Hypothetical protein	1.70×10^3	sll1835	7470159	23.8 / 4.58	28832 / 4.9
5	30S ribosomal protein S1 [b]	6.79×10^4	slr1356	2500385	38.3 / 4.57	36570 / 4.6
6	30S ribosomal protein S1	4.15×10^7	slr1356	2500385	40.1 / 4.57	36570 / 4.6
	3-isopropylmalate dehydrogenase	2.19×10^6	slr1517	2497264	/ 4.7	38668 / 4.7
7	Heat shock protein GrpE	3.02×10^6	sll0057	2495092	32.8 / 4.58	27568 / 4.6
8	Ribulose bisphosphate carboxylase large subunit [b]	2.09×10^5	slr0009	1710041	54.5 / 4.60	52497 / 5.8
9	Ribulose bisphosphate carboxylase large subunit	8.26×10^4	slr0009	1710041	54.5 / 4.64	52491 / 5.8
10	Phycocyanin β subunit [b]	5.25×10^5	sll1577	2493300	19.9 / 4.67	18127 / 5.0

Appendix 1 continued

Spot No.	Protein Identification	MOWSE Score	ORF	Accession No. NCBI	Gel MW (kDa)/pI	Predicted MW (Da)/pI [c]
11	Ribulose bisphosphate carboxylase large subunit	4.89×10^4	slr0009	1710041	54.5 / 4.66	52491 / 5.8
12	DnaK protein [b]	8.39×10^4	sll0170	118730	81.2 / 4.67	67614 / 4.7
13	Ribulose bisphosphate carboxylase large subunit	4.68×10^4	slr0009	1710041	54.5 / 4.69	52491 / 5.8
14	DnaK protein	5.75×10^7	sll0170	118730	29.2 / 4.71	67614 / 4.7
15	Phycocyanin β subunit	5.94×10^4	sll1577	2493300	19.8 / 4.71	18127 / 5.0
16	Phosphoribosylformyl glycinamidine synthetase II	3.66×10^3	sll1056	7428512	92.0 / 4.71	82819 / 4.7
17	Putative oxppcycle protein Opac	4.37×10^9	slr1734	2498704	46.5 / 4.71	52034 / 5.0
18	Allophycocyanin α chain	3.87×10^3	slr2067	266765	18.5 / 4.73	17412 / 4.9
19	DNA polymerase III beta subunit	8.56×10^4	slr0965	2494196	53.1 / 4.73	42088 / 4.7
20	RNA polymerase alpha subunit	4.83×10^7	sll1818	2500603	40.9 / 4.76	35004 / 4.7
	Carboxyl-terminal protease	2.67×10^6	slr1751	7448480		46833 / 5.1

Appendix 1 continued

Spot No.	Protein Identification	MOWSE Score	ORF	Accession No. NCBI	Gel MW (kDa)/pI	Predicted MW (Da)/pI [c]
21	**Hypothetical protein**	1.93×10^3	slr1854	7470520	27.7 4.78	22293 4.7
22	**Hypothetical protein**	1.23×10^3	slr1590	7470465	32.2 4.79	32605 4.9
23	Phycocyanin β subunit	1.81×10^3	sll1577	2493300	21.1 4.80	18127 5.0
24	**ATP dependant Clp protease proteolytic subunit**	5.13×10^3	slr0164	7435702	25.6 4.80	24882 4.9
25	Phycocyanin β subunit	1.32×10^6	sll1577	2493300	19.5 4.80	18127 5.0
26	**Regulatory components of sensory transduction system**	2.23×10^5	slr0947	7444022	28.8 4.80	26264 4.8
27	**ATP synthase β subunit** [b]	2.71×10^8	slr1329	114570	56.7 4.65	51733 4.9
	Ribulose bisphosphate carboxylase large subunit	7.02×10^5	slr0009	1710041		52491 5.8
28	**Hypothetical protein**	3.05×10^3	sll0887	7469953	60.0 4.80	47600 4.8
29	ATP synthase β subunit	7.74×10^5	slr1329	114570	56.7 4.82	51733 4.9
30	**Hypothetical protein**	1.25×10^7	sll0245	7451191	43.5 4.82	39317 4.8

Appendix 1 continued

Spot No.	Protein Identification	MOWSE Score	ORF	Accession No. NCBI	Gel MW (kDa)/pI	Predicted MW (Da)/pI [c]
31	60 kDa chaperonin 2 [b]	5.62×10^5	sll0416	1705799	67.9 / 4.82	57775 / 4.9
32	ATP synthase β subunit	5.70×10^5	slr1329	114570	56.7 / 4.84	51733 / 4.9
33	60 kDa chaperonin 2	1.39×10^6	sll0416	1705799	67.9 / 4.85	57775 / 4.9
34	**Hypothetical protein**	3.34×10^3	slr0848	7470292	31.5 / 4.86	31791 / 4.8
35	ATP synthase β subunit	2.03×10^{13}	slr1329	114570	56.0 / 4.85	51733 / 4.9
36	Phycobilisome LCM core-membrane linker polypeptide [b]	2.21×10^7	slr0335	7469407	106.0 / 4.85	100296 / 9.2
37	Phenylalanyl-tRNA synthase	1.63×10^4	sll1553	2500989		87888 / 4.9
38	Membrane protein	1.36×10^3	sll1621	3915480	23.2 / 4.87	21167 / 4.9
39	**Ketol-acid reductoisomerase (acetohydroxy-acid isomerase)** [b]	2.57×10^3	sll1363	2506910	35.9 / 4.86	35822 / 4.9
39	Phycocyanin β subunit	4.11×10^4	sll1577	2493300	19.3 / 4.88	18127 / 5.0
40	Allophycocyanin β chain [b]	1.66×10^4	slr1986	266766	17.4 / 4.88	17216 / 5.4

Appendix 1 continued

Spot No.	Protein Identification	MOWSE Score	ORF	Accession No. NCBI	Gel MW (kDa)/pI	Predicted MW (Da)/pI
41	**Ribose 5-phosphate isomerse**	3.32×10^5	slr0194	6226034	27.1 / 4.88	24753 / 4.9
42	Allophycocyanin β chain	8.20×10^4	slr1986	266766	17.4 / 4.88	17216 / 5.4
	Phycocyanin α subunit [b]	7.91×10^4	sll1578	2493297		17587 / 5.3
43	Phycocyanin β subunit	1.81×10^3	sll1577	2493300	20.9 / 4.89	18127 / 5.0
44	**Hypothetical protein**	7.28×10^4	slr0552	7469394	25.9 / 4.89	26722 / 4.9
45	**Hypothetical protein**	1.77×10^3	slr0923	6136561	15.5 / 4.90	12638 / 5.0
46	**Hypothetical protein**	4.31×10^3	slr1963	7470547	33.6 / 4.91	34659 / 4.9
47	**Molybdopterin biosynthesis MoeB protein**	4.54×10^4	sll1536	7447427	46.0 / 4.92	42759 / 4.9
48	Ketol-acid reductoisomerase (acetohydroxy-acid isomerase)	1.46×10^8	sll1363	2506910	35.3 / 4.93	35822 / 4.9
49	Molybdopterin biosynthesis MoeB protein	2.13×10^4	sll1536	7447427	45.5 / 4.93	42759 / 4.9
50	Phycocyanin α subunit	1.67×10^4	sll1578	2493297	17.7 / 4.96	17587 / 5.3

Appendix 1 continued

Spot No.	Protein Identification	MOWSE Score	ORF	Accession No. NCBI	Gel MW (kDa)/pI	Predicted MW (Da)/pI[c]
51	Phycocyanin α subunit	1.72×10^4	sll1578	2493297	42.2 4.95	17587 5.3
52	Phycobilisome LCM core-membrane linker polypeptide	4.45×10^5	slr0335	7469407	106.0 4.95	100296 9.2
	Elongation factor EF-G	1.14×10^4	slr1463	2506375		76750 4.9
53	ATP synthase α subunit	1.44×10^6	sll1326	114530	58.3 4.95	53966 5.0
	Glutamate-ammonia ligase	2.48×10^4	slr1756	7437907		53000 5.0
54	ClpB protein[b]	7.95×10^3	slr0156	7435715	84.5 4.98	101392 5.2
55	Glutamate-ammonia ligase[b]	1.97×10^4	slr1756	7437907	58.3 5.00	53000 5.0
56	Rehydrin	6.39×10^3	slr1198	7432672	25.1 5.02	23560 5.1
57	Phycocyanin α subunit	8.27×10^3	sll1578	2493297	17.4 5.08	17587 5.3
58	Hypothetical protein	2.83×10^4	sll1582	7470103	43.1 5.12	129023 6.7
	DNA mismatch repair protein muts[b]	1.23×10^4	sll1165	7404405		97587 5.6

Appendix 1 continued

Spot No.	Protein Identification	MOWSE Score	ORF	Accession No. NCBI	Gel MW (kDa)/pI	Predicted MW (Da)/pI [c]
58	Hypothetical protein	8.40×10^3	slr0104	1723098	43.1 / 5.12	90255 / 8.5
	Sensory transduction histidine kinase	7.71×10^3	sll1871	7470843		74935 / 5.1
	DNA mismatch repair protein	7.47×10^3	sll1165	7448108		101387 / 5.7
59	Transketolase [b]	2.82×10^4	sll1070	7433612	79.6 / 5.23	71726 / 5.4
60	ClpB protein	1.89×10^4	slr0156	7435715	19.2 / 5.20	101392 / 5.2
61	Primosomal protein N [b]	6.96×10^5	sll0270	3183135	74.0 / 5.34	93307 / 8.9
	ClpB protein	4.95×10^4	slr0156	7435715		101392 / 5.2
	Hypothetical protein	1.12×10^4	slr0359	7470226		141663 / 5.6
62	Primosomal protein N	3.38×10^4	sll0270	3183135	38.6 / 5.43	93307 / 8.9
	Hypothetical protein	3.25×10^4	sll1424	7470079		55649 / 5.6
	Glycogen phosphorylase	1.61×10^4	slr1367	7433822		98306 / 5.8

Appendix 1 continued

Spot No.	Protein Identification	MOWSE Score	ORF	Accession No. NCBI	Gel MW (kDa)/pI	Predicted MW (Da)/pI [c]
62	Aspartate kinase	1.61×10^4	slr0657	7469734	38.6 / 5.43	63534 / 5.2
	Hypothetical protein	7.67×10^3	slr1968	7470549		104313 / 5.5
63	RNA polymerase beta prime subunit	8.10×10^3	sll1789	2500624	53.1 / 5.46	144778 / 4.7
	ClpB protein	4.00×10^3	slr0156	7435715		101392 / 5.2
	DNA mismatch repair protein muts	1.07×10^3	sll1165	7404405		97587 / 5.6
64	Elongation factor EF-G [b]	5.15×10^{14}	slr1463	2506375	106.0 / 4.97	76750 / 4.9
65 [a]	GCPE	9.00×10^3	slr2136	8928139	20.0 / 4.98	44176 / 5.6
65 [a]	Precorrin methylase	7.27×10^3	slr1135	7470365	20.0 / 4.98	85347 / 6.1
66	Enolase [b]	6.01×10^3	slr0752	3023705	49.3 / 4.99	46529 / 5.0
67	60kD chaperonin 1	4.55×10^5	slr2076	2506274	66.8 / 4.99	57653 / 5.0
68	Periplasmic iron-binding protein [b]	1.19×10^7	slr0513	7469675	34.7 / 4.99	38156 / 5.8

Appendix 1 continued

Spot No.	Protein Identification	MOWSE Score	ORF	Accession No. NCBI	Gel MW (kDa)/pI	Predicted MW (Da)/pI [c]
69	**Phosphoglycerate kinase**	5.67×10^4	slr0394	2499503	41.8 / 5.00	41784 / 5.0
70	Allophycocyanin β chain	3.38×10^3	slr1986	266766	16.9 / 5.01	17216 / 5.4
71	Hypothetical protein	2.82×10^3	slr1852	7460207	25.0 / 5.03	21835 / 5.1
72	GlpX protein	4.80×10^4	slr2094	7444705	43.5 / 5.05	37075 / 5.1
73	Enolase	2.67×10^5	slr0752	3023705	40.1 / 5.06	46529 / 5.0
74	Periplasmic iron-binding protein	2.23×10^6	slr0513	7469675	34.4 / 5.07	38156 / 5.8
75	Protein synthesis elongation factor Tu [b]	6.18×10^5	sll1099	2494260	48.1 / 5.09	43733 / 5.2
76	**Hypothetical protein**	1.39×10^4	slr1855	7452257	70.2 / 5.10	43733 / 5.2
77	Phycocyanin α subunit	8.43×10^3	sll1578	2493297	17.4 / 5.08	17587 / 5.3
78	**Argininosuccinate synthase**	1.20×10^5	slr0585	2492989	48.7 / 5.10	44485 / 5.1
79	**Polyribonucleotide nucleotidyltransferase** [b]	1.75×10^6	sll1043	7447093	96.2 / 5.11	77832 / 5.1

Spot No.	Protein Identification	MOWSE Score	ORF	Accession No. NCBI	Gel MW (kDa)/pI	Predicted MW (Da)/pI [c]
80	Phosphoribulokinase	4.00×10^8	sll1525	322055	39.4 / 5.12	37915 / 5.2
81	**Dihydroxyacid dehydratase**	1.40×10^6	slr0452	6685569	62.8 / 5.14	58646 / 5.1
82	Protein synthesis elongation factor Tu	3.66×10^{10}	sll1099	2494260	47.6 / 5.14	43733 / 5.2
83	6-phosphogluconate dehydrogenase	3.22×10^7	sll0329	1703020		52874 / 5.1
84	Polyribonucleotide nucleotidyltransferase	2.01×10^4	sll1043	7447093	96.2 / 5.14	77832 / 5.1
85	Phycocyanin α subunit	2.12×10^4	sll1578	2493297	17.4 / 5.13	17587 / 5.3
86	Periplasmic iron-binding protein	2.34×10^6	slr0513	7469675	34.4 / 5.15	38156 / 5.8
87	**Aspastyl-tRNA synthase**	1.01×10^3	slr1720	2500971	72.7 / 5.17	67210 / 5.2
88	Protein synthesis elongation factor Tu	1.13×10^{11}	sll1099	2494260	47.6 / 5.19	43733 / 5.2
89	**IMP dehydrogenase subunit**	2.93×10^6	slr1722	7427693	39.4 / 5.19	40235 / 5.2
	Pentose-5-phosphate-3-epimerase	6.72×10^3	sll0807	2829613	26.1 / 5.19	24971 / 5.2

Appendix 1 continued

Spot No.	Protein Identification	MOWSE Score	ORF	Accession No. NCBI	Gel MW (kDa)/pI	Predicted MW (Da)/pI [c]
90	Aspartate kinase [b]	4.28×10^4	slr0657	7469734	67.9 / 5.21	63534 / 5.2
91	Phosphoribosyl aminoimidazole carboxy formyl fomyltransferase	1.78×10^3	slr0597	7994675	54.5 / 5.22	59327 / 5.6
92 [a]	Sec A	4.69×10^{13}	sll0616	1256593	51.1 / 5.23	107009 / 5.0
	DNA topoisomerase	2.48×10^{12}	slr2058	2501241		99340 / 8.9
93	Protein synthesis elongation factor Tu	1.16×10^4	sll1099	2494260	47.0 / 5.24	43733 / 5.2
94	Allophycocyanin β chain	3.37×10^3	slr1986	266766	17.0 / 5.24	17216 / 5.4
95	Allophycocyanin β chain	8.24×10^4	slr1986	266766	16.6 / 5.26	17216 / 5.4
96	2-isoproplylmalate synthase	1.76×10^5	slr0186	1346444	55.2 / 5.28	57414 / 5.3
97 [a]	Hypothetical protein	2.76×10^5	sll0539	7469891	33.3 / 5.29	45185 / 6.2
	Methyl accepting chemotaxis protein	7.70×10^4	slr1044	7470740		93210 / 4.3
98	Phycocyanin α subunit	8.43×10^3	sll1578	2493297	17.0 / 5.29	17587 / 5.3

Appendix 1 continued

Spot No.	Protein Identification	MOWSE Score	ORF	Accession No. NCBI	Gel MW (kDa)/pI	Predicted MW (Da)/pI [c]
99	Elongation factor TS	5.32×10^3	sll1261	2494280	21.2 / 5.29	24231 / 5.4
100 [a]	**S-adenosylhomocysteine hydrolase** [b]	2.02×10^7	sll1234	6094235	17.0 / 5.31	46214 / 5.5
101	Adenylate kinase	2.66×10^3	sll1815	6647539	20.5 / 5.34	20254 / 5.4
102	Transketolase	9.75×10^4	sll1070	7433612	76.7 / 5.38	71726 / 5.4
103 [a]	DNA mismatch protein MUTS	4.32×10^{17}	sll1165	7404405	17.0 / 5.37	97586 / 5.7
	DNA helicase	7.33×10^{16}	sll1143	7436414		90396 / 6.1
104	S-adenosylhomocysteine hydrolase	2.42×10^5	sll1234	6094235	47.6 / 5.42	46214 / 5.5
105 [a]	Soluble lytic transglycosylase	1.59×10^{16}	slr0534	7469379	49.9 / 5.50	95981 / 5.0
	Hypothetical protein	1.54×10^{14}	slr1135	7470365		85347 / 6.1

[a] Samples where no data was collected in AutoMS mode so the data was re-collected manually, calibrated using internal tryptic fragments (842.5, 1045 and 2211) and searched at 50ppm mass accuracy. [b] Indicates proteins identified in more than one spot on the gel.
[c] Predicted p*I* and MW values acquired from PEDANT (http://pedant.gsf.de) (Frishman *et al.*, 2001, 2003)
The following spots have multiple identifications, indicating these protein spots are mixtures (42, 58, 61, 62, 65, 82, 92, 97, 103, & 105).
Identifications in **bold** text are, at the time of submission, novel proteins identified in this study not previously seen on 2D gels.